



Biakhmetov, Bauyrzhan (2025) *Comparison of centralized and decentralized municipal plastic waste management producing value-added resources: economics, environmental impacts and optimisation*. PhD thesis.

<https://theses.gla.ac.uk/85023/>

Copyright and moral rights for this work are retained by the author

A copy can be downloaded for personal non-commercial research or study, without prior permission or charge

This work cannot be reproduced or quoted extensively from without first obtaining permission from the author

The content must not be changed in any way or sold commercially in any format or medium without the formal permission of the author

When referring to this work, full bibliographic details including the author, title, awarding institution and date of the thesis must be given

Enlighten: Theses

<https://theses.gla.ac.uk/>
research-enlighten@glasgow.ac.uk



University of Glasgow

**Comparison of centralized and decentralized municipal plastic
waste management producing value-added resources: economics,
environmental impacts and optimisation**

Bauyrzhan Biakhmetov

**Submitted in the fulfilment of requirements for the degree of Doctor of Philosophy
(PhD)**

School of Engineering

College of Science and Engineering

University of Glasgow

July 2024

Abstract

Plastic waste is a global issue that severely threatens the environment if not managed properly. Municipal plastic waste is widely treated in unsustainable ways such as landfill and incineration that generally do not contribute to the circular economy or to the principles of the UN's sustainable development goals (SDGs). Mechanical recycling is not able to handle all municipal plastic waste generated due the technological limitations. Chemical recycling, specifically pyrolysis, is considered an alternative solution or supplementary to mechanical recycling because of its potential to recover fuels and chemicals from non-recycled municipal plastic waste.

In this study, large-scale centralized and small-scale decentralized diesel and hydrogen production from NMPW (non-recycled municipal plastic waste) using pyrolysis-based thermochemical conversion technologies were compared in terms of environmental footprint and economic feasibility, specifically focusing on GWP (Global Warming Potential) and NPV (Net Present Value). Glasgow was chosen as the case city for this study. LCA (Life Cycle Assessment) was applied to evaluate the GWP of all systems. The results showed that centralized systems had lower GWP compared to decentralized systems, despite their greater transportation distances. The GWPs of diesel production for centralized and decentralized systems were 801 and 1,345 kg CO₂-eq per tonne of NMPW, respectively. Hydrogen production, however, had much higher GWPs of 7,110 and 7,990 kg CO₂-eq per tonne of NMPW for centralized and decentralized systems, respectively. The end use of diesel produced has a greater carbon footprint than the end use of hydrogen. The carbon saving from the displacement of fossil hydrogen was two times higher than that from diesel displacement. After considering the end use of products and displacement, the net GWP of large-scale hydrogen production is 2,496.53 kg CO₂-eq per tonne of NMPW, which is better than the net GWP of

small-scale diesel production (2,766.3 kg CO₂-eq per tonne of NMPW) and close to the net GWP of large-scale diesel production (2,114.44 kg CO₂-eq per tonne of NMPW).

After completing the assessment of the environmental footprint, in Cost-Benefit Analysis (CBA), the economic feasibility of centralized large-scale and decentralized small-scale diesel and hydrogen production systems from NMPW was compared by defining their NPVs. Across all scenarios, only centralized large-scale diesel production, with and without carbon capture and storage, exhibited total positive net present values (£22,240,135 and £24,449,631, respectively), indicating their economic feasibility. The decentralized small-scale hydrogen production system with carbon capture and storage yielded the lowest net present value result (-£2391) per tonne of treated non-recycled municipal plastic waste. Particularly, the production of diesel and hydrogen from non-recycled municipal plastic systems, with carbon dioxide emissions to the environment, demonstrated better economic performance than the same systems capturing and storing carbon dioxide, attributable to its higher capital and operational expenditures. Also, sensitivity analysis revealed that the fuel sales price and OPEX had the most significant impact on the net present values.

In the MOO (Multi-Objective Optimization) study, 900 diesel and hydrogen-producing scenarios from NMPW were developed, and the data thus generated was then used for inventory analysis to calculate their GWPs and NPVs. After that, the long short-term memory recurrent neural network was applied to define temporal dependencies and dynamics of systems, which was integrated with Monte Carlo simulations of variables to expand scenarios from 900 to 700,000 and to predict their GWPs and NPVs. Finally, a Pareto front was derived from the GWPs and NPVs, from which the best scenarios in terms of balance between environmental and economic performance was identified using the TOPSIS and LINMAP approaches. The TOPSIS approach defined a scenario that aligns perfectly with the ideal scenario, achieving the lowest GWP (-2570.42 kg CO₂-eq. per tonne of NMPW) and the highest

NPV (£300,315.65 per tonne of NMPW). This demonstrates that the TOPSIS method effectively balances environmental and economic performance of NMPW management system. In contrast, the LINMAP approach obtained a less optimal scenario, with a moderate GWP reduction (-1025.28 kg CO₂-eq. per tonne of NMPW) and a negative NPV (-£1,402.92 per tonne of NMPW). This means that the TOPSIS approach is recommended for selecting optimal scenarios, as it provides the best balance between environmental and economic performance for NMPW management systems utilizing pyrolysis-based thermochemical conversion technologies.

Based on the LCA, CBA, and MOO studies, several recommendations were developed for practical applications, and a few of them are worth highlighting. Currently, among the scenarios considered in this study, only diesel production from NMPW in a large-scale plant is economically feasible and can achieve a negative GWP if a CCS unit is applied. Additionally, pyrolysis plants should be located close to feedstock collection sources to reduce transportation costs and minimize environmental impact. When selecting between large-scale NMPW systems and small-scale systems utilizing pyrolysis-based thermochemical conversion processes, the large-scale option is recommended due to its superior environmental and economic performance.

To My Family

Acknowledgements

I would like to thank to my supervisor, **Dr. Siming You**, for his invaluable help and encouragement throughout my entire PhD journey. His professionalism, expertise, and extensive network enabled me to complete a significant piece of work and explore new horizons within my research scope. Dr. You has not only supervised me but also invested considerable effort in my development as a scientist. Under his guidance, I feel that I have truly grown as a researcher. Also, I would like to note that my family was unable to join me in Glasgow at the start of my PhD due to the COVID-19 pandemic. They joined me later when the restrictions were eased. During this challenging time, my supervisor provided me with much-needed support, for which I am heartfelt grateful.

During my PhD journey, I had the great opportunity to collaborate with admired experts in pyrolysis-based thermochemical conversion technologies, including **Prof. Young-Kwon Park** from the University of Seoul, **Prof. Abay Dostiyarov** from Energo University, and **Prof. Yong Sik Ok** from Korea University. Their expertise and mentorship were instrumental in helping me achieve robust results and enhancing the credibility of my study.

Additionally, I would like to express my gratitude to the esteemed expert **Prof. David Flynn** for his guidance in making my study more inclusive and obtaining more accurate results. His feedback and comments on the prepared drafts of papers and my thesis were invaluable in improving them.

In my PhD project, I used numerous programs, and I was unfamiliar with some of them, particularly those related to spatial analysis. I would like to thank **Prof. Qunshan Zhao** and **Miss Yue Li** for spending their precious time guiding me in working with ArcGIS Pro and the DIGIMAP dataset. Their collaboration significantly enriched my study.

My groupmates and I have had numerous online and face-to-face meetings to discuss each other's research projects. I found these meetings invaluable for viewing our projects from different perspectives and improving them further. Many thanks to my groupmates, **Simon Ascher, Yize Li, Jade Lui, Yi Fang, Weicheng Peng, Asam Ahmed, Luís Rodrigues, and Rohit Gupta**, for their valuable advice. Also, I would like to mention the time I spent learning coding in Python with my friend Yi Fang, and many thanks to him for sharing his knowledge and skills in coding.

Besides support from the academia, there was great continuous support from my family. My beloved wife, **Aigerim Biakhmetova**, who is “my strength and stay,” has been a source of inspiration during this journey. I have two wonderful kids, **Bexultan Akylbek** and **Bekarys Akylbek**, and I am deeply grateful to them for being my motivation and for saying that I am the best dad. This journey was not only a PhD chapter of my life, but it was also a special chapter for our family, during which my second son, Bekarys, was born. It was a great experience to be a PhD student and the dad of a newborn baby at the same time, filled with happy moments.

I would also like to acknowledge the **Bolashaq International Scholarship** for providing funding for my study. The Bolashaq International Scholarship is a unique program that offers many talented individuals the opportunity to study at top universities worldwide.

Table of Contents

Chapter 1 Introduction	1
1.1. Background	1
1.2. Aims and Objectives	8
1.3. Contribution of Thesis	9
1.4. Thesis Outlines and Thesis-Related Publications.....	12
Chapter 2 Critical Literature Review	16
2.1. Sustainable Waste Management	17
2.1.1. Sustainable Development.....	17
2.1.2. Circular Economy and Sustainable Waste Management	18
2.2. Plastic Waste Crisis.....	20
2.4. Municipal Plastic Waste Recycling	23
2.5. Pyrolysis-Based MPW Management Systems	26
2.5.1. MPW Pretreatment	27
2.5.2. Thermochemical Conversion Process.....	29
2.5.3. In-line Technologies Applied after Pyrolysis and the Products Obtained from Them.....	41
2.6. Present Life Cycle Assessment Studies on Pyrolysis-Based Conversion of Non- recycled Municipal Plastic Waste into the Diesel and Hydrogen	48

2.7. Present Techno-Economic Studies on Pyrolysis-Based Conversion of Non-Recycled Municipal Plastic Waste into the Diesel and Hydrogen	49
2.8. Multi-Objective Optimization of Chemical Recycling of Municipal Plastic Waste	52
2.9. Centralized and Decentralized Waste Management Systems	54
2.10. Conclusion	55
Chapter 3 Comparing Carbon-Saving Potential of the Pyrolysis of Non-Recycled Municipal Plastic Waste: Influences of System Scales and End Products.....	
3.1. Methodology	58
3.1.1. Scenario description.....	58
3.2. Life cycle Assessment	61
3.2.1. Goal and Scope Definition	61
3.2.2. Life cycle inventory analysis.....	61
3.2.3. Interpretation and sensitivity analysis.....	84
3.3. Results and Discussion	86
3.3.1. Environmental Impacts of Four Scenarios.....	86
3.3.3. Sensitivity analysis	94
3.4. Conclusions.....	97
Chapter 4 Transportation and Process Modelling-Assisted Techno-Economic Assessment of Resource Recovery from Non-Recycled Municipal Plastic Waste.....	
4.1. Methodology	98
4.1.1. Scenario Descriptions	100
4.1.2. Model Development	108

4.1.3. Cost-benefit Analysis	115
4.1.4. Sensitivity analysis	124
4.2. Results and Discussion	125
4.2.1. Inputs and Outputs of the Developed Models	125
4.2.2. Cost-Benefit Analysis Results	134
4.3. Sensitivity Analysis	141
4.4. Conclusions	143
 Chapter 5 Multi-Objective Optimization of Non-Recycled Municipal Plastic Waste Management Systems Producing Value-Added Resources.....	
5.1. Methodology	146
5.1.1. Overview of, and Scenarios for Hydrogen and Diesel Production Systems From NMPW	149
5.1.2. Model Development for Scenarios Considered.....	152
5.1.3. Life Cycle Assessment and Cost-Benefit Analysis.....	153
5.1.4. LSTM-RNN Model	165
5.1.5. Multi-Objective Optimization	166
5.2. Results and Discussion	169
5.2.1. Environmental and Economic Performance of Systems	169
5.2.2. Multi-Objective Optimization and Final Decision Selection	173
5.3. Conclusions	175
 Chapter 6 Conclusions and Recommendations	
6.1. General Conclusions.....	176

6.2. Recommendations for Future studies and Practical Applications	178
Appendix	182
References	197

List of Figures

Figure 1.1. Estimation of hydrogen demand in the transportation sector in Scotland.....	6
Figure 1.2. Estimation of hydrogen demand across sectors such as industry, power, heat, and transportation in the UK for 2030 and 2035 (Department for Energy Security & Net Zero, 2023a).....	7
Figure 1.3. Layout of the thesis. MPW: Municipal Plastic Waste; CAPEX: Capital Expenditure; OPEX: Operational Expenditure; LCA: Life Cycle Assessment; CBA: Cost-Benefit Analysis; and LSTM-RNN: Long Short-Term Memory Recurrent Neural Network.....	15
Figure 2.1. An illustration of pyrolysis-based plastic waste treatment systems.....	26
Figure 2.2. Applications of products received from the pyrolysis of MPW.....	42
Figure 2.3. Methods for producing hydrogen-rich gas through pyrolysis-based processes from plastic waste.....	47
Figure 2.4. Pareto optimal solutions.....	53
Figure 3.1. Detailed process flows for four scenarios: C1, D1, C2, and D2.....	62
Figure 3.2. Glasgow city neighbourhoods' territory with road networks, dwellings and waste collection points.....	67
Figure 3.3. a) GWP for each scenario, where the FU is 1 tonne of MPW; b) GWP for each scenario, where the FU is 100 km travelled by bus.....	87
Figure 3.4. The GWP breakdown of the four scenarios based on (a) the stages involved in the production of hydrogen and diesel, and (b) scope 1-3 emissions.....	92
Figure 3.5. Sensitivity map illustrating the impact of factors on GWP ((a) FU is 1 tonne of MPW; (b) FU is 100 km travelled by bus).....	95

Figure 4.1. Schematic diagram of the proposed framework.....	99
Figure 4.2. Comparison of C1, D1, C2 and D2 scenarios in terms of different sub-processes: a) MPW collection and transportation systems; b) processes involved in the thermo-chemical conversion of NMPW into diesel and hydrogen, and c) product and by-product transportation. *Other separated waste fractions were not considered in this study.....	105
Figure 4.3. Schematic diagrams of the conversion of NMPW to diesel and hydrogen (the top and bottom flow diagrams represent the C1/D1 and C2/D2 scenarios, respectively). In the C2 and D2 scenario diagram, the dryer was not included as a Duplicate Manipulator was used in the C1 and D1 scenario diagram to replicate the dryer process for the C2 and D2 scenarios..	114
Figure 4.4. Verification of modelling results of thermochemical processes simulated in Aspen plus.....	133
Figure 4.5. PVs for all cash flows over operational time and NPV results for all scenarios, with and without CCS.....	139
Figure 4.6. Comparison of LCOHs across the hydrogen producing scenarios.....	140
Figure 4.7. Sensitivity map depicting the effect of factors on NPV results for the different scenarios.....	142
Figure 5.1. Methodology diagram utilized in this MOO study.....	163
Figure 5.2. The factors distinguishing the scenarios considered: MPW transportation systems, ways to address GHG emissions at FPFs, thermos-chemical conversion processes of NMPW into fuels, and scales of FPF. MRF- Material Recovery Facility; FPF- Fuel Production Facility; MPM- Municipal Plastic waste; NMPW- Non-recycled Municipal Plastic Waste; UK ETS- United Kingdom Emissions Trading System; CCS- Carbon Capture and Storage; and PSA- Pressure Swing Adsorption.....	166

Figure 5.3. Explanation diagram of the mathematical basis of MOO.....185

Figure 5.4. Environmental (GWP) and economic (NPV) statistics for a set of 900 scenarios..189

Figure 5.5. Pareto front, and the final TOPSIS and LINMAP best scenarios.....192

List of Tables

Table 2.1. Comparison of the carbon-saving potential of plastic pyrolysis, incineration, and landfill.....	25
Table 2.2. Main catalysts used in MPW pyrolysis.....	36
Table 2.3. Overview of MPW pyrolysis plants operating globally: process characteristics and setups.....	39
Table 2.4. Comparison of properties of conventional diesel, crude pyrolysis oil, and distilled diesel-range pyrolysis oil.....	44
Table 3.1. Scenario description in terms of waste transportation, PtE technologies, product distribution and annual capacity.....	60
Table 3.2. Various inputs and outputs for all four scenarios considered in detail.....	75
Table 3.3. The carbon (GWP) saving by the displacements of heating energy, electricity, diesel, hydrogen and carbon nanotubes per FU (1 tonne of non-recycled MPW) for all scenarios.....	90
Table 4.1. Description of blocks (Figure 4.3) and their parameters applied in Aspen Plus simulation.....	113
Table 4.2. Equipment costs for the base year and updated costs for the reference year based on the scale and cost factors considered in the analysis.....	121
Table 4.3. Equations used to calculate CAPEX and OPEX.....	123
Table 4.4. Transport distances.....	125
Table 4.5. Mass and energy balances for the C1 and D1 scenarios.....	127

Table 4.6. Mass and energy balances for the C2 and D2 scenarios.....	129
Table 4.7. The summary of incomes and expenditures in GBP.....	137
Table 5.1. Mass and energy flows of diesel production from NMPW at the FPFs with annual capacities of 15,500 tonnes (1,800 kg/h), 8,000 tonnes (900 kg/h), and 3,300 tonnes (380 kg/h).....	170
Table 5.2. Mass and energy flows of hydrogen production from NMPW at the FPFs with annual capacities of 15,500 tonnes (1,800 kg/h), 8,000 tonnes (900 kg/h), and 3,300 tonnes (380 kg/h).....	173
Table 5.3. Equipment/unit cost for reference year (2022) calculated based on the base year cost obtained from the existing literature, and scale and cost factors.....	179
Table 5.4. Variables and their upper and lower bounds as applied in Monte Carlo simulations.....	184
Table 5.5. GWPs and NPVs of diesel producing NMPW pyrolysis plants based on the selected locations (Barrhead and Grangemouth).....	191
Table 5.6. GWPs and NPVs of ideal and negative-ideal scenarios, as well as the final TOPSIS and LINMAP best scenarios.....	193

Abbreviation

CAPEX	Capital Expenditure
CCS	Carbon Capture and Storage
CEPCI	Chemical Engineering Plant Cost Index
EU	European Union
FPF	Fuel Production Facility
FU	Functional Unit
GHG	Greenhouse Gas
GWP	Global Warming Potential
HDPE	High Density Polyethylene
LCA	Life Cycle Assessment
LDPE	Low Density Polyethylene
LSTM	Long Short-Term Memory
ML	Machine Learning
MOO	Multi-Objective Optimization
MRF	Material Recovery Facility
MPW	Municipal Plastic Waste
NMPW	Non-Recycled Municipal Plastic Waste
NPV	Net Present Value
OPEX	Operational Expenditure
PET	Polyethylene Terephthalate
PP	Polypropylene
PS	Polystyrene
PSA	Pressure Swing Adsorption

PtD	Plastic-to-Diesel
PtE	Plastic-to-Energy
PtH	Plastic-to-Hydrogen
PVC	Polyvinyl Chloride
RNN	Recurrent Neural Network
UK ETS	United Kingdom Emissions Trading System
WGS	Water Gas Shift

Chapter 1 Introduction

1.1. Background

One of the biggest global environmental challenges humankind faces is plastic pollution. To promote the transition from a linear economy to a circular economy and minimize plastic pollution, municipal plastic waste (MPW) needs to be recycled (Praveenkumar et al., 2024). Various initiatives and programs have been developed worldwide to improve plastics circularity. For example, 1000 organizations (multinational corporations, small- and medium-sized enterprises, non-governmental organizations, and other stakeholders) primarily involved in the production, use, and management of packaging plastics, which account for more than 20% of global packaging plastic, have worked together to boost recycling rates since 2018 (Ellen MacArthur Foundation, 2020, Ellen MacArthur Foundation, 2023). EU has an ambition to achieve 55% plastic packaging recycling by 2030, while significant changes in MPW collection and sorting practices, plastic product design, and market-level interventions are necessary to achieve this goal (Antonopoulos et al., 2021). For instance, plastic product design plays an essential role in enhancing the recyclability of packaging plastics. The EU provides a series of guidelines and commitments to support this effort, including: 1- promoting the use of mono-polymer materials as their designs are easier to recycle compared to multi-layered materials, which are typically inseparable and often end up in landfills or incineration; and 2- reducing or eliminating problematic additives, which interfere with mechanical and chemical recycling processes, is essential to improving recycling results (European Commission, 2024).

Mechanical recycling dominates in MPW management in the EU (Lase et al., 2023). However, mechanical recycling is not applicable to all kinds of MPW and there are still significant amounts of MPW that cannot be mechanically recycled or, indeed, do not even undergo recycling at all. For example, in the UK, MPW, whether part of recyclables (plastics,

glass, and paper) or general municipal solid waste (MSW), is typically transported to Material Recovery Facilities to be sorted by waste fraction types. Polyethylene Terephthalate (PET) and High-density polyethylene (HDPE) bottles are easily separated and mechanically recycled. However, other MPW containing recyclable plastics is mainly sorted to make plastic bales, as it cannot be further separated to the required purity for mechanical recycling (Burgess et al., 2021). In some waste management systems, non-recycled plastic waste can be converted into Refuse-Derived Fuel (RDF), which is then used as an alternative fuel to replace fossil fuels for generating heat and power. However, in most cases, non-recycled plastic waste is usually dumped in landfill or incinerated, both of which generate a high carbon footprint (Eriksson and Finnveden, 2009, Horodytska et al., 2019). Similarly, in Scotland, MPW that cannot be recycled is typically incinerated to recover energy or disposed of in landfills (SEPA, 2024). The result of study by Haig et al. (2018), as described in Table 2.1, shows that MPW pyrolysis can result in a negative net GWP, whereas incineration and landfilling do not achieve this. Hence, we need to explore the use of alternative technologies to lower the carbon footprint of non-recycled municipal plastic waste (NMPW) management.

One of the waste management methods that is considered more sustainable than landfill or incineration is the production of diesel from non-recycled MPW. First, using non-recycled MPW as feedstock for chemical recycling reduces landfill waste and the associated environmental pollution risks. Secondly, plastic pyrolysis can significantly reduce the GWP of plastic waste management systems or even achieve negative GWP by replacing fossil fuel-based materials with the products generated (Haig et al., 2018, Garcia-Gutierrez et al., 2023). Additionally, while the production of diesel, hydrogen, or other value-added materials from plastic waste is not fully renewable, it is more sustainable than extracting fossil fuels and using them to produce these materials.

Diesel shortages and soaring prices are amongst the major challenges experienced by many countries due to unstable geopolitical situations worldwide (Millard, 2022). In 2019, 3,216,360 tonnes of oil equivalent energy were consumed by the transport sector (Department for Business, 2021), with around 60% in the form of diesel in Scotland (Haig et al., 2018). INEOS in Grangemouth is the only crude oil refinery plant in Scotland, and it only serves a quarter of Scotland's road transport fuel demands (Haig et al., 2018); with the majority of fuel used in the transport sector being imported. It is worth noting that the majority of north-western Europe's oil refineries are configured to produce petrol rather than diesel, which further negatively affects Scotland's transport fuel security.

Petroleum prices, especially diesel, and consumption are closely linked to the overall petroleum situation in the UK. Diesel consumption has increased over time, while petrol consumption shows the opposite trend (RAC Foundation, 2024). This shift can be explained by factors such as the greater fuel efficiency of diesel vehicles compared to petrol vehicles, governmental tax incentives promoting diesel to reduce carbon footprints, and diesel's dominance in the logistics sector, as most freight industries rely on diesel (Department for Energy Security and Net Zero, 2019, IEA, 2021). It is worth noting that domestic diesel production has decreased in recent years, while diesel imports have followed the opposite trend (Department for Energy Security and Net Zero, 2024). Diesel produced from non-recycled MPW can be blended with conventional diesel, and this blended fuel can be used in diesel vehicles. This approach may contribute to improving Scotland's and the UK's overall energy security by reducing dependence on diesel imports while promoting a more sustainable method of MPW management. Regarding the economic feasibility of diesel production from plastic waste, some studies suggest that such production can be economically viable under current conditions if appropriate technologies and policies are implemented (Garcia-Gutierrez et al., 2023). One of the objectives of this project is to assess the economic feasibility of diesel

production from non-recycled MPW under the current economic conditions in Scotland and to develop practical recommendations.

Hydrogen can also be recovered from non-recycled MPW, which has the potential to contribute to Scotland's ambitious plan for a future hydrogen economy. The transport sector was the biggest emitter of greenhouse gases (GHG) in Scotland, with a net emission of 9.5 MtCO₂-eq in 2018 (Scottish Government, 2022). Significant share of this emission comes from diesel usage. As an overall strategy to reach the zero-emission target in the transport sector, the UK and Scottish Governments have decided to ban fossil fuel car sales by 2030 and 2032, respectively (Scottish Environment Protection Agency, 2019, UK, 2020). This means that non-fossil fuel vehicles working on electricity and hydrogen will play a greater role (Haugen et al., 2022, Manigandan et al., 2023). While electric vehicles are poised to continue dominating the market over hydrogen fuel cell vehicles, it is beneficial to broaden consumer choice in the proliferation of low GHG emission vehicles (Kim et al., 2020). Additionally, despite one of the main advantages of electric vehicles being their relatively higher energy efficiency in fuelling (the operational efficiency of hydrogen fuel cell vehicles is 40-60%, while that of electric vehicles is over 77%) (U.S. Department of Energy, 2024a, U.S. Department of Energy, 2024b) or a more established charging infrastructure, hydrogen fuel cell technologies applied in heavy-duty vehicles such as buses and trucks have the potential to compete with heavy-duty electric vehicles due to specific economic and mileage advantages. For instance, it was reported that a hydrogen fuel cell truck costed around \$135,503-249,900, whereas an electric truck costed \$164,641-585,000 (Cunanan et al., 2021). A full electric battery is enough for driving 62–500 miles, while 660-1104 miles can be fulfilled by a hydrogen fuel cell truck. Moreover, a hydrogen fuel cell truck has a lighter energy storage system than an electric truck, and thus potentially has a larger cargo weight (Cunanan et al., 2021). To sum up, despite electric vehicles being more widely used than hydrogen fuel cell vehicles, heavy-duty vehicles powered by

hydrogen are expected to increase as they can compete with electric ones due to the specific advantages described above.

Glasgow has already taken action to increase the number of low emissions vehicles, particularly those powered by hydrogen fuel cells. Twenty waste collection and transportation lorries fuelled by hydrogen are planned to be delivered to the Glasgow City Council (Glasgow City Council, 2021). Transport Scotland has provided funding of £805,000 to convert 23 winter gritters working on diesel to dual fuel hydrogen (Glasgow City Council, 2019). Additionally, the Glasgow City Council has an ambitious plan to make all of its cars emission-free by the end of 2029 (Glasgow City Council, 2019). It is expected that the demand for hydrogen fuel in the transport sector in Glasgow, and Scotland and UK in general, will increase significantly. For example, based on estimates from Scotland's national economic development agency, hydrogen demand in the transportation sector, as described in Figure 1.1, is projected to increase exponentially, with annual demand potentially exceeding 12.5 TWh by 2045 (Scottish Enterprise, 2023). Most of this increase will be driven by waterborne transportation. Any shortage in hydrogen supply should be prevented so as not to affect the operational costs of hydrogen fuel cell vehicles.

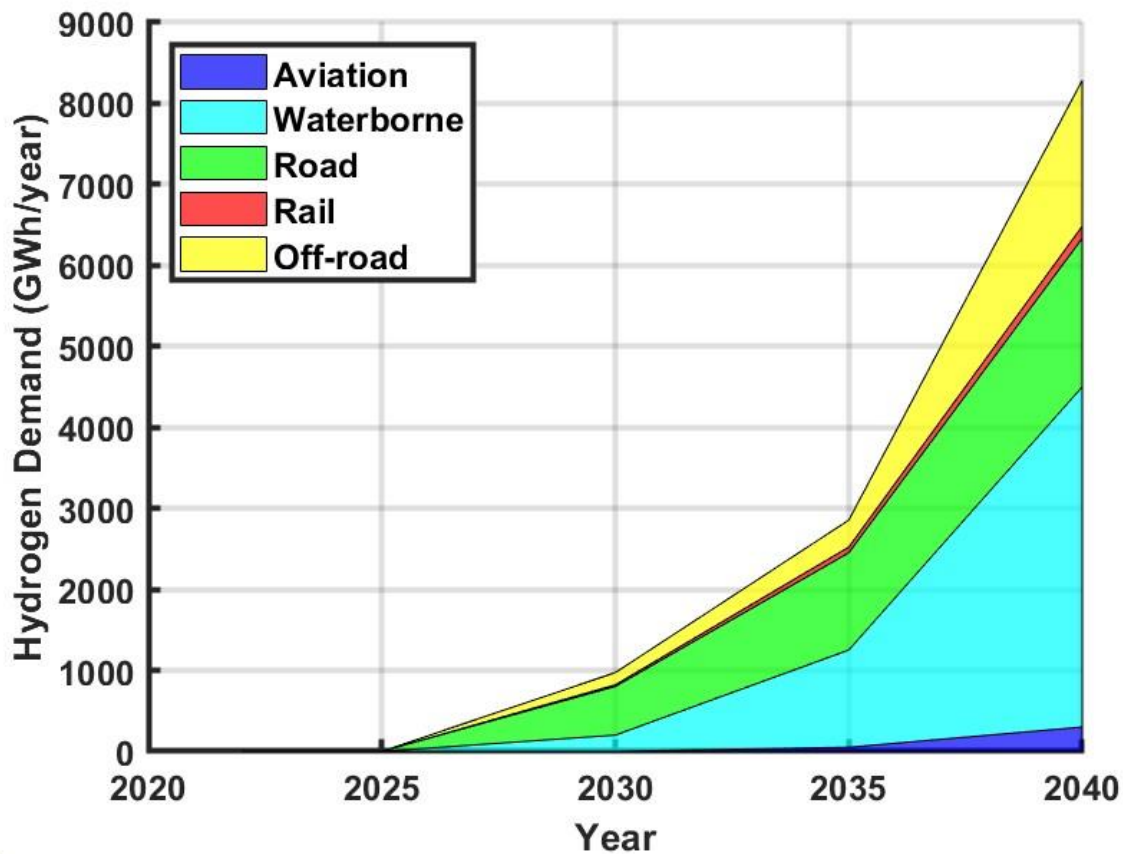


Figure 1.1. Estimation of hydrogen demand in the transportation sector in Scotland (Scottish Enterprise, 2023).

Besides its usage in the transportation sector, hydrogen is utilized in various other sectors such as industry, heating, agriculture, and more. The current general hydrogen demand in the UK is approximately 10–27 TWh per year, with a large share attributed to the industrial sector (Hydrogen UK, 2023). General hydrogen demand is expected to continuously increase, and Figure 1.2 illustrates the projected hydrogen demand by sector in the UK for 2030 and 2035. By 2035, the annual hydrogen demand in the industrial sector is expected to reach 25–55 TWh, which alone—without considering other sectors—will exceed the current general hydrogen demand. In 2030, the annual hydrogen demand for transportation is projected to be 1–4 TWh, increasing significantly to 20–30 TWh by 2035. Additionally, Figure 1.2 shows that hydrogen will also be actively used in heat and power generation. This indicates that hydrogen

demand will rise not only in the transportation sector but also in other sectors, such as industry, heat, and power generation.

Hydrogen is typically produced from natural gas, which has a great carbon footprint (Williams, 2020). However, the UK government has aimed to produce 10 GW of hydrogen annually from fossil fuel-free sources for the transportation and industrial sectors by 2030 (Department for Energy Security and Net Zero and Department for Business, 2022). The use of MPW to produce hydrogen could contribute the UK's aim to produce hydrogen from fossil fuel-free sources.

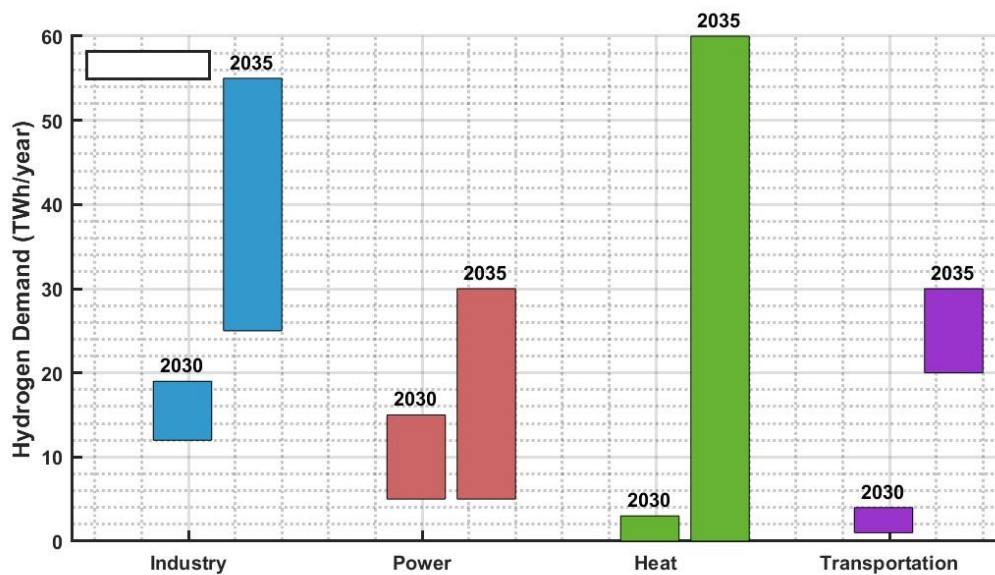


Figure 1.2. Estimation of hydrogen demand across sectors such as industry, power, heat, and transportation in the UK for 2030 and 2035 (Department for Energy Security & Net Zero, 2023a).

Waste management systems can be divided into centralized large-scale systems and decentralized small-scale systems. The main differences between these systems lie in their scale and the transportation requirements. Centralized systems are typically large-scale and are usually located farther from waste collection areas compared to decentralized systems, which

are smaller in scale and closer to waste sources. Centralized large-scale systems are generally preferable when transportation is not considered. However, including transportation can negatively impact their economic and environmental performances. There are several reasons for this: first, in centralized systems, large quantities of MPW feedstock must be transported over long distances and since MPW has a relatively low density, this leads to increased economic and environmental costs. Second, the availability and quality of infrastructure can further amplify environmental footprints and economic costs.

Decentralized systems have the potential to compete with centralized systems due to the minimal distances covered by trucks used for feedstock, product, and by-product transportation. Proximity to MPW sources minimizes fuel consumption, which inevitably reduces environmental impact and enhances the economic performance of these systems. However, it is important to note that small-scale waste management plants, without accounting for transportation, are generally more costly per unit of treated waste compared to centralized large-scale systems. Therefore, it is pivotal to assess their environmental and economic performances to define systems with a balanced environmental footprint and economic feasibility. Detailed knowledge gaps related to diesel and hydrogen-producing systems from NMPW, as well as their environmental and economic aspects, are discussed in the next chapter.

1.2. Aims and Objectives

The main aim of this PhD study is to compare centralized large-scale and decentralized small-scale pyrolysis-based diesel and hydrogen production systems from NMPW in terms of their environmental footprint and economic feasibility. Additionally, the study aims to develop ideal systems with balanced environmental and economic performances. These “ideal systems” are defined as those with minimal environmental footprints, measured by metrics such as GHG

emissions, and high economic feasibility, assessed through indicators like NPVs (Net Present Value). To achieve the aims mentioned above, the following objectives were set:

- 1) Model and simulate the transportation aspects for centralized large-scale and decentralized small-scale diesel and hydrogen production systems to obtain more accurate results.
- 2) Model and simulate the pyrolysis-based thermochemical conversion of NMPW into diesel and hydrogen as previous studies have identified knowledge gaps related to the credibility of results obtained from modelling and simulating this process. These gaps are discussed in detail in subsection 2.7.
- 3) Assess the carbon footprint (GHG emissions) of centralized large-scale and decentralized small-scale diesel and hydrogen production systems in the understanding of transportation-related emissions, and providing insights into product selection between diesel and hydrogen based on carbon footprint.
- 4) Define the economic feasibility of centralized large-scale and decentralized small-scale diesel and hydrogen production systems.
- 5) To integrate machine learning, LCA, and CBA to evaluate a wide range of hydrogen and diesel production scenarios from NMPW. This objective also involves using machine learning algorithms to predict the GWP and NPV of scenarios based on input data. Multi-objective optimization will then be applied to define ideal scenarios where GWP does not exceed NPV, and vice versa, ensuring a balance between environmental and economic performance. The ultimate goal is to analyse these ideal scenarios and select the best-performing system using TOPSIS and LINMAP methods.

1.3. Contribution of Thesis

The contribution of the thesis can be divided into three main aspects:

Modelling. Most studies related to waste management systems based on thermochemical processes contain two main parts: transportation and thermochemical conversion. For the transportation part, most studies related to waste management systems, particularly MPW, rely on general assumptions without detailed modelling and accurate numbers. In this thesis, modelling and simulation of transportation related to MPW management systems for centralized large-scale systems and decentralized small-scale systems were conducted in ArcGIS Pro. Data from the Digimap dataset was used in ArcGIS Pro to determine transportation distances, which were subsequently used to calculate the environmental impact and transportation costs.

Also, there is a knowledge gap in simulating the thermochemical conversion of NMPW into fuels, particularly hydrogen, using Aspen Plus. For instance, as discussed in detail in subsection 2.7, some previously published studies use kinetic parameters for tire pyrolysis in the simulation of plastic pyrolysis processes that produce diesel or hydrogen. This raises concerns regarding the reliability of the obtained results. Existing LCA and CBA studies related to hydrogen production from MPW or NMPW are based on data obtained from lab-scale studies, and there are few studies that apply Aspen simulations. In this study, the conversion processes of MPW into hydrogen and diesel were simulated in Aspen Plus, as it offers a cost-effective and flexible approach to modelling. The obtained simulation results were compared with experimental data and findings from other simulation studies. The results of this comparison are presented in subsection 4.2.1. To summarize, modelling the thermochemical conversion process and validating the simulation results against lab-scale studies enhances the reliability of this study.

Assessing carbon footprint and economic feasibility. Little is known about the influences of system scales and end product selection on the carbon footprints and economic feasibility of plastic waste treatment. Most MPW management studies considered large-scale systems, which

are associated with higher economic feasibility. However, some studies noted that the carbon-saving potential and economic benefits of small-scale systems should be compared with large-scale systems, as short transportation distances positively influence the environmental and economic performance of the systems.

Additionally, most studies compared the carbon-saving potential and economic feasibility of diesel recovery from MPW through thermochemical conversion processes with landfills or incineration. Undoubtedly, the recovery of value-added materials or fuels from MPW is better than landfills or incineration based on waste management hierarchy and circular economy principles. However, there are knowledge gaps in comparing the thermochemical conversion of MPW to value-added materials or fuels with different setups, for example, hydrogen and diesel production through fast pyrolysis-steam reforming and slow-pyrolysis-oil distillation, respectively.

The UK recently launched a GHG emissions trading scheme on January 1, 2021, to promote the reduction of GHG. However, its effectiveness related to the MPW systems working on thermochemical conversion processes is not well understood. In this study, the environmental and economic performance of large-scale and small-scale pyrolysis-based hydrogen and diesel-producing systems from MPW was assessed under the newly launched GHG emissions trading scheme.

Multi-objective optimization by using machine learning. To the best of my knowledge, there are no studies related to the optimization of the environmental and economic performance of pyrolysis-based MPW and NMPW management systems producing hydrogen and diesel. It is pivotal to have more scenarios to define optimal or best scenarios with balanced environmental and economic performance. In this study, machine learning (ML) was used to increase the

number of diesel and hydrogen-producing scenarios, and optimal and best scenarios were selected from them using Pareto front, TOPSIS, and LINMAP methods.

1.4. Thesis Outlines and Thesis-Related Publications

The thesis contains main six chapters as described in Figure 1.3, and there are publications related to each of these chapters. In this sub-section, the brief content of each chapter is discussed.

Chapter 1 briefly discusses MPW and the attempts to mitigate this issue. It covers the reasons why mechanical recycling cannot handle the generated MPW, resulting in most of the MPW ending up in incinerators or landfills. The potential of pyrolysis-based chemical recycling of NMPW to produce transportation fuels (diesel and hydrogen) is evaluated. The main aims, objectives, and contributions of the thesis are then presented. Finally, the general thesis outline, including a flowchart for easy explanation and relevant publications, is described. The subsection 1.1, "Background" is an adjusted introduction from paper [3] listed in the last publications.

Chapter 2 covers a critical literature review on topics related to the plastic waste crisis, sustainable waste management, and the role of pyrolysis-based waste management systems in mitigating the plastic waste crisis and shifting to more circular economy systems. The stages involved in pyrolysis-based waste management systems and the applications of products obtained from them are also discussed in detail. Finally, the knowledge gaps related to LCA, CBA and MOO of pyrolysis-based waste management systems are defined in this chapter. Some parts of publications [2] [3], [4], and [5] were adjusted and integrated in this chapter.

Chapter 3 compares the GWPs of centralized large-scale and decentralized small-scale diesel and hydrogen production systems, applying LCA approach. First, the goal and scope of this study were defined, and an inventory analysis was conducted to obtain mass and energy

balances for the developed scenarios. Based on these balances, the carbon footprints of the scenarios were assessed. Finally, the GWP results were interpreted, and a sensitivity analysis was conducted. In many waste management system studies, transportation aspects are not properly modelled and simulated. In this chapter, the transportation aspects of centralized large-scale and decentralized small-scale diesel and hydrogen-producing systems from NMPW were modelled and simulated using ArcGIS Pro software. It is worth noting that publication [3] was integrated into this chapter.

Chapter 4 focuses on comparing the economic feasibility of centralized large-scale and decentralized small-scale diesel and hydrogen production systems from NMPW. First, transportation distances and mass and energy balances for the developed scenarios were obtained using ArcGIS Pro and Aspen Plus, respectively. Then, this generated data was used to select and size equipment units, which are applied to calculate CAPEX, OPEX, and incomes. Finally, NPVs for all scenarios were obtained, and the influence of variables on them was assessed. Publication [4] was adjusted and integrated into this chapter.

Chapter 5 examines ideal centralized large-scale and decentralized small-scale diesel and hydrogen production systems from NMPW in terms of minimum environmental footprint and maximum economic feasibility. First, a certain number of scenarios were developed, and their GWPs and NPVs were calculated. Then, these scenarios were expanded using ML-driven approaches to identify a broader range of choices for defining the ideal scenarios with balanced environmental and economic performance. Finally, the Pareto Curve approach was applied to identify a range of scenarios with balanced GWPs and NPVs, and the LINMAP and TOPSIS approaches were used to define the best scenarios from them. In this chapter, publication [5] was integrated.

Chapter 6 summarizes all the findings of this PhD project and discusses recommendations for future studies and practical applications based on the results obtained.

List of publications related to this PhD project:

- 1) Biakhmetov, B., You, S. and Dostiyarov, A., 2022. Sustainable waste management and circular economy. In *Low Carbon Stabilization and Solidification of Hazardous Wastes* (pp. 545-554). Elsevier.
- 2) Biakhmetov, B., Dostiyarov, A., Ok, Y.S. and You, S., 2023. A review on catalytic pyrolysis of municipal plastic waste. *Wiley Interdisciplinary Reviews: Energy and Environment*, 12(6), p.e495.
- 3) Biakhmetov, B., Li, Y., Zhao, Q., Ok, Y.S., Dostiyarov, A., Park, Y.K., Flynn, D. and You, S., 2024. Comparing carbon-saving potential of the pyrolysis of non-recycled municipal plastic waste: Influences of system scales and end products. *Journal of Cleaner Production*, p.143140.
- 4) Biakhmetov, B., Li, Y., Zhao, Q., Dostiyarov, A., Flynn, D. and You, S., 2025. Transportation and process modelling-assisted techno-economic assessment of resource recovery from non-recycled municipal plastic waste. *Energy Conversion and Management*, 324, p.119273.

List of publications currently under review and preparation related to this PhD project:

- 5) Multi-objective optimization of non-recycled municipal plastic waste management systems producing value-added resources by incorporating life cycle assessment, cost-benefit analysis and machine learning (under preparation).

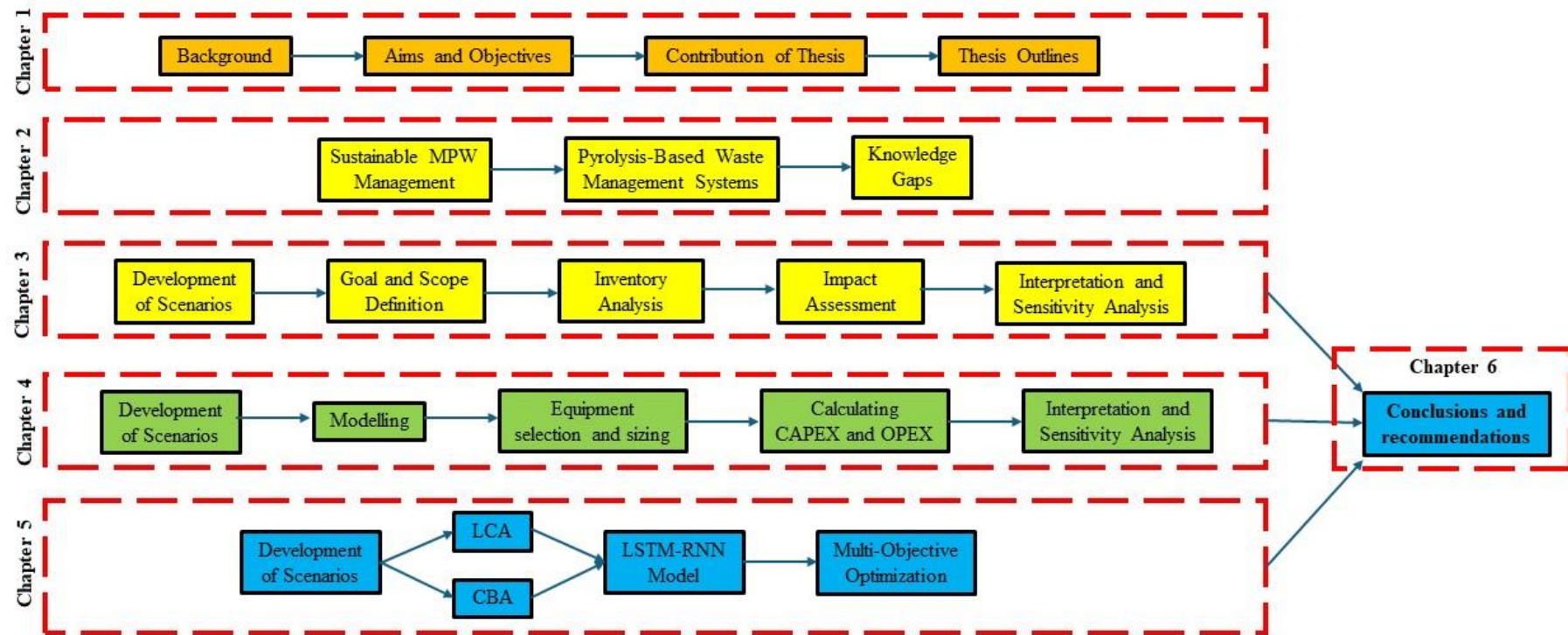


Figure 1.3. Layout of the thesis. MPW: Municipal Plastic Waste; CAPEX: Capital Expenditure; OPEX: Operational Expenditure; LCA: Life Cycle Assessment; CBA: Cost-Benefit Analysis; and LSTM-RNN: Long Short-Term Memory Recurrent Neural Network.

Chapter 2 Critical Literature Review

In Chapter 1, the aims and objectives of this work, along with its contribution, are described. Chapter 2 is divided into three parts. In the first part (sub-sections 2.1–2.4), the global plastic waste crisis, its environmental impacts, and sustainable waste management are discussed. Additionally, the role of recycling in the waste management hierarchy is evaluated to understand its contribution to sustainable waste management. In the second part (sub-section 2.5), the stages of municipal plastic waste (MPW) management systems based on pyrolysis-based processes are discussed in detail, particularly focusing on transportation, feedstock pretreatment, and the thermochemical conversion of MPW into fuels (diesel and hydrogen). This section emphasizes process parameters and setups—such as reactor types, pyrolysis process temperature, catalysts, residence time, and pressure—that have a profound impact on product qualities and yields. Additionally, existing pyrolysis plants that process plastic waste are analysed to understand the practical application of these parameters and setups. In the final part (sub-sections 2.6–2.8) of this chapter, existing LCA and TEA studies assessing the environmental footprint and economic performance of plastic waste management systems, particularly those involving pyrolysis-based processes, are discussed to identify the knowledge gaps. LCA and TEA studies separately provide results such as the GWP and NPV of systems. Typically, the optimal system achieving a balance of minimum GWP and maximum NPV, is defined through MOO studies. Finally, the methodologies for conducting MOO studies are explored to identify the most efficient systems for producing hydrogen and diesel via pyrolysis-based processes.

2.1. Sustainable Waste Management

2.1.1. Sustainable Development

Since the second industrial revolution, humankind has faced a multitude of problems due to extreme (over)exploitation and (over)consumption of natural resources (Grooten and Almond, 2018). The speed at which natural resources are being exploited by human activities is far greater than their recovery rate. For example, one of the most important global problems, namely climate change, appears to be continuously accelerating. It has been proven by measurable parameters that average global temperatures and greenhouse gas emissions into the atmosphere are increasing. Annual carbon dioxide emissions totalled 3 Gt in the middle of the last century compared with their current level of 9.5 Gt (Friedlingstein et al., 2019). If this trend continues the carbon budget will be exceeded, leading to more human health-related and ecological problems, such as the spread of viruses, extreme weather conditions, flooding, drought, storms, bushfires, starvation, *etc.*

A variety of problems have been caused by the irrational overexploitation of natural resources. Tons of metals, silicon, organic materials, rare elements, and plastics fabricated from oil and gas are being consumed or used for daily human life. However, improper disposal of waste products is causing environmental problems. The current global population is around 7.6 billion and could reach 9.8 billion by 2050 and 11.2 billion by 2100 (Biakhmetov et al., 2022). To solve or mitigate these problems, it is critical to develop sustainable human actions under the concept of the circular economy.

Sustainability and the circular economy are closely interconnected. Sustainability was defined in the report issued by the Bruntland Commission in 1987 as:

“Development that meets the needs of the present without compromising the ability of future generations to meet their own needs.” (Imperatives, 1987)

The circular economy is a relatively recent global concept proposed to mitigate the problems caused by the conventional, linear economic business model. The main difference between the circular and linear economies is that the former seeks not to generate any type of waste or co-products, use unnecessary inputs, or have outputs to meet human demands, whereas the latter's overriding approach is that of extract-produce-use-dispose (Sauvé et al., 2016).

One of the essential problems which must be solved to prevent more catastrophic outcomes is that of increasing waste generation. Currently, 2.01 billion tonnes of waste is generated annually and it is anticipated that this number could reach 3.4 billion tonnes by 2050 (Kaza et al., 2018). A small part of global waste is treated in sustainable ways, but the majority is disposed of unsustainably, resulting in environmental problems: 19% of waste is treated using material recovery technologies, 11% incinerated, 33% openly dumped, while the remaining 37% of waste ends up in landfill (Grooten and Almond, 2018). Many landfills do not have appropriate physical barriers to prevent leachate movement into soil and groundwater. Consequently, the groundwater around landfills often has a high concentration of heavy metals and toxic substances (Samadder et al., 2017). Also, marine debris represents a global tragedy, as the marine environment and the creatures living in it have been amongst the most seriously affected by such debris (Grooten and Almond, 2018). Most marine litter is plastic in nature and tiny particles of such can be found in the bodies of turtles, more than half of whales, 36% of seals, and 40% of birds, amongst other creatures (Grooten and Almond, 2018). In accordance with sustainable development principles, the negative impact of generated waste needs to be minimized or even eliminated.

2.1.2. Circular Economy and Sustainable Waste Management

Increasingly, world organisations and individuals alike are working on ways to save our planet, by shifting to sustainable development. Humankind needs to find the balance between thriving

as a species and saving the environment in which it thrives. Achieving a circular economy could bring about this balance. This requires that humankind should try to achieve zero waste, or at least minimize it, as it represents a loss of resources, and, typically, its disposal is associated with environmental pollution. Ideally, waste generation is prevented or returned to the economy, where all materials are circulated in a completely closed loop.

The rate of waste generation is positively correlated with various factors such as urbanization, population, and economic development growth rates. Currently, around 2.01 billion tonnes of waste is generated annually, 34% of which comes from 16% of the world population, namely the developed countries (Kaza et al., 2018). On average, the global rate of waste generation per capita per day is 0.74 kg. In the developed economy the average per capita waste generation is 4.54 kg, whereas, in countries with low-income, this figure is a mere 0.11 kg (Kaza et al., 2018). The tendencies towards urbanization, population, and growth in economic development are accelerating, suggesting that the rate of waste generation will continue to increase, especially in low- and middle-income countries. It is anticipated that annual global waste generation will reach 2.59 billion tonnes by 2030 and 3.4 billion tonnes by 2050 (Kaza et al., 2018).

The waste management hierarchy has been promoted as a means of achieving sustainable waste management. The number of countries starting to promote sustainable waste management is gradually increasing and 186 UN countries signed the 12 Sustainable Development Goals of the 2030 Agenda for Sustainable Development, in which the waste management hierarchy is defined (Clark and Wu, 2016). According to the Waste Framework Directive 2008/98/EC (Directive, 2008), the principle of the waste management hierarchy is that the waste generation should be firstly prevented; after that, the generated waste should be reused, recycled, or recovered, with a final step of disposal of remaining waste which cannot be recycled due to a loss of resource and environmental pollution. The waste management

hierarchy aims to work for the benefit of the environment and to return resources into the production cycle. The waste management hierarchy has become increasingly focused on extending the lifespan of products or services to prevent waste and minimize resource consumption. Many researchers have suggested new, more complex waste management hierarchies. One of these considers that prevention of waste through extending the lifespan of products and by smarter product use and manufacture is the main concept underlying the new waste management hierarchy as it pertains to the circular economy aiming to reduce humanity's environmental footprint, minimizing the need for resource extraction (Potting et al., 2017).

2.2. Plastic Waste Crisis

Plastic is a cheap and ubiquitous material due to its versatility, durability and adaptability, and 368 million tonnes of plastic were produced globally in 2019 (Plastics Europe, 2020). One-half of the plastics currently produced are single-use plastics (Giacovelli, 2018), and only 2% of these single-use packaging plastics flow in closed-loop recycling, despite the recycling symbol having appeared on plastic items for more than 40 years (Ellen MacArthur Foundation, 2016). During the Covid-19 pandemic, the generation of single-use plastics that do not flow in closed-loop recycling rises due to the increasing usage of PPE (Yuan et al., 2021). The production of plastics has increased 200-fold since the middle of the last century (Geyer, 2020); currently, around 6% of annual oil demand is used for plastic production, which is expected to reach 20% by 2050 (Ellen MacArthur Foundation, 2016).

Plastic waste is one of the main causes of three intertwined world disasters, i.e. environmental pollution, climate change, and natural resource scarcity. The GHG emitted from the fossil fuel-based plastics produced in 2015 is 1.8GtCO_{2eq} for a whole life cycle perspective (excluding recycling), accounting for 3.8% of global GHG emissions that year (Zheng and Suh, 2019). The largest share (60%) of emissions came from the production of polymers, including

resource extraction and polymer production stages (Zheng and Suh, 2019). For example, producing one kilogram of PET requires 84 MJ of energy: 31 MJ in the form of crude oil, which includes both the energy content of the crude oil and the energy consumed for its extraction, and 53 MJ for converting crude oil into polymers, including net heating energy, energy losses, and other associated energy uses (Gervet, 2007).

End-of-life plastic is usually disposed of unsustainably, which poses environmental pollution for the terrestrial and marine ecosystem. Jambeck et al. (2015) calculated that 4.8-12.7 million metric tonnes of plastic debris entered the ocean. Lack of information due to the complexity of tracking plastic pollution systems worldwide through transmission pathways (terrestrial, aquatic, and atmospheric pathways) makes the plastic problem challenging to resolve (Bank et al., 2021). For example, there are no standardized methods to quantify and extract plastic particles in a soil (Dissanayake et al., 2022).

Worldwide, various campaigns have attempted to address these issues. More than 500 organizations including >200 businesses responsible for more than 20% of global packaging plastics, and 27 financial institutions with overall \$4 trillion worth of assets have set the target of keeping plastics within a circular economy and out of the environment at their sources by 2025 (Ellen MacArthur Foundation, 2020). The European Union (EU) also developed the Plastics in the Circular Economy legislation and the Circular Economy Action Plan, to drive sustainable plastic waste management (European Commission, 2020). It was estimated that shifting five key industries (i.e. cement, aluminium, steel, plastics, and food) to the circular economy could reduce global GHG emissions by 40% by 2050, with plastics contributing significantly to this reduction (Ellen MacArthur Foundation, 2019).

Except for its economic burdens on mankind, plastic waste also has a profound footprint on the environment and living species on terrestrial and marine systems (Ok, 2020). Total 60-

99 million tonnes of plastic waste was disposed of in an unsustainable manner and ended up in the environment, whilst annual mismanaged plastic waste could reach 155–265 million tonnes by 2060 under the business-as-usual scenario (Lebreton and Andrady, 2019). Annually, 11% (19-23 million tonnes) of plastic waste ended up in the ocean, and this figure could well exceed 90 million tonnes per year by 2030 if the business-as-usual scenario is continued (Borrelle et al., 2020). Overall, 150 million tonnes of plastic debris was floating in the oceans (McKinsey Center for Business and Environment, 2015), and plastic waste usually reaches world's oceans through rivers, which is referred to as one of the major plastic waste transportation systems (van Emmerik and Schwarz, 2020). The annual world economic burden due to plastic debris reaching the oceanic system is \$8 billion (Kershaw, 2016).

Significantly concerns have been raised about the adverse impacts of plastic pollution on marine ecosystems and beyond. The plastic debris is a cause of feeding impairment (Savinelli et al., 2020) and entanglement of marine species (Jepsen and de Bruyn, 2019, Nisanth and Kumar, 2019), and disturbs natural carbon dioxide circulation (Shen et al., 2020). In a recent study, two-thirds of marine and estuarine fish species were found to have ingested plastics; indeed, the last decade's records suggests that the average frequency of microplastic occurrence in marine species has doubled since 2010 (Savoca et al., 2021). A recent study estimated that the entire population of sea turtles, 41.46% of all marine mammals, and 44% of all sea birds have plastics in their stomachs (Kühn and Van Franeker, 2020). Many of the deaths amongst marine species are associated with film-like plastics, fishing nets and latex/balloons (Roman et al., 2020). Seabirds play a transfer role for plastics received through marine foraging to terrestrial zones, which contributes to their spread (Grant et al., 2021). Furthermore, microplastics can enter the food chain, posing a potential threat to human health (De-la-Torre, 2020). Despite the various and considerable evidence about the severe ecological effect of plastic waste, more studies are needed to fully understand problems related to plastics (Bucci

et al., 2020), especially their effect on the terrestrial system (de Souza Machado et al., 2018, Kumar et al., 2020).

2.4. Municipal Plastic Waste Recycling

There are a few factors that make plastic waste more problematic than other types of waste. The plastic recycling rate is the lowest amongst the three most-used materials (i.e. plastic, paper and glass) for packaging. For example, in the UK, the recycling rates of plastic, paper and glass materials were reported to be 44.9%, 81.9%, and 67.1%, respectively (DEFRA (Department of Economic and Social Affairs Population Division), 2018). MPW is usually managed in unsustainable ways, incineration, landfill dumping, etc., and the associated GHG could triple by 2030 (Advisors et al., 2019). The world needs to take bold and urgent action to curb what appears to be a mounting plastic-related disaster (Sarkar et al., 2021).

Ideally, the waste should be treated within the framework of the waste management hierarchy, which is considered as a sustainable way of achieving this goal. According to the Waste Framework Directive 2008/98/EC, the principle of the waste management hierarchy is preventing-reusing-recycling-recovering-disposing (European Commission, 2018), where the prevention of plastic waste arising, the reuse of plastics, and plastic waste recycling need to be prioritized. Reuse of plastics has potential economic and environmental benefits over single-use plastics, but the use of plastics for the same purposes on a large scale is legislatively and technically limited (Coelho et al., 2020). In the case of plastic recycling, even in European countries with advanced waste management technologies, only 32.5% of a total of 29.1 million tonnes of post-consumer plastics was recycled in 2018, whilst 42.6% were used as resources for energy recovery, and 24.9% ended up in landfill (Plastics Europe, 2020). Unrecycled and unrecyclable post-consumer plastics should be treated for energy recovery purposes rather than

being sent to landfill in order to gain maximum environmental, economic, and social benefits in terms of their contributions to the circular economy (Van Caneghem et al., 2019).

There are two types of plastic recycling technologies: the mechanical and chemical. For the former, plastic waste is sorted, washed, shredded, melted and granulated into pellets which can be used as some ready raw materials for plastic goods production; the latter requires the use of various technologies such as chemolysis, pyrolysis, fluid catalytic cracking, gasification, etc. (Ragaert et al., 2017, Singh et al., 2017). The main disadvantages of the mechanical recycling method include thermal-mechanical degradation causing random chain scission and crosslinking (Ragaert et al., 2017), and limited effectiveness for heterogeneous plastics due to varying melting parameters (Singh et al., 2017). Plastics rejected from the mechanical recycling method due to contamination could be treated by the chemical recycling technologies, for example, pyrolysis, which is more tolerant to higher levels of plastic contaminations (Holger et al., 2019, Ragaert et al., 2017). Sorted and washed plastic usually contains contaminants such as metals, flame retardants, and small amounts of organics, which remain as solid bottom residues after the pyrolysis process (Schade et al., 2024). In the pyrolysis reactor, long polymer hydrocarbon chains are broken down into shorter ones, and they are in vapor form as the pyrolysis temperature is typically above 400°C (Haig et al., 2018). These hydrocarbon chains are pumped into the condenser, where oil-range hydrocarbons are separated from gas-range hydrocarbons. In mechanical recycling, sorted and washed plastic is melted, but long polymer hydrocarbon chains do not actively break down into shorter chains as they do in pyrolysis (Schade et al., 2024). Contaminants are not easily separated from the melted plastic.

Furthermore, the impact of climate change due to pyrolysis is less than the other widely used waste management technologies such as incineration (Somoza-Tornos et al., 2020, Gear et al., 2018). For example, the results of the study by Haig et al. (2018) illustrated in Table 2.1, clearly show that the net carbon-saving potential of plastic waste pyrolysis is much greater than

that of incineration or landfill. In plastic waste pyrolysis, oil-based products are produced, and the transportation and processing stages to produce oil are responsible for a large share of GHG emissions. However, the produced oil displaces fossil-fuel-based oil, resulting in GHG displacement that is greater than the emitted GHGs. The net GHG emissions of landfill are greater than those of pyrolysis but less than those of incineration. The main GHG emissions from landfill arise from the degradation of organic contamination present in plastic waste. Also, plastic waste dumped in landfills is associated with the loss of resources that could be used as feedstock to produce value-added products. In the case of incineration of contaminated plastic waste, net GHG emissions are the greatest compared to the other options. Hence, pyrolysis of MSPW should be prioritized over incineration and landfill which lead to losses of valuable resources, a linear economy principle, and greater environmental concerns (Davidson et al., 2021).

Table 2.1. Comparison of the carbon-saving potential of plastic waste pyrolysis, incineration, and landfill.

	Input, CO ₂ -eq per tonne plastic waste	Transportation, CO ₂ -eq per tonne plastic waste	Processing, CO ₂ -eq per tonne plastic waste	Displacement, CO ₂ -eq per tonne plastic waste	Net emissions, CO ₂ -eq per tonne plastic waste
Plastic waste pyrolysis	13	197.2	55.6	-425.5	-159.7
Plastic waste incineration	-	15.1	2,408	-565.5	1857.6
Plastic waste landfill	-	15.1	55.7	-	70.8

2.5. Pyrolysis-Based MPW Management Systems

Pyrolysis is the process whereby waste undergoes thermal treatment in the absence of oxygen/air breaking down polymers and monomers into smaller hydrocarbon molecules in the form of three main products (i.e. oil, gas and solid residue) (Ragaert et al., 2017, Chen et al., 2014b, Davidson et al., 2021). Despite the fact that pyrolysis is one of the most heavily researched technologies for resource recovery from plastic waste (Davidson et al., 2021) and is a quite commercially mature technology (Jeswani et al., 2021), there are few plastic pyrolysis plants worldwide (Jeswani et al., 2021). Typically, pyrolysis-based MPW management systems comprises collection and transportation of waste, sorting, pre-treatment of feedstock, pyrolysis, and purification of received products (Yuan et al., 2022), and all these processes involved in the systems are illustrated in Figure 2.1. Detailed discussions about these processes can be found in subsections 2.5.1, 2.5.2, and 2.5.3.

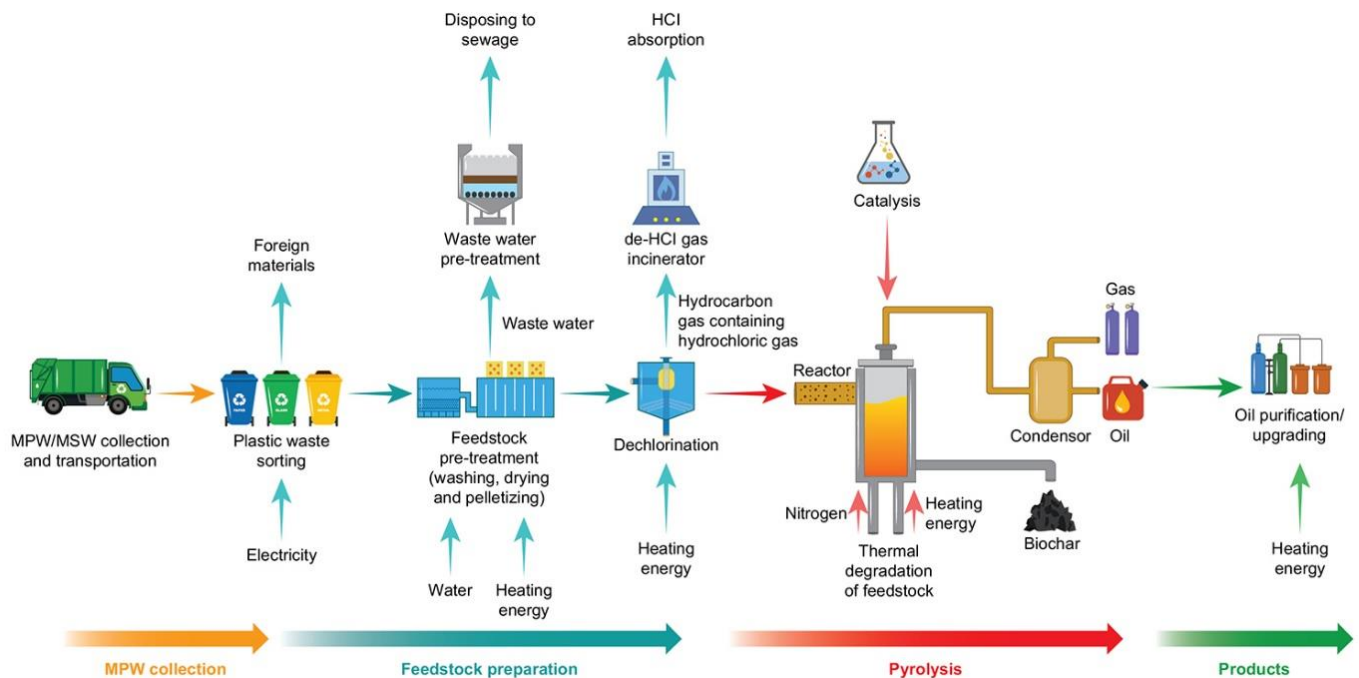


Figure 2.1. An illustration of pyrolysis-based plastic waste treatment systems (Biakhmetov et al., 2023).

2.5.1. MPW Pretreatment

The main purpose of the pretreatment stage is to prepare the MPW feedstock for the primary thermochemical conversion process. One of the key factors that could adversely affect the thermochemical conversion process is the presence of contamination or additives in the MPW. To address these issues, MPW is typically washed, dried, or subjected to low-temperature pretreatment to remove additives such as chlorine. These methods are described in detail in sub-sections 2.5.1.1 and 2.5.1.2.

2.5.1.1. Plastic washing

A sorting step is necessary to eliminate unwanted materials that can affect the quality of the production, and to ensure the optimal performance of the pyrolysis process (Jeswani et al., 2021). Despite undergoing a sorting stage, MPW is often still contaminated with organic matter such as soil and plants, and non-organic materials such as glue, dye, and labels that can adversely affect the pyrolysis process and product quality.

MPW normally goes through a washing process to remove contamination. For example, MPW of the province of Granada in Spain contains 10-14wt.% of dirt (Calero et al., 2018); contamination of organic origins can be effectively removed by a washing process with water at room temperature, whilst, to remove non-organic materials such as glue, paint, and fat, the washing process needs hot water (Calero et al., 2018). Calero et al. (2018) in their study used 10 litres of water to wash a kilogram of plastics for 30 min, and wastewater from the washing process needed to be treated before discharging into the sewage system to meet local legislation requirements: wastewater to be discharged into the sewage network of the Granada City Council has to show the chemical oxygen demand at not more than 1400 mgO₂/L (Calero et al., 2018). Sometimes, wastewater that has not been treated can be directly discharged into sewage if the dirt in the wastewater does not exceed certain limits (Calero et al., 2018).

Recommended temperature of water for hot washing of plastics was 60°C (Al-Sabagh et al., 2016, Awaja and Pavel, 2005).

2.5.1.2. Dryer

Thermal pre-treatment as a drying process is an important step to control the moisture content of feedstock for the pyrolysis process. Increasing moisture content in feedstock reduces the reaction temperature in the pyrolysis reactor, and consequently, the process of cracking of feedstock into lighter molecules can be incomplete or prolonged (Chen et al., 2014a, Kaewluan and Pipatmanomai, 2011, Li et al., 1999, Karamarkovic and Karamarkovic, 2010). For instance, Li et al. (1999) studied how moisture content affected pyrolysis time and found increasing moisture content of the wood-chips from 5.25 to 14.83% doubled pyrolysis time from 6 to 12 min. This revealed that the overall efficiency of the pyrolysis process was reduced with increasing moisture content of the feedstock. The moisture content of polymers in MSPW can vary depending on location, weather patterns, and polymer type. The moisture content of PE, PET, PP, PS and EPS in MSW sampled in the province of Granada, Spain, has been found to be 11.78 wt%, 8.9 wt%, 1.58 wt%, 20.98 wt% and 16.1 wt%, respectively (Calero et al., 2018). The moisture content of MPW needs to be analysed to define the optimal parameters for the drying process.

2.5.1.3. De-chlorination

In addition to the contaminants that can be removed by the washing and drying processes, polymers can contain chemical additives that are used to improve certain physical characteristics (e.g., tensile strength, plasticity, fire-resistance, etc.) of plastics and the chemical contaminations of such can negatively affect the pyrolysis process. One of the widely used additives is chlorine, which is mainly added to produce fire-resistant plastics. The PVC polymers used for packaging have a high chlorine content (Wang et al., 2020). The pyrolysis of plastics containing chlorine produces chlorinated hydrocarbon molecules, which causes

problems with corrosion and making oil more halogenated (Qureshi et al., 2020). Thermal pre-treatment of polymers at low temperature before feeding into the pyrolysis reactor can be used to de-chlorinate the feedstock (Wu and Williams, 2013, Fukushima et al., 2009). In the pre-treatment process, plastic waste is melted in a low-temperature treatment reactor operating at temperature range 300-330°C, and then, chlorine containing gases are evaporated (Fukushima et al., 2009). Hydrocarbon gases containing hydrochloric gases separated by evaporation at the low temperature are pumped into the de-HCl gas incinerator for combustion to reclaim hydrochloric acid (Fukushima et al., 2009). The use of the dichlorination step depends on the concentration of chlorine in plastics. Some pyrolysis reactor designs are able to tolerate a high concentration of chlorine, up to 35% (Haig et al., 2018).

2.5.2. Thermochemical Conversion Process

After the pre-treatment steps to remove unwanted contaminants, the plastic waste feedstock is fed into the pyrolysis reactor, where the feedstock is thermally decomposed into highly saturated hydrocarbon vapor in the absence of air/oxygen (Jeswani et al., 2021, Chen et al., 2014b). This process requires a significant amount of heating energy to drive the thermal degradation of plastics. Various energy sources can be used depending on the setup and the desired product qualities, such as electricity, fossil fuels, or produced pyrolysis gas. After the pyrolysis reactor, the condensable gases contained in vapour are collected in the form of oil via condensation while the remaining incondensable gas is collected as pyrolysis gas (Jeswani et al., 2021). Inside the pyrolysis reactor, nitrogen is used as an inert gas to purge and to replace air/oxygen to avoid feedstock oxidation (Maniscalco et al., 2021, Anene et al., 2018). The oil and gas produced does need some conditioning to reach the desired quality by various forms of purification, for example, distillation (Fukushima et al., 2009). Heavy oil with unwanted matter content can be upgraded by thermal treatment with catalysts to gasoline and diesel-like

products with low chloride and high alkane and aromatic contents (Lopez-Urionabarrenechea et al., 2015).

Various process parameters can be adjusted to achieve the desired yield and quality of products (oil, gas, and solid residues) (Sharuddin et al., 2016). A high proportion of oil and gas can be produced from the same feedstock, but the specific product output depends on the selected process parameters. For example, increasing the temperature enhances the yield of gas products while reducing the yield of oil products. The selection of process parameters also depends on the properties of the plastic feedstock. For instance, plastic feedstock with high volatile matter favours the production of more oil. If gas is the desired product from such feedstock, higher temperatures can be applied, or specific catalysts can be used in the pyrolysis process. In the following subsections, key process parameters (reactor type, temperature, residence time, pressure, and catalysts) are discussed in detail. A summary of MPW pyrolysis plants operating globally is provided in Table 2.3, along with a discussion of their key process characteristics and setups.

2.5.2.1. Reactor

One of the main factors that could affect the quality of products and their yields is reactor type. There are various types of reactors that can be used to pyrolyze MPW, namely fixed bed, fluidized bed, rotary kiln, microwave, batch or semi-batch, plasma pyrolysis reactors, and so forth. Fluidized bed, a fixed-bed, batch, the rotary kiln, and semi-batch reactors should be highlighted as they are widely used on a commercial scale due to either their very simple designs or their efficiencies. Fixed-bed reactors have a simple design and are usually operated at lower temperatures, which is more suited to the production of liquids, but they have the disadvantage of poor heat transfer. Fluidized bed reactors are relatively suitable to deal with materials such as MPW, which is a poor heat conductor, as the fluidization serves to improve heat transfer between plastic particles (Kaminsky et al., 2004). This contributes to improved

homogenization of the temperature inside the reactor and allows for a rapid heating rate, which allows for reduced residence time and, consequently, a reduction in the formation of residue and increased production of lighter hydrocarbons (Singh et al., 2019). Despite fluidized bed reactors having numerous advantages, they do have issues about defluidization as a result of the agglomeration of molten MPW feedstock (Dai et al., 2022). This reduces both the quality of products and the efficiency of thermal conversion process. Conical spouted bed reactors, which notably have a more complex design, can be used to minimize the defluidization issue.

For batch reactors, MPW is fed into the reactor prior to the pyrolysis process, and products are removed after complete thermal conversion (Serra et al., 2022). Semi-batch reactors are not completely closed systems, as are the batch reactors, as reagents or products can be added or removed while the pyrolysis process is ongoing (Serra et al., 2022). The main disadvantages of the reactors are that (a) feedstock cannot be continuously fed into the reactors, and there is an issue about system scale-up, and (b) poor heat transfer (Dai et al., 2022, Inayat et al., 2021, Lopez et al., 2017). However, the issue with poor heat transfer can be minimized by installing a stirrer inside the reactors.

Rotary kiln reactors also see widespread use due to its easily adjustable parameters such as residence time, temperature, and so forth. However, heating energy is usually transferred from the reactor walls to the plastic particles inside the reactor, resulting in issues regarding the homogenization of the temperature inside the reactor. This can cause overcracking or incomplete cracking of hydrocarbon chains, which negatively affects the product quality. Metal or ceramic balls can be loaded inside the reactor to minimize this issue (Dai et al., 2022).

Many recently developed reactors can be used for plastic waste pyrolysis, but most of them have not been well-studied. For example, researchers have significant interest in microwave technology as it shows advantages such as rapid heating and minimal energy loss

(Fernández et al., 2011). However, the efficiency of the pyrolysis process in microwave reactors depends on the dielectric properties of the feedstock, which are typically low for plastic waste. The primary limitation to the widespread use of microwave reactors, compared to other reactor types, is the lack of sufficient data (Sharuddin et al., 2016). In this subsection, reactor types that are widely used in plastic pyrolysis and have adequate supporting data are discussed. While all of these reactors are actively used in laboratory-scale experiments, fluidized-bed, fixed-bed, batch, rotary kiln, and semi-batch reactors are also found on an industrial scale. These reactors are favoured for their simple design and efficiency, which likely contribute to their widespread adoption in industrial applications.

2.5.2.2. Temperature

Plastics consist of long hydrocarbon chains, which are broken down into shorter chains during the pyrolysis process. This process requires heating energy, and the temperature reflects the level of heating energy inside the pyrolysis reactor. Hydrocarbon molecules are held together by Van der Waals forces between carbon atoms, and thermal energy is required to overcome these weak intermolecular forces, resulting in the breaking of intermolecular bonds (Sobko, 2008).

The thermal decomposition reactions of polymer chains inside a pyrolysis reactor can be adjusted by temperature. It is worth noting that different plastic types exhibit varying decomposition behaviours. MPW typically contains six main types of plastics: LDPE, HDPE, PP, PS, PVC, and PET. Thermogravimetric analysis and derivative thermogravimetric analysis curves are commonly used to study the thermal decomposition of plastic waste. The former shows weight change over time and temperature, while the latter displays peaks that reflect to specific stages of weight loss (Kumar and Singh, 2011).

In the studies by Chin et al. (2014) and Marcilla et al. (2009), it was observed that HDPE and LDPE begin thermal decomposition at 378-404°C and 360-385°C, respectively, and fully decompose at 500-540°C. PET and PP show similar decomposition behaviour in the range of 400-500°C (Çepelioğullar and Pütün, 2013, Aboulkas and El Bouadili, 2010). In the case of PVC and PS, they have a lower starting point compared to other plastic types. The temperature ranges for the thermal decomposition of PVC and PS are 220–520°C and 350–500°C, respectively (Çepelioğullar and Pütün, 2013, Sharuddin et al., 2016).

Most studies highlight that, in terms of the decomposition efficiency of mixed plastic waste and obtaining products with appropriate quality, 500°C is the optimal temperature (Lopez et al., 2011, Sharuddin et al., 2016). Most plastic pyrolysis plants operate within the range of 400-500°C (Haig et al., 2018), as shown in Table 2.3, where most plants producing liquid product operate at temperatures below 500°C. Despite different plastic types having varied thermal decomposition behaviours as described above, this temperature range is optimal for their complete conversion into liquid and gaseous hydrocarbons.

2.5.2.3. *Catalysts*

In the plastic pyrolysis, catalysts can be used to speed up the chemical reactions that occur during the cracking of polymer chains. Choosing an optimal catalyst for MPW pyrolysis on an industrial scale is essential as the MPW pyrolysis plant requires a large amount of catalyst. To date, many types of catalysts have been developed to deal with plastic pyrolysis such as ZSM-5 (Mangesh et al., 2020b), Ziegler-Natta (Kumagai and Yoshioka, 2016), HZSM-5, FCC, HY zeolite (Wang et al., 2021) and MCM-41. In particular, mesoporous molecular sieve catalysts are widely used for polymer pyrolysis. The main difference between mesoporous molecular sieve catalysts and other forms of catalyst is in their topology, as mesoporous molecular sieve catalysts have an ordered pore structure. Also, it is worth noting existing catalysts have been

modified by for example, the impregnation of transition metals into catalyst structures to improve their catalytic performance.

Using catalysts in plastic waste pyrolysis offers several advantages, as described below:

(1) Adjustment of the yields of products. Selecting catalysts based on their pore structure and pH for the pyrolysis process helps to control the yields and distribution of pyrolysis products (Pan et al., 2021). For example, using certain acid catalysts such as HY, H β , HZSM-5, and HUSY zeolites enhances the quality of the resultant oil (Aguado et al., 2008, Chen et al., 2020, Elordi et al., 2009, López et al., 2011b, Lopez et al., 2017, Marcilla et al., 2009, Serrano et al., 2012). Anene et al. (2018) compared oils received from the non-catalytic and catalytic pyrolysis of HDPE, LDPE, PP, and a mixture of LDPE and HDPE in the presence of zeolite-type catalysts in a laboratory-scale batch reactor at 460°C. The oil produced from the pyrolysis in the presence of zeolite-type catalyst mainly contained gasoline fraction carbons (C₇-C₁₂), and no diesel fraction (C₁₃-C₂₀) or heavy fraction (C₂₁-C₄₀) as would otherwise be gained from non-catalytic pyrolysis (Anene et al., 2018).

(2) The formation of undesirable substances during polymer pyrolysis can be inhibited or reduced through the choice of catalyst. For example, ZSM-5 is effective at reducing the amount of solid residue, sulphur, nitrogen, and phosphorous in the resultant oil (Miskolczi et al., 2009).

(3) Increased efficiency of the pyrolysis process. The presence of a catalyst during the pyrolysis process accelerates chemical reactions and the decomposition of polymers as the participation of the catalyst reduces the activation energy of the associated reactions. For example, Miskolczi et al. (2006) found that the presence of FCC, ZSM-5, or clinoptilolite in the pyrolysis of polymers can reduce the activation energy by 40 kJ/mol. This inevitably

increases the conversion rate of MSW, and which usually proceeds at a lower temperature than non-catalytic pyrolysis.

However, there are also some disadvantages associated with using catalysts in plastic waste pyrolysis:

(1) Deactivation of catalysts. After the pyrolysis process, deactivation occurs due to the deposition of coke on the surface of the catalysts (López et al., 2011c). The catalysts with the strong acid sites and micropores promote greater deactivation process (Chen et al., 2021, Huang et al., 2009). For example, zeolites, which are considered highly acidic catalysts, are mainly deactivated due to acid-site poisoning (Argyle and Bartholomew, 2015, Bibby et al., 1992, Magnoux et al., 1987, Nakasaka et al., 2015). Another way to minimize the problem of deactivation of the catalyst caused by deposition of coke is to reduce its formation during pyrolysis. Typically, deactivated catalysts need to be regenerated or replaced by fresh catalyst, which in both cases will clearly result in additional costs (López et al., 2011a). Another way to minimize the deactivation issue is to select the catalyst based on its topology (shape of selectivity) (Castano et al., 2011); for example, HZSM-5 has pores like channels, which prevent the entry of bulky coke molecules into pores, maintaining its catalytic activity for longer (Schirmer et al., 2001).

(2) Additional expenditure for catalysts. Despite benefits such as better product selectivity, lowering the activation energy of polymers, and saving thermal energy, additional costs are associated with the purchase, regeneration, and disposal of catalysts. To make catalytic pyrolysis more attractive, widely available, and cheap, alternative catalysts such as clay or fly ash have been studied.

Plastic pyrolysis plants globally producing diesel or other liquid products typically operate in a non-catalytic pyrolysis mode, as shown in Table 2.3. This is likely because the use

of catalysts often leads to excessive cracking of polymers, resulting in an increased production of gaseous products. In these plants, the specific types of catalysts used are not mentioned, making it challenging to analyse the details comprehensively. Furthermore, as noted earlier, a large quantity of catalysts is required for plastic pyrolysis, which significantly increases costs.

The catalysts that can be used in MPW pyrolysis is illustrated in Table 2.2. Some catalysts could favour liquid formation, and some could be used to produce more gas or char. For example, zeolite or clay-based catalysts recommended themselves in producing liquid, but zeolite catalysts promote the production of a high-quality liquid containing diesel or gasoline range carbon such as lighter aliphatic hydrocarbons (Serra et al., 2022). Also, zeolite catalysts such as FCC or ZSM-5 have been widely used in oil and gas industry since the last century, and currently they are popular catalysts to pyrolyze plastic waste (Fadillah et al., 2021). It is worth noting that despite both, zeolite and clay-based catalysts being desirable to receive liquid, the use of zeolite catalysts results in a formation of a higher coke and lower oil than clay-based catalysts due to their acidic nature (Hafeez et al., 2019, Manos et al., 2001, Serra et al., 2022). Clay-based catalysts usually need to be modified to produce a high-quality oil (Serra et al., 2022).

Table 2.2. Main catalysts used in MPW pyrolysis.

Product(s) favoured	Catalyst	Key findings
They are preferable to produce an increased amount of oil.	Clay-based catalyst	<ul style="list-style-type: none"> Made from a cheap abundant raw material (Budsareechai et al., 2019, Patil et al., 2018). Catalytic performance not good as widely used zeolite catalysts (Manos et al., 2001).
	ZSM-5 and HZSM-5	<ul style="list-style-type: none"> HZSM-5 exhibited greater ability to reduce coke formation than other zeolites catalysts, which is important to prolonging its life cycle (Garforth et al., 1997).
	Y Zeolite	<ul style="list-style-type: none"> Deactivated faster than other zeolite catalysts due to active coke formation (Onwudili et al., 2019).

		<ul style="list-style-type: none"> Oil produced contains increased proportions of aromatics such as benzene and toluene (Onwudili et al., 2019).
	MCM-41	<ul style="list-style-type: none"> Promote the production of the oil containing more gasoline-range hydrocarbons (Ma et al., 2017).
	FCC	<ul style="list-style-type: none"> Obtained by combining Y zeolites with alumina-silica (Degnan, 2000).
	Fly ash catalysts	<ul style="list-style-type: none"> Cheap catalysts as they are the by-products of <i>e.g.</i>, pulverised coal combustion (Ram and Masto, 2014). Lower catalytic performance than zeolite and metal-based catalysts (Singh et al., 2020).
	Red Mud	<ul style="list-style-type: none"> An industrial waste from alumina production (Álvarez et al., 1999, Eamsiri et al., 1992, Llano et al., 1994). Lower catalytic performance than zeolite and metal-based catalysts (de Marco et al., 2009).
They are preferable to produce an increased amount of gas.	Metal-based catalysts	<ul style="list-style-type: none"> Ni-based catalysts are common metal-based catalysts to produce hydrogen-rich gas due to their high catalytic performance compared to Fe, Co and Cu-based catalysts (Acomb et al., 2016, Aupretre et al., 2002). Main issue being deactivation due to coke deposition (Karimi et al., 2021, Prabu and Chiang, 2022). Fe-based catalysts produce higher yields and quality of carbon nanotubes than other widely used metal catalysts (<i>e.g.</i>, Ni, Co, and Cu) (Acomb et al., 2016, Liu et al., 2013). Polyolefin plastics are preferred to produce purer and cleaner carbon nanotubes and higher yields of hydrogen (Hernadi et al., 2000).

2.5.2.4. Residence time

Residence time refers to the average duration volatile particles spend in the pyrolysis reactor and is one of the main factors influencing product yields and quality. The longer the residence time, the more lighter, thermally stable, and non-condensable hydrocarbon molecules are

produced (Ludlow-Palafox and Chase, 2001). This means that increasing the residence time enhances the conversion rate of heavier molecules into lighter ones. Additionally, it is worth noting that the impact of residence time on product yield is constrained by the pyrolysis process temperature. If the reactor does not reach a critical temperature, the residence time may have minimal effect on product yield. For example, in study by Mastral et al. (2002), increasing the residence time from 0.64 to 2.6 s had no significant effect on product yields when the pyrolysis temperature was below 685°C. Thus, residence time should be carefully adjusted based on the pyrolysis temperature to achieve optimal product yields.

2.5.2.5. Pressure

Most lab-scale and industrial pyrolysis plants, as described in Table 2.3, work at atmospheric pressure. Nevertheless, several studies have assessed the impact of pressure on product yields and quality. Generally, the effect of pressure on product distribution is constrained by temperature, similar to the effect of residence time discussed above. Pressure has a more significant impact at lower pyrolysis temperatures than higher ones. For example, Murata et al. (2004) found that non-condensable hydrocarbons increased from 6 wt% to 13 wt% at 410°C, whereas the increase was less significant, from 4 wt% to 6 wt%, at 440°C when pressure was raised from 0.1 MPa to 0.8 MPa in HDPE pyrolysis. Consequently, it is recommended to increase pressure in plastic pyrolysis processes conducted at lower temperatures as it has a greater effect on product distribution compared to pyrolysis at higher temperatures.

Table 2.3. Overview of MPW pyrolysis plants operating globally: process characteristics and setups.

Pyrolysis plant	Location	Feedstock	Products	Capacity	Operation temperature	Process type (Catalytic/Non-catalytic)	Residence time	Operating pressure	Reference
Promeco	Italy	80 wt% plastic, with the remainder being contaminants and other materials	Diesel/gasoline	-	350°C	Non-catalytic pyrolysis	15-30 mins	-	(Promeco, 2024)
Plastic2Oil	USA	Mixed plastic	70 wt% diesel and 30wt% gasoline	7,000 tonnes of plastics per year	Low operating temperature	-	-	-	(Plastic2Oil, 2024)
Plastic Advanced Recycling Corporation	USA	Mixed plastic	50–70 wt% crude oil, 15–25 wt% gas, and 15–25 wt% residue	10,000 tonnes of plastics per year	<500°C	Catalytic pyrolysis	-	Atmospheric pressure	(Plastic Advanced Recycling Corp, 2024)
Niutech Environment Technology Corporation	China	Scrap tyre and mixed plastic	Diesel/gasoline and heavy oil	-	Low operating temperature	-	-	-	(Niutech Environment Technology)

									Corporation, 2024)
Klean Industries	Canada	Mixed plastic	70 wt% diesel, ±10 wt% gas, and ±30 wt% monomers	3,500 tonnes of plastics per year	Low operating temperature	Non-catalytic pyrolysis	-	-	(Industries, 2024)
GreenMantra Technologies	Canada	Mixed plastic	Waxes, lubricants, and crude oil	-	Low operating temperature	-	-	-	(GreenMantra Technologies, 2024)
Quantum Lifecycle	Canada	Mixed plastic	Diesel	6,000 tonnes of plastics per year	-	Non-catalytic pyrolysis	-	-	(Quantum Lifecycle, 2024)
Agilyx	USA	Mixed plastic	80 wt% crude oil, 12 wt% gas and 8 wt% residue	3,500 tonnes of plastics per year	593.3°C	Non-catalytic pyrolysis	5 hours per batch	Atmospheric pressure	(Agilyx, 2024)

2.5.3. In-line Technologies Applied after Pyrolysis and the Products Obtained from Them

Pyrolysis of MSPW produces oil, gas, and char (Benavides et al., 2017). The quality or distribution of products from the pyrolysis of plastic can be adjusted by the appropriate selection of process parameters (pyrolysis reactor, catalyst, residence time, and pressure), as discussed in subsections 2.5.2.1 to 2.5.2.5 (Qureshi et al., 2020). For example, oil with similar quality to diesel can be received (Santaweesuk and Janyalertadun, 2017), but there are still certain limitations to completely replacing conventional diesel. The way in which pyrolysis product can be applied depends on their quality and in-line technologies applied after the pyrolysis to upgrade products obtained. In this section, the application of products received from the pyrolysis of MPW is discussed, and Figure 2.2 is used to help our understanding of such. Also, in-line technologies such as oil distillation and gas synthesizing that can be used to upgrade pyrolysis oil and gas are discussed, respectively.

The gas obtained from the pyrolysis of MPW is usually combusted to generate power and heat energy (Haig et al., 2018, Kanattukara et al., 2023). The heat energy can be used for the thermal decomposition of feedstock in a pyrolysis reactor. However, pyrolysis gases can contain certain impurities, and consequently, an upgrade or cleaning process needs to be used to obtain high-quality gas (Huang et al., 2022). Another way to obtain upcycled and more valuable products from plastic waste is the synthesis of carbon nanotubes and hydrogen-rich gas from hydrocarbon volatiles obtained from plastic waste pyrolysis (Jiang et al., 2022, Wang et al., 2023b). The pyrolysis setups and technologies for producing hydrogen-rich gas are discussed in Subsection 2.5.3.2.

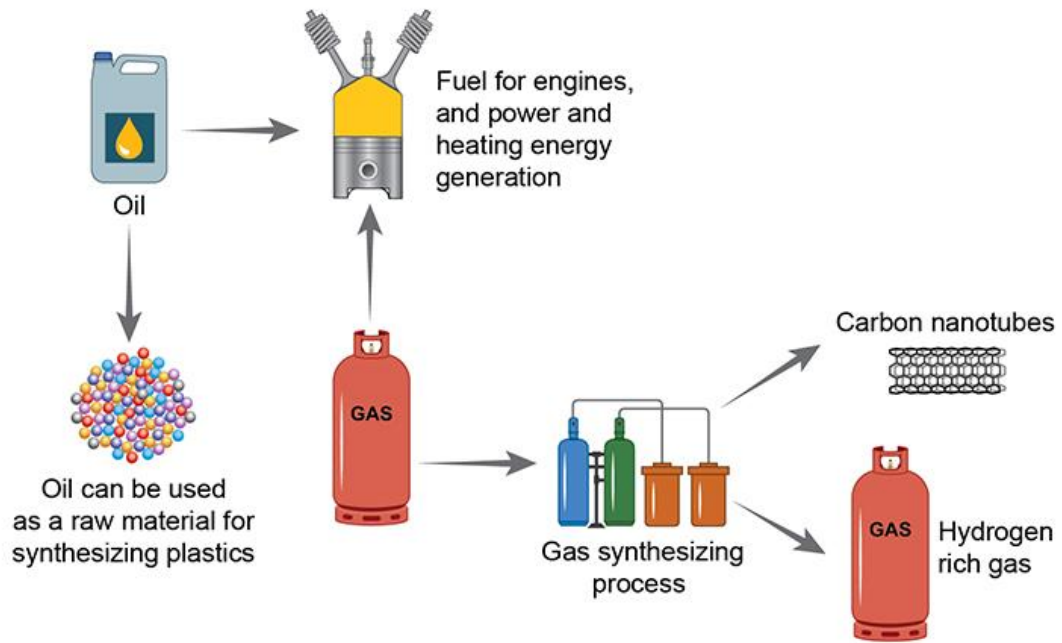


Figure 2.2. Applications of products received from the pyrolysis of MPW.

2.5.3.1. Production of diesel-range oil from pyrolysis crude oil

Liquid oil and wax produced from plastic pyrolysis can be stored more effectively than other energy resources, which gives the freedom to use it as an energy resource (Ikäheimo et al., 2019). Also, it has a higher heating value than other fuels, at 42.1–49.4 MJ/kg (Kunwar et al., 2016). The pyrolysis oil produced from plastic waste pyrolysis, after undergoing an upgrading process (distillation), can be blended with conventional diesel and gasoline, depending on its properties, and then used as fuel for engines.

The pyrolysis oil produced cannot be used as a drop-in fuel for diesel engines as it contains a wide range of hydrocarbons (C1-C22), and therefore it is typically considered crude oil. A distillation process is applied to separate diesel-range hydrocarbons from the crude oil, resulting in what is defined as diesel-range plastic pyrolysis oil. The remaining by-products from the plastic pyrolysis oil distillation process are referred to as the residue of the distillation process or lube oil cuts. The operational principle of the pyrolysis oil distillation process is

simple: diesel-range hydrocarbons are separated from non-diesel-range hydrocarbons based on differences in their boiling points.

Although the oil obtained from the distillation contains diesel-range hydrocarbons, it can only partially replace conventional diesel. Most existing studies recommended blending pyrolysis-based diesel with conventional diesel in a ratio of up to 15-20 wt.% depending on the properties of the plastic-based diesel (Das et al., 2020, Rajak et al., 2022, Januszewicz et al., 2023, Mangesh et al., 2020a). The mixed plastic-based and conventional diesel must meet certain standards to be used, in terms of e.g., flash point, calorific value (35.8 to 38.6 MJ/L), cetane number (40 to 55), viscosity, aromatic content, boiling temperature (163-357°C), and others (Wexler et al., 2005).

The study by Faisal et al. (2023a) compared conventional diesel, crude pyrolysis oil, and distilled pyrolysis oil in terms of key properties essential for meeting fuel quality standards. The results are presented in Table 2.4. The calorific values of both crude pyrolysis oil and distilled pyrolysis oil are within the range observed for conventional diesel. However, in many studies, the calorific value of conventional diesel is higher than that of crude oil derived from plastic pyrolysis (Mani et al., 2011). The flash points of crude and distilled pyrolysis oils are also comparable to those of conventional diesel. Notably, the flash point of pyrolysis oil can be easily adjusted through the distillation process, which separates carbon fractions with the required boiling points.

The kinematic viscosity of diesel is an important property, as it defines the fuel's ability to flow easily and its effectiveness in forming a combustible mist when injected into a diesel engine (Faisal et al., 2023c). If the kinematic viscosity exceeds the required range, it can lead to issues such as incomplete combustion and excessive soot and smoke production due to poor fuel atomization (Chandran et al., 2020). As shown in Table 2.4, the kinematic viscosity of

crude pyrolysis oil does not meet the standards for conventional diesel fuel, whereas the kinematic viscosity of distilled pyrolysis oil aligns with the required specifications.

The most critical property for fuel ignition in diesel engines is the cetane number (Lapuerta et al., 2008, Atabani et al., 2012). The pyrolysis diesel may contain unsaturated hydrocarbons, which have lower cetane numbers, resulting in slower ignition and poorer combustion performance compared to saturated hydrocarbons (Mangesh et al., 2020b, Mangesh et al., 2020a). In table 2.4, the cetane numbers of distilled pyrolysis oil fall within the range of conventional diesel, unlike those of crude pyrolysis oil. Thus, the mixing ratio needs to be adjusted to ensure that the allowed content of unsaturated hydrocarbons in the fuel is not exceeded.

Table 2.4. Comparison of properties of conventional diesel, crude pyrolysis oil, and distilled diesel-range pyrolysis oil.

Property	Conventional diesel	Crude pyrolysis oil	Distilled diesel-range pyrolysis oil
Calorific value, MJ/kg	42-46	44-45.2	45.8-46.8
Flash point, °C	55-61.5	<20	63-77
Kinematic viscosity, mm ² /s	1.9-4.5	1.32-1.75	2-3
Cetan numbers	>40	~30	~50

One of the primary products of plastic waste pyrolysis is crude oil, a valuable fuel with a high heating value compared to other fuels. However, it cannot be used as a drop-in fuel because it typically contains a high proportion of heavy hydrocarbon fractions. To address this, plastic pyrolysis crude oil is distilled to separate diesel-range hydrocarbon fractions based on their boiling points. Key properties such as flash point, calorific value, kinematic viscosity, and cetane numbers of distilled plastic pyrolysis oil are comparable to those of conventional diesel.

Despite its similarities, distilled pyrolysis oil cannot fully replace conventional diesel. It is typically blended with conventional diesel at ratios of up to 15-20%, as its slightly higher cetane numbers may lower combustion efficiency in diesel engines. Therefore, distilled diesel-range plastic pyrolysis oil and conventional diesel must be blended at an optimal ratio to ensure the combustion performance of the blended fuel is not significantly affected.

2.5.3.2. Hydrogen and Carbon nanotubes production from

Plastic pyrolysis gas can be a resource for power and heat generation, or otherwise, some part of it can be returned to the pyrolysis system to produce the electricity and heating energy necessary for the pyrolysis of the polymers (Benavides et al., 2017). The calorific value of gas is relatively higher than other fuels, for example Kumagai and Yoshioka (2016) noted it was 50 MJ/kg. The most ideal polymers for the production of high-quality gas with high calorific value are PE and PP (Honus et al., 2018b, Honus et al., 2018a). The flammability limits of the gas produced from the pyrolysis of PE, PP, PS, and PVC are the same as the flammability limit of natural gas; PET, however, has high upper flammability limits.

Besides pyrolysis gas, a more valuable gaseous product—hydrogen-rich gas—can be obtained from plastic waste. Plastic waste is fed into a fast pyrolysis reactor, where it is converted into volatiles containing a wide range of hydrocarbon fractions, from light hydrocarbons (C1–C20) to heavy hydrocarbons (C21+) (Arregi et al., 2020). These volatiles then undergo synthesis to produce syngas, which can be achieved through three different methods, as outlined in Figure 2.3.

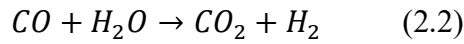
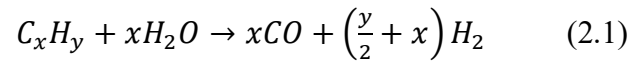
In the first method described in Figure 2.3, metal-based catalysts such as Ni/Al₂O₃ and Ni/Mn/Al are used to catalyse the conversion of hydrocarbon volatiles into syngas, which typically contains hydrogen and carbon monoxide (Li et al., 2023, Wu et al., 2014). Additionally, in this process, carbon nanotubes are produced as hydrocarbon volatiles

decompose and diffuse on the catalysts. This occurs when hydrocarbon molecules are broken down into elemental carbon and hydrogen gas in the presence of transition metals, with the carbon being deposited on the surface of the metal-based catalysts (Dai et al., 2023).

The carbon nanotubes obtained from the process can be used in various ways, from serving as a fuel for heating and electricity generation, attributed to their high carbon content, to becoming value-added materials due to their unique characteristics such as extraordinary strength and stiffness, relatively high electrical and thermal conductivity, and chemical stability (Inshakova et al., 2020). To comply with circular economy practices and maximize resource recovery, carbon nanotubes should be used as value-added materials instead of being employed as fuel for heating energy and electricity generation. A number of studies indicate that simple carbon nanotubes produced from waste can be utilized as reinforcement to LDPE, resulting in improved tensile and Charpy impact properties (Borsodi et al., 2016), in the automotive and construction industries, as well as in the production of lithium-ion batteries (Dagle et al., 2017). However, carbon nanotubes obtained from MPW termed crude carbon nanotubes as they contain undesired amorphous carbons or can be polluted with metal-based catalysts (Guo et al., 2007). Thus, they can be purified and then modified to acquire properties close to required property depending on the application purpose (Wang et al., 2022a). However, these additional processes, which involve upgrading carbon nanotubes, require significant resources, such as deionized water, acids, calcium oxide, and energy inputs. This substantially impacts the economic feasibility of such systems.

In the second way, instead of utilizing metal-based catalysts, steam is employed to convert hydrocarbon volatiles into syngas. The general chemical reactions for synthesizing hydrocarbon volatiles are represented by equations (2.1) and (2.2). Initially, hydrocarbon molecules react with steam, forming carbon monoxide and hydrogen. Subsequently, a portion

of the carbon monoxide undergoes the water-gas shift reaction, producing carbon dioxide and additional hydrogen.



In the third method, syngas is generated through the combined effects of metal-based catalysts and steam. Additionally, carbon nanotubes are produced, similar to the first method. However, the resulting carbon nanotubes often have defects, such as poor morphological characteristics and low purity, which make them a less favourable product (Wu et al., 2014).

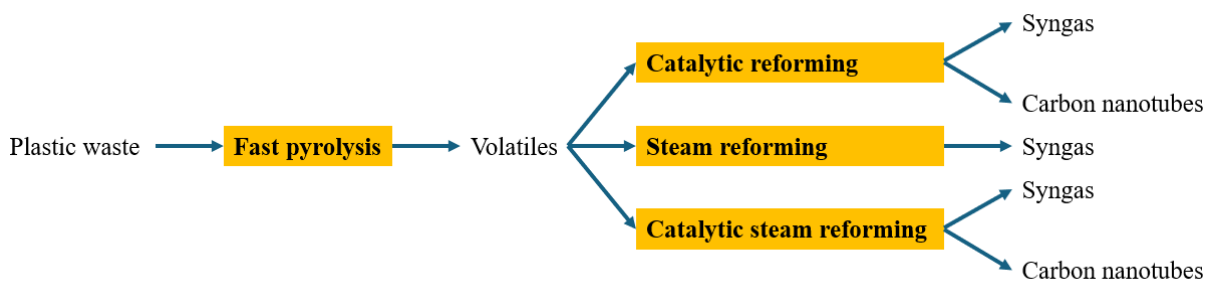


Figure 2.3. Methods for producing hydrogen-rich gas through pyrolysis-based processes from plastic waste.

In addition to diesel-range oil, gas is also produced from plastic waste pyrolysis, which can be used as a fuel for power and heat generation. Furthermore, syngas, often referred to as hydrogen-rich gas in many studies, can be produced from plastic waste by employing pyrolysis-based conversion technologies. Hydrocarbon volatiles obtained from the fast pyrolysis of plastic waste are synthesized to produce hydrogen-rich gas.

2.6. Present Life Cycle Assessment Studies on Pyrolysis-Based Conversion of Non-recycled Municipal Plastic Waste into the Diesel and Hydrogen

In general, MPW management systems can be deployed in either centralized or decentralized modes. The main difference between the two is regarding the scale and efficiency, which affect their environmental and economic performance. Recently, the number of comparative LCA studies of centralized and decentralized systems have been increased to define their relative environmental footprints (Quinteiro et al., 2020, Gupta et al., 2022). In many cases, centralized systems are preferable due to their better economic benefits, but they can nevertheless have a worse or better environmental performance than decentralized systems depending on several factors. To the best of our knowledge, there have been limited studies on the influences of system scales on the carbon footprints of diesel and hydrogen production from pyrolysis-based MPW treatment. The existing LCA of MPW pyrolysis and other waste management technologies focuses on large or centralized MPW. However, Pires Costa et al. (2022) mentioned in their study that large-scale centralized pyrolysis facilities should be compared with small-scale pyrolysis facilities built locally as there was still an argument as to how GHG emissions from transportation could affect the overall results. A large-scale waste pyrolysis facility is usually located some distance away from the city, and the density of plastic waste is low. In this case, the transportation of waste, pyrolysis products, and by-products for large-scale facilities may have a significant carbon footprint, as compared to small-scale facilities that can be located nearer to waste collection points.

The majority of existing studies have not considered the environmental burden of the end-of-life use of products resulting from plastic waste pyrolysis (Bora et al., 2020, Khoo, 2019). It is important to assess the quantity of products derived from plastic waste and the extent of the environmental burden/benefit that comes from using such products. Moreover, Pires Costa et al. (2022) highlighted that there were plenty of LCA studies where plastic waste

pyrolysis was compared with incineration and landfill. It is well known that plastic waste pyrolysis can achieve better environmental performance than these waste management methods (Krüger et al., 2020). For instance, as discussed in sub-section 2.4, the results of study by Haig et al. (2018), net GWP of incineration of one tonne of MPW is 1857.6 CO₂-eq per tonne plastic waste, whereas net GWP of diesel production via MPW pyrolysis is -159.7 CO₂-eq per tonne plastic waste. However, there is a knowledge gap in comparing the various types of plastic waste pyrolysis technologies with each other (Pires Costa et al., 2022).

2.7. Present Techno-Economic Studies on Pyrolysis-Based Conversion of Non-Recycled Municipal Plastic Waste into the Diesel and Hydrogen

In the available techno-economic assessment (TEA) studies related to fuel production from MPW pyrolysis, diesel, as one of the more widely used transportation fuels, has been compared with other fuels such as naphtha, ethanol, gasoline, *etc* (Haig et al., 2018). However, to the best of our knowledge, there are limited or no existing TEAs that comprehensively compare the economics of pyrolysis-based diesel and hydrogen production from MPW. Only a few TEA studies have assessed hydrogen production from plastic waste using pyrolysis-based technologies. For example, in study by Yi et al. (2024), the economic feasibility of hydrogen production from plastic waste pyrolysis-based processes was assessed, but it was not compared with the production of other fuels through pyrolysis-based processes for plastic waste. Similarly, in the study by Paneru et al. (2024), high-temperature pyrolysis (600°C) was applied to convert plastic waste into syngas, from which hydrogen was separated. The production cost of hydrogen from plastic waste was also determined. In these studies, only a few setups for pyrolysis-based processes were considered. However, there are many other configurations that can be applied to produce hydrogen, such as varying the temperature ranges, employing different setups for converting pyrolysis volatiles into hydrogen-rich gas, or using a wider range of catalysts. Exploring alternative setups for pyrolysis-based conversion technologies could

help identify optimal configurations for hydrogen production in more economically feasible ways. Additionally, these studies could be enhanced by incorporating models for transportation or CCS, which would provide more comprehensive results.

As mentioned in sub-section 2.6, waste management systems can be categorized as either centralized or decentralized, depending on system efficiency and scale. The techno-economic feasibility of pyrolysis-based diesel and hydrogen production from MPW should be affected by the scale of system. However, the extent of the influence of system scale on the feasibility does not exist yet. Furthermore, the influence of system scale is also influenced by product selection and transportation factors. Particularly, despite that waste transportation has little impact on the environment its cost can significantly affect the overall cost of waste management systems (Ascher et al., 2019). Therefore, it is important to incorporate accurate transportation modelling in the TEA of pyrolysis-based diesel and hydrogen production from MPW (Yadav et al., 2022).

In many TEA studies related to waste management, energy-intensive technologies are applied, which often have a significant carbon footprint (Fang et al., 2023, Lui et al., 2022a). These studies assess the use of CCS to evaluate the economic feasibility of waste management systems with CCS, especially when a carbon tax is applied. The findings vary, with some studies demonstrating economic feasibility, while others do not. For example, Lui et al. (2022a) stated that in systems using natural gas-based technologies for waste treatment, CCS combined with a carbon tax is not economically feasible due to the low cost of natural gas, which offsets the costs associated with GHG emissions. Conversely, the study by Geissler and Maravelias (2021) suggested that CCS can be economically viable if thermochemical conversion plants are scaled up.

Based on the discussion in the previous paragraph, maximizing the carbon-saving potential of pyrolysis-based diesel and hydrogen production from MPW requires considering CCS and its impact on economic feasibility through the application of a carbon tax (Fang et al., 2023, Lui et al., 2022a). Additionally, the scale of MPW pyrolysis plants should be evaluated to understand how it influences the integration of a CCS unit within the system.

The UK government implemented the UK Emissions Trading System (UK ETS) as a market trade measure in 2021, with its primary goal being to incentivize GHG reduction (UK Government, 2023). This is a newly implemented tool in the UK, and its effectiveness has not been well studied. MPW management systems utilizing thermochemical conversion technologies such as pyrolysis, gasification, etc., emit GHGs, and the economic motivation of these systems to capture carbon emissions should be assessed under schemes similar to the UK ETS. It is essential to compare the costs of employing UK ETS and other options in dealing with GHG emissions. This comparison could help define the optimal solution for the thermochemical conversion of NMPW to transportation fuels under the market situation.

Mass and energy balances of thermochemical conversion processes are typically employed to select and size equipment in cost-benefit analyses (Martins et al., 2023). For diesel and hydrogen production from MPW, mathematical modelling of the thermochemical conversion, in particular pyrolysis, is challenging due to the complexity of the reactions that occur during such processes and the large numbers of product components involved (Ismail et al., 2017). Aspen Plus is one of the widely used process modelling tools to simulate thermochemical conversion of different feedstocks and to calculate mass and energy flows. However, there are a very few studies that use Aspen Plus in the simulation of diesel and hydrogen production from MPW via pyrolysis-based conversion technologies, and indeed the majority of such are questionable regarding the reliability of their results. For example, in the study by Rodriguez et al. (2018), kinetic reaction constants of tire pyrolysis are used in the Aspen simulation of

MPW pyrolysis, though there are issues concerning the reliability of Aspen simulations in such circumstances. In the study by Al-Rumaihi et al. (2023), two RYIELD reactors were used to simulate the pyrolysis process; in the first reactor, non-conventional materials (polymer feedstock) were decomposed into conventional components based on the ultimate composition of the feedstock, whilst in the second reactor products were obtained based on the ultimate composition without using equilibrium reactions. These kinds of Aspen simulation are certainly questionable in terms of their reliability.

2.8. Multi-Objective Optimization of Chemical Recycling of Municipal Plastic Waste

The feasibility of waste management systems is typically assessed via LCA and CBA studies, which determine the environmental footprints and economic benefits of such systems, respectively (Afzal et al., 2023, Yadav et al., 2022). LCA and CBA studies cannot separately determine the most feasible systems. MOO (Multi-Objective Optimization) is currently the best approach to determining systems with delicately balanced environmental footprints and economic benefits (Wang et al., 2022b, Fang et al., 2024). It is particularly useful for addressing conflicting objectives, such as reducing GWP while increasing NPV, or resolving situations where these metrics yield contradictory results.

In MOO studies, Pareto-optimal solutions can be applied to define the states when each of the objectives, environmental and economic performance, cannot be improved without compromising the other (Musharavati et al., 2022). Figure 2.4 illustrates a set of solutions with objectives x and y . Solutions where x cannot be increased without decreasing y , or vice versa, are considered Pareto-optimal solutions. The line connecting all Pareto-optimal solutions is referred to as the Pareto curve.

TOPSIS or LINMAP approaches can then be applied to calculate the ideal value from the Pareto-optimal solutions (Li et al., 2020). TOPSIS ranks all Pareto solutions by evaluating their closeness to the ideal solution and their distance from the non-ideal solution. LINMAP, on the other hand, identifies the closest solution to the ideal by calculating distances in a space where each dimension represents a different objective.

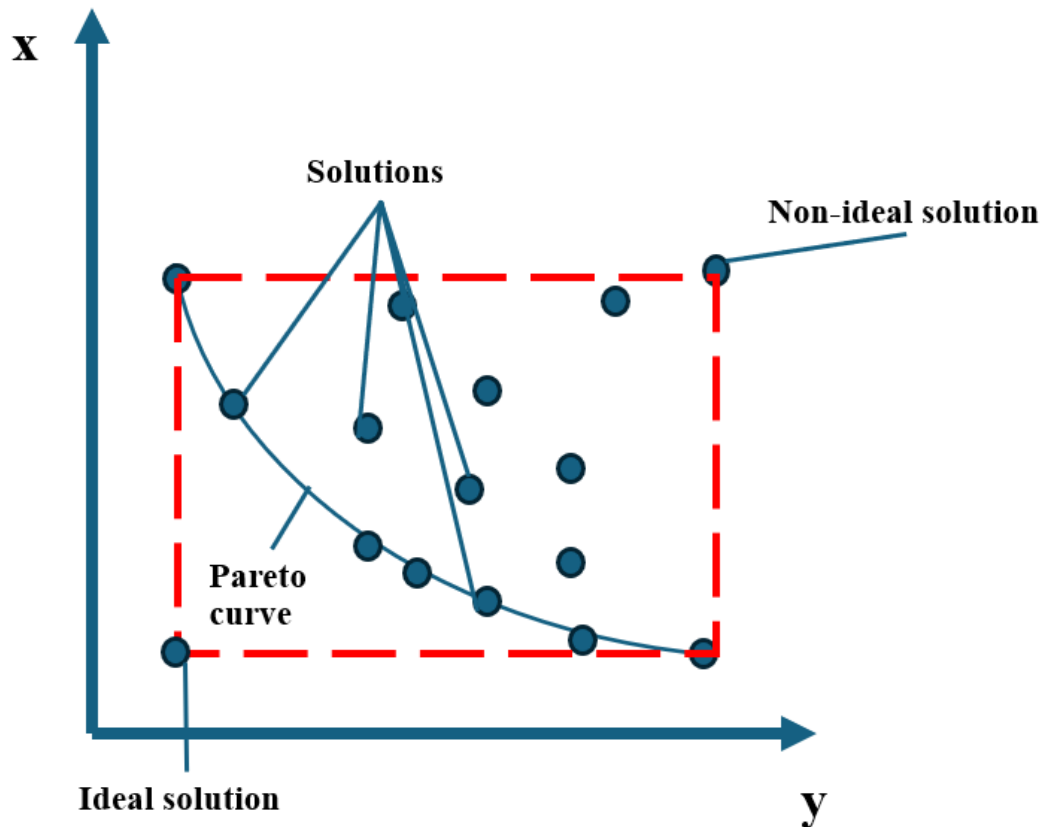


Figure 2.4. Pareto optimal solutions.

Several scenarios or solutions can be proposed for converting NMPW into diesel and hydrogen, with Pareto-optimal solutions identified to achieve balanced GWP and NPV outcomes. Among these Pareto-optimal solutions, the most favourable scenarios can be selected. Also, considering factors that have significant impacts on GWP and NPV results in the MOO study can provide a more inclusive and deeper understanding of the systems, and then define a general framework for system optimization.

2.9. Centralized and Decentralized Waste Management Systems

As described in Sub-section 2.6, waste management systems can be categorized by their scale and location as centralized large-scale and decentralized small-scale systems. Transportation plays a crucial role in defining the environmental and economic performance of these systems. Decentralized small-scale waste management facilities can be located near waste collection sources, which positively affects the economic feasibility of the systems and reduces the environmental burden associated with transportation. However, large-scale waste management facilities are generally more economically preferable. For instance, the cost of equipment per functional unit is lower for large-scale systems compared to small-scale waste management facilities. This is demonstrated in Table 4.2, where the equipment costs for large-scale and small-scale pyrolysis plants are compared.

Despite the advantages of centralized large-scale systems, decentralized systems could have specific benefits in the context of Glasgow. Decentralized small-scale systems could be located near existing material recovery or transfer stations, allowing feedstock to be directly supplied and supporting preprocessing activities (Glasgow City Council, 2025). Additionally, small-scale plants, unlike centralized ones, can be easily integrated into Glasgow's neighbourhoods due to their lower utility and land requirements.

In this study, hydrogen and diesel production from NMPW were considered. Hydrogen production in a local pyrolysis plant has advantages, such as proximity to local markets, which eliminates the need for long-distance transportation. Hydrogen transportation is particularly costly; for example, according to the Department for Energy Security & Net Zero (2023c), transporting 1 kg of hydrogen over 25 km costs approximately £4 for a truck with a 500 kg workload capacity. Furthermore, small-scale facilities can be easily adapted or adjusted based on local demand or feedstock supply.

To summarize, despite the economic advantages of centralized large-scale waste management systems, such as pyrolysis plants, over decentralized small-scale systems, the latter should still be considered due to their potential to be competitive. Key areas can be identified to reduce the environmental footprint and fuel production costs of decentralized systems.

2.10. Conclusion

Plastic is one of the most widely used materials worldwide due to its low production cost and unique properties, such as being lightweight, durable, versatile, and waterproof. Plastic production has increased 200-fold since the 1950s, and currently, half of the plastics produced are single-use. This means that after being used once, they typically end up as waste. Under the principles of the circular economy and the sustainable waste management hierarchy, the generated MPW needs to be recycled to prevent it from polluting the environment and to keep it within the economy.

MPW refers to plastic waste generated in urban or residential areas. It typically includes the following types of plastic: LDPE, HDPE, PP, PS, PVC, and PET. In many countries, particularly in well-developed nations, MPW is usually transported to Material Recovery Facilities (MRF) after collection. At these facilities, the most commonly recycled types of plastic, HDPE and PET, are separated and sent for mechanical recycling. The rest of MPW is often managed in unsustainable ways, such as incineration or landfilling, both of which are associated with resource loss and environmental pollution. Chemical recycling, particularly pyrolysis-based processes, can play a complementary role to mechanical recycling by increasing the amount of MPW returned to the economy and reducing the volume of MPW managed in unsustainable ways.

Pyrolysis is a thermochemical conversion process that converts feedstock into oil, gas, and solid products in the absence of air. It involves several key process parameters (reactor type, operating temperature, catalysts, residence time, and pressure) that can be adjusted to achieve desired product quality and yields. Plastic pyrolysis plants operating globally were analysed based on these key process parameters. It was observed that most of these plants produce diesel or other liquid products, operate at lower temperatures (<500°C), and utilize non-catalytic pyrolysis modes.

Diesel and hydrogen can be obtained from MPW pyrolysis, each involving distinct pyrolysis-based conversion technologies. Plastic pyrolysis produces crude oil, which must undergo an upgrading process, such as oil distillation. The distillation process separates diesel-range hydrocarbons from heavy hydrocarbons. Although pyrolysis-derived diesel has properties close to those of conventional diesel, it cannot fully replace conventional diesel. Many studies recommend blending pyrolysis diesel with conventional diesel at a ratio of 15–20%. For hydrogen production, hydrocarbon volatiles obtained from plastic pyrolysis are synthesized to produce hydrogen-rich gas. Hydrogen is then separated from this gas.

The main objectives of this study are to assess the carbon footprint and economic feasibility of diesel and hydrogen production from MPW using pyrolysis-based processes. LCA and TEA approaches are applied to achieve these goals. Notably, most existing LCA and TEA studies focus on comparing the environmental footprint and economic feasibility of pyrolysis-based plastic waste management systems with conventional methods such as incineration or landfilling. However, there are limited studies comparing different pyrolysis-based plastic waste management systems with one another, despite the variety of process parameters and setups that can be assessed. Furthermore, these studies could be expanded to incorporate additional factors for more comprehensive results. For instance, modelling the transportation

component, evaluating the effectiveness of the newly implemented carbon tax in the UK, or assessing the impact of the UK ETS could provide valuable insights.

LCA and TEA studies alone cannot independently identify the optimal system with balanced GWP and NPV results from various pyrolysis-based MPW management systems. MOO approach can be applied to determine the optimal systems that meet the condition where improvements in GWP or NPV cannot be achieved without compromising the other. Finally, methods such as LINMAP and TOPSIS can be utilized to select the best systems from these optimal scenarios.

Chapter 3 Comparing Carbon-Saving Potential of the Pyrolysis of Non-Recycled Municipal Plastic Waste: Influences of System Scales and End Products

In the previous chapter, the plastic waste crisis was discussed, and the role of pyrolysis was evaluated. Additionally, the production of hydrogen and diesel from NMPW through pyrolysis-based conversion technologies was described. Finally, the knowledge gaps in the present LCA, CBA, and MOO studies related to hydrogen and diesel producing systems from NMPW were identified.

In this chapter, the carbon footprints of centralized large-scale and decentralized small-scale pyrolysis-based conversion of NMPW into value-added resources are compared. The chapter aims to address objectives 1 and 3 described in subsection 1.2 and to fill the knowledge gaps outlined in subsection 2.6. Specifically, the transportation component of NMPW management systems was modelled and simulated to provide more reliable GWP results, rather than relying on general assumptions. Additionally, the GWP of all systems was determined using the LCA methodology. As mentioned in sub-section 1.4, this chapter is based on the paper published in the Journal of Cleaner Production (Biakhmetov et al., 2024).

3.1. Methodology

3.1.1. Scenario description

Glasgow is the fourth largest in the UK with a population of 614,520 in 2021 (Population UK, 2023). It is also the largest city in terms of waste generation: 258,941 tonnes of MSW or 408 kg/capita/year were generated in 2021 (Scottish Environment Protection Agency, 2023). MPW that is not suitable for mechanical recycling usually ends up in landfill or is sent to other countries, amounting around 15,000 tonnes. In this study, plastics that are

non-recycled or rejected by recycling processes are defined as a feedstock for pyrolysis systems.

Four scenarios are defined as illustrated in Table 3.1: C1, D1, C2, and D2. Scenarios C1 and C2 denote centralized plants, whilst scenarios D1 and D2 denote decentralized plants. The annual capacity of the centralized pyrolysis plant is ~15,500 tonnes of MPW, that is all non-recycled MPW generated in Glasgow is transported to this site for treatment. Overall, annual MPW generation in Glasgow is more than 21,000 tonnes, around 5,500 tonnes of which goes through mechanical recycling (Scottish Environment Protection Agency, 2023). The rest of NMPW is considered as feedstock for the centralized pyrolysis plant.

The capacity of the decentralised plants is set to be 3,300 tonnes per year, which corresponds to the capacity of typical small commercial-scale pyrolysis plants, as reported by (Haig et al., 2018). In scenarios C1 and D1, MPW transported to the plant is treated by pyrolysis to produce crude oil substitute, which is then distilled to produce oil containing diesel-range hydrocarbons. The main products in the C2 and D2 scenarios are hydrogen, carbon nanotubes and diesel, which are recovered by two-step pyrolysis-catalytic reforming in the presence of metal-based catalysts. Diesel and hydrogen produced from all scenarios are used as fuel for buses in Glasgow.

Table 3.1. Scenario description in terms of waste transportation, PtE technologies, product distribution and annual capacity.

	Scenarios			
	C1	D1	C2	D2
Waste transportation	MPW is collected and transported to a transfer station, where non-recycled MPW is separated and baled before being transported to the pyrolysis plant, which is located 100 km away from the transfer station.	MPW is collected and transported to the transfer station, where non-recycled MPW is separated and directly sent to the pyrolysis plant, which is located near the transfer station.	MPW is collected and transported to a transfer station, where non-recycled MPW is separated and baled before being transported to the pyrolysis plant, which is located 100 km away from the transfer station.	MPW is collected and transported to the transfer station, where non-recycled MPW is separated and directly sent to the pyrolysis plant, which is located near the transfer station.
PtE technologies	Pyrolysis + oil distillation	Pyrolysis + oil distillation	Two-step pyrolysis-catalytic reforming + pressure swing adsorption/oil distillation	Two-step pyrolysis- catalytic reforming + pressure swing adsorption/oil distillation
Products	Diesel	Diesel	Hydrogen/Carbon nanotubes/Diesel	Hydrogen/Carbon nanotubes/Diesel
Annual capacity	15,500 tonnes	3,300 tonnes	15,500 tonnes	3,300 tonnes

* The capacity of the decentralized plants is set to be 3,300 tonnes per year, which corresponds to the capacity of typical small commercial-scale pyrolysis plants, as reported by (Haig et al., 2018).

3.2. Life cycle Assessment

3.2.1. Goal and Scope Definition

LCA was conducted based on the ISO 14040 and 14044 standards, and proceeds in four sequential stages: goal and scope definition; inventory analysis; impact assessment; and interpretation (ISO, 2006a, Ascher et al., 2024). The goal of the LCA study is to ascertain and compare the environmental footprints of large-scale centralized and small-scale decentralized MPW pyrolysis systems. The scope of this study considers six stages, namely (a) collection and transportation of MSW containing MPW, (b) feedstock pre-treatment, (c) pyrolysis, (d) product upgrading processes, (e) fuel supply, and (f) end-of-life use. GWP, as one of the main environmental impact categories, was considered in terms of global impact within a timeframe of 100 years and the Centrum voor Milieukunde Leiden (CML) 2001 method was applied to calculate GWP. In this LCA study, two different functional units (FU) were considered, namely, the treatment of 1 tonne of NMPW from a waste management perspective, and 100 km travelled by bus.

3.2.2. Life cycle inventory analysis

Life cycle inventory analysis defines the inputs and outputs (materials, energy, products, by-products, and emissions) of each stage involved in the systems. Data for foreground processes such as MPW sorting, pyrolysis, product purification, *etc.*, were obtained from research papers and documents, whilst data for background processes, such as electricity and diesel generation and distribution, were obtained from GaBi software databases. The system boundary and mass and energy flows were simulated in the GaBi software and their balance for all four scenarios is shown in Figure 3.1. In the figure, processes within the red boxes represent those occurring at the pyrolysis plant site, while processes in the yellow boxes indicate those conducted at the transfer station. The detailed inputs and outputs (electricity,

materials, and other resources) for each process involved in each system can be found in Table 3.2.

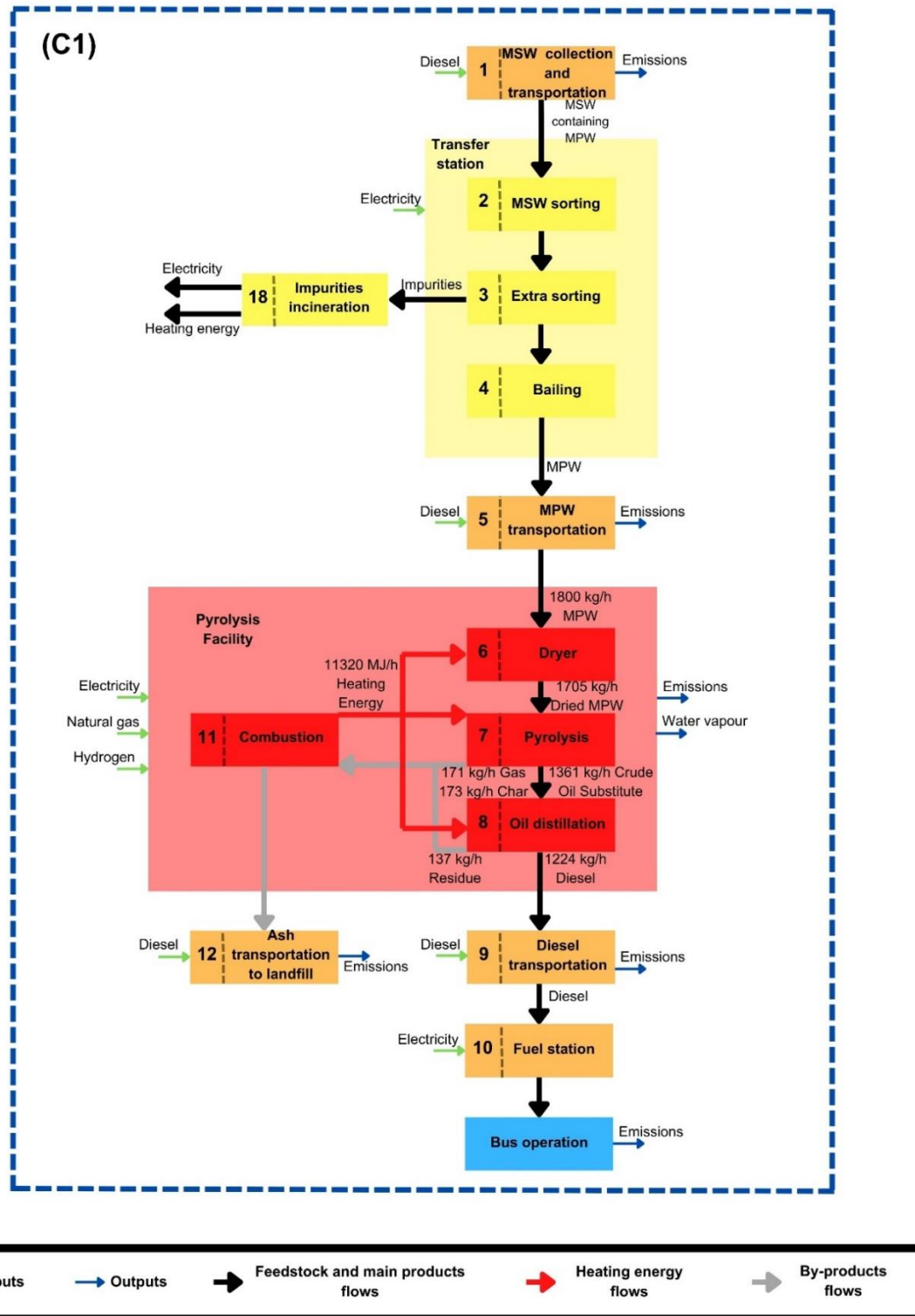


Figure 3.1. Detailed process flows for four scenarios: C1, D1, C2, and D2.

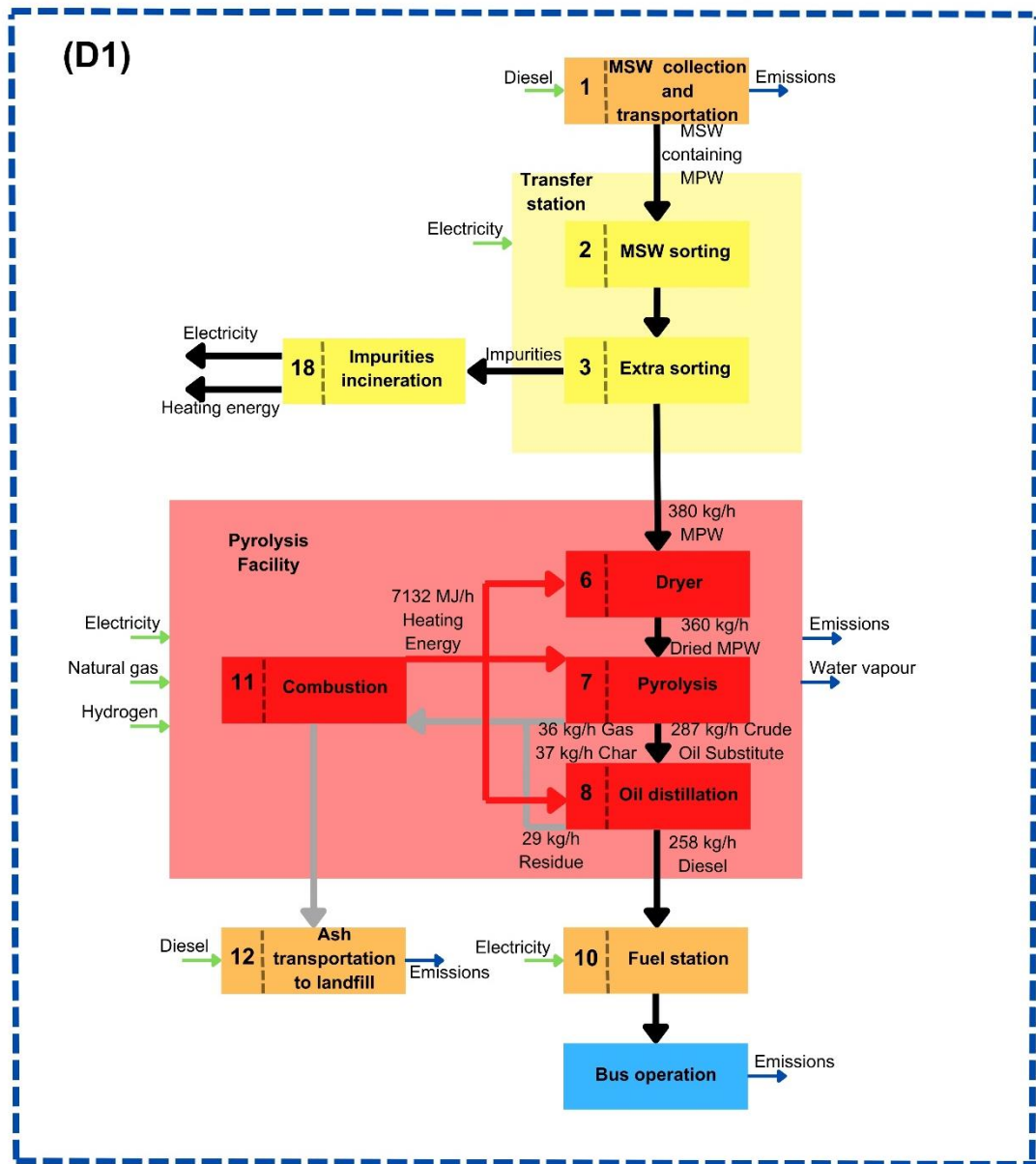


Figure 3.1. (continued).

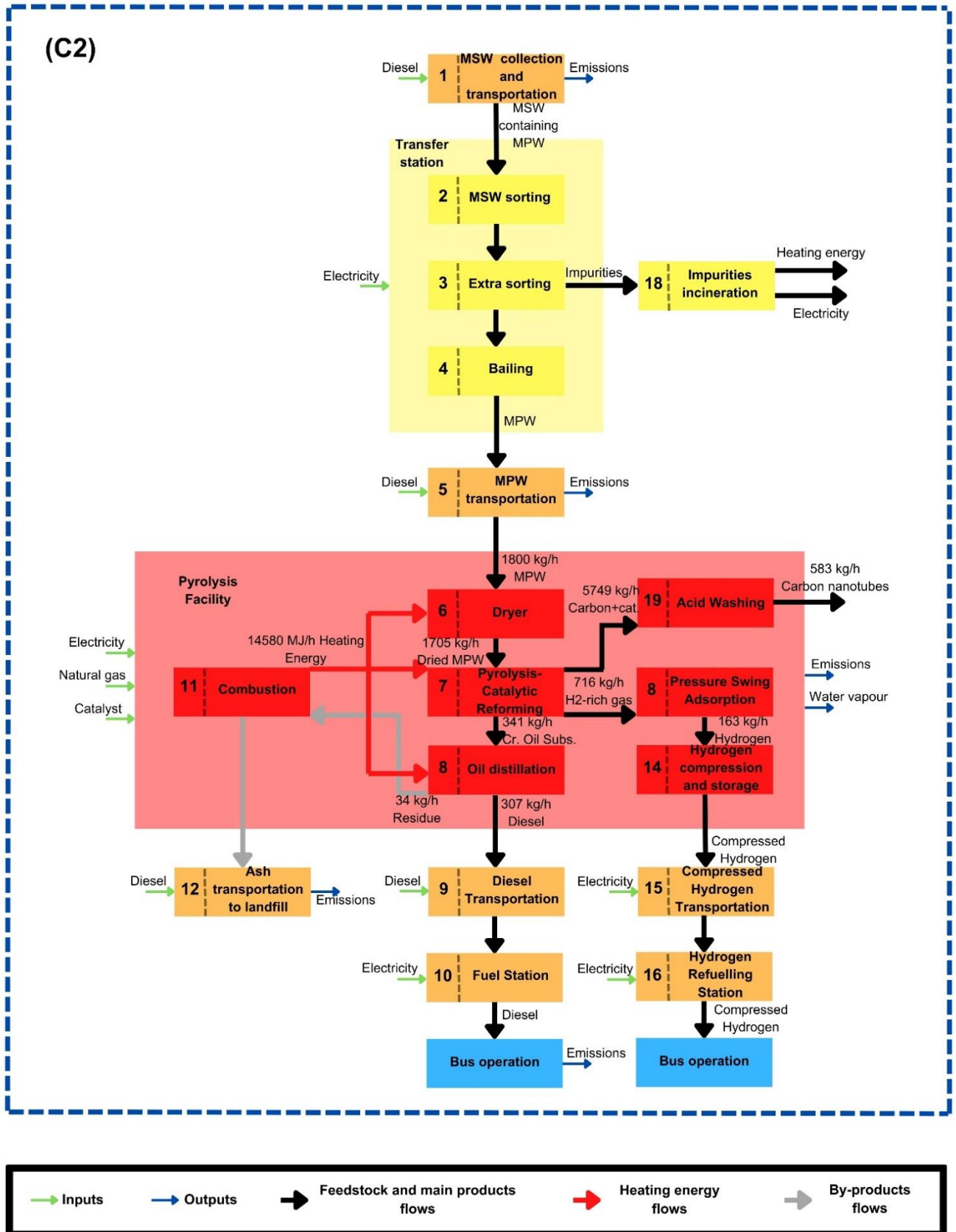


Figure 3.1. (continued).

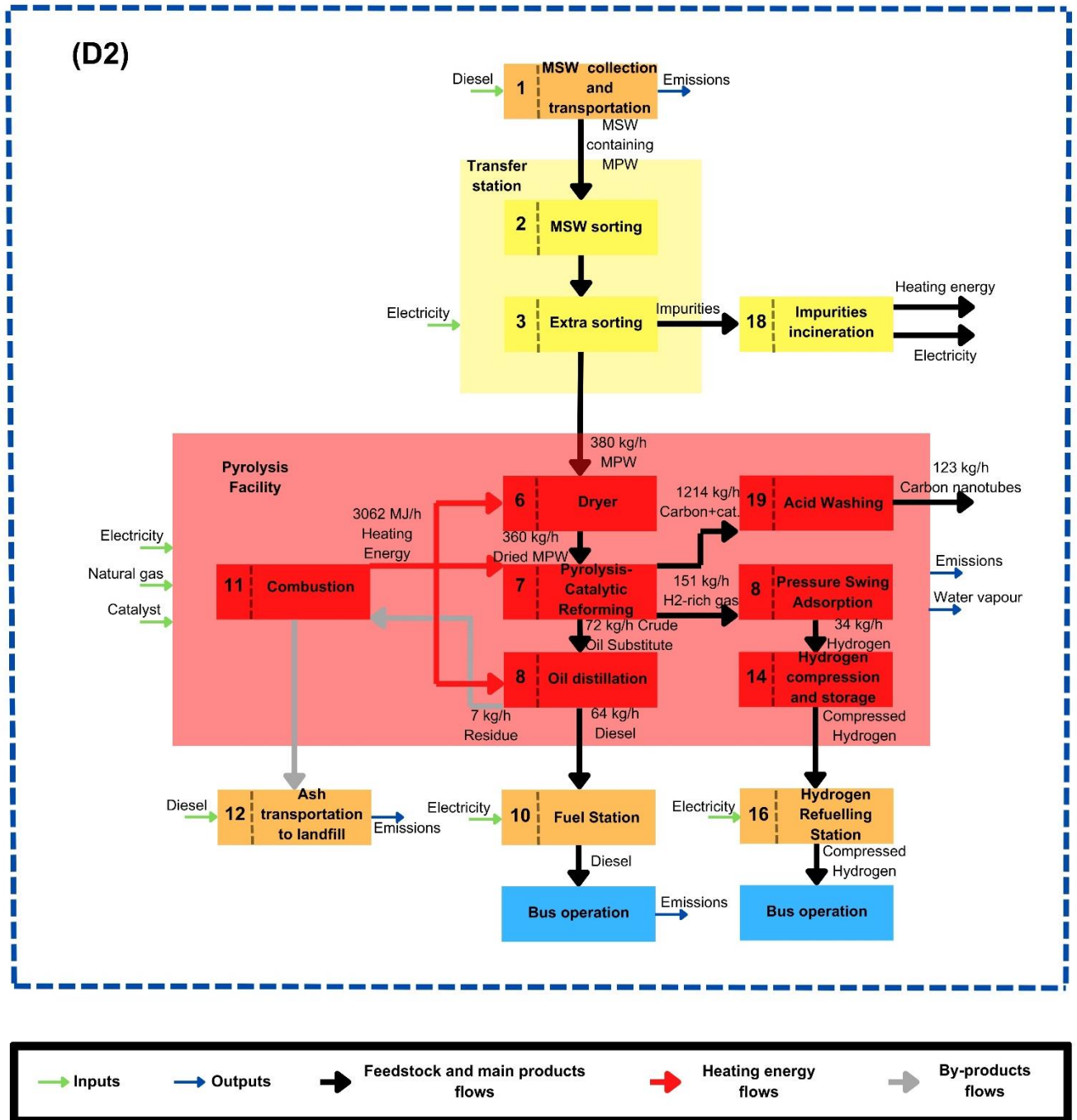


Figure 3.1. (continued).

3.2.2.1. MPW collection, transportation and sorting systems

MSW waste is collected every eight days (Glasgow City Council, 2023a). It was assumed that a lorry working with diesel collects 10-15 tonnes of MSW per trip and the maximum mass capacity of such lorries is 14-16 tonnes or 30.6 m³ (PE International, 2015).

The density of MSW is 408.5 kg/m^3 , which is within the range of MSW densities stated in other studies related to waste collection and transportation (Jaunich et al., 2016). It is worth noting that MPW density can vary depending on several factors, such as composition, compaction, moisture content, etc., but the chosen density represents the average value for MSW. Overall, 25% and 75% of the diesel used for MPW collection is consumed in the idling and driving of automated side loader trucks, respectively (Jaunich et al., 2016). Approximately 17.7 million MSW bins are collected per year in Glasgow (Glasgow City Council, 2015). It can thus be assumed that the average weight of MSW collected per stop is around 10.57 kg, 8.3% of which is plastics.

The collection and transportation of NMPW were modelled using the ArcGIS Pro. First, the four different datasets were received from the Digimap platform, namely neighbourhood areal classification, topography with road network data for Glasgow, OS Open UPRN, and UK buildings (EDINA Society Digimap Service, 2022c, EDINA Society Digimap Service, 2011, EDINA Society Digimap Service, 2022b, EDINA Society Digimap Service, 2022a). Then, all four datasets are integrated into ArcGIS Pro to produce the map containing the road networks and dwellings within the neighbourhoods of Glasgow as illustrated in Figure 3.2. The obtained map does not include waste collection points. It was assumed that these points are located on the closest road to the dwellings, and the geoprocessing tool ‘Generate Near Table (Analysis)’ was used to position them on the road in the ArcGIS Pro. Finally, 1000 points were randomly selected to determine their average distance, which is 17.3 m. This average value reflects the urban areas within Greater Glasgow, whose territorial boundaries can be seen on the right side of Figure 3.2. The main factors affecting the average distance between waste collection points include population density, urban layout, and the distribution and number of collection points. Selecting over 1000 points does not remarkably affect the result.

Additionally, it is worth noting that some property locations are positioned outside the building footprints in the analysis, and thus, all selected points were visually assessed to account for this discrepancy. Visually assessing and manually measuring the distances is labour-intensive. However, selecting around 2000 points does not significantly affect the result.

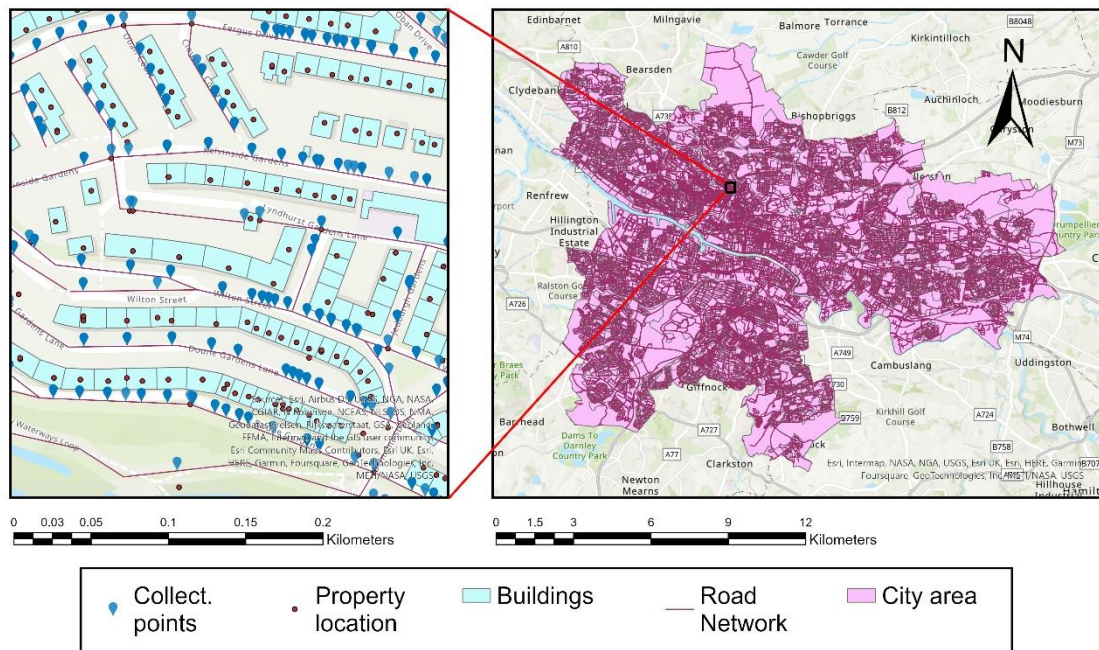


Figure 3.2. Glasgow city neighbourhoods' territory with road networks, dwellings and waste collection points.

PtE plants in the UK are usually located beyond the outskirts of cities (on average around 100 km away) (PE International, 2015); it is considered that the pyrolysis plant for the C scenarios is located 100 km away from Glasgow. For the C scenarios, prior to transportation to the pyrolysis facility, the MPW is baled, with each bale's weight being around 400 kg (Haig et al., 2018). Overall, 48 MPW bales are fit into a lorry for transportation. It is worth noting that the source providing the bale weight does not specify its density. Therefore, in this analysis, the weight of the bale is used as the sole key parameter without considering its volume.

First, MSW collected is transported to the sorting facility, where MPW is separated from other waste fractions. The MPW composition was defined based on the dataset obtained from Zero Waste Scotland (2010) and Foster (2008), and is shown in Table 1A in the Appendix. Sorted MPW mainly contains PE (28.5 wt.%), PP (22.2 wt.%), and PS (4 wt.%), which is favourable for the pyrolysis process; MPW also contains impurities (16.5 wt.%) and undesirable plastics such as PET (15.3 wt.%) and PVC (3.5 wt.%) for the pyrolysis process (Krüger et al., 2020). The MPW composition, featured by the particularly high content of PE and PP plastics, medium content of PET, and low content of PS and PVC, aligns with other studies defining MPW composition for developed countries (Bodzay and Bánhegyi, 2016, López et al., 2010, Edjabou et al., 2021). Extra sorting is applied to separate polyolefin MPW from them. The efficiency of the sorting process and the composition of sorted non-recycled MPW were assumed based on the data for the Meilo sorting plant in Germany, as it is one of the widely applied sorting setups (Krüger et al., 2020). Sorted non-recycled MPW mainly contains PE, PS, PP, and a small amount of PVC (< 0.5 wt.%) and PET (< 3 wt.%). The pyrolysis technology vendors reported that pyrolysis is tolerant of MPW containing up to 10% wt. PVC and 15% wt. PET (Haig et al., 2018). In this study, the PVC and PET content in MPW is much lower than the recommended limits for pyrolysis.

The presence of unwanted materials in plastic feedstock can affect the quality of resultant products and the pyrolysis process itself (Jeswani et al., 2021, Borsodi et al., 2011). The impurities received after the extra sorting have lower calorific value compared to non-recycled MPW sent to the PtE facilities. However, they contain a relatively high carbon content and can thus be sent to an incineration plant to recover electricity and heating energy. For D scenarios, it was assumed that the extra sorting facilities are near to waste incineration facilities around Glasgow (hence, transportation is minimum and not considered), whilst the impurities obtained from the extra sorting are transported to the incineration plant located 50 km away

from the extra sorting facilities for C scenarios. The outputs and inputs of incineration are described in detail in the next subsection. The GWP burden allocation of the MSW sorting process was performed with regard to the mass of sorted waste streams (Civancik-Uslu et al., 2021).

3.2.2.2. MPW-to-Energy Production

For all scenarios, the impurities obtained after the extra sorting are incinerated to produce electricity fed into the grid systems and heating energy used for local businesses or district heating. Incinerating one tonne of impurities produces 4.1 MJ of electricity and 12.15 MJ of heating energy (Jeswani et al., 2021). It is worth noting that heating energy and electricity generated from the impurities have carbon saving by displacing the heating energy generation from natural gas and electricity in the UK grids.

Before the plastics are fed into the pyrolysis reactor, they need to be dried as a high content of moisture could cause various issues such as temperature reduction in the reactor, prolonging the pyrolysis process, and increasing the production of unwanted gas and oil (Chen et al., 2014a). The heating energy consumed by the large (C1 and C2 scenarios) and small dryers (D1 and D2 scenarios) is 0.45 and 1.36 MJ/kg feedstock, respectively, with 5.3% of the feedstock mass being evaporated as moisture (Haig et al., 2018).

Dried MPW is fed into the pyrolysis reactor, where the feedstock in the pyrolysis reactor is broken down into lighter molecules in the absence of air (Chen et al., 2014b). The main difference between scenarios C1/D1 (diesel production) and C2/D2 (hydrogen production) is that for the former scenarios, an oil distillation process is applied after pyrolysis, while for the latter, a catalytic reforming process is applied.

For scenarios C1 and D1, dried MPW is degraded into less complex hydrocarbon chains in the form of vapor in the pyrolysis reactor. The condensable hydrocarbon molecules are then

condensed and separated from gas and solid products. The liquid obtained after the condensation process is considered as crude oil substitute, which is subsequently pumped into the oil distillation system to produce diesel-like oil that can be mixed with diesel. The oil obtained after the distillation process is called diesel-like pyrolysis oil, as it contains hydrocarbon molecules within the conventional diesel range (C₅-C₁₈) (Haig et al., 2018). The yields of diesel-like oil, gas, and solid products and residues are 71.81 wt.%, 10.03 wt.%, and 18.16 wt.%, respectively. Overall, 5.7 MJ of heating energy is consumed per kg of dried feedstock for the pyrolysis process in scenario C1, while for scenario D1, three times more heating energy is consumed (Haig et al., 2018). Also, the gas and char produced from the pyrolysis process and residue from the oil distillation process are combusted to produce the necessary heat for the pyrolysis plants, and thus have a carbon footprint. In scenarios C1 and D1, approximately 90 kg of pyrolysis char are produced per FU, 1 tonne of non-recycled MPW, and their combustion emits approximately 300 kg CO₂-eq (Ahamed et al., 2020). It is worth noting that the pyrolysis process consumes more than 90% of the heating energy used in the plants, and the rest is consumed by the processes such as dryer, oil distillation, *etc.*

Two-stage pyrolysis-catalytic reforming of MPW in the presence of a metal-based catalyst is applied to produce hydrogen-rich gas and carbon nanotubes (Acomb et al., 2016, Prabu and Chiang, 2022). In the first stage, in the pyrolysis reactor, plastic feedstock is broken down into mixture of shorter hydrocarbon volatiles at 500°C. In the second stage, hydrocarbon molecules volatiles are pumped into another catalytic reforming reactor, where they are decomposed and diffused on the nickel-based catalyst in an oxygen-free environment at a temperature of 700-800°C (Yao and Wang, 2020, Li et al., 2023, Biakhmetov et al., 2023). Overall, around 2.5 tonnes of Ni-based catalyst is used per FU (1 tonne of non-recycled MPW) in the C2 and D2 scenarios, and GWP associated with it was assumed based on the study by Ahamed et al. (2020). The GWP of producing 1 kg of nickel-based catalyst is 1.54 kg CO₂-eq,

with half of them associated with direct emissions occurring during catalyst preparation. The main products of catalytic reforming process are hydrogen-rich gas (42 wt.%) and carbon nanotubes (38 wt.%). Additionally, a small amount of liquid product containing hydrocarbon molecules C₆-C₂₂ is produced which is then distilled to achieve diesel-like oil quality (Cai et al., 2021).

The carbon nanotubes obtained from the process can be used in various ways, from serving as a fuel for heating and electricity generation, attributed to their high carbon content, to becoming value-added materials due to their unique characteristics such as extraordinary strength and stiffness, relatively high electrical and thermal conductivity, and chemical stability (Inshakova et al., 2020). To comply with circular economy practices and maximize resource recovery, carbon nanotubes are used as value-added materials instead of being employed as fuel for heating energy and electricity generation in this study. However, carbon nanotubes obtained from MPW termed crude carbon nanotubes as they contain undesired amorphous carbons or can be polluted with metal-based catalysts (Guo et al., 2007). Thus, they can be purified and then modified to acquire properties close to required property depending on the application purpose (Wang et al., 2022a).

Carbon nanotubes obtained from the catalytic reforming process are deposited on the nickel-based catalysts and need to be separated. An acid washing process is applied for this purpose, using hydrochloric acid (HCl) and deionized water as input materials (Griffiths et al., 2013). The main waste output of this process, wastewater, is sent to the wastewater treatment plant where Ni metals are easily recovered by adding calcium oxide (Ahamed et al., 2020). The acid washing process does not have any direct GHG emissions, but it is highly a material intensive process due to the HCl and deionized water inputs. Consequently, there are indirect GHG emissions associated with preparation of these input materials. Also, it is believed that the combustion of carbon nanotubes is less environmentally and economically friendly,

because of significant resource inputs into the acid washing process for their production. If carbon nanotubes are used as value-added materials, there will be carbon saving by displacing fossil fuel-based carbon nanotubes production, positively affecting the overall GWP of non-recycled MPW management systems producing hydrogen and carbon nanotubes.

There is lack of data about the amount of energy used in two-stage pyrolysis-catalytic reforming process. This study considered data from other thermo-chemical technologies that are similar to the two-step pyrolysis-catalytic reforming considered in this study. Hydrogen-rich gas is the main product of two-stage pyrolysis-catalytic reforming, containing more than 30 wt.% hydrogen, 20 wt.% methane, and other hydrocarbon gases (C₂-C₄). Hydrogen-rich gas is pumped to be treated by the polybed pressure swing adsorption (PSA) technology, where hydrogen is separated from other gases, which is used due to the following advantages: (a) it is the most commercially available technology to produce ultrapure hydrogen (99.99+%) (Luberti and Ahn, 2022, Meyers, 2016, Yang, 1997, Ruthven and Pressure, 1994, Voss, 2005), and (b) it has relatively high hydrogen recoveries (60-90%) (Ronald Long, 2011). Since not all hydrogen is recovered after the PSA process, the remaining gas still contains a proportion of hydrogen and methane, which is combusted to recover heating energy for auxiliary demands of the systems. Overall, 322.17 MJ of electricity is consumed by the PSA process to process 357.97 kg of hydrogen-rich gas produced from the pyrolysis-catalytic reforming process for scenarios C2 and D2 (Valente et al., 2019, Lui et al., 2022b). The crude oil substitute produced from the two-stage pyrolysis-catalytic reforming process is distilled to produce pyrolysis diesel.

Also, it is worth noting that the CCS unit was not included in the LCA study for all scenarios, as the main purpose of LCA is to assess the carbon footprint of the primary systems. However, the CCS unit was considered in the CBA study (Chapter 4) to evaluate its economic feasibility, including potential savings from reduced emissions penalties.

3.2.2.3. Distribution and End-of-life Use of Products

In Scotland, a large share of fuel (petrol and diesel) for transport is sourced through INEOS's oil refinery located on the Firth of Forth in Grangemouth, Scotland, and it is assumed for the purpose of this study that distilled pyrolysis diesel, with a density of 850 kg/m^3 , is transported to this plant (Haig et al., 2018). The shortest and most optimal route to this oil refinery from Glasgow is via the M80 motorway, the distance for which is around 45 km. Mixed diesel from oil refinery plant is transported back to the fuel station in Glasgow, where buses are fuelled.

The pyrolysis oil obtained after the distillation process has properties very close to those of conventional diesel (Faisal et al., 2023b). The diesel engine does not require considerable modification to use a mixture of conventional diesel and pyrolysis diesel produced from MPW. The most important factor is the effect of pyrolysis diesel on engine performance and emissions characteristics (Sekar et al., 2022, Biakhmetov et al., 2023, Ramalingam et al., 2018, Erdoğan et al., 2019). The negative effects of pyrolysis diesel, such as poor combustion, knocking, or combustion noise, can be mitigated by modifying the blending ratio of conventional and MPW diesel. It should be stated that pyrolysis diesel produced from a mixture of plastics cannot fully substitute conventional diesel or be blended with conventional diesel at a high ratio (Biakhmetov et al., 2023). Also, the pyrolysis diesel obtained and then transported to the oil refinery plant could still contain some impurities and undesired hydrocarbon chains. However, this issue can be sorted out, as the oil refinery plant has the capability to adjust the composition of pyrolysis diesel or remove all undesired components through the purification or other processes it has (Haig et al., 2018).

The hydrogen produced in scenarios C2 and D2 is used to support local hydrogen fuel cell electric buses in Glasgow. Additional energy is required to store and transfer hydrogen. Overall, 11.34 MJ of electricity was required per kilogram of hydrogen, with 4.14 MJ for

compression and the remaining energy used for storage (Lui et al., 2022b). The hydrogen produced, usually at around 10-20 bar pressure, is compressed to 200 bar for storing and transportation purposes (Lozanovski et al., 2011). The pyrolysis diesel produced in scenarios C2 and D2 is transported to the oil refinery located outside of Glasgow which is the same as scenarios C1 and D1. The fuel consumption part of the comparison study by Ally and Pryor (2016) is used to assess the carbon footprint of bus operations powered by fuel from MPW pyrolysis.

The main by-product in all scenarios is ash received from the combustion process to produce heating energy. Ultimate and proximate analyses of MPW in many studies show that MPW contains a small amount of ash (Park et al., 2012, Aboulkas and El Bouadili, 2010, Rajendran et al., 2020, Sharuddin et al., 2017), which can typically deposit with carbon and other inert solid products at the bottom of the reactor during the pyrolysis process, which is considered a solid product. In this study, the overall solid product was combusted due to the high carbon content, and the ash was left as a by-product. Based on data released by the Scottish Environment Protection Agency (2015), the ash produced is defined as a non-hazardous inert material, and transported to landfill without any pretreatment (50 km road transport).

Table 3.2. Various inputs and outputs for all four scenarios considered in detail.

No. (corresponding to the processes illustrated in Figure 3.1)	Process stage		Scenarios				Comments	References
			C1	D1	C2	D2		
1	MSW collection and transportation to sorting and bailing facility	Inputs				Gross weight of truck is 20-28 tonne (Euro 4)	GaBi database	
		MSW, kg	12,000	12,000	12,000			12,000
		Diesel, kg	1.24	1.24	1.24			1.24
		Outputs						
		MSW, kg	12,000	12,000	12,000			12,000
		GHG from vehicles, kg CO ₂ -eq	3.7	3.7	3.7	3.7		
2	MPW sorting	Inputs				Other waste fractions separated are excluded	Krüger et al. (2020)	
		MSW, kg	12,000	12,000	12,000			12,000
		Electricity, MJ	190	190	190			190
		Outputs						
		MPW with impurities, kg	1,000	1,000	1,000			1,000

		Other waste fractions, kg	11,000	11,000	11,000	11,000	from the systems	
3	Extra sorting	Inputs					Impurities separated are excluded from the systems	Krüger et al. (2020)
		MPW with impurities, kg	1,000	1,000	1,000	1,000		
		Electricity, MJ	58	58	58	58		
		Outputs						
		MPW, kg	900	900	900	900		
		Impurities, kg	100	100	100	100		
4	Bailing	Inputs					35.28 MJ of electricity is consumed per a tonne of MPW	Liljenström and Finnveden (2015)
		MPW, kg	900	900	900	900		
		Electricity, MJ	31.8	-	31.8	-		
		Outputs						
		MPW, kg	900	900	900	900		
5	MPW transportation to the pyrolysis facility	Inputs					Gross weight of truck is 32 tonne (Euro 4), the distance between the sorting and pyrolysis	GaBi database
		MPW, kg	900	900	900	900		
		Diesel, kg	2.2	-	2.2	-		
		Outputs						
		MPW, kg	900	900	900	900		
		GHG from vehicles, kg CO ₂ -eq	8.5	-	8.5	-		

							facilities is 100 km	
6	Dryer	Inputs					Dried MPW moisture composition of around 5%	Haig et al. (2018)
		MPW, kg	900	900	900	900		
		Heating energy, MJ	408.2	1224.7	408.2	1224.7		
		Electricity, MJ	180	180	180	180		
		Outputs						
		Dried MPW, kg	852.3	852.3	852.3	852.3		
		Water vapour, kg	47.7	47.7	47.7	47.7		
7	Pyrolysis/Pyrolysis -Catalytic reforming	Inputs					One-stage pyrolysis is applied to produce oil (T1=400- 500°C), whilst two- stage pyrolysis- catalytic reforming is applied to	Lui et al. (2022b), Haig et al. (2018), Khoo (2009), Cai et al. (2021), Ahamed et al. (2020) and Griffiths et al. (2013)
		Dried MPW, kg	852.3	852.3	852.3	852.3		
		Heating energy, MJ	4,860	14,580	7,290	21,870		
		Catalyst, kg	-	-	2,551	2,551		
		Outputs						
		Crude oil substitute, kg	680.4	680.4	170.5	170.5		
		Gas, kg	85.5	85.5	-	-		
		Hydrogen-rich gas, kg	-	-	358	358		
		Solid product, kg	86.4	86.4	-	-		

		Carbon nanotubes+catalyst, kg	-	-	2,874	2,874	produce hydrogen-rich gas (T1=500°C and T2=800°C).	
8	Oil distillation	Inputs					Hydrogen received from natural gas is used for C1 and D1 scenarios, whilst C2 and D2 scenarios use their own hydrogen	Haig et al. (2018), GaBi database
		Crude oil substitute, kg	680.4	680.4	170.5	170.5		
		Hydrogen, kg	6.8	6.8	1.7	1.7		
		Heating energy, MJ	392	1176.1	491.1	491.1		
		Outputs						
		Distilled diesel, kg	612	612	153.3	153.3		
		Residue, kg	68.4	68.4	17.1	17.1		

							produced from MPW	
9	Diesel transportation to the oil refinery plant, and back to Glasgow	Inputs					Gross weight of truck is 20-28 tonne (Euro 4)	GaBi database
		Distilled diesel, kg	612	612	153.3	153.3		
		Diesel, kg	2.3	1	0.6	0.3		
		Outputs						
		Distilled diesel, kg	612	612	153.3	153.3		
		GHG from vehicles, kg CO ₂ -eq	7.1	3.2	1.8	0.8		
10	Fuel station	Inputs					1.06 MJ of electricity consumed per kg of diesel at the fuelling station	Lucas et al. (2012)
		Distilled diesel, kg	612	612	153.3	153.3		
		Electricity, MJ	646.8	646.8	162	162		
11	Combustion of gas and by-products to produce heating energy	Inputs					Carbon emission factor is 0.2904 kg CO ₂ -eq./kg. The heating	GaBi database, Haig et al. (2018) and (Ahamed et al., 2020)
		Gas, kg	85.5	85.5	-	-		
		Solid product, kg	86.4	86.4	-	-		
		Residue, kg	68.4	68.4	17.1	17.1		
		Natural gas, kg	-	233.1	157	481.2		
		Outputs						

		Heating energy, MJ	7,329.1	16,980.8	8,189.3	23,585.8	values of gas, solid product, residue, and natural gas are 20, 31, 43, and 47.5 MJ/kg, respectively .	
		GHG from the combustion process, kg CO ₂ -eq	342	900.8	436.5	1,327.8		
		Ash, kg	93.5	93.5	10.4	10.4		
12	Ash transportation to landfill	Inputs					Gross weight of truck is 32 tonne (Euro 4)	GaBi database
		Ash, kg	93.5	93.5	10.4	10.4		
		Diesel, kg	0.2	0.2	0.02	0.02		
		Outputs						
		GHG from vehicles, kg CO ₂ -eq	0.5	0.5	0.02	0.02		
13	Pressure swing adsorption	Inputs					Hydrogen recovery efficiency is around 90%	Cai et al. (2021), Valente et al. (2019), and Lui et al. (2022b)
		Hydrogen-rich gas, kg	-	-	358	358		
		Electricity, MJ	-	-	322.2	322.2		
		Outputs						
		Hydrogen, kg	-	-	83.4	83.4		

		Other gases, kg	-	-	274.6	274.6		
14	Hydrogen compression and storage	Inputs					Hydrogen is compressed from 10-20 bar pressure to 200 bar	Cai et al. (2021), GaBi database, Lui et al. (2022b)
		Hydrogen, kg	-	-	81.7	81.7		
		Electricity, MJ	-	-	926.2	926.2		
		Hydraulic oil, kg	-	-	0.1	0.1		
		Outputs						
		Compressed Hydrogen, kg	-	-	81.7	81.7		
		Used Hydraulic Oil, kg	-	-	0.1	0.1		
		Waste Heat, MJ	-	-	1	1		
15	Compressed hydrogen transportation	Inputs					Gross weight of truck is 32 tonne (Euro 4)	GaBi database, Lui et al. (2022b)
		Compressed Hydrogen, kg	-	-	81.7	-		
		Diesel, kg	-	-	0.3	-		
		Outputs						
		Compressed Hydrogen, kg	-	-	81.7	-		
		GHG from vehicles, kg CO ₂ -eq	-	-	1	-		
16		Inputs						

	Refuelling hydrogen fuel vehicles	Compressed Hydrogen, kg			81.7	81.7	14.4 MJ of electricity consumed per kg of hydrogen	Pi et al. (2016), Lui et al. (2022b)
		Electricity, MJ			1,176.1	1,176.1		
17	Impurities transportation to incineration plant	Inputs					Gross weight of truck is 32 tonne (Euro 4)	GaBi database
		Impurities, kg	100	-	100	-		
		Diesel, kg	0.25	-	0.25	-		
		Outputs						
		GHG from vehicles, kg CO ₂ -eq	0.74	-	0.74	-		
18	Impurities incineration	Inputs					The net electricity and heating energy efficiencies are 11.3% and 33.3%, respectively. Carbon emission factor is	(Jeswani et al., 2021) and
		Impurities, kg	100	100	100	100		
		Outputs						
		Electricity, MJ	414	414	414	414		
		Heating energy, MJ	1,215	1,215	1,215	1,215		
		Greenhouse gases from the incineration, kg CO ₂ -eq	299	299	299	299		

							2.99 kg CO2-eq./kg.	
19	Acid washing	Inputs					HCl is produced by chlorination and halogen exchange reactions, which are widely used methods in the industry. Carbon nanotubes recovery efficiency is 90%.	GaBi database, (Ahamed et al., 2020), (Griffiths et al., 2013) and (Isaacs et al., 2010)
		Carbon nanotubes+catalyst, kg	-	-	2,874.4	2,874.4		
		Deionized water, kg	-	-	36,990.7	36,990.7		
		HCl, kg	-	-	4,566.8	4,566.8		
		Outputs						
		Carbon nanotubes, kg	-	-	291.5	291.5		
		Wastewater, kg	-	-	44,140.4	44,140.4		
20	Wastewater treatment	Inputs					Quicklime is typically used to recover Ni.	
		Wastewater, kg	-	-	44,140.4	44,140.4		
		Quicklime (CaO), kg	-	-	1,015.2	1,015.2		

3.2.3. Interpretation and sensitivity analysis

This LCA phase includes a description of the final results and checks the completeness of the study as a whole. Also, breakdowns of GWP results based on the stages involved in the production of hydrogen and diesel, as well as scope 1-3 emissions, are described to provide a more inclusive and accurate results. Finally, sensitivity analysis is conducted to understand how some of the uncertainties affect the final results. Various uncertainties could affect the final GWP results, and some such that have profound impact were chosen. These are described below:

- The distance from the transfer station to the MPW pyrolysis plant for centralized scenarios was assumed based on the distance reported in other studies (PE International, 2015). In the study by Haig et al. (2018), a few options for the locations of centralized MPW pyrolysis plants in Scotland were suggested, one of which was on the outskirts of Glasgow. This means there is no need for the transfer station, as any MPW collected can be transported directly to the pyrolysis facility. In another option, the MPW pyrolysis facility was located 230 km away from Glasgow.
- The distance between MPW collection points. During the data collection about MPW collection and transportation, it was found that the average distances between collection points could vary.
- MPW feedstock composition. Contamination of feedstocks with other materials such as glue, paint, dirt, food, and other inert materials reduces the proportion of usable plastic, which is the main source of any oil or gas produced. Inert materials are usually deposited onto the char produced (Williams et al., 2023). Also, polymer composition (some polymers such as PET or PVC) has negative effects on the conversion efficiencies of systems from feedstock to diesel or hydrogen fuel, whilst rigid plastics can be more suitable for the pyrolysis process than film plastics as the latter lead to the

production of increased amounts of residue (Haig et al., 2018). In the sensitivity analysis, the upper and lower bounds for contamination and the content of undesired polymers (PET and PVC) for all scenarios are $\pm 20\%$. This variation impacts the usable MPW content for the thermochemical conversion process, as well as the energy usage for removing contamination and the content of undesired polymers.

- The efficiency of hydrogen recovery from the gas produced. In this study, the maximum hydrogen recovery from PSA (90%) was considered. However, the efficiency of hydrogen recovery from PSA can vary from 60% to 90% (Ronald Long, 2011), and affects the overall GWP. It is worth noting that many PSA systems have efficiencies close to 85–90% under optimal conditions. Nonetheless, the broader range of PSA efficiency was considered to account for potential variability in less efficient systems.
- Heating energy used for the conversion process. There are many factors affecting the amount of heating energy required for the conversion process such as the scale of reactors, conversion efficiency, *etc.* In Haig et al. (2018), it is noted that the heating energy can vary depending on the scale of the facility. The variations of the input heating energy are $\pm 10\%$.

After defining the upper and lower bounds of the various uncertainties, Monte Carlo simulations were used to assess their impacts on the GWP results. Monte Carlo simulations are a technique used for forecasting or decision-making under a range of uncertain factors. In this study, the simulations generated random values for each uncertainty factor mentioned above. Triangular distributions were used for the analysis as it clearly shows probability density across a defined range (Doubilet et al., 1985). Overall, 1000 iterations were run for each uncertainty factor. Selecting the number of iterations is important, as it affects balancing result accuracy and computational efficiency. Most studies select 1,000 iterations because it provides a reasonable balance between these factors (Lui et al., 2022a, Steiger, 2010). Thereafter, the

percentage change in GWP for each uncertainty factor was calculated for all four scenarios using equation (3.1).

$$Change (\%) = \frac{GWP_{mont.car.} - GWP_{main}}{GWP_{main}} \times 100\% \quad (3.1.)$$

where GWP_{main} is the main result of the scenarios, and $GWP_{mont.car.}$ is the range of results (minimum to maximum values) from the Monte Carlo simulation for each uncertainty factor, illustrating the potential variability in GWP outcomes.

3.3. Results and Discussion

3.3.1. Environmental Impacts of Four Scenarios

The results of GWP calculations for all scenarios are illustrated in Figure 3.3a (FU = 1 tonne of feedstock) and Fig 3.3b (FU = 100 km travelled by bus). Each scenario includes four parts: (a) MPW collection, transportation, and sorting systems, (b) MPW-to-energy production, (c) distribution and end-of-life-use of products and byproducts; and (d) displacement of fossil fuel-based diesel, hydrogen, heating energy and electricity.

The GWP of MPW collection, transportation, and sorting systems for the D scenarios is 22.51 kg CO₂-eq. per tonne of MPW, whilst the GWP for the centralized systems is 1.5 times higher than for the decentralized systems. For scenario C1 and C2 systems, a higher carbon footprint can be explained by the fact that the MPW feedstock is transported to MPW pyrolysis facilities that are located 100 km away from the city. Also, MPW sorted from other waste fractions needs to be bailed before transportation. Figure 3.3 (a) shows that the carbon footprint associated with MPW collection, transportation, and sorting systems is 4.13% overall for scenario C1 and around 1.67% for scenarios D1 and followed by 0.46% and 0.28% for scenarios C2 and D2, respectively. In Figure 3.3 (b), scope 1 emissions for centralized MPW

collection, transportation, and sorting systems are 33.22%, while they are 16.41% for decentralized MPW collection, transportation, and sorting systems. This difference can be explained by direct GHG emissions from driving truck from the transfer station to the pyrolysis facility.

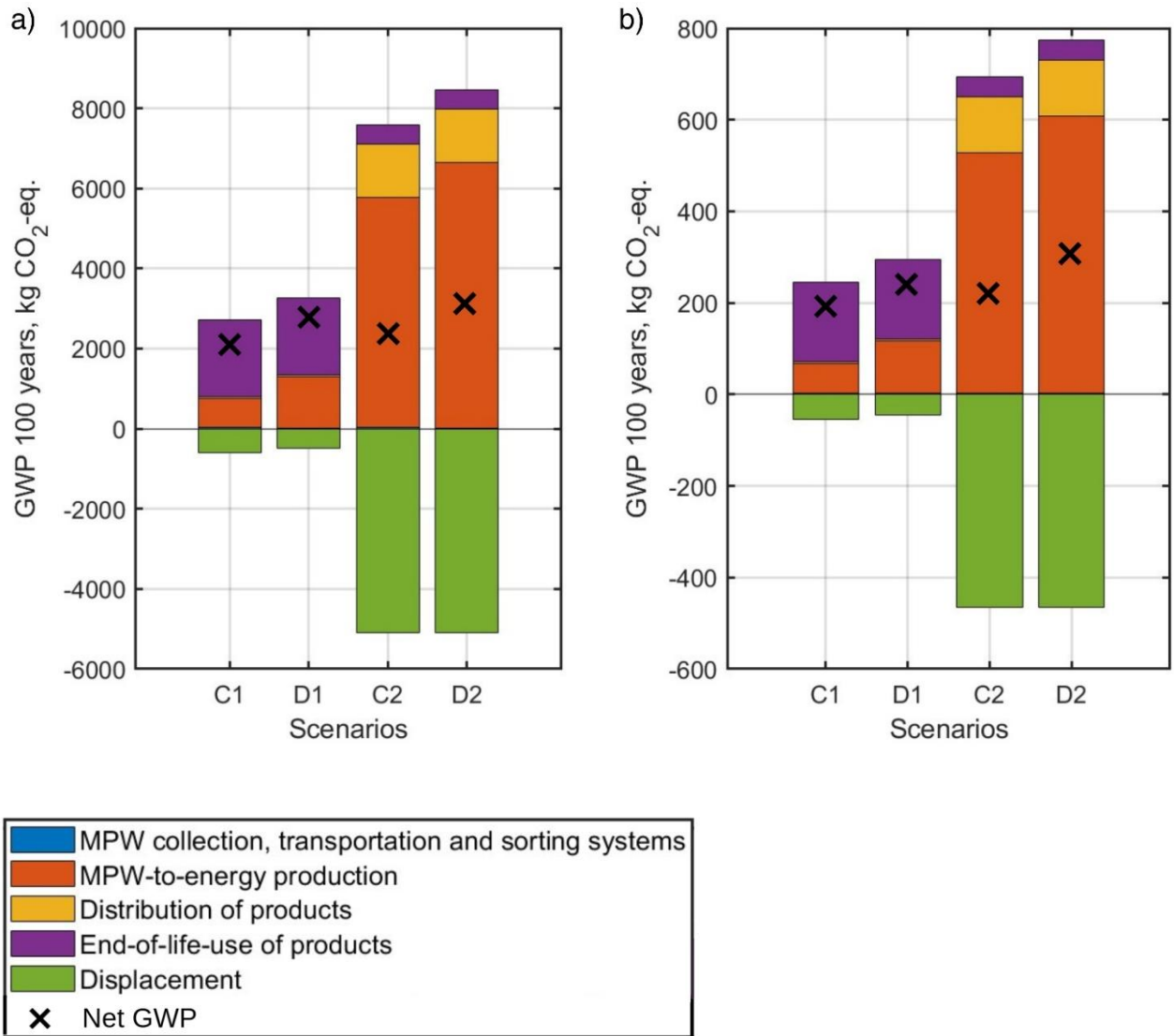


Figure 3.3. a) GWP for each scenario, where the FU is 1 tonne of MPW; b) GWP for each scenario, where the FU is 100 km travelled by bus.

The MPW-to-energy production stage in Figure 3.3 includes incineration of impurities from the extra sorting process, feedstock pretreatment, pyrolysis, and oil distillation for scenarios C1 and D1, whilst for scenarios C2 and D2 it includes incineration of impurities,

feedstock pretreatment, two-stage pyrolysis-catalytic reforming, oil distillation, PSA and acid washing. Hydrogen production is more energy intensive than diesel production and, consequently, its environmental footprint is much higher. The pie charts displayed in Figure 3.4 (a) indicate the share of each stage involved to produce hydrogen and diesel with respect to the overall carbon footprints. In Figure 3.4 (a), the GWP proportion of MPW-to-energy production is also much higher than other parts, namely (a) MPW collection, transportation, and sorting, and (b) product and byproduct distribution. It is worth noting that GHG emissions from MPW-to-energy production are ordered from low to high as C1, D1, C2, and D2. The share of scope 1 emissions from MPW-to-energy production is over 90% for the C1 and D1 scenarios, while the C2 and D2 scenarios have much lower scope 1 emissions, with indirect GHG emissions being dominant. The plastic-to-hydrogen and carbon nanotubes conversion process is not only highly energy-intensive but also demands other resources (catalyst, deionized water, HCl, *etc.*) in large quantities, resulting in high indirect GHG emissions.

The GWP of the distribution of products stage is less than that of the MPW-to-energy production stage and higher than that of the MPW collection, transportation, and sorting stage. Also, it is worth noting that the GWP of distribution of products and byproducts for scenarios C2 and D2 is almost 7 times higher than scenarios C1 and D1 as storage and transportation of hydrogen is more energy and resource intensive as compared to diesel. Moreover, wastewater sent to the wastewater treatment plant is processed by adding quicklime to recover metals, resulting in high shares of scope 1 and 2 emissions for the C2 and D2 scenarios.

The end-of-life-use and displacement stages are significant as they change the overall results of this study. The end-of-life-use of hydrogen and diesel produced for all scenarios are fuels for public transport - buses. Scenarios C1 and D1 produce diesel to drive 1107.71 km each of them and their GWP is 1915.6 kg CO₂-eq. per tonne of MPW. Diesel and hydrogen produced in scenarios C2 and D2 are enough to drive 1094 km, their GWP is 479.92 kg CO₂-

eq. per tonne of MPW. It is worth noting that the results are slightly changed (by 1.2%) when the FU of 100 km driven by bus is applied. These results highlight the fact that it is meaningful to assess the environmental footprint based on the consideration of different types of FUs for these kinds of studies.

The carbon saving associated with the displacement of fossil fuel-based diesel, hydrogen, carbon nanotubes, and energy production further improve the environmental performance of the systems, as detailed in Table 3.3. The carbon saving obtained from the heating energy displacement for the C1 scenario is the highest compared to other scenarios. Overall, in the C1 scenario, 7,329 MJ of heating energy is produced per FU (1 tonne of non-recycled MPW) from the waste product on the pyrolysis site, which is much higher than the consumed heating energy for the thermochemical conversion process (5,660 MJ). In other scenarios (D1, C2 and D2), the combustion of waste products (pyrolysis char, pyrolysis gas, and oil distillation residue) does not produce enough heating energy for the whole systems, and as a result, natural gas is combusted to fill the deficiency. For all the scenarios, there is carbon saving from displacing grid heat with the heating energy obtained from the incineration of sorting process residues as shown in Table 3.3. The carbon savings by displacements for C2 and D2 scenarios are 10 times of those for C1 and D1 scenarios, mainly attributed to significant emissions from the production of hydrogen and carbon nanotubes from fossil fuels that are displaced. It is also worth noting that the carbon saving potential of C2 and D2 scenarios per FU is the same.

Table 3.3. The carbon (GWP) saving by the displacements of heating energy, electricity, diesel, hydrogen and carbon nanotubes per FU (1 tonne of non-recycled MPW) for all scenarios.

	Heating energy		Electricity		Diesel		Hydrogen		Carbon nanotubes	
	MJ	CO ₂ -eq.	MJ	CO ₂ -eq.	kg	CO ₂ -eq.	kg	CO ₂ -eq.	kg	CO ₂ -eq.
C1	2,884	185.34	414	30.64	612.01	385.87	-	-	-	-
D1	1,215	78.09	414	30.64	612.01	385.87	-	-	-	-
C2	1,215	78.09	414	30.64	153.33	96.67	81.67	690.95	291.49	4,197
D2	1,215	78.09	414	30.64	153.33	96.67	81.67	690.95	291.49	4,197

Overall, centralized systems show better environmental performance than decentralized systems. Notably, D2 shows the worst net environmental performance (3,376 kg CO₂-eq. per tonne of MPW), whilst C1 indicates the best net environmental performance (2,114 kg CO₂-eq. per tonne of MPW). Despite that the hydrogen and diesel production stage for scenarios C2 and D2 has higher GWP than the diesel production stage for scenarios C1 and D1, the former scenarios outperformed the latter scenarios in terms of carbon saving by displacements overall. It can be explained that diesel buses emit GHG while hydrogen fuel cell buses do not. Also, the carbon saving by the displacement of fossil fuel-based hydrogen using the hydrogen from the pyrolysis is greater than that from the GWP reduction by the displacement of fossil fuel-based diesel using the diesel from the pyrolysis, and the carbon saving from carbon nanotubes significantly improve the environmental performance of C2 and D2 scenarios.

The GWP results for all scenarios with assumptions are positive, but they could turn to negative values if changes are applied. For example, centralized systems can be located as close as possible to the transfer station, which reduced the GHG emission associated with the non-recycled MPW transportation. Alternatively, the carbon dioxide emitted from thermochemical processes can be captured and stored in geologic formations, which can further reduce the overall GWP. These possibilities could be addressed by future studies. This LCA study exclusively focuses on comparing the GWP of hydrogen and diesel production from MPW as pyrolysis-catalytic reforming is an energy-intensive technology that can have a profound impact on GWP. However, GWP abatement is not the only environmental impacts that are relevant to the deployment of the technology. It is recommended future research can explore other impact categories, such as acidification, eutrophication, PM_{2.5}, water depletion, *etc.*, based on similar system boundaries defined in this study.

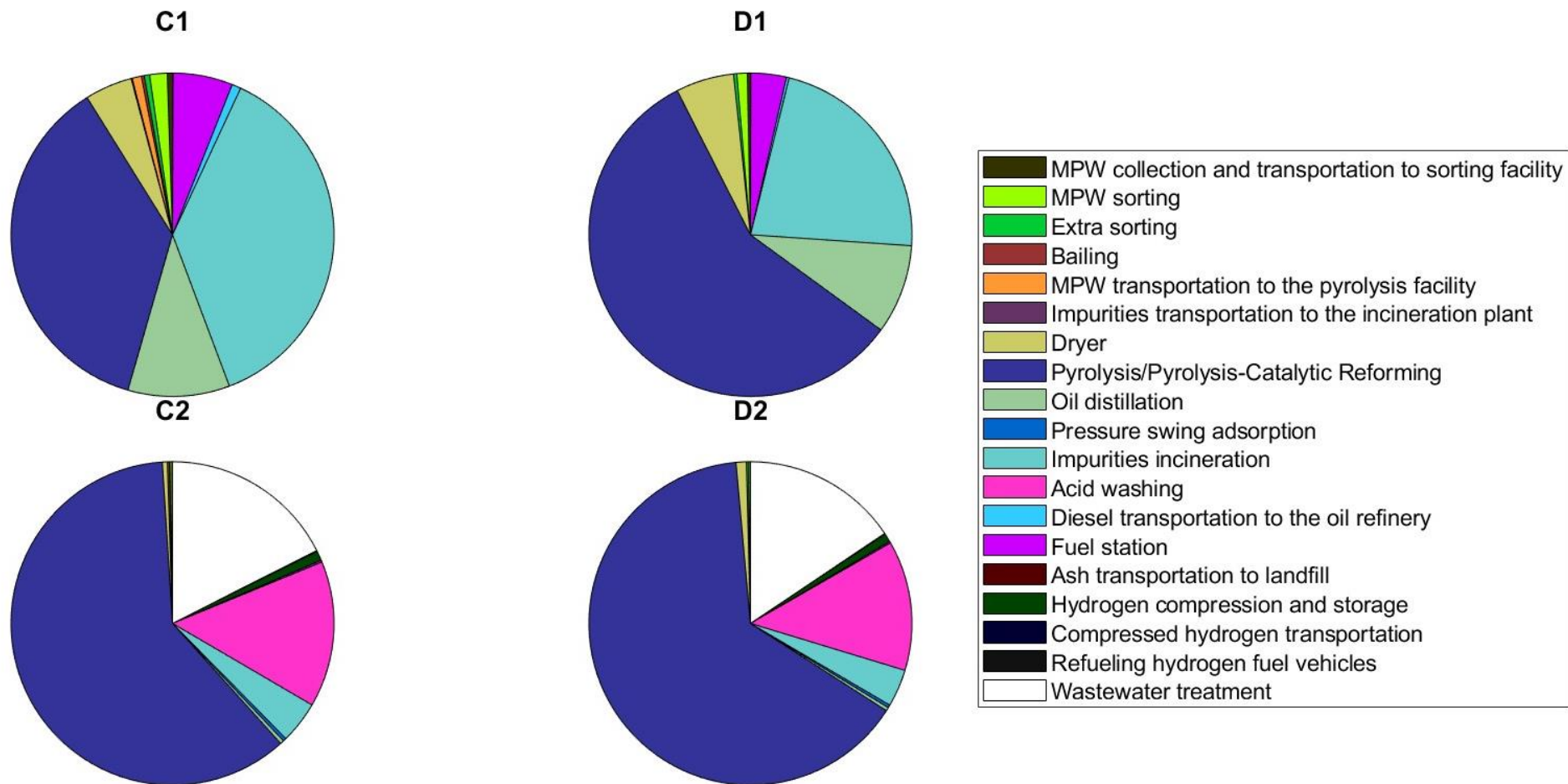
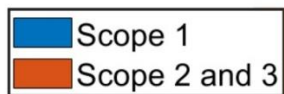
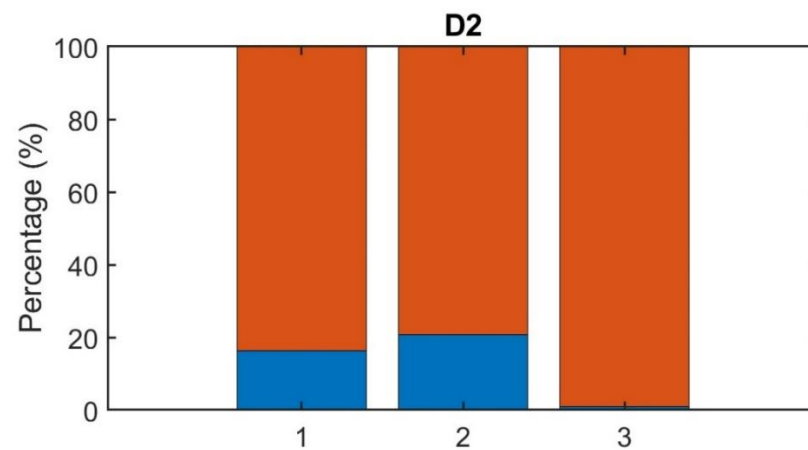
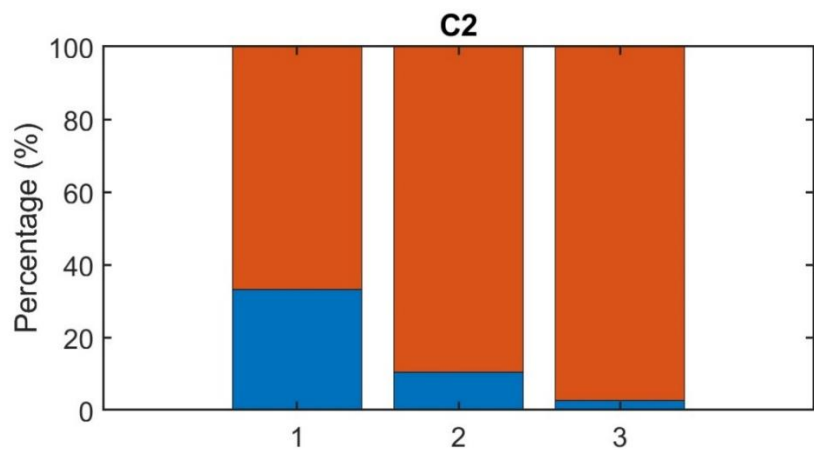
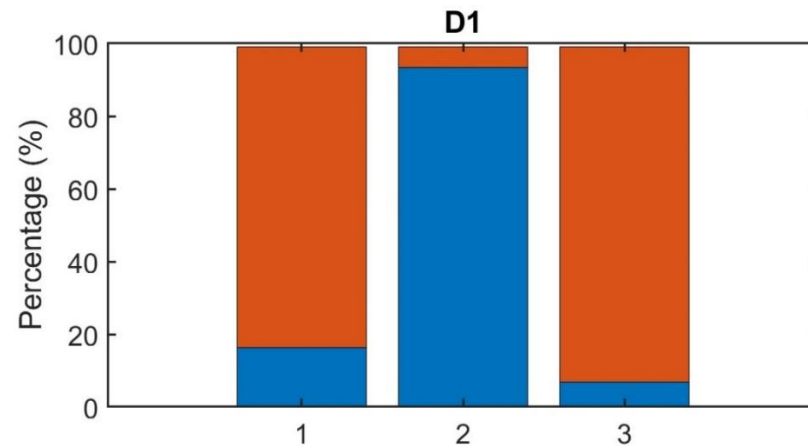
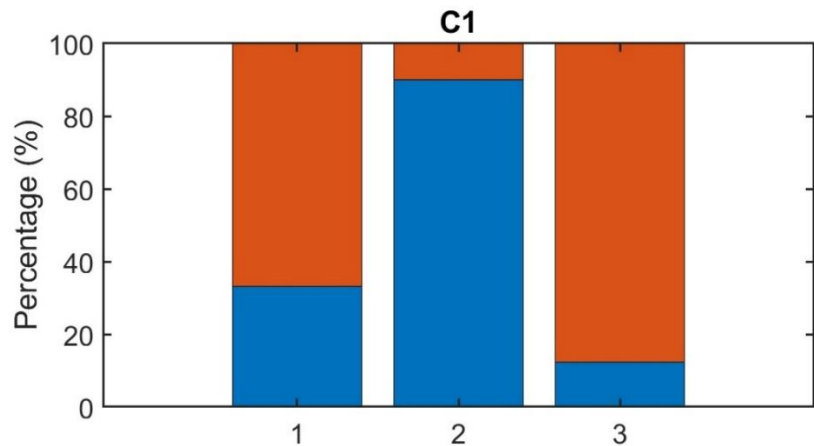


Figure 3.4. The GWP breakdown of the four scenarios based on (a) the stages involved in the production of hydrogen and diesel, and (b) scope 1-3 emissions. It is worth noting that the percentages of the GWP breakdown can be found in Table 2 of the Appendix



- 1- MPW collection, transportation, and sorting
- 2- MPW-to-energy conversion
- 3- Distribution of products and byproducts

Figure 3.4. (continued).

3.3.3. Sensitivity analysis

The impacts of various factors/parameters on GWP for all four scenarios are assessed as shown in Figure 3.5. The results indicate that the uncertainty factor of heating energy used for the conversion process has the greatest influence on the D1 scenario. The changes in GWP related to heating energy for centralized large-scale systems are $\pm 3\text{--}4\%$, which is much lower than the $\pm 6\text{--}9\%$ observed in decentralized small-scale systems.

MPW composition, on the other hand, shows an opposite trend, where changes for centralized systems are higher than for decentralized systems. For example, the change for the C1 scenario is $\pm 0.8\%$, while the D1 scenario shows a change of $\pm 0.3\%$. Regarding the distance from the transfer station to the pyrolysis plant, there are no changes for decentralized systems, whereas centralized systems show variations of $\pm 0.5\text{--}5\%$.

Additionally, Figure 3.5 highlights the differences in changes between diesel and hydrogen scenarios. In general, the uncertainty factors considered in this sensitivity analysis have a greater impact on diesel-producing scenarios than on hydrogen-producing scenarios. For instance, regarding the distance between MPW collection points, diesel-producing scenarios exhibit changes of $\pm 0.25\text{--}0.65\%$, whereas changes for hydrogen-producing scenarios are limited to $\pm 0.04\text{--}0.05\%$.

a)

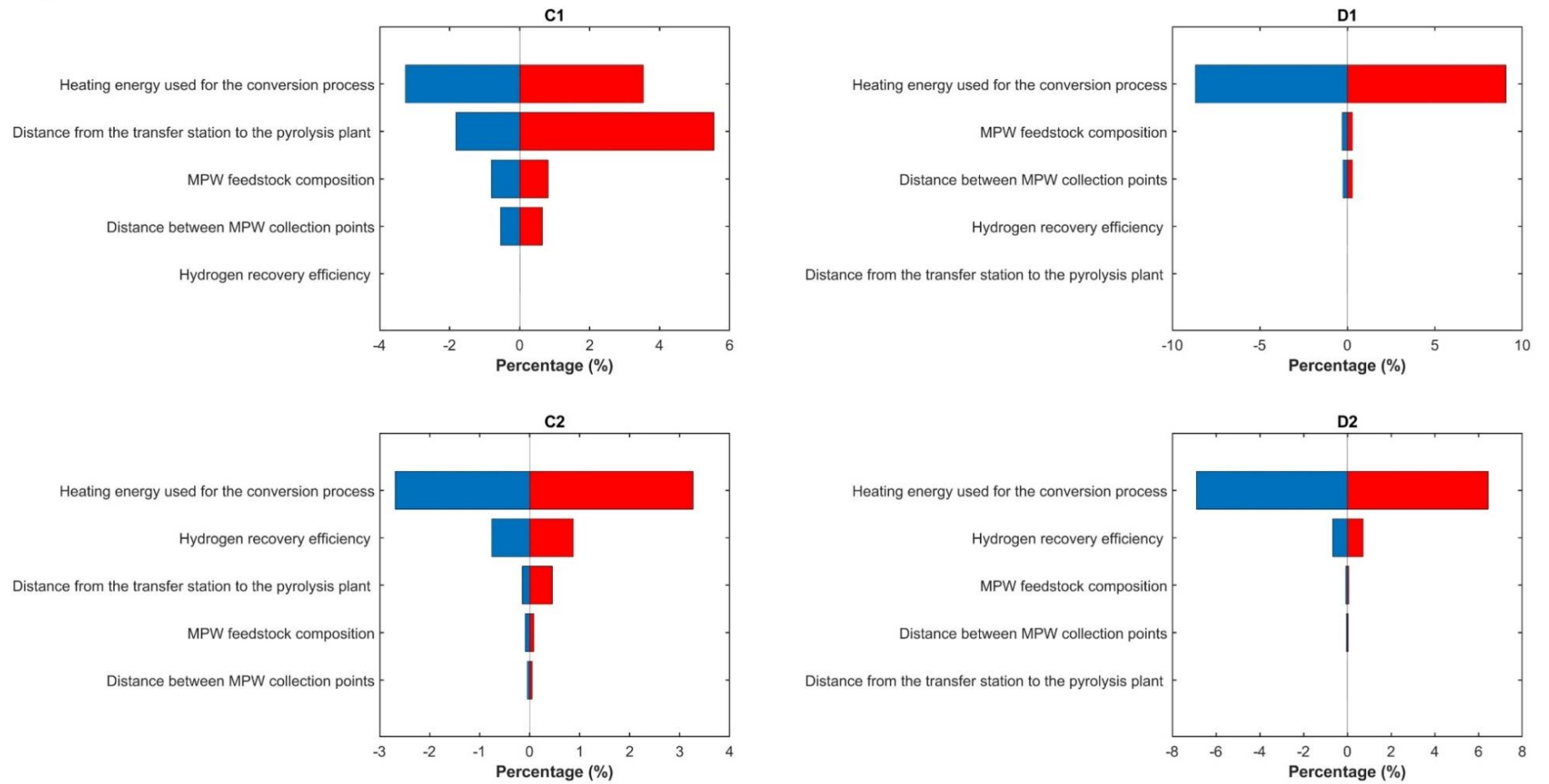


Figure 3.5. Sensitivity map illustrating the impact of factors on GWP ((a) FU is 1 tonne of MPW; (b) FU is 100 km travelled by bus)

b)

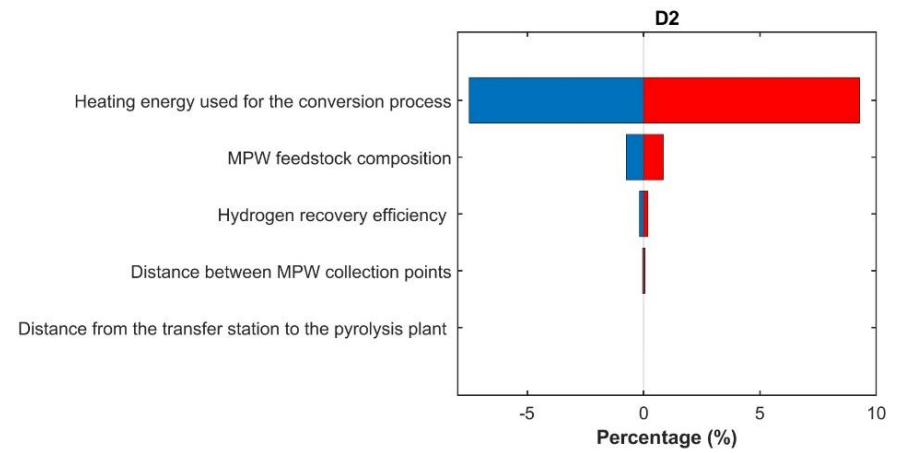
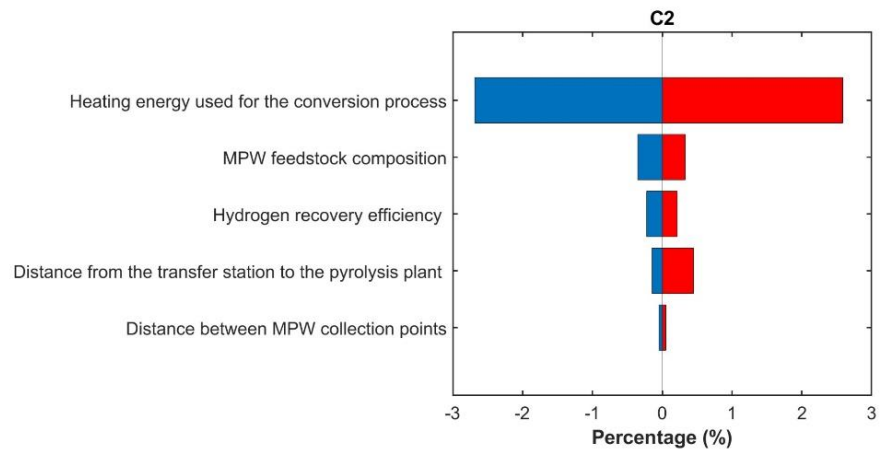
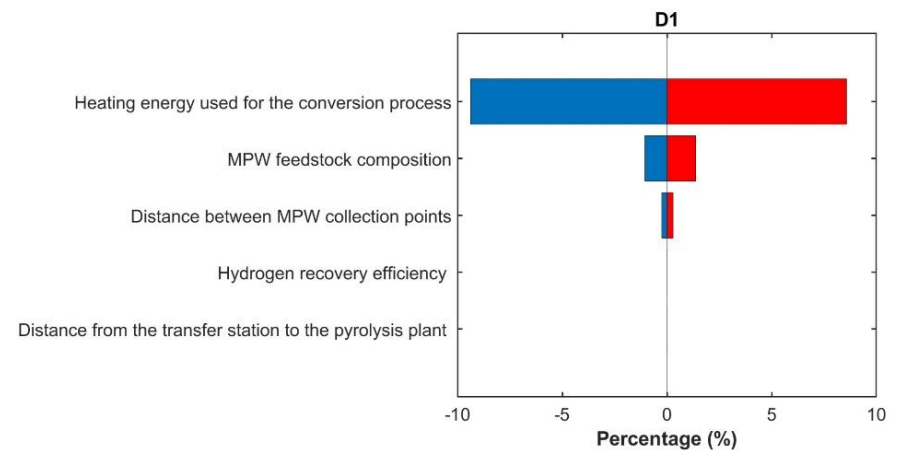
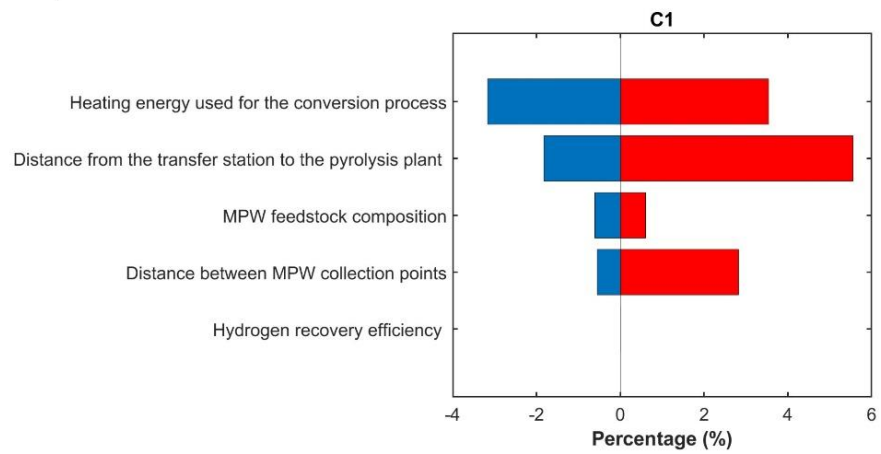


Figure 3.5. (continued).

3.4. Conclusions

This chapter investigated the GWP of centralized and decentralized pyrolysis systems that convert non-recycled MPW to diesel and/or hydrogen. Centralized, large-scale systems producing hydrogen and diesel show better environmental performance than decentralized, small-scale systems. The GWP of hydrogen production is much higher than that for diesel production but the compensation from the end-of-life use of fuels, and the displacement of their production from fossil fuels, as well as heating energy, electricity, and carbon nanotubes, significantly affect the overall GWP results. Decentralized hydrogen production shows the highest GHG emissions (7,989.6 kg CO₂-eq. per tonne of feedstock). Sensitivity analysis shows that centralized systems are less influenced by uncertainty factors compared to the decentralized ones.

After defining the environmental footprint of the systems, it is important to understand their economic feasibility, as the most environmentally efficient systems are not always economically viable. This issue for centralized large-scale and decentralized small-scale diesel and hydrogen production systems from NMPW is addressed in the next chapter.

Chapter 4 Transportation and Process Modelling-Assisted Techno-Economic Assessment of Resource Recovery from Non-Recycled Municipal Plastic Waste

In the previous chapter, the carbon footprint of centralized large-scale and decentralized small-scale NMPW management systems was compared. This chapter logically continues from the previous chapter, where the economic performance of centralized large-scale and decentralized small-scale NMPW systems was defined and compared. This chapter aims to meet objectives 2 and 4, and to fill the knowledge gaps defined in subsection 2.7, in detail, simulate thermochemical conversion processes in Aspen Plus for all considered systems, and defining their economic performance, specifically NPVs.

In the previous chapter, the CCS unit was not considered in all scenarios to evaluate the carbon footprint of the primary systems. While including a CCS unit can positively impact reducing carbon emissions, it comes with trade-offs in the form of carbon taxes, as well as CAPEX and OPEX expenses. Additionally, the UK recently launched the UK ETS to trade GHG emissions, but its economic effectiveness for waste management systems utilizing energy-intensive technologies such as pyrolysis has not been well studied. In this chapter, the economic feasibility of capturing GHG emissions versus emitting them into the atmosphere is compared.

The content of this chapter is based on the published paper in the journal *Energy Conversion and Management* (Biakhmetov et al., 2025).

4.1. Methodology

The methodology is divided into two parts: 1- Modelling, and 2- CBA (Cost-Benefit Analysis). The proposed framework is illustrated in Figure 4.1. In the modelling part, mass and energy

balances for the thermochemical conversion of NMPW into diesel and hydrogen were obtained through Aspen Plus simulation. These results were validated against existing studies. Kinetic parameters for the Aspen Plus simulation were also used. Digimap datasets, containing road networks and dwelling locations in Glasgow, were integrated into ArcGIS Pro to determine the distances between waste collection points, transfer stations, and pyrolysis sites. The mass and energy balances, along with transportation distance data generated for all scenarios, were then subsequently utilized in the CBA. Equipment types (dryer, pyrolysis, SR, oil distillation, WGS, and other units) were selected for all scenarios based on the analysis of their material and energy inputs and outputs, and their Capital Expenditure (CAPEX) and Operational Expenditure (OPEX) were calculated and used to determine their Net Present Value (NPV). Finally, the factors that could have a great impact on NPV results were defined, and sensitivity analysis was conducted to determine their specific impacts on the results.

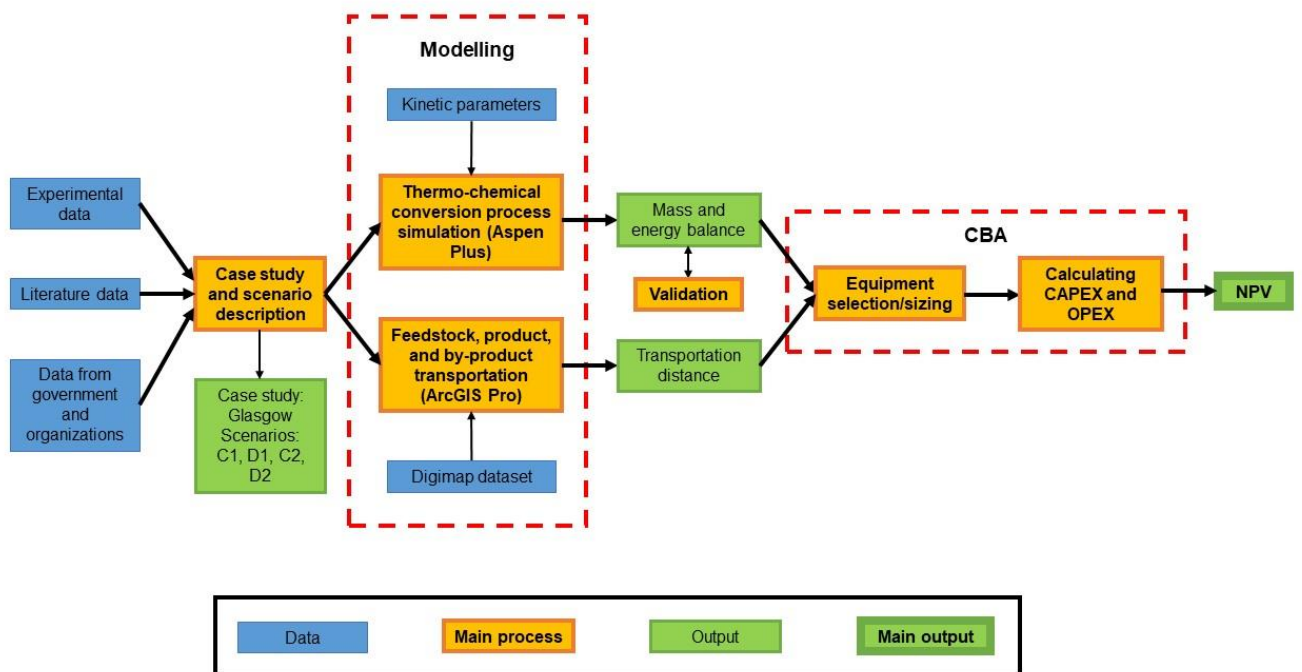


Figure 4.1. Schematic diagram of the proposed framework.

4.1.1. Scenario Descriptions

In this TEA study, one of the largest cities in the UK, Glasgow, was chosen as a case study city same as in LCA study, Chapter 3. This TEA study utilises a detailed case study, as to enhance the ability to assess real-world application of diesel and hydrogen production from NMPW, and to understand the influence of development factors towards the economics of relevant systems. As outlined in Chapter 3, sub-section 3.1.1, the amount of NMPW feedstock for the pyrolysis plants was defined. Overall, annual MPW generation in Glasgow is more than 21,000 tonnes, around 5,500 tonnes of which goes through mechanical recycling (Scottish Environment Protection Agency, 2023). The remaining 15,500 tonnes of NMPW were designated as feedstock. In Glasgow, UK, there are two types of bins where MPW can be disposed, namely recycling and general waste bins (Glasgow City Council, 2023c). Recyclables such as paper, card packaging, drinks cans, food tins, and most of PET and HDPE drink and milk bottles are typically put in the recycling bins. PET and HDPE can be easily separated for other waste fractions and mechanically recycled. Thus, HDPE and PET are most widely recycled compared to other municipal plastics in the UK (British Plastic Federation, 2024). Other NMPW that disposed to the general waste bins with other waste fractions was considered as the feedstock in this TES. The composition of NMPW stream transported to the transfer station was assumed based on the current waste management systems and MSW composition in the UK which described in the supplementary materials.

In this TEA study, four different scenarios, similar to those in the LCA study in Chapter 3, were considered: C1 - centralized large-scale diesel production from NMPW, D1 - decentralized small-scale diesel production from NMPW, C2 - centralized large-scale hydrogen production from NMPW, and D2 - decentralized small-scale hydrogen production from NMPW. In the LCA study, the GWPs of diesel and hydrogen production from NMPW were defined without considering CCS, to assess the carbon footprint of the primary processes

involved in fuel production. As described in Sub-section 2.7, the UK recently launched the UK ETS to facilitate trading of GHG emissions allowances permitted to be released into the environment, with the primary goal of reducing emissions. The allowed amount of GHG emissions will decrease over time, and its price is expected to rise further. However, the current effectiveness of the UK ETS in regulating waste management systems employing energy-intensive technologies, such as pyrolysis or gasification, is not well studied. Therefore, all four scenarios were assessed with and without a CCS unit to evaluate the economic feasibility of carbon capture. All scenarios and their associated processes are illustrated in Figure 4.2.

Three main products are typically obtained from pyrolysis of MPW, namely oil, gas, and solid products, the first two of which require additional steps to be upgraded to transportation fuels (diesel and hydrogen). It is worth noting that different pyrolysis modes and various in-line technologies after the primary pyrolysis step are applied in hydrogen and diesel production. For diesel, pyrolysis and oil distillation as an in-line technology are applied. Additionally, in the hydrogen-producing scenarios considered in the LCA study, slight adjustments were made to process parameters in this TEA study to enhance hydrogen yield. Specifically, Steam Reforming (SR) and Water Gas Shift (WGS) processes are implemented after the pyrolysis reactor.

The MPW collection and transportation systems to the pyrolysis sites for all scenarios are detailed in Figure 4.2(a). The MSW collected from the general waste bins of households is transported to the transfer station located on the outskirts of the city for the C1 and C2 scenarios. NMPW is separated from other waste fractions and then is baled to be transported to the pyrolysis plant. In this TEA study, it was assumed that PET and HDPE are effectively separated, and the remaining MPW was defined as NMPW. In the D1 and D2 scenarios, the MSW containing MPW collected is transported to the transfer station which is located near to

the small-scale diesel and hydrogen production facilities. Notably, these facilities are located on the outskirts of the city.

Diesel and hydrogen production from NMPW have different pyrolysis modes and in-line technologies, as shown in Figure 1(b). In the C1 and D1 scenarios, the pyrolysis temperature is 400°C as this is sufficient to devolatilize the feedstock and is recommended for increasing the yield of oil-like products (Haig et al., 2018). The devolatilization temperature of plastics primarily depends on the heating rate, and it can be adjusted by increasing or decreasing the heating rate. For example, the devolatilization temperature for PS is 387°C at a heating rate of 5°C/min, while it rises to 428°C at a heating rate of 20°C/min (Nisar et al., 2019). It is assumed that the heating rate of 5°C/min was selected to fully devolatilize NMPW at 400°C. In the C1 and D1 scenarios, the pyrolysis temperature is 400°C, and the vapour received from the reactor is pumped into the condenser (Haig et al., 2018). Crude oil is received from the condenser, which is then purified to produce diesel-range oil.

For hydrogen production, fast pyrolysis is typically utilized to generate volatiles which are directly fed into SR and then into WGS reactors to produce hydrogen-rich gas (Shahabuddin et al., 2020). In this study, NMPW goes through fast pyrolysis at 500°C because this is the optimal temperature required to fully devolatilize the plastic feedstock (Santamaria et al., 2021, Singh et al., 2019). In the second SR reactor, syngas is obtained from the reactions of volatiles and steam at 700-800°C. After that, the syngas produced goes through the cleaning unit to remove solid particles and sulphur (Lui et al., 2022a). Then, the cleaned syngas is pumped to the WGS reactor where carbon monoxide reacts with steam to form hydrogen and carbon dioxide. Finally, hydrogen is separated from other gases via single-stage PSA (Pressure Swing Adsorption). In all scenarios, by-products (pyrolysis char, gas, and residues) obtained are combusted to produce heating energy for the main conversion processes. In the scenarios where

they cannot produce sufficient heating energy for this purpose, natural gas is used as a supplementary fuel.

In the C1 and D1 scenarios, diesel produced from NMPW pyrolysis is transported to the oil refinery plant where it is mixed with conventional diesel as it cannot be used alone (Mangesh et al., 2020b). As described in Sub-section 2.5.3.1, the diesel produced from NMPW has properties, such as a lower cetane number and the presence of impurities, which could negatively affect the properties of conventional diesel. Therefore, the produced diesel is transported to the oil refinery plant to undergo further upgrading or blending to meet the required standards for conventional diesel.

In scenarios C2 and D2 the main product is hydrogen, which is transported to the hydrogen refuelling station for hydrogen fuel cell buses for the C2 scenario. The transportation of hydrogen produced for scenario D2 was not considered as it is assumed that the pyrolysis facility is located near to the hydrogen refuelling station (Department for Energy Security and Net Zero and Department for Business, 2022). Captured carbon dioxide emissions from the combustion process are compressed for transport and storage purposes.

Besides technical and logistical details, there are other environmental factors that have profound impacts on the NPV of scenarios. The main environmental factor is GHG emissions, as pyrolysis-based thermochemical conversion processes are energy-intensive, and the heating energy used for these conversion processes is produced from the combustion of by-products and natural gas. GHGs (carbon dioxide (CO₂), nitrous oxide (N₂O), and perfluorocarbons (PFCs)) emitted from combustion to the environment are regulated under UK ETS regulations, and a standard metric, carbon dioxide equivalent (CO₂-eq.), is used to account for overall GHG emissions. Two different methodologies can be applied to define GHG emissions under the UK ETS regulations depending on the sources of GHG emissions: direct measurement and fuel

emission factors. The latter is used when direct measurement is not applicable. In general, the UK ETS is designed to financially incentivize GHG emissions reductions from high-emitting sectors. The total GHG emissions allowed to be emitted will be reduced over time for all participants under the UK ETS, encouraging them to find ways to reduce GHG emissions.

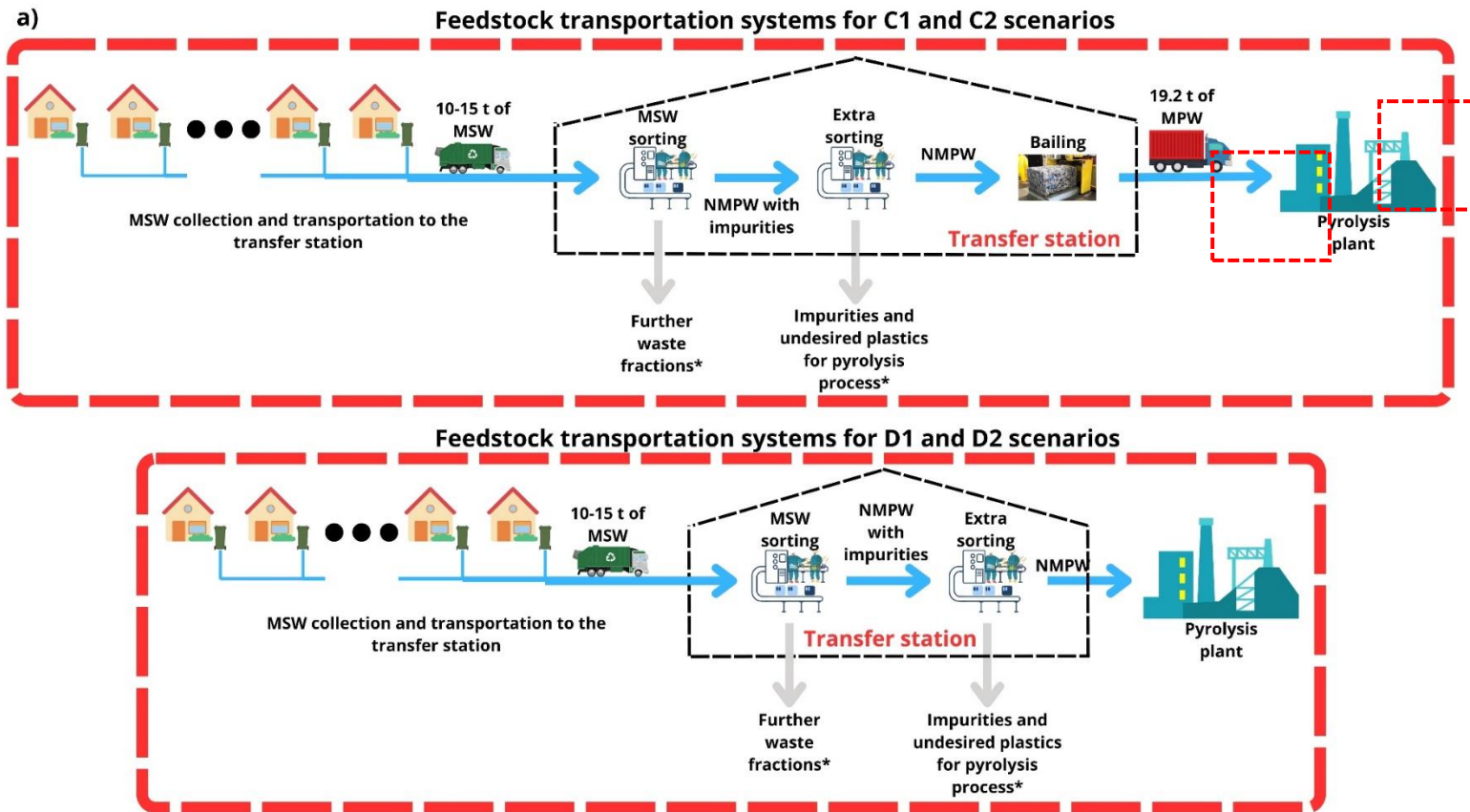
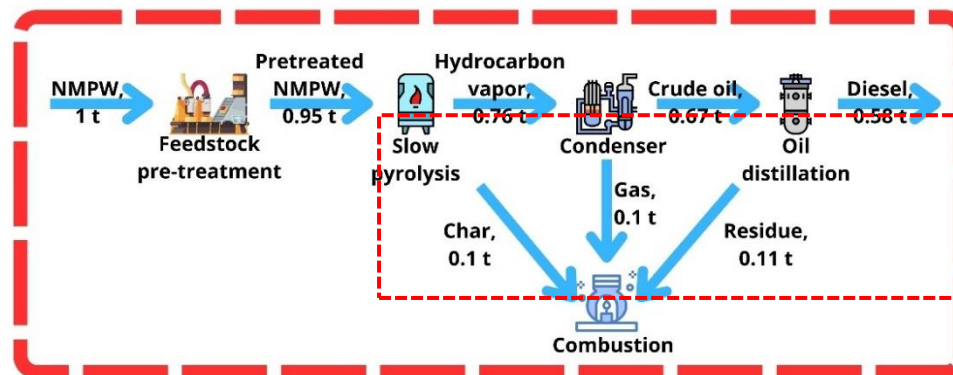


Figure 4.2. Comparison of C1, D1, C2 and D2 scenarios in terms of different sub-processes: a) MPW collection and transportation systems; b) processes involved in the thermo-chemical conversion of NMPW into diesel and hydrogen, and c) product and by-product transportation. *Other separated waste fractions were not considered in this study. The main differences between the scenarios are highlighted with red boxes and dashed red lines

b)

Processes involved in the thermo-chemical conversion of NMPW into diesel for C1 and D1 scenarios



Processes involved in the thermo-chemical conversion of NMPW into hydrogen for C2 and D2 scenarios

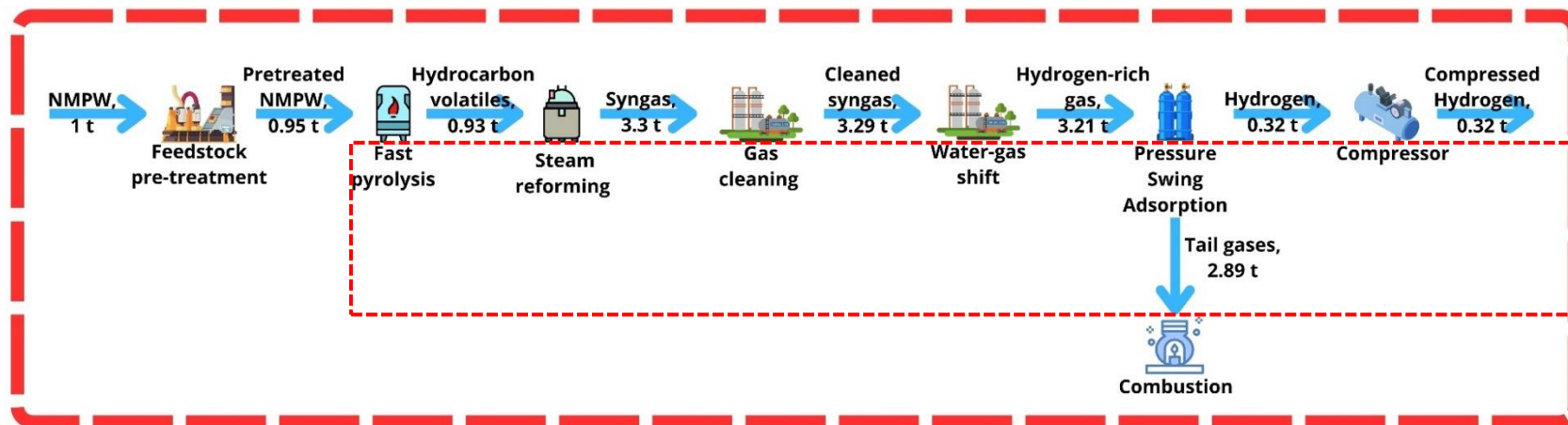


Figure 4.2. (continued).

c)

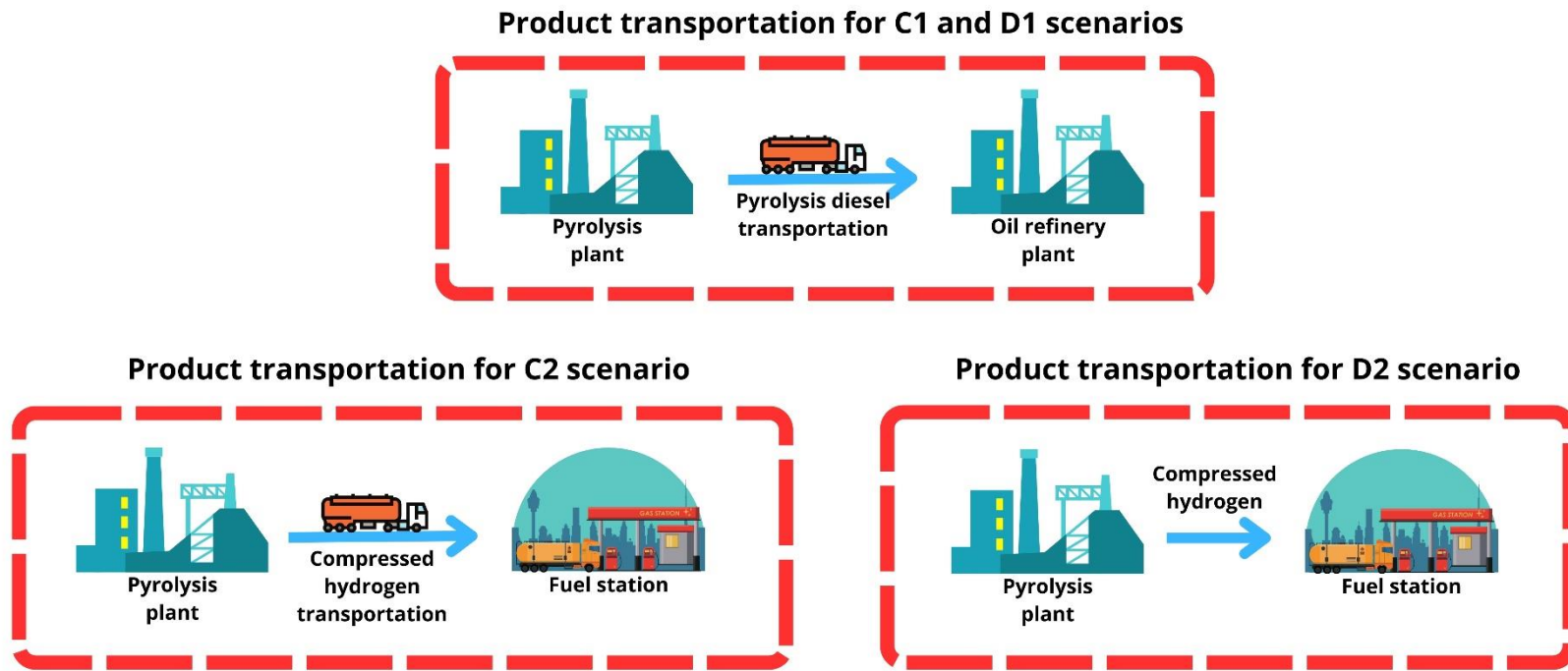


Figure 4.2. (continued).

4.1.2. Model Development

4.1.2.1. Feedstock, Product, and By-product Transportation

The collection and transportation of NMPW, modelled using the ArcGIS Pro software in Chapter 3 (sub-section 3.2.2), was used for this CBA study in this chapter. The main results of this are that the average distance between waste collection points is 17.3 m, and the distance between the transfer station and the pyrolysis site, which is important for the C1 and C2 scenarios, is 100 km.

It was assumed that centralized large-scale fuel production facilities are located in the northeast of Scotland, given the presence of an oil refinery plant in Grangemouth on the Firth of Forth (Haig et al., 2018). While the exact location of these facilities is not specified, a general assumption was made that the distance between the oil refinery and the C1 fuel production facility is approximately 50 km. Additionally, there is a high concentration of infrastructure related to carbon capture, storage, and transportation in the northeast of Scotland, which would allow the cost of CCS to be reduced (SGN and Wood, 2021). For example, CO₂ can be transported from cities such as Dunbar, Mossmorran, and Grangemouth (where the oil refinery is located) to geological formations in the North Sea (Brownsort et al., 2016). Thus, it is reasonable to locate the centralized large-scale pyrolysis plant near the oil refinery and carbon transportation infrastructures. It was assumed that these fuel production facilities are situated close to carbon transportation pipelines, enabling direct pumping of captured carbon into them. For decentralized small-scale facilities, carbon transportation pipelines are not available around Glasgow, and thus trucks were used to transport compressed carbon dioxide to the northeast of Scotland, where carbon storage and transportation infrastructure is available.

4.1.2.2. Thermochemical Conversion of NMPW into Value-added Resources

In the LCA study (Chapter 3), existing literature was used to estimate the inputs and outputs of each process involved in producing fuels. Regarding diesel production, there are sufficient industrial-scale studies providing reliable data for developing scenarios. However, in the case of hydrogen production from plastic waste, the results of lab-scale studies were mostly used to estimate the inputs and outputs of each process involved in hydrogen production. In this Chapter 4, the Aspen Plus V10 software was used to simulate the main thermochemical conversion processes (fast and slow pyrolysis) and in-line processes (SR, oil distillation, WGS, etc.). The obtained results were compared with the findings of existing studies, lending greater credibility to the results presented in this chapter.

First, the simulation process was started with the main input to the systems, NMPW, which is defined as a non-conventional component. The proximate and approximate composition of plastics, LDPE, PP, HDPE, and PS in the NMPW is reported in the Appendix. HCOALGEN and DCOALIGT models are typically used to calculate enthalpies and densities when proximate, ultimate, and sulphur analysis results for non-conventional components are available (Martins et al., 2023). These models were applied for all non-conventional components in this simulation. The method assistant tool available in the software was used to choose the optimal thermodynamic model for conventional components, which in this instance was the Peng-Robinson equation of state. The Peng-Robinson method is notably applied to gain more accurate phase equilibrium predictions in modelling hydrocarbon mixtures at high temperatures, and its equation of state is expressed as:

$$P = \frac{RT}{V - b} - \frac{a}{V^2 + 2bV - b^2}$$

where P is the pressure, R is the universal gas constant, T is the temperature, V is the molar volume, and a and b are substance-specific constants.

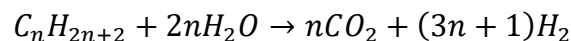
The characteristics of all blocks involved in the simulation process and schematic flow diagrams in Aspen Plus V10 are shown in Table 4.1 and Figure 4.3, respectively. In the first stage (dryer), moisture is removed from NMPW, where a moisture content of 5 wt.% before the drying was assumed based on the study by Haig et al. (2018). The moisture content can vary depending on many factors, such as the time of year and weather conditions. However, LCA study (Chapter 3) shows that variations in moisture have little impact on GWP results due to the relatively low energy requirement compared to other processes. Also, the cost of dryer equipment is much lower than other equipment which can be seen in Table 4.2. Therefore, variations in moisture content were not considered in this CBA study, as it is assumed that they do not have a significant impact on NPV results.

For the pyrolysis and fast pyrolysis stages, the RYield reactor block was applied as the chemical reactions that occur during the pyrolysis process are complex. The RYield reactor is typically employed when only the input and output materials are available or when the reactions occurring in the reactor are complex. The data that describe product yields and compositions from the studies by Haig et al. (2018) and López et al. (2010) were applied for the C1 and D1 scenarios, whilst the data from the studies by Barbarias et al. (2018) and Predel and Kaminsky (2000) were applied for the assumed composition of the volatiles obtained from the fast pyrolysis for the C2 and D2 scenarios.

For the C1 and D1 scenarios, after the pyrolysis process, solid product was separated by a cyclone system. The remaining hydrocarbon vapour was then cooled from 500°C to 300°C, and gases (methane, ethane, ethylene, propene, propane, and hydrogen) were separated from the hydrocarbons in the liquid form (Sahu et al., 2014). This liquid is defined as ‘crude oil’ due to the wide range of hydrocarbons (C₁-C₂₂) it contains, with some of them containing sulphur-based molecules. In the Aspen simulation, the crude oil is pumped to the desulphurisation stage where the sulphur content is reduced by adding hydrogen, which stimulates the breaking of C–

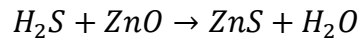
S bonds (Sun et al., 2023, Serefentse et al., 2019, Mello et al., 2023). Diesel-range hydrocarbons (C_7-C_{19}) are then separated from the heavy oil hydrocarbons, which is defined as a residue (C_{20+}).

Volatiles obtained from fast pyrolysis typically contain gaseous hydrocarbons (C_{1-4}), oil hydrocarbons (C_{5-20}), and wax hydrocarbons (C_{21+}), and a recovery rate of these volatiles from fast pyrolysis feedstock is 97-99% (Arregi et al., 2020). Overall, the volatiles obtained contain over 90 hydrocarbon components, with the majority being oil and wax hydrocarbons. These volatiles are fed into the SR reactor to be converted into syngas at 700-800°C (Wu et al., 2014). Instead of considering all over 90 hydrocarbon components, 19 virtual components representing all oil and wax hydrocarbons were chosen to simplify the modelling of the thermochemical conversion process that occurs in the SR reactor (Wang et al., 2023a). In selecting the 19 virtual components, 90 hydrocarbons were grouped based on their physical properties and intermolecular forces. One virtual hydrocarbon was then selected for each group, with its intermolecular force representing the average of the grouped hydrocarbons' intermolecular forces. The majority of the feedstock contains HDPE and LDPE, the fast pyrolysis of which produces more hydrocarbons with linear chain structures (Predel and Kaminsky, 2000). Thus, it was assumed that the majority of virtual hydrocarbons are saturated hydrocarbons with the chemical formula C_nH_{2n+2} . The overall chemical reaction between steam and hydrocarbons in the SR reactor that combines the primary and secondary reactions, can be stated as follows:



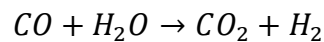
The RStoic reactor is selected for the SR process, as it enables modelling of reactions based on the properties of the reactants and the reaction conditions. Consequently, the reaction efficiencies are not 100%, and the syngas obtained after the SR reactor mainly contains

hydrogen and carbon monoxide, as well as a small volume of other gases and liquid hydrocarbons. Also, the syngas contains a small volume of H₂S which needs to be removed by adding ZnO. The chemical reaction for desulfurization is as follows:



Most of the other contaminants remain in the solid product after the pyrolysis process. It was assumed that the hydrocarbon volatiles do not contain any other contaminants, or if present, they exist in such small quantities that they do not affect the quality of the final products.

Cleaned syngas is pumped to the WGS reactor to maximize hydrogen production. Since the SR process cannot fully convert all hydrocarbons and steam into carbon dioxide and hydrogen, a significant amount of carbon monoxide is produced. In the WGS reactor, carbon monoxide reacts with steam, resulting in an increased hydrogen yield. The chemical reaction is as follows:



The stream obtained from the WGS reactor is then cooled, and water and liquid hydrocarbons are separated from the stream. The stream, which then contains only gases, is pumped to the PSA where the hydrogen, with a purity of 99.999%, is separated from other tail gases. The tail gases that are left after the PSA still contains hydrogen, methane, and other hydrocarbon gases besides carbon dioxide, and are thus combusted for heat recovery purposes.

Finally, the results of diesel and hydrogen production yields were adapted to the FU (functional unit) of a tonne of NMPW to facilitate comparison with the results of existing studies, aiming to assess the credibility of the modelling of the thermochemical conversion processes using Aspen Plus (Haig et al., 2018, Yi et al., 2024, Krüger et al., 2020, Khoo, 2019).

Table 4.1. Description of blocks (Figure 4.3) and their parameters applied in Aspen Plus simulation.

Process	Block (corresponding to Figure 4.3)	Aspen Model	Parameters/Description
C1 and D1 scenarios			
Dryer	B1	RYield reactor	T=100°C, P=1 atm
	B2	Flash2	
Slow Pyrolysis	PYRO	RYield reactor	T=500°C, P=1 atm
	CYCL-1	Sep	100% solid separation
	COOLER-1	Heater Exchanger	T ₁ =500°C, T ₂ =300°C, P=1 atm
	SEP-1	Sep2	100% liquid separation
Crude Oil Distillation	DISTIL	DSTWU	T=300-400°C, P=30-130 atm, average recovery efficiency of diesel range hydrocarbon is 99%, minimum number of stages is 48, reflux ratio is 0.61, pressures for condenser and reboiler are 6- psia
C2 and D2 scenarios			
Dryer	B1	RYield reactor	T=100°C, P=1 atm
	B2	Flash2	
Fast Pyrolysis	FPYRO	RYield reactor	T=500°C, P=1 atm
Steam Reforming	SR	Rstoic reactor	T=700-800°C, P=1 atm
Syngas cooling and cleaning	B1	Heater Exchanger	T _{out} =400°C
	DESULFUR	Rstoic reactor	ZnO was added to remove sulfure
Water Gas Shift	WGS	Rstoic reactor	100% of CO reacts with H ₂ O, T _h =350°C (high temperature-shift), T _l =200°C (low temperature-shift)
	COOLER	Heater Exchanger	T ₁ =700°C, T ₂ =25°C, P=1 atm
	B4	SEP2	100% liquid separation
Pressure Swing Adsorption	PSA	SEP	90% hydrogen separation

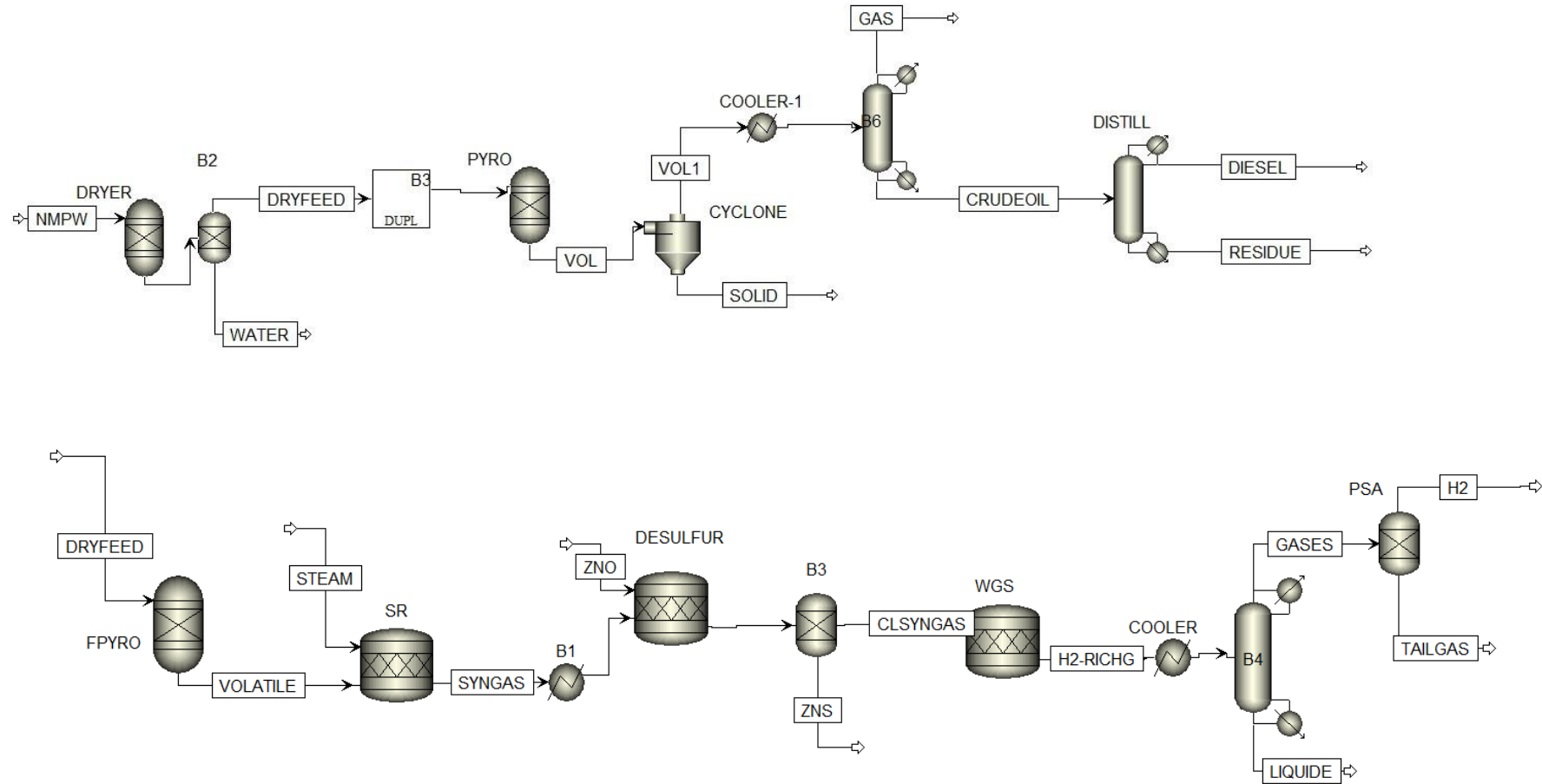


Figure 4.3. Schematic diagrams of the conversion of NMPW to diesel and hydrogen (the top and bottom flow diagrams represent the C1/D1 and C2/D2 scenarios, respectively). In the C2 and D2 scenario diagram, the dryer was not included as a Duplicate Manipulator was used in the C1 and D1 scenario diagram to replicate the dryer process for the C2 and D2 scenarios.

4.1.3. Cost-benefit Analysis

NPV is calculated to compare the economic feasibilities of the scenarios. NPV shows the current value of all cash flows that occur over the lifetime of systems (25 years). A number of studies and reports related to petroleum refinery waste management plants, waste-to-energy facilities, waste recycling facilities, and chemical plants were analysed. Most of these facilities have an operational lifespan of 25 years, which supports the assumption of a 25-year operational period for the pyrolysis plant . NPV for all scenarios was calculated as per the equation below (Fang et al., 2023):

$$NPV = \sum_{n=1}^{n=25} \frac{(I_n - OPEX_n - T_n - TAX_n)}{(1+i)^n} - CAPEX \quad (4.1)$$

where *CAPEX* is the CAPital EXpenditure; *OPEX_n* is the OPERational EXpenditure for the *n*-th operational year; *T_n* is the transportation cost for the *n*-th operational year; *TAX_n* is the payment for GHG emissions for the *n*-th operational year, *I_n* is the income received from selling fuels (hydrogen and diesel) and gate fees for the *n*-th operational year, and *i* is the discount rate, which is 5% (Lui et al., 2022a).

4.1.3.1. Transportation Cost

The Arcgis Pro software was employed to calculate the distances travelled by waste collection trucks, which were then converted into travel time based on an assumed average truck speed. The average time between stops (0.2 min), the average stop duration (0.2 min), and the average tip time (17 min) were incorporated into the calculation (Jaunich et al., 2016). The total time per trip to collect and transport MPW to transfer station was calculated by summing these components with the travel time. The average charge for MPW collection per trip was estimated based on the waste collection charge (£153.5 per hour) for 2023 (Glasgow City Council, 2023b).

The reference year for this study was 2022, and Consumer Price Index (CPI) values were considered to convert base year costs to reference year costs for items that were not from 2022. For example, the waste collection charge for 2023 mentioned above was converted to its equivalent in 2022 using equation (4.2) below:

$$C_{tr.2022} = C_{tr.x} \left(\frac{CPI_{2022}}{CPI_x} \right) \quad (4.2)$$

where $C_{tr.2022}$ is the cost for the reference year, $C_{tr.x}$ is the cost for the base year, and CPI_{2022} and CPI_x are the $CPIs$ for the reference and base years, respectively.

It is worth noting that the reference year, 2022, falls within the post COVID pandemic period, raising questions about how the selected reference year represents the trend in CPI, as many countries experienced economic changes during and after the pandemic. During the COVID period (2020–2021), in the UK, consumer price inflation was approximately 2%, increasing slightly to 2.1% in 2022 and stabilizing around 2% in 2023 and 2024 (Statista, 2025). As seen, despite the pandemic being over, the CPI is gradually increasing over the years, rather than decreasing or remaining at the same level. Since 2022 provided the latest CPI data available at the time of conducting the TEA studies, it was selected as the reference year. If the economy stabilizes further, the CPI is expected to remain close to the 2022 level or slightly higher. To summarize, the CPI for 2022 can be selected as the reference year for this TEA study, as it represents an approximate trend in CPI.

The MSW collected is transported to the transfer station where the MPW is separated from other waste fractions. Sorting and bailing costs of the NMPW were estimated according to the study by Gradus (2020). The bailed NMPW is transported to the diesel and hydrogen production facilities, and its cost was calculated following the approach described by Haig et al. (2018). A fixed price per journey (£225) and additional cost per mile (£1.3) for 2018 were used to calculate the transportation cost from the transfer station to the pyrolysis site. The Eq.

(4.2) was used to convert the base year (2018) values to the reference year (2022) values. The transportation cost of bailed NMPW from the transfer station to the pyrolysis site is £351.22 per journey (based on a fixed price per journey = £258.44 and an additional cost per km = £0.93).

Transportation of 1 kg of compressed hydrogen from the centralized large-scale facility to hydrogen refuelling station in Glasgow costs around £1 per 100 km (Department for Energy Security & Net Zero, 2023c). The tariff for diesel transportation from the transfer station to the pyrolysis plant was obtained from the study Haig et al. (2018).

4.1.3.2. Carbon Tax Cost

For the scenarios without CCS, expenses regarding carbon dioxide emissions depend on the volume of emitted carbon dioxide and where it ends up. The UK ETS carbon price used for carbon dioxide emitted into the atmosphere is quite volatile due to being subject to the open-market system, and in this study the average price (£75.42 per tonne) for the reference year was considered (Ian, 2023). The average cost of transportation of compressed carbon dioxide for the reference year was calculated based on the 2020 price, as described in Eq.(4.3), amounting to £31.33 per tonne carbon dioxide (Department for Energy Security and Net Zero, 2021). For the scenarios with CCS, the efficiency of capturing carbon dioxide is 90%, and the carbon tax is applicable for the remaining carbon dioxide emitted into the atmosphere in the CBA (Singh et al., 2011).

4.1.3.3. Incomes

Overall, two types of income were considered, namely the waste gate fee, and selling products (hydrogen, diesel, and electricity). The waste gate fee is paid to the pyrolysis sites for converting MPW to fuels, and on average it was £110 per a tonne of managed waste for 2022 (Steven and Ashley, 2022). This gate fee does not include any additional costs associated with

transportation or other processes outside the pyrolysis plant. The income from selling the diesel produced was calculated based on the study by Haig et al. (2018), and is £648 per tonne of fuel for the reference year. Since the pyrolysis plant serves a similar role to that of a petroleum refinery—producing diesel but not distributing it directly to customers—the wholesale price of diesel, which is lower than the retail price at petrol stations, was used in this study.

In the case of hydrogen, its market is not as well developed as the diesel and gasoline markets in the UK and in general whole world. There are only a few hydrogen refuelling stations available compared to the diesel or gasoline fuel stations across the UK. The price of hydrogen in these refuelling stations varies greatly, ranging between £10 and £15 per kilogram of fuel, indicating that its price is highly variable in the UK market. The UK has established a Hydrogen Business Model, as to underpin and enable its ambitions of 10 GW low carbon hydrogen production by 2030 (Department for energy Security & Net Zero, 2023b). One of its main aims is to incentivize low carbon hydrogen production by covering the production cost gaps between high and low carbon hydrogen production (high carbon hydrogen is hydrogen produced from fossil fuels; low carbon hydrogen is hydrogen produced through the electrolysis using renewable energy or thermochemical conversion of biomass and different types of waste). Due to the lack of sufficient data regarding hydrogen sales prices in the UK, the average hydrogen sales price data available on the Hydrogen Valley platform was used. It shows that the hydrogen sales price varies between €3-4 and >€10 per kg of hydrogen across the EU (Hydrogen Valley platform, 2024). The sales price of 43.75% of hydrogen produced is in the range of €4-6 per kg of hydrogen in the EU. Therefore, a price of €5 (£4.26) per kilogram of hydrogen was adopted for this study. Although the selected sale price for hydrogen is relatively low compared to green hydrogen, it reflects the broader market reality.

The EU, and particularly the UK, are working on the development of the hydrogen market by investing in large projects, infrastructure, and shaping market and regulatory rules

(van der Spek et al., 2022). Promoting a hydrogen economy is also able to strengthen energy security by democratizing the energy landscape and mitigating the adverse impact of volatile fossil fuel prices, as not all countries have fossil fuel resources, unlike renewables (Carlson et al., 2023). Moreover, the EU and UK have the ambition to reduce green hydrogen production costs to less than €2 and £2.5 per kg of hydrogen, respectively, and increase hydrogen production and storage capacity by 2030 (Department for Energy Security and Net Zero and Department for Business, 2022, Burgess, Statista, 2022). Consequently, reducing hydrogen production costs inevitably reduces the sales price of hydrogen in the market. Therefore, calculating the LCOH (Levelized Cost of Hydrogen) for the C2 and D2 scenarios is important with regard to assessing the economic feasibility of systems under the direction of current development of the hydrogen market. The LCOH for the C2 and D2 scenarios were calculated by dividing the sum of all expenses by the amount of hydrogen produced:

$$LCOH = \frac{\sum_{n=1}^{n=25} \frac{(OPEX_n + T_n + TAX_n)}{(1+i)^n} + CAPEX}{\sum_{n=1}^{n=25} M_n} \quad (4.3)$$

Smart Export Guarantee tariffs are applied to calculate the value of the electricity fed back into the grid system, which will vary greatly depending on the energy supply companies involved. In 2022, these tariffs ranged from 1 p/kWh to 5.57 p/kWh of electricity in the UK (The Renewable Energy Hub, 2023). For this study, a rate of 5 p/kWh of electricity was adopted, as large energy supply companies typically paid between 4 p and 5.57 p/kWh in 2022.

It is worth noting that Smart Export Guarantee tariffs have been increasing over time. For example, Scottish Power offers tariffs of 12–15p/kWh in 2024 (Scottish Power, 2024). If the 2024 tariff were applied to this study, it would not significantly affect the final NPV results, as electricity is only produced in the C1 scenario, and the income from selling electricity accounts for just 0.04% of the total income.

4.1.3.4. CAPEX and OPEX

To calculate the OPEX and CAPEX for fuel production facilities, one must first utilize the mass and energy balances of NMPW-to-hydrogen/diesel for equipment selection and sizing, a summary of which can be seen in Table 4.2. The scale factor for the equipment related to the waste treatment processes and main conversion reactor is typically between 0.6 and 0.8, and was employed in this study (Wu et al., 2023, You et al., 2016). The reference cost of equipment was calculated using Eq. (4.4) and Eq. (4.5). The base costs of equipment were determined from existing studies in the literature and reports, as illustrated in Table 4.2, and were converted to British Pounds (£) using the average exchange rate for the base year. The Chemical Engineering Plant Cost Index (*CEPCI*) was employed to calculate the reference year cost from the base year cost via:

$$C_{2022} = C_{base} \left(\frac{CEPCI_{2022}}{CEPCI_{base}} \right) \quad (4.4)$$

where C_{2022} and C_{base} are the reference and base year costs, respectively, and $CEPCI_{2022}$ and $CEPCI_{base}$ are the *CEPCI* values for the reference and base years, respectively. It is worth noting that the *CEPCI* value for 2022 was used as the reference year as it was the latest available one (Chemical Engineering, 2023). Also, the effect of scale was considered in calculating the equipment cost via:

$$C_{eq.} = C_{2022} \left(\frac{S_{ref}}{S_{base}} \right)^n \quad (4.5)$$

where $C_{eq.}$ is the cost of equipment designed for the scenarios, n is the exponent scale factor for equipment cost, and S_{ref} and S_{base} are the reference and base capacities, respectively.

Table 4.2. Equipment costs for the base year and updated costs for the reference year based on the scale and cost factors considered in the analysis.

Equipment	Scenarios	Base year	Base capacity	Base cost	Cost factor	Scale Factor	Reference year	Reference capacity	Reference cost	Reference
Dryer Unit	C1 and C2	2018	1.25 t/h	\$2,000,000	1.35	0.7	2022	1.8 t/h	£2,616,591	(Haig et al., 2018)
	D1 and D2	2018	1.25 t/h	\$2,000,000	1.35	0.7	2022	0.4 t/h	£914,229	(Haig et al., 2018)
Pyrolysis Unit	C1	2018	0.4 t/h	\$2,000,000	1.35	0.7	2022	1.7 t/h	£5,588,847	(Haig et al., 2018)
	D1	2018	0.4 t/h	\$2,000,000	1.35	0.7	2022	0.4 t/h	£2,029,785	(Haig et al., 2018)
Fast Pyrolysis Unit	C2	2021	10 t/h	\$22,000,000	1.15	0.7	2022	1.7 t/h	£5,327,182	(Yadav et al., 2022)
	D2	2021	10 t/h	\$22,000,000	1.15	0.7	2022	0.4 t/h	£1,934,752	(Yadav et al., 2022)
Steam Reforming Unit	C2	2022	0.15 t/h	€275,000	1	0.75	2022	1.7 t/h	£1,448,599	(Al-Qadri et al., 2023)
	D2	2022	0.15 t/h	€275,000	1	0.75	2022	0.4 t/h	£489,392	(Al-Qadri et al., 2023)
Oil Distillation Unit	C1	2018	1 t/h	\$2,500,000	1.35	0.7	2022	1.4 t/h	£3,211,069	(Haig et al., 2018)
	D1	2018	1 t/h	\$2,500,000	1.35	0.7	2022	0.3 t/h	£1,092,307	(Haig et al., 2018)
Syngas Cleaning Unit	C2	2022	0.25 t/h	€1,177,000	1	0.67	2022	6 t/h	£8,440,442	(Al-Qadri et al., 2023)
	D2	2022	0.25 t/h	€1,177,000	1	0.67	2022	1.3 t/h	£3,029,325	(Al-Qadri et al., 2023)
	C2	2007	233.6 t/h	\$12,918,000	1.55	0.67	2022	6 t/h	£861,818	(Rath et al., 2011)

Water Gas Shift Unit	D2	2007	233.6 t/h	\$12,918,000	1.55	0.67	2022	1.3 t/h	£309,312	(Rath et al., 2011)
Pressure Swing Adsorption Unit	C2	2007	32.99 t/h	\$38,047,000	1.55	0.6	2022	5.8 t/h	£10,401,199	(Rath et al., 2011)
	D2	2007	32.99 t/h	\$38,047,000	1.55	0.6	2022	1.2 t/h	£4,041,433	(Rath et al., 2011)
Hydrogen Compressor Unit	C2	2009	166 t/h	€9,000,000	1.56	0.68	2022	0.6 t/h	£263,909	(Manzolini et al., 2013)
	D2	2009	166 t/h	€9,000,000	1.56	0.68	2022	0.1 t/h	£78,039	(Manzolini et al., 2013)
Carbon Capture Unit	C1	2016	82 t/h	€43,274,000	1.51	0.7	2022	1.3 t/h	£2,935,567	(Rath et al., 2011)
	D1	2016	82 t/h	€43,274,000	1.51	0.7	2022	0.5 t/h	£1,503,871	(Rath et al., 2011)
	C2	2016	82 t/h	€43,274,000	1.51	0.7	2022	33.2 t/h	£28,361,440	(Rath et al., 2011)
	D2	2016	82 t/h	€43,274,000	1.51	0.7	2022	9.8 t/h	£12,072,296	(Rath et al., 2011)

The equipment unit purchase costs (Table 4.2), and labour costs and material and utility inputs were used to calculate the total CAPEX and OPEX (Table 4.3) (Umenweke et al., 2023). The CAPEX contains direct and indirect costs, whilst the OPEX is divided into fixed and variable operating costs. One of the main components of the fixed operating cost is the labour cost, which is dependent on the number of operating staff. The overall number of operators for each scenario was calculated via the following equation (Mukherjee et al., 2022):

$$N_o = \sqrt{(31.7P^2 + 0.23N + 6.29)} \quad (4.6)$$

where P is the number of solid handling steps and N is the number of non-particulate (gas- and liquid-phase) processing steps. The overall number of operators required for each scenario is 12, which was multiplied by the gross annual average pay (£27,710) in Scotland for 2022 to obtain the labour cost (The Scottish Parliament, 2023).

Table 4.3. Equations used to calculate CAPEX and OPEX.

Name	Estimation factors and formulas
Total equipment unit purchase cost	$C_{totaleq.} = \sum C_{eq.}$
Installation cost	$C_{eq.instal.} = 0.4C_{totaleq.}$
Instrumentation and control cost	$C_{instr.} = 0.26C_{totaleq.}$
Mechanical, electrical, and plumbing cost	$C_{m.e.p.} = 0.41C_{totaleq.}$
Building cost	$C_{build.} = 0.1C_{totaleq.}$
Outdoor space work cost	$C_{out.} = 0.12C_{totaleq.}$
Direct cost	$C_{direct} = C_{totaleq.} + C_{eq.instal.} + C_{instr.} + C_{m.e.p.} + C_{build.} + C_{out.}$
Indirect cost	$C_{indirect} = 0.22C_{direct}$
Fixed capital investment	$FCI = C_{direct} + C_{indirect}$
Working capital	$WC = 0.15FCI$
Pre-operating and organization costs	$C_{startup} = 0.05FCI$
CAPEX	$CAPEX = FCI + WC + C_{startup}$
Labor cost	$C_{labour} = N_o * S_{average}$
Supervisory and management cost	$C_{sup.} = 1.25C_{labour}$
Maintenance and miscellaneous expenses	$C_{maint.} = 0.04FCI$
Fixed operating cost	$FOC = C_{labour} + C_{sup.} + C_{maint.}$
Total utility cost	$C_{utility} = C_{electricity} + C_{water} + C_{natural\ gas}$
Operating supplies cost	$C_{supplies} = C_{catalyst} + C_{hydrogen} + \dots$
Variable operating cost	$VOC = C_{utility} + C_{supplies}$
OPEX	$OPEX = FOC + VOC$

The average prices of electricity and natural gas for the reference year in the UK were used to calculate the variable operating costs. Gas and electricity prices vary according to the annual scale of utility consumption for non-domestic sectors in the UK, and this factor was also considered in the analysis (Department for Energy Security and Net Zero, 2023a). Ash and solid by-products produced by the combustion and processes are sent to landfill, and the gate fee paid for landfill, including transportation, is £78 per tonne of waste (Steven and Ashley, 2022).

4.1.4. Sensitivity analysis

Various factors (CAPEX, OPEX, transportation, carbon tax, fuel sales price, inevitably waste gate fee, and average distance between waste collection points) can have significant impacts on the NPV. To compare the influences, sensitivity ratios per changes of key factors with a variation of $\pm 10\%$ were calculated using (Fang et al., 2023):

$$SR = \left| \frac{\frac{NPV_i^b - NPV_i^m}{NPV_i^b}}{\frac{\varphi_i^b - \varphi_i^m}{\varphi_i^b}} \right| \quad (4.7)$$

where NPV_i^b and NPV_i^m are baseline and modified NPV results, respectively; φ_i^b and φ_i^m are baseline and modified factors' value.

It is also worth noting that exploring a wider range of factors with greater variations, such as the selling price of electricity or diesel, conversion efficiency, and others, could provide more comprehensive insights. However, the purpose of this sensitivity analysis is to offer a consistent and comparable measure of the influence of the selected factors on the NPV.

4.2. Results and Discussion

4.2.1. Inputs and Outputs of the Developed Models

A summary of the transportation distances for the products and by-products is given in Table 4.4. On average, the truck makes 1183 stops to collect general bin waste and covers over 20 km per trip in all scenarios. In the C1 and C2 scenarios, the bailed sorted NMPW is transported to hydrogen and pyrolysis diesel production plants located 100 km away. Additionally, empty returns were taken into account for the bailed NMPW transportation in calculating the cost of transportation.

Table 4.4. Transport distances.

Transported material	Transport from	Transport to	Distance, km
MPW	Households	Transfer station	25
NMPW*	Transfer station	Pyrolysis facility	100
Pyrolysis diesel	Pyrolysis facility	Oil refinery plant	100
Hydrogen*	Pyrolysis facility	Hydrogen refuelling station	100
Compressed carbon dioxide**	Pyrolysis facility	Carbon storage and transportation infrastructure	70

*These transportation distances are only for centralized NMPW management systems. **These transportation distances are only for decentralized NMPW management systems.

A summary of the main inputs and outputs obtained from the mass and energy balance analysis for the C1/D1 and C2/D2 scenarios is presented in Tables 4.5 and 4.6, respectively. It is evident that the large-scale systems (C1 and C2) exhibit higher efficiencies in heating energy consumption compared to the small-scale systems (D1 and D2). For example, for the C1 system, the heating energy consumption for drying, pyrolysis, and oil distillation is 11,356 MJ/h, which is significantly lower than the heating energy recovered from the combustion of by-products, at 16,239.18 MJ/h. Consequently, a CHP system was implemented to utilize

excess heating energy to generate electricity, amounting to 4,883.68 MJ/h for the C1 scenario. Conversely, for the D1 scenario, the heating energy consumption for all processes totalled 7,191.82 MJ/h, much greater than the heating energy recovered from the combustion of by-products (3,427.37 MJ/h). Therefore, natural gas was combusted to compensate for the heating energy deficiency in this scenario.

In all scenarios, thermochemical conversion processes consume a significant amount of energy. For instance, for the large-scale plant in the C2 scenario, fast pyrolysis and SR processes consume 9751 MJ/h and 36,332 MJ/h of energy, respectively, which are much greater than the energies consumed by any other stages. Moreover, the thermochemical conversion processes require steam to produce hydrogen-rich gas for the C2 and D2 scenarios, which results in the increased energy consumption for these systems.

Across all scenarios, approximately 90% of total carbon dioxide emissions are captured and sent to deep geological formation sites in the North Sea. For large-scale plants, the transportation of captured carbon is not considered within the systems, as these plants are situated near existing carbon dioxide transportation infrastructure that convey the captured carbon to storage sites in the North Sea. Conversely, in the case of decentralized small-scale plants, captured carbon is transported to the northeast of Scotland, as illustrated in Table 4.4, where a carbon storage and transportation infrastructure is available.

Table 4.5. Mass and energy balances for the C1 and D1 scenarios.

Process stage		C1	D1	Comment	Reference
	Inputs				
Dryer Unit	NMPW, kg/h	1,800	380	After the dryer, the moisture content of NMPW is less than 1 wt%	Aspen Plus simulation, (Haig et al., 2018), (C3)
	Heating energy, MJ/h	816	517		
	Outputs				
	Dried NMPW, kg/h	1,710	361		
	Water vapour, kg/h	90	19		
Pyrolysis Unit	Inputs			T=500°C, P=1 atm	Aspen Plus simulation, (Haig et al., 2018), (C3)
	Dried NMPW, kg/h	1,710	361		
	Heating energy, MJ/h	9,751	6,176		
	Outputs				
	Crude Oil, kg/h	1,368	289		
	Gas, kg/h	171	36		
	Solid product, kg/h	171	36		
Oil Distillation Unit	Inputs			Residue contains hydrocarbons heavier than diesel-range hydrocarbons	Aspen Plus simulation, (Haig et al., 2018), (C3)
	Crude Oil, kg/h	1,368	289		
	Heating energy, MJ/h	788	499		
	Hydrogen, kg/h	14	3		
	Outputs				
	Pyrolysis diesel range oil, kg/h	1,187	251		
	Residue, kg/h	181	38		

Heat Recovery and Electricity Generation Unit	Inputs		RStoic reactor was used to simulate this process. Heat recovery efficiency is 80% of produced heating energy; fuel to electricity conversion efficiency is 33-36%.	Aspen Plus simulation, (EPA, 2023), calculated	
	Gas, kg/h	171			36.1
	Solid product, kg/h	171			36.1
	Residue, kg/h	181			38
	Natural gas, kg/h	-			94
	Air, kg/h	7,010			3,211
	Outputs				
	Net heating energy, MJ/h	11,356			7,192
	Electricity, MJ/h	4,884			-
	Exhaust gasses, kg/h	7,475			3,400
Ash, kg/h	58	15			
Carbon Capture Unit	Inputs		The carbon capture efficiency is 90%. The energy penalty for this unit is 7.9% of the Lower Heating Value (LHV) points.	(Singh et al., 2011), (Rubin et al., 2007) and (Peeters et al., 2007)	
	Exhaust gasses, kg/h	7,475			3,400
	Electricity, MJ/h	1,604			339
	Outputs				
	Scrubbed gasses, kg/h	6,204			2,908
Captured and compressed carbon dioxide, kg/h	1,271	493			

Table 4.6. Mass and energy balances for C2 and D2 scenarios

Process stage		C1	D1	Comment	Reference
	Inputs				
Dryer Unit	NMPW, kg/h	1,800	380	After the dryer, the moisture content of NMPW is less than 1 wt%	Aspen Plus simulation, (Haig et al., 2018), (C3)
	Heating energy, MJ/h	816	517		
	Outputs				
	Dried NMPW, kg/h	1,710	361		
	Water vapour, kg/h	90	19		
Fast Pyrolysis Unit	Inputs			T=500°C, P=1 atm	Aspen Plus simulation, (Ahamed et al., 2020), (C3)
	Dried NMPW, kg/h	1,710	361		
	Heating energy, MJ/h	9,751	6,176		
	Outputs				
	Volatiles, kg/h	1,676	354		
	Solid product, kg/h	34	7		
Steam Reforming Unit	Inputs			T=700-800°C, P=1 atm.	Aspen Plus simulation, (Yi et al., 2024)
	Volatiles, kg/h	1,676	354		
	Steam, kg/h	4,283	904		
	Heating energy, kg/h	36,332	7670		
	Outputs				
	Syngas, kg/h	5,959	1,258		
Syngas Cooling and	Inputs				

Cleaning Unit	Syngas, kg/h	5,959	1,258	Overall, 100% of zinc sulphide is recovered from the reaction of hydrogen sulphide and zinc oxide.	Aspen Plus simulation, (Lui et al., 2022b), (Spallina et al., 2016), and (Lui et al., 2022a)
	Electricity, kg./h	534	113		
	Zinc oxide, kg/h	89	19		
	Outputs				
	Cleaned syngas, kg/h	5,938	1,253		
	Zinc sulphide, kg/h	111	23		
Water Gas Shift Unit	Inputs			Carbon monoxide is reacted with steam to maximize hydrogen production	Aspen Plus simulation, (Lui et al., 2022b), and (Lui et al., 2022a)
	Cleaned syngas, kg/h	5,938	1,253		
	Electricity, MJ/h	178	38		
	Outputs				
	Hydrogen rich gas, kg/h	5,794	1,223		
	Water, kg/h	144	30		
Pressure Swing Adsorption Unit	Inputs			Hydrogen recovery efficiency is 90%	Aspen Plus simulation, (Ronald Long, 2011), (C3)
	Hydrogen-rich gas, kg/h	5,794	1,223		
	Electricity, MJ/h	5,215	1,101		
	Outputs				
	Hydrogen, kg/h	569	120		
	Tail gas, kg/h	5,224	1,103		
	Inputs				(Lui et al., 2022b), (C3)
	Hydrogen, kg/h	569	120		

Hydrogen Compression and Storage Unit	Electricity, MJ/h	6,457	1,363	Hydrogen is compressed to 200 bar	
	Outputs				
	Compressed hydrogen, kg/h	569	120		
Heating Energy and Steam Generation Unit	Inputs			2.5 MJ of energy is required to produce 1 kg of steam	Aspen Plus simulation, GaBi database
	Tail gas, kg/h	5,161	1,103		
	Air, kg/h	26,757	5,708		
	Natural gas, kg/h	1,300	277		
	Water, kg/h	4,283	904		
	Outputs				
	Heating energy, kg/h	46,899	14,363		
	Exhaust gasses, kg/h	33,184	9,766		
	Steam, kg/h	4,283	904		
Carbon Capture Unit	Inputs			The carbon capture efficiency is 90%. The energy penalty for this unit is 7.9% of the Lower Heating Value (LHV) points.	(Singh et al., 2011), (Rubin et al., 2007) and (Peeters et al., 2007)
	Exhaust gasses, kg	33,184	9,766		
	Electricity, MJ	5,477	1,612		
	Outputs				
	Scrubbed gases, kg/h	25,473	7,497		
	Captured and compressed carbon dioxide, kg/h	7,711	2,269		

The credibility of the developed Aspen models with regards to the thermochemical conversion of NMPW into fuels (diesel and hydrogen) was assessed by comparing the results of diesel and hydrogen production yields with those of other studies. Figure 4.4 reports the yields of diesel and hydrogen production per tonne of MPW feedstock, and the percentage differences between this study's results and those of other studies. A number of studies were selected for comparison based on similarities in technological and thermochemical conversion setups. However, it was not possible to select studies with identical setups to those in this study due to as the difficult of matching various factors such as the composition of MPW feedstock, temperature, and residence time of the thermochemical conversion processes. It is worth noting that this study was based on Glasgow (UK), and there are few available studies that are directly comparable due to the differences in the systems, technologies and process designs. Hence, the results of the comparison are indicative and will more tend to support collective understanding of cost hotspots and the development of a more complete picture about the economic outlook of similar technologies.

Overall, diesel production yield is 659 kg per tonne of NMPW for the C1 and D1 scenarios, whilst 316 kg of hydrogen is produced per tonne of NMPW for the C2 and D2 scenarios. The results of the verification analysis show that the deviation in diesel production yields between this study and others is generally less than 5%, while in the case of hydrogen production yields, the deviation is more than 20%. This difference can be explained by the availability of existing studies assessing diesel production from MPW, allowing for more accurate parameter selection in model development for the C1 and D1 scenarios. There are limited studies related to hydrogen production from MPW through fast pyrolysis-SR, the majority of which are lab-based studies. However, the model developed for hydrogen production can still be utilized despite the deviation being relatively significant as it could indicate the general potential of hydrogen production from NMPW. Future studies could

potentially address this issue to develop a more accurate model of hydrogen production through fast pyrolysis-SR by increasing the available data regarding hydrogen production from MPW through this process.

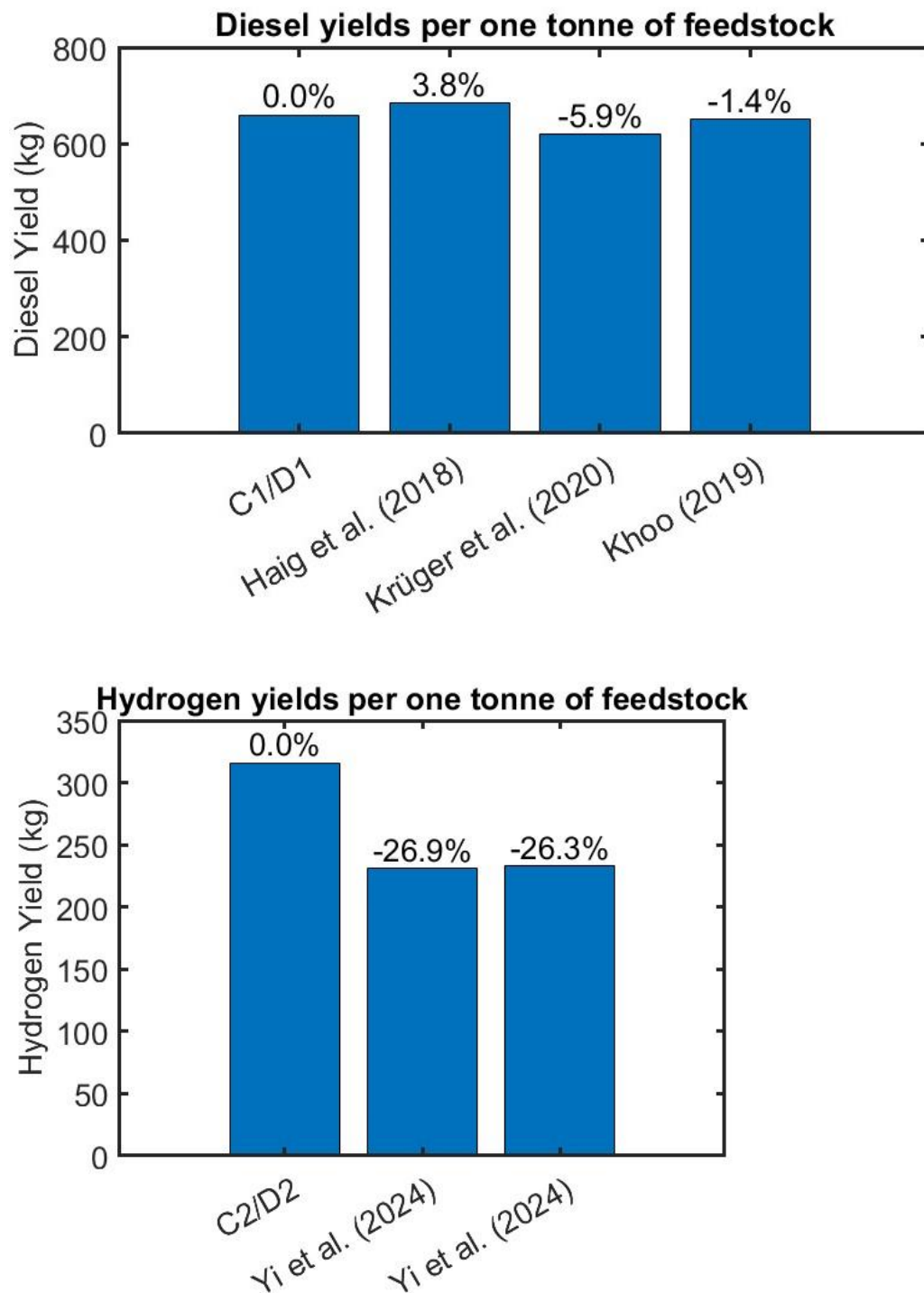


Figure 4.4. Verification of modelling results of thermochemical processes simulated in Aspen plus.

4.2.2. Cost-Benefit Analysis Results

The detailed results of the CBA, including all expenditures and incomes, as well as the total NPV results for each scenario, are reported in Table 4.7 and illustrated in Figure 4.5. Across all scenarios, only centralized large-scale diesel production from NMPW has a positive NPV (£22,240,135 and £24,449,631 for C1 with and without CCS, respectively). The lowest negative NPV is from the C2 scenario with CCS (-£435,744,891) and without CCS (-£326,392,536) compared to the other two scenarios, with the D1 and D2 scenarios showing negative NPV results. However, the C2 scenario demonstrates better economic performance than the D2 scenario when their NPV results are adapted to one tonne of treated NMPW. The NPVs per tonne of treated NMPW for C2 with and without CCS are -£1125 and -£842, respectively, which are higher than the NPVs per tonne of treated NMPW for the D2 scenario with (-£2391) and without (-£1525) CCS. This suggests that when waste management systems with different scales, as in this study, are compared, it is important not only to assess the total NPV of systems but also their NPV results as normalized to the FU, such as per a certain amount of treated waste.

When comparing centralized large-scale and decentralized small-scale waste management systems, aside from the scales and efficiencies of the systems, transportation plays a crucial role. In some existing studies, it was supposed that transportation costs should be higher for centralized systems than decentralized (Pires Costa et al., 2022). It is indeed the case that transportation cost per FU for centralized large-scale systems is lower than for the decentralized small-scale systems considered in this study. For example, the transportation cost per tonne of treated NMPW is £221 for the C1 scenario without CCS, which is approximately 10% lower than for the D1 scenario without CCS. However, the CBA of the transportation part revealed that poor or undeveloped infrastructure related to waste management systems could negatively affect the cost of product and by-product transportation. In this study, it was assumed

that centralized large-scale plants are located in the northeast of Scotland, close to carbon dioxide transportation pipelines and storage infrastructure, while compressed carbon dioxide captured from decentralized small-scale facilities located on the outskirts of Glasgow needs to be transported to the northeast of Scotland due to the lack of carbon dioxide transportation and storage infrastructures around the city. Thus, in systems with CCS units, the transportation costs per tonne of treated NMPW for decentralized systems are higher than those for centralized systems. For example, the transportation costs for the D2 scenario with CCS are £694 per tonne of treated NMPW, which is much higher than the transportation costs for the C2 scenario with CCS (£525 per tonne of treated NMPW). This implies that in the development and analysis of the transportation components of waste management systems, factors such as distance and the condition or availability of infrastructure affecting transportation costs need to be accounted for.

Two options to deal carbon dioxide emissions were considered, namely emitting it into the atmosphere under the UK ETS regulations or capturing it for storage it in deep geological formations. In the case of emitting carbon dioxide into the atmosphere, £916,814, £358,666, £5,564,475, and £1,651,525 need to be paid annually for the C1, D1, C2, and D2 scenarios under the UK ETS regulations, respectively. This payment can be reduced by 90% for all scenarios if the CCS unit is used to capture carbon dioxide emissions. This results in other expenditures for the CAPEX and OPEX of CCS unit, of course, and for transportation of compressed captured carbon dioxide. From Table 4.7 and Figure 4.5, it can be seen that capturing carbon dioxide for diesel and hydrogen production from NMPW is not economically beneficial as the NPV results for systems that include CCS are lower than the results for systems without CCS for all scenarios. Thus, the question arises regarding the effectiveness of UK ETS in promoting the CCS option and reducing GHG emissions from the waste management systems using energy-intensive technologies. This issue should be investigated in

depth to find ways of making capturing carbon dioxide more economically viable or developing scenarios that strike the balance between carbon footprint and economic benefits.

There are a few sources of income in all scenarios such as waste gate fees, and selling product fuels (diesel and hydrogen) and electricity. The income from selling the fuels (diesel and hydrogen) produced is much greater than the income possible from other sources. For example, in the D1 scenario, selling diesel resulted in £1,409,783 per year, which accounts for around 80% of the total income.

The results of this study showed that the real-world demonstrator scenario C1 producing diesel, is economically feasible, whereas other alternatives are not. The alternative scenarios were developed based on the consideration of the current situation in Glasgow, and there are ways to potentially improve NPVs. For example, diesel and hydrogen production through pyrolysis-based technologies are thermal energy-intensive. In all scenarios, natural gas and by-products (tail gases, oil distillation residues, etc.) are used to generate the necessary heating energy. This results in GHG emissions and expenses related to addressing them. Integrating low-carbon energy generation technologies (such as wind or solar energy) with hydrogen and diesel production systems from NMPW can reduce GHG emissions. However, there are additional expenses associated with deploying renewables. This study showed that capturing carbon dioxide is not economically attractive due to the high CAPEX and OPEX of the CCS unit and the underdeveloped CCS infrastructure around Glasgow. In future alternative scenarios, the development of CCS infrastructure and other tools, such as government subsidies to reduce the cost of CCS, can be considered for boosting both profitability and carbon saving potential of the systems.

Table 4.7. The summary of incomes and expenditures in GBP.

	Scenarios							
	C1 with CCS	C1 without CCS	D1 with CCS	D1 without CCS	C2 with CCS	C2 without CCS	D2 with CCS	D2 without CCS
Process information								
Annual NMPW input, t	15,500	15,500	3,300	3,300	15,500	15,500	3,300	3,300
Operational lifetime, years	25	25	25	25	25	25	25	25
Annual saleable hydrogen output, t	-	-	-	-	4,903	4,903	1,044	1,044
Annual saleable diesel output, t	10,222	10,222	2,176	2,176	-	-	-	-
Annual saleable electricity output, kWh	7,845,820	11,681,636	-	-	-	-	-	-
CAPEX								
Total fixed capital investment, £	40,106,390	31,905,003	15,478,189	11,276,674	161,270,996	82,034,804	63,890,788	30,163,208
Total working capital, £	6,015,958	4,785,750	2,321,728	1,691,501	24,190,649	12,305,221	9,583,618	4,524,481
Total pre-operating costs and organization costs, £	2,005,319	1,595,250	773,909	563,834	8,063,550	4,101,740	3,194,539	1,508,160
Total CAPEX, £	48,127,668	38,286,004	18,573,827	13,532,009	193,525,195	98,441,765	76,668,946	36,195,849
OPEX								
Annual fixed operating cost, £	2,352,426	2,024,370	1,367,298	1,199,237	7,199,010	4,029,562	3,303,802	1,954,698
Annual variable operating cost, £	38,948	38,948	787,637	597,519	16,382,125	13,972,789	3,872,157	3,113,909
Total annual OPEX, £	2,391,373	2,063,318	2,154,935	1,796,756	23,581,135	18,002,351	7,175,958	5,068,607
Transportation								
Annual feedstock collection, segregation, and transportation cost, £	3,234,252	3,234,252	628,217	628,217	3,234,252	3,234,252	628,217	628,217
Annual compressed carbon dioxide transportation, £	0	0	134,093	0	0	0	617,450	0
Annual product transportation, £	186,979	186,979	39,808	39,808	4,903,497	4,903,497	1,043,970	1,043,970
Total annual transportation cost, £	3,421,231	3,421,231	802,118	668,025	8,137,749	8,137,749	2,289,637	1,672,187
Carbon Tax Cost (UK ETS)								

Total annual Carbon Tax Cost (UK ETS), £	91,681	916,814	35,867	358,666	556,447	5,564,475	165,153	1,651,525
Income								
Annual gate fee income, £	1,705,000	1,705,000	363,000	363,000	1,705,000	1,705,000	363,000	363,000
Annual product sales income, £	17,227,713	17,419,503	3,584,316	3,584,316	49,034,973	49,034,973	10,439,704	10,439,704
Total annual income, £	18,932,713	19,124,503	3,947,316	3,947,316	50,739,973	50,739,973	10,802,704	10,802,704

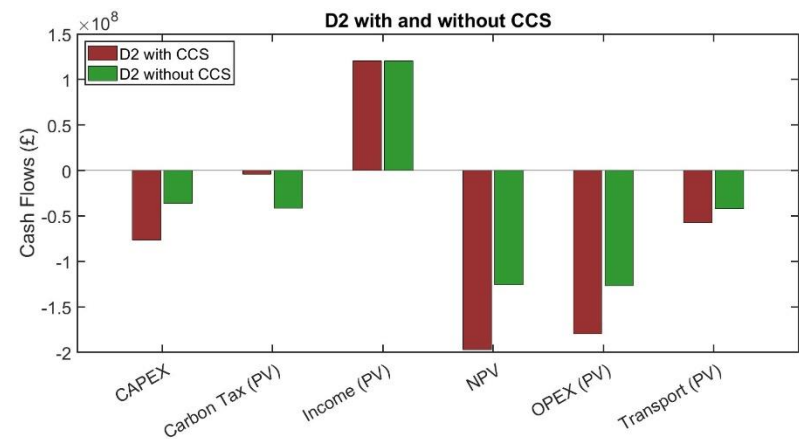
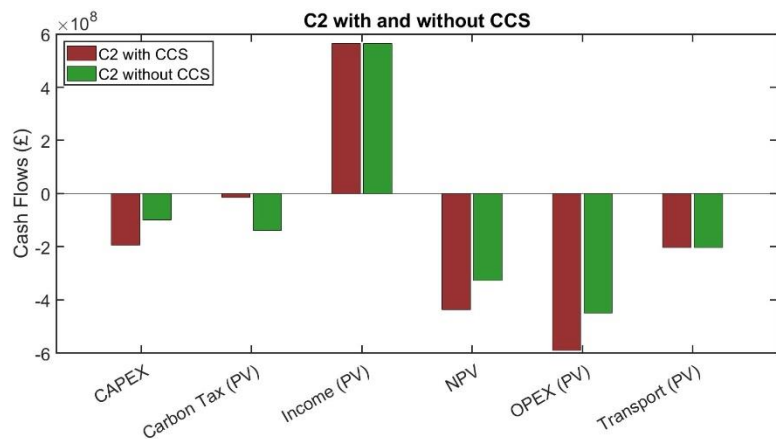
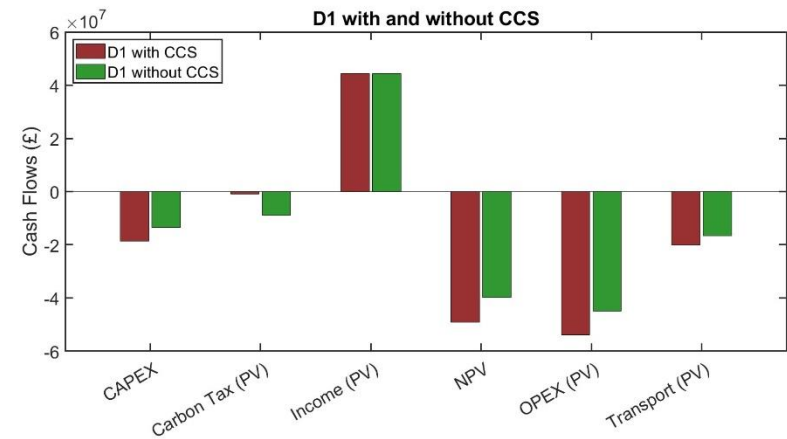
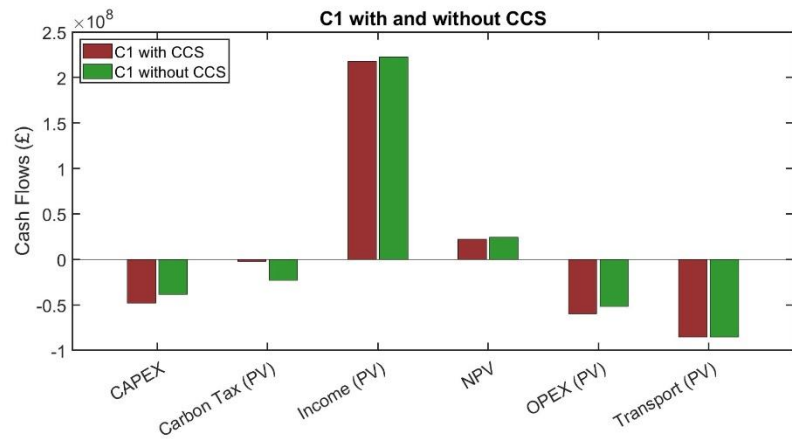


Figure 4.5. PVs for all cash flows over operational time and NPV results for all scenarios, with and without CCS.

4.2.2.1. Levelized Cost of Hydrogen

For the NPV calculation, the average sales price of hydrogen was considered. However, as described in section 4.1.3.3, the hydrogen market is currently not well developed, and the hydrogen sale price is relatively variable compared to the price of diesel. Moreover, the UK and EU have the ambition to reduce the production costs of green hydrogen soon, which will affect the hydrogen sale price. Thus, the LCOH for hydrogen production scenarios with and without CCS were calculated to clarify the cost structure and competitiveness with hydrogen production technologies.

The LCOH per kg of hydrogen for the C2 and D2 scenarios with and without CCS is illustrated in Figure 4.6. The lowest LCOH is £7.27 per kg of hydrogen for the centralized large-scale system without CCS, whilst the highest LCOH is £12.16 per kg of hydrogen for the decentralized large-scale system with CCS. It is worth noting that capturing carbon dioxide for both the centralized and decentralized systems increases the LCOH.

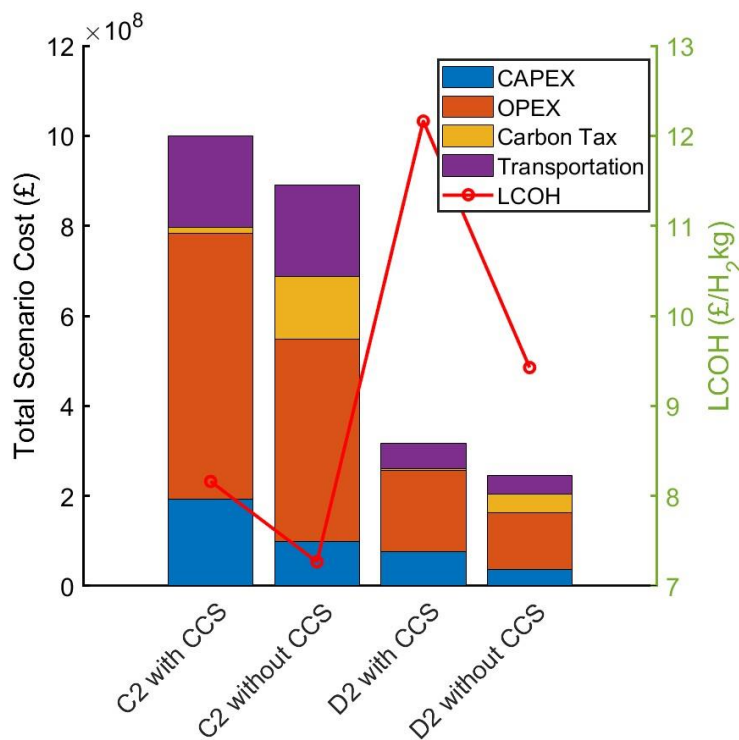


Figure 4.6. Comparison of LCOHs across the hydrogen producing scenarios.

4.3. Sensitivity Analysis

The sensitivity ratio results of key factors are illustrated in Figure 4.7. Notably, sensitivity ratios of CAPEX and OPEX for the scenarios with CCS are higher than those for the scenarios without CCS. However, the sensitivity ratios of carbon tax present a contrasting outcome, with lower values observed for scenarios with CCS compared to those without CCS. According to Ouderji et al. (2023), if the threshold sensitivity ratio value was considered to be 0.2, and a ratio higher than the threshold indicates a high level of impact. The source does not provide a detailed explanation for selecting 0.2, but this benchmark is widely applied in the sensitivity analysis of many studies (Fang et al., 2023). Accordingly, factors such as OPEX and fuel sales prices exhibit high influence on the results across all scenarios with ratios higher than 0.2.

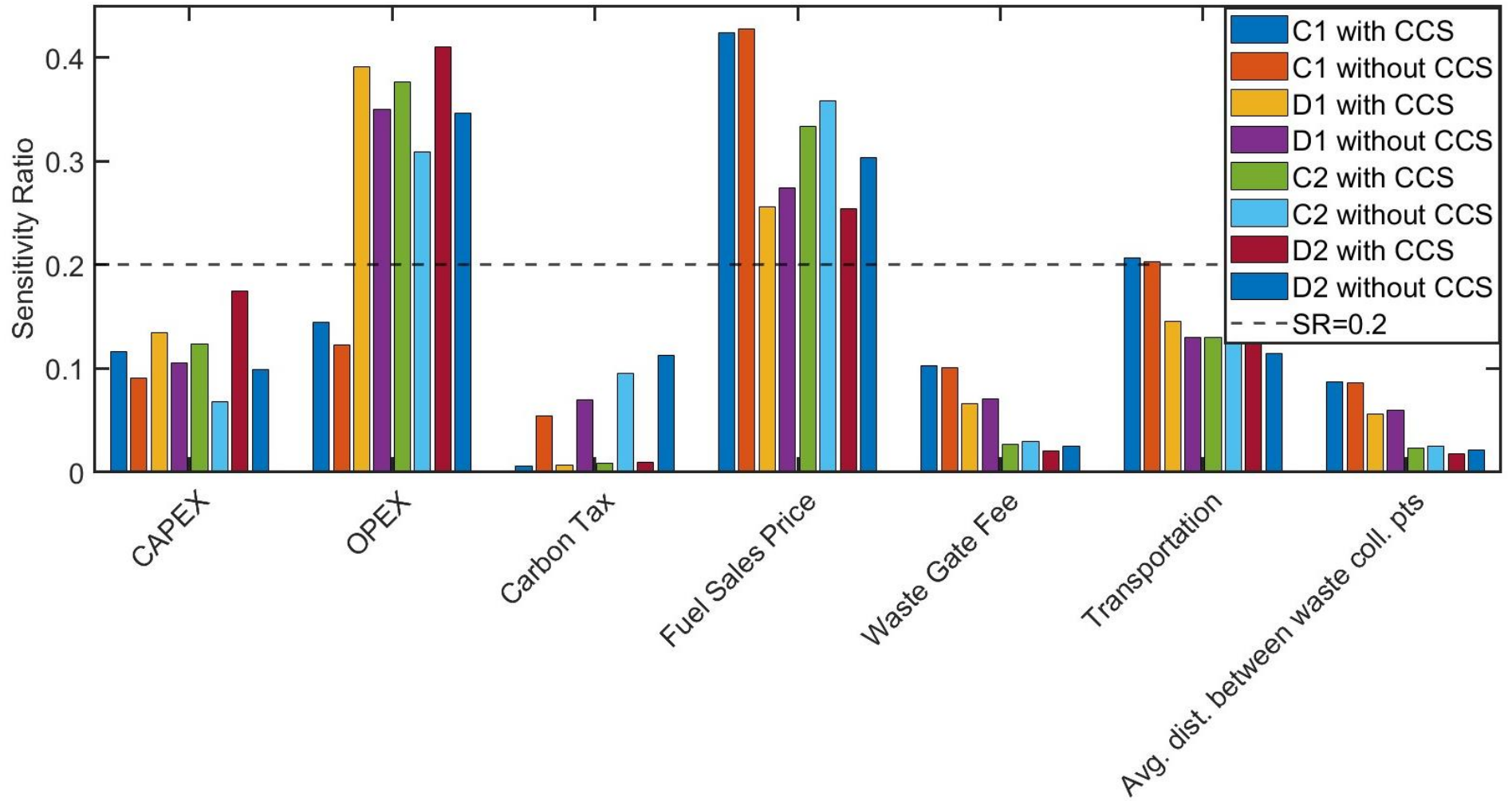


Figure 4.7. Sensitivity map depicting the effect of factors on NPV results for the different scenarios.

4.4. Conclusions

To improve the understanding of the techno-economic feasibility of pyrolysis-based resource recovery from NMPW, our research focused on the design of an assessment framework integrating transportation and process modelling into CBA. The framework was applied to evaluate the economics of 4 scenarios, including centralized large-scale and decentralized small-scale diesel and hydrogen production from NMPW with and without CCS. It is worth noting that existing TEA studies assessing hydrogen production primarily consider renewables (wind and solar energy) and biomass as sources of hydrogen production. There are limited TEA studies assessing hydrogen production from MPW or NMPW. This study can serve as a pioneering effort for future research to define the potential of hydrogen production from MPW, thus helping to deliver a more comprehensive roadmap of hydrogen economy.

Only centralized large-scale diesel production, namely the C1 scenario, showed a positive NPV and profitability, whilst the others' were negative. Centralized large-scale diesel production without CCS has the highest NPV of £24,449,631, whilst the centralized large-scale hydrogen production with CCS has the lowest NPV of -£435,744,891. However, for NPV per tonne of treated NMPW, the lowest NPV per tonne for treated NMPW (£-2391) is associated with decentralized hydrogen production with CCS. This suggests the relevance of assessing total NPV and NPV per given amount of treated waste or obtained product. Carbon tax is not effective enough to promote the reduction of carbon dioxide emissions from under current economic conditions as the NPV results for scenarios with CCS are lower than those without CCS. This issue warrants further investigation. Also, multi-objective optimization studies should be conducted to obtain NMPW management systems with balanced environmental and economic benefits.

It is also worth noting that in Chapters 3 and 4, the environmental and economic performance of four different systems was analysed, but the number of scenarios could be increased by varying the input data. This approach would allow for the selection of ideal scenarios from a broader range of possibilities, resulting in a more comprehensive study. This knowledge gap is addressed in the next chapter.

Chapter 5 Multi-Objective Optimization of Non-Recycled Municipal Plastic Waste Management Systems Producing Value-Added Resources

In Chapter 3, the environmental footprints of centralized large-scale and decentralized small-scale NMPW management systems producing diesel and hydrogen were assessed using LCA. Chapter 4 presents a CBA study that evaluates the economic feasibility of these systems. From the results of the LCA study, it can be observed that, in general, the environmental performance of diesel production is better than that of hydrogen production. However, when considering the displacement effects from substituting fossil fuel-based diesel and hydrogen, as well as the end-use of the produced fuels, centralized large-scale hydrogen production demonstrated better environmental performance than decentralized small-scale diesel systems and comparable environmental performance to centralized large-scale diesel production systems.

The CBA study, however, determined that only the centralized large-scale diesel production system had a positive NPV, indicating its economic feasibility. Additionally, this study assessed the economic feasibility of incorporating a carbon capture unit under the recently launched UK ETS, a GHG emission trading scheme in the UK. It was found that the current carbon tax price is not an effective economic tool for waste management systems utilizing high-energy-intensive technologies, such as pyrolysis, as modelled in this study.

In both the LCA and CBA studies, four different scenarios were developed and assessed in terms of environmental and economic performance. However, many more scenarios can be developed by varying input data, such as the transportation distance between the transfer station and the pyrolysis plant or by adjusting the carbon tax as traded on platforms with open market rules. Additional factors could also be considered in newly developed scenarios. Expanding the number of scenarios allows for the selection of ideal scenarios with balanced environmental footprints and economic feasibility. The main aim of this PhD project is to define systems with

optimally balanced environmental and economic performance. In this chapter, a MOO study was applied to identify these optimal scenarios.

Also, in Chapters 3 and 4, the exact location of the pyrolysis plant was not discussed; only general assumptions were made based on other studies related to waste management systems within the UK. In this chapter, potential locations for the pyrolysis plant are discussed, along with their impact on the environmental and economic performance of NMPW management systems.

5.1. Methodology

The main stages involved in the methodology are described in Figure 5.1. Basic input data obtained from Chapters 3 and 4 were used in this MOO study (Chapter 5). First, 900 scenarios for the diesel and hydrogen producing NMPW management systems were developed based on existing studies and data from governmental and international organizations, and Chapter 3 and 4. It is worth noting that varying certain inputs, as discussed in Section 5.1.1, allows for the development of these 900 scenarios. The number of scenarios depends on how the inputs are varied. All scenarios contain two main parts: 1- transportation of NMPW feedstock, products and by-products; and 2- thermochemical conversion of NMPW into fuels. Then, the simulation of transportation parts in ArcGIS Pro, along with the thermochemical conversion of NMPW into fuels in Aspen Plus, was conducted to generate a dataset for the 900 scenarios. Following this, the dataset generated was fed into LCA and CBA to calculate the GWPs and NPVs of 900 scenarios, respectively. This dataset was subsequently enriched through Monte Carlo simulation of the main input variables, such as transportation distance, construction cost, *etc.*, and the LSTM-RNN model was trained to predict sequences of data with long-range dependencies, thereby increasing the number of scenarios from 900 to 700,000 and obtaining their GWPs and NPVs. Finally, Pareto Front were determined from the GWPs and NPVs, and

the TOPSIS and LINMAP approaches were employed to define the best scenarios from the Pareto Front. At the conclusion of this study, its main findings were discussed.

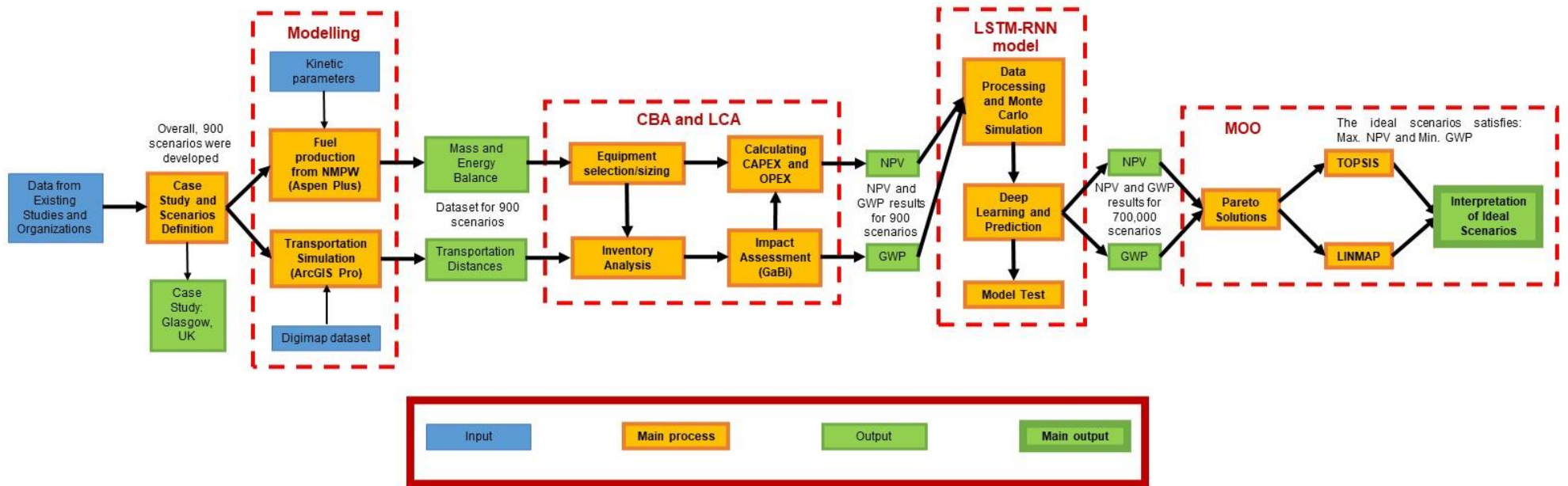


Figure 5.1. Methodology diagram utilized in this MOO study.

5.1.1. Overview of, and Scenarios for Hydrogen and Diesel Production Systems From NMPW

Overall, 900 scenarios were considered for the production of transportation fuels from NMPW systems in Glasgow based on LCA and CBA studies in Chapter 3 and 4, respectively; their main distinguishing factors are reported in Figure 5.2. Five options for NMPW transportation were considered. In the first option, NMPW is directly transported to the FPF (Fuel Production Facility), as it is located near to Glasgow. In other options, NMPW is first transported to the MRF, and then to the FPF. Four different distances between MRF and FPF were considered, namely 50, 100, 150, and 230 km.

Two of these options, a pyrolysis plant located near Glasgow and a pyrolysis plant located 50 km away from Glasgow, represent realistic locations for such facilities. In the first option, Barrhead—a small town located near Glasgow (14.5 km by road from the southwestern edge of Glasgow)—was selected. For the second option, a significant industrial area, Grangemouth (approximately 50 km by road from Glasgow), was chosen. The results of analysis by Haig et al. (2018) served as the basis for selecting these two locations.

In Chapters 3 and 4, two different scales of FPF (pyrolysis plant) were considered. In this chapter, an additional scale is included alongside the previously considered ones: 3,300, 8,000, and 15,500 tonnes of feedstock per year. In this study, two types of transportation fuel, hydrogen and diesel, can be obtained from NMPW, and two different technological methods and setup parameters are applied to produce them. Simulation and detailed mass and energy balances of thermochemical conversion processes to produce hydrogen and diesel can be found in the following sub-sections.

In the UK, there are two ways to address GHGs received from energy-intensive thermochemical conversion of NMPW into fuels: 1- buying allowance through the UK ETS

(United Kingdom Emissions Trading System) to cover GHG emissions (Ian, 2023); and 2- Carbon Capture and Storage (CCS) involving capturing carbon dioxide at the FPFs, and transporting it to, and storing it under, ex-oil and -gas reservoirs underground (Department for Energy Security and Net Zero, 2021). Both these options were considered in the scenarios.

In Chapter 4, the CBA study assessed the impact of the UK ETS value for the reference year 2022 (£75.42 per tCO₂-eq.) (Ian, 2023). This value is also used in this MOO study. It is expected that the UK ETS value will increase over time as the allowed GHG emissions to the environment are reduced. More comprehensive results could be obtained by considering different scenarios with varying UK ETS values in this study. Department for Energy Security and Net Zero (2023b) modelled the UK ETS value up to 2050. Based on this modelling, the average upper (£137.87 tCO₂-eq.) and lower (£79.96 tCO₂-eq.) bounds assumed based on the modelling carbon values during the lifespan of diesel and hydrogen production systems from NMPW were considered in the scenarios developed. The efficiency of most of the carbon capture units varies between 85 and 90%, and thus these parameters were considered as well.

Also, chapter 4 showed that selling price of hydrogen can vary greatly due to the market not being well developed, and fuel price, in particular, can have a profound impact on the economic feasibility of NMPW management systems. Based on this analysis, in the hydrogen producing scenarios three different hydrogen selling prices were considered: £2.5, £4.26, and £8.53 per kg of hydrogen (Hydrogen Valley platform, 2024).

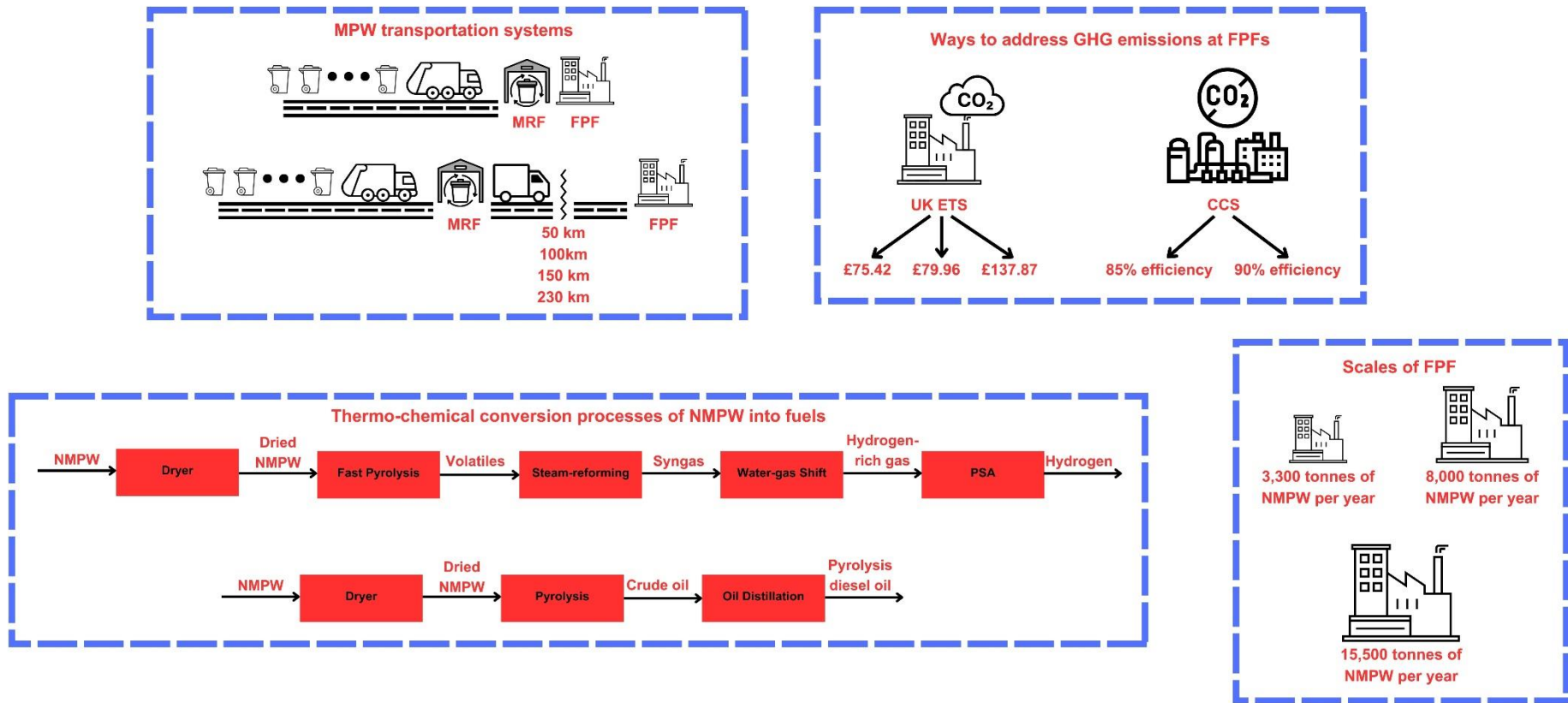


Figure 5.2. The factors distinguishing the scenarios considered: MPW transportation systems, ways to address GHG emissions at FPFs, thermo-chemical conversion processes of NMPW into fuels, and scales of FPF. MRF- Material Recovery Facility; FPF- Fuel Production Facility; MPM- Municipal Plastic waste; NMPW- Non-recycled Municipal Plastic Waste; UK ETS- United Kingdom Emissions Trading System; CCS- Carbon Capture and Storage; and PSA- Pressure Swing Adsorption.

5.1.2. Model Development for Scenarios Considered

5.1.2.1. Transportation

The transportation aspects of the developed scenarios were modelled and simulated using ArcGIS Pro based on the methodology described in subsection 3.2.2. First, MPW is collected and transported to the MRF. In the MRF, the MPW is separated from other waste fractions, and then extra sorting is employed to segregate all mechanically recyclable plastic types such as PET and HDPE. The remaining plastic waste is defined as NMPW, which is feedstock for the pyrolysis-based thermochemical conversion process to produce hydrogen or diesel. Segregated NMPW is baled for transport to the FPF. Five locations for the FPF were considered in this study: the FPFs are located 0 km, 50 km, 100 km, 150 km, and 230 km from the MRF, and nearby it. Two of these locations, 0 km and 50 km, are based on realistic sites for FPFs—a small town, Barrhead, near Glasgow, and an industrial area, Grangemouth, respectively.

5.1.2.2. Thermochemical Conversion of NMPW into Hydrogen and Diesel

NMPW transported to the FPF is thermochemically converted into diesel and hydrogen. All processes involved in this conversion processes were simulated in the Aspen Plus software using methodology described in sub-section 4.1.2. As depicted in Figure 5.2, three different scales of hydrogen and diesel production facility were simulated: 3,300, 8,000, and 15,500 tonnes of NMPW per year. The flowsheets of conversion processes to produce diesel and hydrogen in Aspen Plus can be seen in Figure 4.3 of Chapter 4.

In Figure 4.3, the top and bottom flowsheets are for diesel and hydrogen production, respectively, and the first process in both is a dryer. Pyrolysis is the main process used for hydrogen and diesel production, each of which have different in-lines processes. For diesel production, dried feedstock goes through slow pyrolysis to produce solids and hydrocarbons in the form of vapour, and then a cyclone is used to separate the solid product. Hydrocarbon

vapour is pumped into the condenser where liquid-range hydrocarbons are separated, which is defined as crude oil, and which undergoes distillation to obtain diesel. For hydrogen production, dried feedstock is converted to volatiles through fast pyrolysis, which is pumped into the SR to obtain syngas. The syngas obtained contained hydrogen sulphide, and which thus needs to go through desulphurisation. A WGS reactor is then used to produce hydrogen-rich gas from the cleaned syngas. Finally, hydrogen is separated from other tail gases by PSA. The detailed parameters and flows of the thermochemical conversion processes involved are summarized in Table 5.1 and 5.2.

5.1.3. Life Cycle Assessment and Cost-Benefit Analysis

LCA and CBA are applied to define the environmental footprint and economic feasibilities of all scenarios, respectively. The data obtained from sub-sections 5.1.2.1 and 5.1.2.2 is fed into the LCA and CBA to calculate GWPs and NPVs, respectively. The scenarios do not have identical scales, and functional units (FU), i.e., one tonne of NMPW, was applied to compare the results. It is worth noting that the methodologies of Chapter 3 and 4 were used in the LCA and CBA analysis parts of this MOO study.

5.1.3.1. Net Global Warming Potential

The net GWPs of the scenarios were defined based on the methodology described in subsection 3.2 of the LCA study. LCA consists of four main parts, namely goal and scope definition; inventory analysis; impact assessment; and interpretation. All these stages are conducted under the ISO 14040 and 14044 standards (ISO, 2006b, ISO, 2006a). The goal of LCA is to compare the GWPs of all scenarios, whilst the scope definition covers subprocesses such as NMPW collection and transportation, thermochemical conversion, and product and by-product transportation. LCA was conducted in commercial LCA software, GaBi, and Ecoinvent Dataset

3.0, and data from existing studies were used. The Centrum voor Milieukunde Leiden (CML) 2001 method was used to calculate GWP within a timeframe of 100 years.

For MPW collection and transportation to MRF, the truck (Euro 4) with gross weight of 20-28 tonnes was used, which transports 10-15 tonnes of waste per a trip (Biakhmetov et al., 2024). The gross weight of the truck (Euro 4) used for NMPW transportation from MRF to FPF is 32 tonnes, and it transports 19.2 tonnes of NMPW per trip. In obtaining the carbon footprint of the transportation part, the empty returns for trucks used to transport feedstock, products, and by-products were also considered.

The detailed mass and energy flows of diesel and hydrogen production from NMPW in the FPF are described in Tables 5.1 and 5.2, respectively. The main input (feedstock) and outputs (products) are NMPW and diesel/hydrogen, respectively. Additionally, there are other inputs such as electricity, diesel, and natural gas, and the carbon footprint of their production is obtained from the simulation in GaBi.

Based on the inventory analysis, the GWPs of the transportation and thermochemical conversion of NMPW into hydrogen and diesel were defined. The diesel and hydrogen produced displace fossil fuel-based conventional diesel and hydrogen, and this displacement was considered in defining the net GWPs of the systems.

Table 5.1. Mass and energy flows of diesel production from NMPW at the FPFs with annual capacities of 15,500 tonnes (1,800 kg/h), 8,000 tonnes (900 kg/h), and 3,300 tonnes (380 kg/h).

Process stage		FPF with capacity of 15,500 tonnes/year	FPF with capacity of 8,000 tonnes/year	FPF with capacity of 3,300 tonnes/year	Comment	Reference
	Inputs					
Dryer Unit	NMPW, kg/h	1,800	900	380	The moisture content of dried NMPW is less than 1 wt%	Aspen Plus simulation, (Haig et al., 2018, Biakhmetov et al., 2024), [4]
	Heating energy, MJ/h	816	612	517		
	Outputs					
	Dried NMPW, kg/h	1,710	855	361		
	Water vapour, kg/h	90	45	19		
Pyrolysis Unit	Inputs				P = 1 atm, T = 500°C,	Aspen Plus simulation, (Haig et al., 2018, Biakhmetov et al., 2024), [4]
	Dried NMPW, kg/h	1,710	855	361		
	Heating energy, MJ/h	9,751	7,313	6,176		
	Outputs					
	Crude Oil, kg/h	1,368	684	288.8		
	Gas, kg/h	171	86	36		
	Solid product, kg/h	171	86	36		
Oil Distillation Unit	Inputs				Residue contains hydrocarbons C ₁₈₊	Aspen Plus simulation, (Haig
	Crude Oil, kg/h	1,368	684	289		

	Heating energy, MJ/h	788	591	499		et al., 2018, Biakhmetov et al., 2024), [4]
	Hydrogen, kg/h	14	7	3		
	Outputs					
	Pyrolysis diesel range oil, kg/h	1,187	594	251		
	Residue, kg/h	181	90	38		
Heat Recovery and Electricity Generation Unit	Inputs				Carbon footprints for producing and combusting 1 kg of natural gas are 0.36 and 2.67 kg CO ₂ -eq.; conversion efficiency of fuel into electricity is 33-36%.	Aspen Plus simulation, (EPA, 2023), calculated, [4]
	Gas, kg/h	171	86	36.1		
	Solid product, kg/h	171	86	36.1		
	Residue, kg/h	181	90	38		
	Natural gas, kg/h	-	10	94		
	Air, kg/h	7,010	5,351	3,211		
	Outputs					
	Net heating energy, MJ/h	11,356	8,517	7,192		
	Electricity, MJ/h	4,884	-	-		
	Exhaust gasses, kg/h	7,475	5,594	3,400		
Ash, kg/h	58	29	15			
Carbon Capture Unit with efficiency of 85% and 90%	Inputs				For each system developed, two carbon capture efficiencies were considered: 85% and 90%.	(Singh et al., 2011), (Rubin et al., 2007), (Peeters et al., 2007), and [4]
	Exhaust gasses, kg/h	7,475	5,594	3,400		
	Electricity, MJ/h	1,604	1,170	339		
	Outputs					
	Scrubbed gases, kg/h	6,275 (85%)/	4,702 (85%)/ 4,649 (90%)	2,935 (85%)/ 2,908 (90%)		

		6,204 (90%)				
	Captured and compressed carbon dioxide, kg/h	1200 (85%)/ 1,271 (90%)	892 (85%)/ 944 (90%)	465 (85%)/ 493 (90%)		

Table 5.2. Mass and energy flows of hydrogen production from NMPW at the FPFs with annual capacities of 15,500 tonnes (1,800 kg/h), 8,000 tonnes (900 kg/h), and 3,300 tonnes (380 kg/h).

Process stage		FPF with capacity of 15,500 tonnes/year	FPF with capacity 8,000 of tonnes/year	FPF with capacity 3,300 of tonnes/year	Comment	Reference
	Inputs					
Dryer Unit	NMPW, kg/h	1,800	900	380	The moisture content of dried NMPW is less than 1 wt%	Aspen Plus simulation, (Haig et al., 2018, Biakhmetov et al., 2024), [4]
	Heating energy, MJ/h	816	612	517		
	Outputs					
	Dried NMPW, kg/h	1,710	855	361		
	Water vapour, kg/h	90	45	19		

Fast Pyrolysis Unit	Inputs				P = 1 atm , T = 500°C	Aspen Plus simulation, (Ahamed et al., 2020, Biakhmetov et al., 2024), [4]
	Dried NMPW, kg/h	1,710	855	361		
	Heating energy, MJ/h	9,751	7,313	6,176		
	Outputs					
	Volatiles, kg/h	1,676	838	354		
	Solid product, kg/h	34	17	7		
Steam Reforming Unit	Inputs				P = 1 atm, T = 700-800°C,	Aspen Plus simulation, (Yi et al., 2024) , [4]
	Volatiles, kg/h	1,676	838	354		
	Steam, kg/h	4,283	2,142	904		
	Heating energy, MJ/h	36,332	18,166	7670		
	Outputs					
	Syngas, kg/h	5,959	2,979	1,258		
Syngas Cooling and Cleaning Unit	Inputs				Zinc oxide is used for desulphurization, and the carbon footprint for producing 1 kg of zinc oxide is 3.86 CO ₂ -eq.	Aspen Plus simulation, (Lui et al., 2022b), (Spallina et al., 2016), (Lui et al., 2022a) , [4]
	Syngas, kg/h	5,959	2,979	1,258		
	Electricity, MJ/h	534	267	113		
	Zinc oxide, kg/h	89	45	19		
	Outputs					
	Cleaned syngas, kg/h	5,938	2,969	1,253		
	Zinc sulphide, kg/h	111	55	23		
Water Gas Shift Unit	Inputs					

	Cleaned syngas, kg/h	5,938	2,969	1,253	More hydrogen is produced from the reaction of steam and carbon monoxide	Aspen Plus simulation, (Lui et al., 2022b), (Lui et al., 2022a), [4]
	Electricity, MJ/h	178	89	38		
	Outputs					
	Hydrogen rich gas, kg/h	5,794	2,897	1,223		
	Water, kg/h	144	72	30		
Pressure Swing Adsorption Unit	Inputs				Overall, 90% of the hydrogen is recovered with a purity of 99.999%	Aspen Plus simulation, (Ronald Long, 2011, Biakhmetov et al., 2024), [4]
	Hydrogen-rich gas, kg/h	5,794	2,897	1,223		
	Electricity, MJ/h	5,215	2,607	1,101		
	Outputs					
	Hydrogen, kg/h	569	285	120		
	Tail gas, kg/h	5,224	2612	1,103		
Hydrogen Compression and Storage Unit	Inputs				Hydrogen is compressed to a pressure of 200 bar	(Lui et al., 2022b, Biakhmetov et al., 2024), [4]
	Hydrogen, kg/h	569	285	120		
	Electricity, MJ/h	6,457	3,223	1,363		
	Outputs					
	Compressed hydrogen, kg/h	569	285	120		
Heating Energy and Steam Generation Unit	Inputs				2.5 MJ of energy and 1 kg of water are consumed to obtain 1 kg of	Aspen Plus simulation, GaBi database, [4]
	Tail gas, kg/h	5,161	2,612	1,103		
	Air, kg/h	26,757	13,518	5,708		
	Natural gas, kg/h	1,300	657	277		

	Water, kg/h	4,283	2,142	904	steam. Carbon footprints for producing and combusting 1 kg of natural gas are 0.36 and 2.67 kg CO ₂ -eq.	
	Outputs					
	Heating energy, MJ/h	46,899	26,092	14,363		
	Exhaust gasses, kg/h	33,184	16,787	7,087		
	Steam, kg/h	4,283	2142	904		
Carbon Capture Unit with efficiency of 85% and 90%	Inputs				For each system developed, two carbon capture efficiencies were considered: 85% and 90%.	(Singh et al., 2011), (Rubin et al., 2007), (Peeters et al., 2007) , [4]
	Exhaust gasses, kg	33,184	16,787	7,087		
	Electricity, MJ/h	5,477	2,771	1,170		
	Outputs					
	Scrubbed gases, kg/h	25,902 (85%)/ 25,473 (90%)	13,103 (85%)/ 12,886 (90%)	5,531 (85%)/ 5,440 (90%)		
	Captured and compressed carbon dioxide, kg/h	7,283 (85%)/ 7,711 (90%)	3,684 (85%)/ 3,901 (90%)	1,555 (85%)/ 1,647 (90%)		

5.1.3.2. Net Present Value

The NPV represents the values of all income and expense cash flows that occur during the lifecycle of a system. The NPVs of all scenarios were calculated using the CBA methodology described in subsection 4.1.3. The mathematical expression for NPV is as follows (Fang et al., 2023):

$$NPV = \sum_{n=1}^{n=25} \frac{(I_n - OPEX_n - T_n - TAX_n)}{(1+i)^n} - CAPEX \quad (5.1)$$

where $CAPEX$ represents the CAPital EXpenditure for development and construction of the FPF, $OPEX_n$ is the OPERational EXpenditure for the n -th operational year, and T_n is the transportation cost for the n -th operational year. TAX_n represents the payment for carbon dioxide emissions for the n -th operational year, while I_n represents the income obtained from selling fuels and gate fees for the n -th operational year, and i is the discount rate (5%) (Lui et al., 2022a). The reference year for this MOO study is 2022, and lifetime for all scenarios is 25 years.

The cost of waste collection and transportation to the MRF was obtained from Table 4.7 in Chapter 4. The overall annual cost for waste collection and transportation to the MRF was divided by the total amount of transported waste. The cost of waste collection and transportation to the MRF is £1,168 per tonne of treated NMPW. NMPW sorted at the MRF is bailed and transported to the FPF, and the fixed cost per journey from the MRF to FPF is £258.44, and £0.93 is applied per km distance travelled (Haig et al., 2018). Mass and energy balances obtained from the Aspen Plus simulations were used to select the unit/equipment size, and their costs, illustrated in Table 5.3, were calculated by considering scale and cost factors. Equations (4.4) and (4.5) in subsection 4.1.3.4 were used to account for costs and scale factors associated with pyrolysis plants. Base year costs were converted to reference year costs by applying the Chemical Engineering Plant Cost Index (CEPCI).

Table 5.3. Equipment/unit cost for reference year (2022) calculated based on the base year cost obtained from the existing literature, and scale and cost factors.

Equipment	Scenarios	Base year	Base capacity	Base cost	Cost factor	Scale Factor	Reference year	Reference capacity	Reference cost	Reference
Dryer Unit	Diesel and hydrogen producing scenarios	2018	1.25 t/h	\$2,000,000	1.35	0.7	2022	1.8 tonne/h	£2,616,591	(Haig et al., 2018), [4]
		2018	1.25 t/h	\$2,000,000	1.35	0.7	2022	0.9 tonne/h	£1,650,255	(Haig et al., 2018), [4]
		2018	1.25 t/h	\$2,000,000	1.35	0.7	2022	0.4 tonne/h	£914,229	(Haig et al., 2018), [4]
Pyrolysis Unit	Diesel producing scenarios	2018	0.4 t/h	\$2,000,000	1.35	0.7	2022	1.7 tonne/h	£5,588,847	(Haig et al., 2018), [4]
		2018	0.4 t/h	\$2,000,000	1.35	0.7	2022	0.9 tonne/h	£3,524,892	(Haig et al., 2018), [4]
		2018	0.4 t/h	\$2,000,000	1.35	0.7	2022	0.4 tonne/h	£2,029,785	(Haig et al., 2018), [4]
Fast Pyrolysis Unit	Hydrogen producing scenarios	2021	10 t/h	\$22,000,000	1.15	0.7	2022	1.7 tonne/h	£5,327,182	(Yadav et al., 2022), [4]
		2021	10 t/h	\$22,000,000	1.15	0.7	2022	0.9 tonne/h	£3,368,186	(Yadav et al., 2022), [4]
		2021	10 t/h	\$22,000,000	1.15	0.7	2022	0.4 tonne/h	£1,934,752	(Yadav et al., 2022), [4]
Steam Reforming Unit	Hydrogen producing scenarios	2022	0.15 t/h	€275,000	1	0.75	2022	1.7 tonne/h	£1,448,599	(Al-Qadri et al., 2023), [4]
		2022	0.15 t/h	€275,000	1	0.75	2022	0.9 tonne/h	£882,953	(Al-Qadri et al., 2023), [4]
		2022	0.15 t/h	€275,000	1	0.75	2022	0.4 tonne/h	£489,392	(Al-Qadri et al., 2023), [4]
Oil Distillation Unit	Diesel producing scenarios	2018	1 t/h	\$2,500,000	1.35	0.7	2022	1.4 tonne/h	£3,211,069	(Haig et al., 2018), [4]
		2018	1 t/h	\$2,500,000	1.35	0.7	2022	0.7 tonne/h	£2,022,893	(Haig et al., 2018), [4]
		2018	1 t/h	\$2,500,000	1.35	0.7	2022	0.3 tonne/h	£1,092,307	(Haig et al., 2018), [4]
Syngas Cleaning Unit	Hydrogen producing scenarios	2022	0.25 t/h	€1,177,000	1	0.67	2022	6 tonne/h	£8,440,442	(Al-Qadri et al., 2023), [4]
		2022	0.25 t/h	€1,177,000	1	0.67	2022	3.1 tonne/h	£5,423,616	(Al-Qadri et al., 2023), [4]
		2022	0.25 t/h	€1,177,000	1	0.67	2022	1.3 tonne/h	£3,029,325	(Al-Qadri et al., 2023), [4]
Water Gas Shift Unit	Hydrogen producing scenarios	2007	233.6 t/h	\$12,918,000	1.55	0.67	2022	6 tonne/h	£861,818	(Rath et al., 2011), [4]
		2007	233.6 t/h	\$12,918,000	1.55	0.67	2022	3.1 tonne/h	£553,782	(Rath et al., 2011), [4]
		2007	233.6 t/h	\$12,918,000	1.55	0.67	2022	1.3 tonne/h	£309,312	(Rath et al., 2011), [4]
Pressure Swing Adsorption Unit	Hydrogen producing scenarios	2007	32.99 t/h	\$38,047,000	1.55	0.6	2022	5.8 tonne/h	£10,401,199	(Rath et al., 2011), [4]
		2007	32.99 t/h	\$38,047,000	1.55	0.6	2022	3 tonne/h	£6,999,626	(Rath et al., 2011), [4]
		2007	32.99 t/h	\$38,047,000	1.55	0.6	2022	1.2 tonne/h	£4,041,433	(Rath et al., 2011), [4]
Hydrogen Compressor Unit	Hydrogen producing scenarios	2009	166 t/h	€9,000,000	1.56	0.68	2022	0.6 tonne/h	£263,909	(Manzolini et al., 2013), [4]
		2009	166 t/h	€9,000,000	1.56	0.68	2022	0.3 tonne/h	£168,465	(Manzolini et al., 2013), [4]
		2009	166 t/h	€9,000,000	1.56	0.68	2022	0.1 tonne/h	£78,039	(Manzolini et al., 2013), [4]
Carbon Capture Unit	Diesel producing scenarios	2016	82 t/h	€43,274,000	1.51	0.7	2022	1.3 tonne/h	£2,935,567	(Rath et al., 2011), [4]
		2016	82 t/h	€43,274,000	1.51	0.7	2022	0.7 tonne/h	£1,849,334	(Rath et al., 2011), [4]

		2016	82 t/h	€43,274,000	1.51	0.7	2022	0.5 tonne/h	£1,503,871	(Rath et al., 2011), [4]
	Hydrogen producing scenarios	2016	82 t/h	€43,274,000	1.51	0.7	2022	33.2 tonne/h	£28,361,440	(Rath et al., 2011), [4]
		2016	82 t/h	€43,274,000	1.51	0.7	2022	17.2 tonne/h	£17,866,999	(Rath et al., 2011), [4]
		2016	82 t/h	€43,274,000	1.51	0.7	2022	9.8 tonne/h	£12,072,296	(Rath et al., 2011), [4]

Total equipment cost was used to calculate the CAPEX and OPEX, the equations used for which are given in Table 4.3 of chapter 4. CAPEX includes fixed capital investment, working capital, and pre-operating and organization costs, whereas OPEX includes fixed and variable operating costs. For each FPF, 12 operators are required, whose average annual gross salary is £27,710 [4]. Electricity and gas prices depend on the consumption scale for the industrial and commercial sectors, and were considered for all scenarios (Department for Energy Security and Net Zero, 2023a). Also, the gate fee for landfilling solid by-products obtained after the combustion process, £78 per tonne of material landfilled, was considered when calculating NPVs (Steven and Ashley, 2022).

5.1.3.3. Assessing the Environmental Footprint and Economic Performance of Pyrolysis Plant Locations

Defining suitable locations for pyrolysis plants could provide valuable insights regarding the potential placement of centralized large-scale and decentralized small-scale plants. Based on the results of study by Haig et al. (2018), two locations were selected to evaluate how locating pyrolysis plants there affects the environmental and economic performance of NMPW management systems: Barrhead, a small town near Glasgow, and Grangemouth, a major industrial area in Scotland located around 50 km from Glasgow.

Barrhead is an ideal location for a pyrolysis plant due to its proximity to Glasgow and the presence of infrastructure such as a material recycling centre, a transfer station, and several landfill sites. For the second location, Grangemouth is a large industrial area that hosts Scotland's only oil refinery, the Grangemouth Refinery. This makes it an ideal location for a diesel-producing pyrolysis plant, as the produced diesel can be directly transported to the nearby refinery. Furthermore, as highlighted in Chapter 4, Grangemouth has existing infrastructure for carbon capture and transportation, which reduces the cost of implementing carbon capture systems, especially energy-intensive hydrogen-producing systems. The impact

of these two locations on the environmental and economic performance of NMPW management systems is analysed and discussed in detail, providing valuable insights for the practical implementation of the proposed systems.

5.1.4. LSTM-RNN Model

The main results of section 5.1.3 are the GWPs and NPVs for 900 scenarios, and the LSTM-RNN model was developed based on these results. The LSTM-RNN model is a deep learning artificial neural network architecture designed for processing complex sequential data to learn long-term dependencies of systems (Fang et al., 2024). Python was used to create the virtual environment used to develop the LSTM-RNN model, and a set import statement needs to be provided for time series and sequential data analysis. NumPy and Pandas libraries were imported for numerical operations and handling arrays, and MinMaxScaler and Sequential were imported as well to normalize data and to build neural networks layer-by-layer, respectively. Also, LSTM, Dense, and Input were used to build RNN, to connect neural network layers, and to specify the shape and type of the input data, respectively.

The dataset obtained from the development of the scenarios and calculating their GWPs and NPVs was split into 80% for training, and 20% each for testing and validation. Based on the results of previously published works and the existing literature, a set of variables with their upper and lower bounds, as illustrated in Table 5.4, was selected for Monte Carlo simulation. Selected variables are uncertain factors that have profound impacts on environmental and economic performances of systems, and that can be adjusted through policymaker interventions or otherwise during the design stage. This approach aims to enrich the dataset, develop additional scenarios, and obtain their GWPs and NPVs. This allows for a more comprehensive analysis with a greater number of developed scenarios, facilitating the identification of a single ideal scenario that balances environmental and economic performance.

Table 5.4. Variables and their upper and lower bounds as applied in Monte Carlo simulations.

Variable	Lower bound	Upper bound
Distance between MRF and FPF, km	0	230
Carbon capture efficiency, %	85	90
Hydrogen selling price, £/kg of hydrogen	2.5	8.53
Carbon tax, £/tCO ₂ -eq.	75.42	137.87
System scale, tonnes of NMPW/year	3,300	15,500

5.1.5. Multi-Objective Optimization

MOO to define the best scenario with balanced GWP and NPV is described in Figure 5.3, and its mathematical bases can be seen in subsections 5.1.5.1-5.1.5.3. Data containing GWPs and NPVs from subsection 5.1.4 were normalized to define the Pareto front. The Pareto front contains a set of non-dominated scenarios where no other scenario is better in both GWP and NPV. For TOPSIS, the ideal solution that satisfies the best values for NPV and GWP and the anti-ideal solution that satisfies the worst values were calculated. The distance of each Pareto scenario from the ideal and anti-ideal solutions was computed, and the relative closeness of each Pareto scenario to the ideal solution was calculated. The highest relative closeness indicates the TOPSIS best scenario. In the case of LINMAP, first, a decision matrix was constructed from the Pareto optimal scenarios, and a pairwise comparison matrix was created to understand the trade-offs between GWPs and NPVs. Then, weights of each GWP and NPV were calculated based on the pairwise comparisons. Finally, Pareto scenarios were ranked by their weighted scores, with the highest being the LINMAP best scenario.

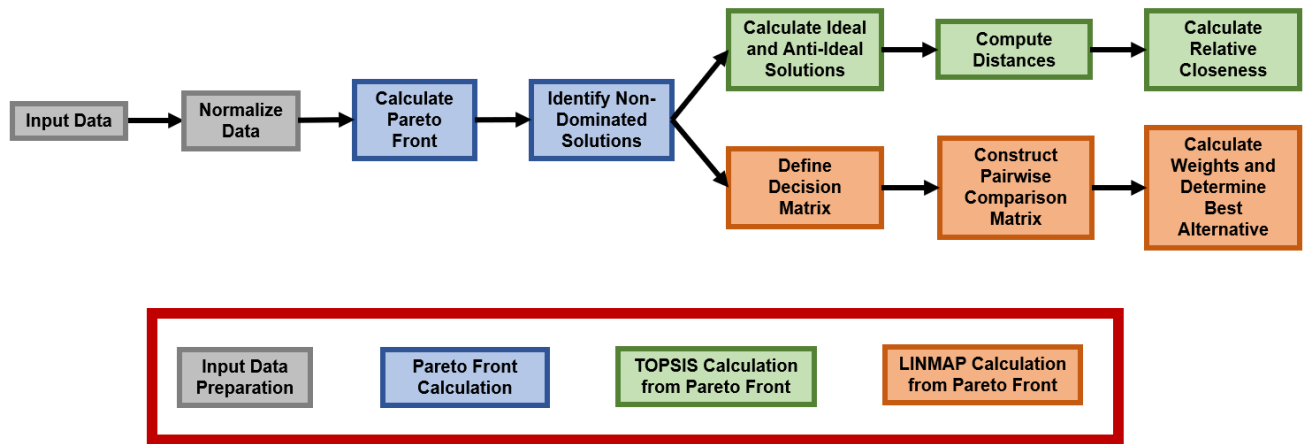


Figure 5.3. Explanation diagram of the mathematical basis of MOO.

5.1.5.1. Pareto Front

In section 5.1.4, the environmental (GWP) and economic (NPV) performance for 700,000 scenarios were obtained. The sustainability, environmental footprint, and economic feasibility of any waste management systems need to be minimized and maximized as appropriate. Pareto's optimal solutions were applied to define the ideal scenarios in terms of balanced environmental and economic objectives, where neither can be improved without compromising the other. In the case of this MOO study, these objectives were GWP and NPV. In multi-objective optimization, Python was used to process data for 700,000 scenarios, and NumPy, Pandas, MinMaxScaler from Scikit-learn, Matplotlib, and Euclidean from Scipy were imported.

Optimal Pareto solutions provide a range of optimal scenarios with balanced environmental and economic performance. TOPSIS and LINMAP approaches were applied to define the single best scenario obtained from the optimal Pareto scenarios. First, for both TOPSIS and LINMAP, a decision matrix was created, and it was converted into a normalized matrix using

$$R_{ij} = \frac{X_{ij}}{\sqrt{\sum_{i=1}^m X_{ij}^2}} \quad (5.2)$$

where R_{ij} is normalized value of the criterion j (e.g., GWP or NPV) for scenario i , X_{ij} is original value of the criterion, and m is the total number of scenarios considered in the decision matrix. The equation (5.2) is used to normalize created decision matrix to eliminate the influence of differing units or scales.

5.1.5.2. TOPSIS

The weighted normalized decision matrix was obtained from the normalized matrix using Equation (5.3). Equal weights were assumed for both GWP and NPV values in the matrix, which means that $\omega_{GWP} = 0.5$ and $\omega_{NPV} = 0.5$.

$$V_{ij} = R_{ij} * \omega_j \quad (5.3)$$

The ideal (A^+) and negative-ideal (A^-) scenarios need to be determined to obtain the TOPSIS best scenarios. They were determined by applying the following conditions:

$$A^+ = (\min V_{GWP}, \max V_{NPV}) \quad (5.4)$$

$$A^- = (\max V_{GWP}, \min V_{NPV}) \quad (5.5)$$

The distances from the scenarios in the Pareto front to the ideal (A^+) and negative-ideal (A^-) scenarios were calculated using Equations (5.6) and (5.7).

$$S_i^+ = \sqrt{(V_{GWP,i} - A_{GWP}^+)^2 + (V_{NPV,i} - A_{NPV}^+)^2} \quad (5.6)$$

$$S_i^- = \sqrt{(V_{GWP,i} - A_{GWP}^-)^2 + (V_{NPV,i} - A_{NPV}^-)^2} \quad (5.7)$$

Finally, the relative closeness to the ideal solution was determined using following equation:

$$C_i^* = \frac{S_i^-}{S_i^+ + S_i^-} \quad (5.8)$$

The obtained C_i^* values typically vary between 0 and 1, and the highest value is defined as the best TOPSIS scenario.

5.1.5.3. LINMAP

First, the ideal scenario was obtained from the decision matrix using Equation (5.4), and the Linear Programming Problem was applied to the matrix. All constraint applied to this Linear Programming Problem is linear as it is able allow to ensure that the optimization remains within the framework of linear programming. The objective of the Linear Programming Problem is to minimize the total weighted distance from the ideal scenarios, and its mathematical expression can be described as follows:

$$\text{minimize } Z = \sum_{i=1}^m d_i, d_i \geq \omega_{GWP}(A_{GWP}^+ - GWP_i) + \omega_{NPV}(A_{NPV}^+ - NPV_i) \quad (5.9)$$

It is worth noting that the sum of the weights must be 1, and they cannot be negative. Finally, the optimal weights were used to calculate the preference scores for all alternatives using Equation (5.10). The scenario with the highest preference score is the best LINMAP scenario.

$$P_i = \omega_{GWP} \times GWP_i + \omega_{NPV} \times NPV_i \quad (5.10)$$

5.2. Results and Discussion

5.2.1. Environmental and Economic Performance of Systems

Overall, 900 scenarios were developed, and their transportation and thermochemical conversion parts were simulated in the ArcGIS Pro and Aspen Plus software suites. Their environmental and economic performances were then assessed by LCA and CBA and the associated GWPs and NPVs for 900 scenarios obtained, as illustrated in Figure 5.4.

Scenarios from 1 to 225 are diesel-producing systems, while the remaining scenarios are hydrogen-producing systems. In general, the GWPs and NPVs of hydrogen-producing scenarios are greater than those of diesel-producing scenarios because hydrogen production from NMPW is more energy-intensive, and its OPEX and CAPEX are much higher. The average NPV and GWP of diesel-producing scenarios are 67 kg CO₂-eq. and £-218 per tonne NMPW, respectively, while those for hydrogen-producing scenarios are -59 kg CO₂-eq. and £-984 per tonne NMPW, respectively.

Applying CCS significantly reduces the carbon footprints of all scenarios. For example, most of the hydrogen-producing scenarios without CCS have a GWP of around 3 tonnes CO₂-eq. per tonne NMPW. The scenarios that include CCS show much lower GWPs, resulting in increased NPVs. Despite a large number of hydrogen-producing scenarios having positive GWPs and negative NPVs, there are 120 hydrogen-producing scenarios showing negative GWPs and positive NPVs. It is worth noting that all of these scenarios have a large annual capacity of 15,500 tonnes of NMPW, and the FPFs are located near the feedstock collection points, with CCS infrastructures available nearby. Additionally, the selling price of hydrogen plays a crucial role in maximizing the economic feasibility of the systems. Government intervention in setting the selling price of hydrogen produced from MPW should be further studied.

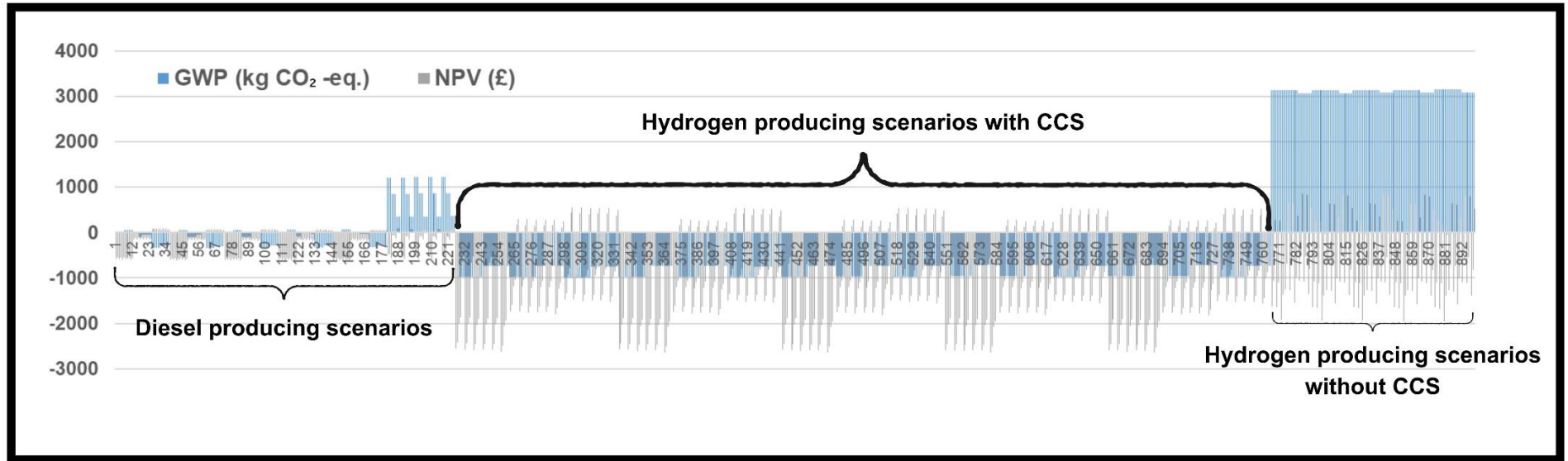


Figure 5.4. Environmental (GWP) and economic (NPV) statistics for a set of 900 scenarios.

5.2.1.1. The Impact of Pyrolysis Plant Locations on the GWPs and NPVs of NMPW Management Systems

Two locations were selected for the pyrolysis plant: Barrhead, a small town near Glasgow, and Grangemouth, a major industrial area in Scotland located approximately 50 km from Glasgow. Overall, GWPs and NPVs for 900 scenarios were obtained, as shown in Figure 5.4. Among these, 360 scenarios are associated with the locations of Barrhead and Grangemouth. Specifically, in 180 scenarios, the pyrolysis plant is located near Glasgow, while in the remaining scenarios, it is situated 50 km away from Glasgow, which corresponds to Grangemouth. To understand the impact of location on the GWP and NPV of the system in detail, one scenario—a large-scale (15,500 tonnes of NMPW per year) diesel-producing system from NMPW with CCS—was selected. The results of this analysis are presented in Table 5.5.

In Table 5.5, it can be observed that the GWP and cost of feedstock transportation per tonne of treated plastic feedstock for the pyrolysis plant located in Grangemouth are higher than those for Barrhead, due to the greater distance from Glasgow to Grangemouth. However, additional GWP and costs are incurred in Barrhead, as the produced diesel and captured carbon need to be transported to the oil refinery and carbon transportation infrastructure in the Grangemouth area.

As seen from the total GWP and costs, there is currently no significant difference in where the pyrolysis plant is located. While a plant near Glasgow eliminates the need for long-distance feedstock transportation, the lack of carbon transportation infrastructure near Glasgow means that produced fuel and captured carbon must still be transported to Grangemouth. If carbon transportation infrastructure were available around Glasgow, it would be more advantageous to locate the pyrolysis plant near Glasgow.

Table 5.5. GWPs and NPVs of diesel producing NMPW pyrolysis plants based on the selected locations (Barrhead and Grangemouth).

	Location	
	Barrhead	Grangemouth
GWP of feedstock transportation per tonne of treated plastic feedstock (kg CO ₂ -eq)	24.85	28.54
Cost of feedstock transportation per tonne of treated plastic feedstock (£)	190.37	206.25
GWP of diesel production from plastic waste per tonne of treated plastic feedstock (kg CO ₂ -eq)	78.43	78.43
Cost of diesel production from plastic waste per tonne of treated plastic feedstock (£)	278.48	278.48
GWP of product and by-product transportation per tonne of treated plastic feedstock (kg CO ₂ -eq)	1.35	0
Cost of product and by-product transportation per tonne of treated plastic feedstock (£)	34.17	0
Overall GWP per tonne of treated plastic feedstock (kg CO₂-eq)	104.63	106.97
Overall cost per tonne of treated plastic feedstock (£)	503.02	484.73

5.2.2. Multi-Objective Optimization and Final Decision Selection

The LSTM-RNN model was trained on 900 scenarios to expand the dataset to 700,000 scenarios and predict their GWPs and NPVs by enriching the input data. Overall, the GWPs and NPVs of 700,000 diesel and hydrogen-producing scenarios were processed to define the Pareto front and identify the best TOPSIS and LINMAP scenarios from the Pareto front. The main aim of MOO analysis is to define the best scenario with balanced environmental and economic performance. The results of the MOO analysis are illustrated in Figure 5.5 and Table 5.5.

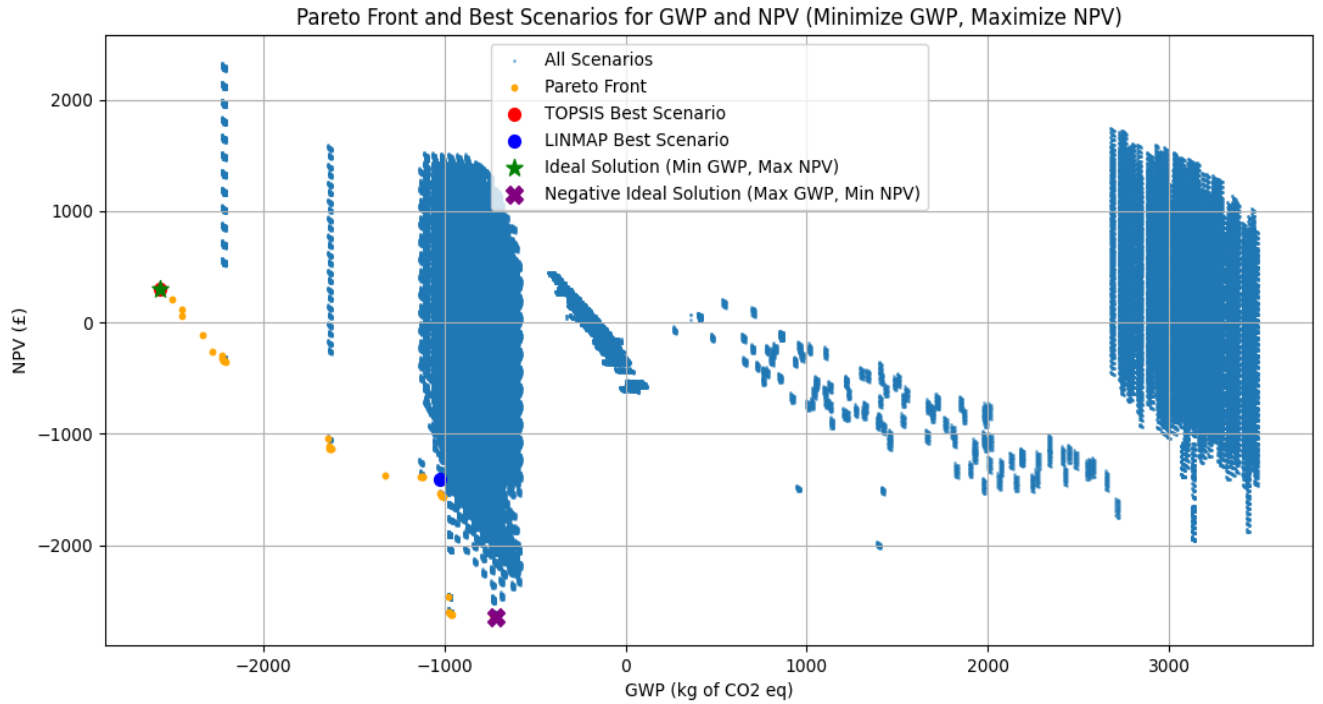


Figure 5.5. Pareto front, and the final TOPSIS and LINMAP best scenarios.

The TOPSIS best scenario is a diesel-producing scenario with a CCS unit. Its annual capacity is 11,385 tonnes of NMPW, and the FPF facility is located near Glasgow. Additionally, it is worth noting that carbon transportation infrastructure is available around the FPF. The GWP and NPV of the TOPSIS best scenario are -2570.42 kg CO₂-eq and £300.32 per tonne NMPW. The LINMAP best scenario is a hydrogen-producing scenario with a CCS unit. Carbon transportation infrastructure is available, and the distance between the MRF and FPF is 0 km, the same as in the TOPSIS scenario. The capacity of the FPF is 12,960 tonnes of NMPW per year. The GWP and NPV of the LINMAP best scenario are -1025.28 kg CO₂-eq and £-1402.92 per tonne NMPW. Its highest preference score, which is the highest, is 0.627946. In both scenarios, TOPSIS and LINMAP, the first one is more preferable due to the lower carbon footprint and higher economic feasibility.

Table 5.6. GWPs and NPVs of ideal and negative-ideal scenarios, as well as the final TOPSIS and LINMAP best scenarios.

Scenarios	GWP (kg CO ₂ -eq. per tonne NMPW)	NPV (£ per tonne NMPW)
Ideal scenario	-2570.42013837	300, 31564735
Negative-ideal scenario	-717.80847156	-2645.74649138
TOPSIS best scenario	-2570.420138	300.315647
LINMAP best scenario	-1025.278402	-1402.924978

5.3. Conclusions

In this study, 900 diesel and hydrogen-producing scenarios from NMPW based on pyrolysis-based thermochemical conversion processes were developed, and their transportation and thermochemical conversion processes were simulated in ArcGIS Pro and Aspen Plus to produce a dataset. The obtained dataset was fed into LCA and CBA to calculate the GWPs and NPVs of the 900 scenarios, respectively. An LSTM-RNN integrated with Monte Carlo simulation of variables was used to expand the scenarios from 900 to 700,000 and predict their GWPs and NPVs. Finally, the Pareto front was defined, and the TOPSIS and LINMAP best scenarios were obtained from it. Both scenarios showed negative GWPs (-2570.42 kg CO₂-eq per tonne NMPW for the TOPSIS scenario and -1025.28 kg CO₂-eq per tonne NMPW for the LINMAP scenario); however, only the TOPSIS scenario showed a positive NPV, which is equal to £300.32 per tonne of NMPW. In both scenarios, TOPSIS is more preferable due to the lower GWP and higher NPV. This demonstrates that the TOPSIS method effectively balances environmental and economic considerations.

Chapter 6 Conclusions and Recommendations

6.1. General Conclusions

The project studied and compared the environmental and economic performance of centralized large-scale and decentralized small-scale diesel and hydrogen-producing systems from NMPW, and then identified the ideal scenarios with balanced environmental and economic performance. To achieve this, LCA, CBA, and MOO studies were conducted.

The results of the LCA study showed that centralized large-scale diesel or hydrogen production systems have better environmental performance than decentralized small-scale systems. For example, the GWP of diesel production for a centralized large-scale system is 801 kg CO₂-eq. per tonne of NMPW, while for a decentralized small-scale system, it is 1,345 kg CO₂-eq. per tonne of NMPW. Additionally, it is important to highlight that hydrogen production has a greater GWP than diesel production. When comparing centralized large-scale diesel and hydrogen production scenarios, the GWP of the hydrogen-producing scenario is seven times greater than that of the diesel-producing scenario. However, the hydrogen-producing scenario benefits from greater carbon credits due to its replacement of fossil fuel-based hydrogen production. After accounting for end-of-life GHG emissions of fuels, the net GWP of the centralized large-scale hydrogen-producing scenario (2,496.53 kg CO₂-eq. per tonne of NMPW) is lower than that of the decentralized small-scale diesel-producing scenario (2,766.3 kg CO₂-eq. per tonne of NMPW) and is close to the centralized large-scale diesel-producing scenario (2,114.44 kg CO₂-eq. per tonne of NMPW).

Defining the environmental footprint of systems alone is not sufficient to identify the most feasible system. In the CBA portion of this project, the economic feasibility of centralized large-scale and decentralized small-scale diesel and hydrogen production systems was assessed by calculating their NPVs. Among the scenarios, only the centralized large-scale diesel-

producing scenario demonstrated a positive NPV (£22,240,135 with a CCS unit and £24,449,631 without CCS), while the rest of the scenarios showed negative NPVs. When the FU (functional unit) of 1 tonne of NMPW was applied, the decentralized small-scale hydrogen production system exhibited the lowest NPV of -£2,391 with CCS and -£1,524 without CCS. Sensitivity analysis revealed that factors such as OPEX and fuel sales prices have a significant influence on the NPV of the systems.

The economic feasibility of capturing GHG emissions versus releasing them into the environment for the systems considered in this study was also compared. Recently, the UK ETS (carbon emission trading scheme) was launched to motivate industries to reduce GHG emissions. Pyrolysis-based thermochemical conversion of NMPW into diesel and hydrogen is energy-intensive, producing GHG emissions. It was found that the UK ETS is not effective for hydrogen or diesel production systems from NMPW, as the cost for releasing GHGs into the atmosphere is less than the cost of CCS.

In the LCA and CBA sections of this project, only four scenarios were considered. However, there is potential to explore more scenarios, which would allow for the identification of an ideal scenario with balanced environmental and economic performance. In the MOO analysis, 700,000 diesel and hydrogen scenarios with different setups and parameters were developed, and their GWPs and NPVs were predicted using machine learning techniques. Subsequently, a Pareto curve with several ideal scenarios showcasing balanced environmental and economic performance was generated, and the best TOPSIS and LINMAP scenarios were identified. The TOPSIS scenario has a GWP of -2570.42 kg CO₂-eq. and an NPV of £300,315.65 per tonne of NMPW, which are significantly better than those of the LINMAP scenario (-1025.28 kg CO₂-eq. and -£1,402.92 per tonne of NMPW). In conclusion, the TOPSIS method effectively selects scenarios with optimally balanced environmental and economic performance.

6.2. Recommendations for Future studies and Practical Applications

Despite the comprehensive studies conducted, several improvement points were identified that can be addressed in future research. These include enhancing the simulation of transportation processes, refining thermochemical conversion models, and expanding the scope of LCA and CBA studies by considering broader scenarios. Additionally, the results of the LCA, CBA, and MOO analyses provide valuable insights for developing recommendations for practical applications.

Recommendations for future studies:

In Chapter 3, ArcGIS Pro was used to model and simulate the transportation part to obtain more accurate results. It is worth noting that this model can be improved to achieve even more precise results by conducting a more comprehensive analysis. For example, in modelling the transportation part, factors such as traffic congestion, weather patterns, road type, and infrastructure quality can be considered.

In Chapter 4, the thermochemical conversion of NMPW into diesel and hydrogen was simulated using Aspen Plus, and the results of both simulations were validated against other studies. The deviation between diesel production results and other studies' results is generally less than 5%, while the deviation between hydrogen production results and other studies' results is around 20%. One of the main reasons for the relatively large deviation of 20% is the limited number of studies related to hydrogen production from MPW through pyrolysis-based thermochemical conversion technologies, which negatively affects the selection of optimal parameters for conversion processes. More experimental and modelling studies related to hydrogen production from MPW or NMPW through pyrolysis-based thermochemical conversion processes are necessary.

In addition to the systems considered in this study, there are many setups of thermochemical conversion processes that can be applied to produce hydrogen from MPW or NMPW, such as catalytic reforming, catalytic steam reforming, or other types of catalysts. Their environmental and economic performance are still not clear.

Besides GWP, there are more environmental categories that can be applied to define their environmental footprints, such as PM2.5, water scarcity, acidification, etc. These environmental categories can be applied in future studies.

CBA showed that the carbon tax is not effective in incentivizing carbon capture for diesel and hydrogen production systems from NMPW. This means that more studies are necessary to find ways to reshape the current systems. For example, in this study, it was found that the availability of carbon transportation infrastructure has a profound impact on the total NPV of systems. In areas where carbon transportation infrastructure is not available, governmental funding in the form of subsidies can be considered. Also, it is worth noting that other technologies for CCS to reduce its cost should be assessed.

In this study, various input data related to thermo-chemical conversion processes are considered, with most parameters being fixed. For example, in scenarios C1 and D1, the pyrolysis temperature was set at approximately 500°C, and the impact of temperature variation and other process parameters on GWP and NPV results was not assessed. In future studies, evaluating the effect of process parameter variations could provide more comprehensive results.

In this study, GWP and NPV were selected as objectives for optimization using machine learning techniques. Future studies should consider other important objectives for optimization such as social impacts, energy efficiency, etc. Additionally, more diverse scenarios can be developed to increase the dataset and assess other technologies. For example, new scenarios

involving the thermochemical conversion of NMPW integrated with other renewable energy sources can be assessed.

In the sensitivity analysis presented in Chapters 3 and 4, the impact of operational parameters such as pyrolysis temperature, retention time, etc., on GWP and NPV results was not conducted. This was deemed unnecessary for this study, as all parameters were selected based on existing studies and industrial practices, ensuring more robust and reliable results that are closely aligned with realistic applications. Varying operational parameters typically results in changes in product quality and yields. For instance, increasing the temperature of the pyrolysis process generally leads to an increase in gas products. However, for the systems considered in this study, an optimal temperature range was selected to prioritize the production of diesel and hydrogen fuels. Furthermore, the developed environment for mass and energy balance and the Aspen simulation model were not adapted for varying operational parameters. Nonetheless, in future studies, a more flexible environment for mass and energy balance and the Aspen simulation of the NMPW pyrolysis process, with the capacity to vary operational parameters, can be developed.

Recommendations for practical applications:

Based on the results of this study, the large-scale diesel-producing scenario utilizing pyrolysis-based thermochemical conversion processes with a CCS unit is recommended for processing NMPW. Among the scenarios considered, only this system demonstrated economic feasibility and negative GWP.

If hydrogen production from NMPW is required, it is recommended to deploy large-scale plants, as small-scale hydrogen-producing systems showed the lowest environmental and economic performance in this study.

It is recommended to locate NMPW management plants producing diesel and hydrogen close to waste collection sources. This reduces costs and GHG emissions associated with transportation, as it is more efficient to transport produced fuel rather than low-density plastic.

One of the main challenges in capturing GHG emissions is the unavailability of carbon capture and transportation infrastructure. For example, in Glasgow, even if a pyrolysis plant is located near the city and a CCS unit is applied, the captured GHGs would still need to be transported to distant areas with carbon capture and transportation infrastructure, significantly increasing the cost of waste management systems.

Appendix

Table 1A. Detailed MPW composition.

MSW generation, tonnes	265,910 (Scottish Environment Protection Agency, 2023)	MSW excluding MPW, tonnes	244,637				
		MPW, tonnes	21,273	Recycled plastic wastes, tonnes	5745 (Scottish Environment Protection Agency, 2023)		
				Non-recyclable plastic wastes, tonnes	15,528	Flexible	Plastic type
		LDPE	25 (Foster, 2008)				
		PP	5 (Foster, 2008)				
		Rigid	PP			17.2 (Foster, 2008)	
			HDPE			13.5 (Foster, 2008)	
			PET			15.3 (Foster, 2008)	
			PVC			3.5 (Foster, 2008)	
		PS	4 (Foster, 2008)				
Contamination	16.5 (Foster, 2008)						

Table 2A. The composition of NMPW transported to the hydrogen and diesel production facilities.

Plastic	The share of plastic in NMPW feedstock, wt%	Ultimate composition, wt %						Proximate composition, wt %				HHV, MJ/kg	LHV, MJ/kg
		C	H	N	Cl	S	O	Ash	Volatile matter	Fixed carbons	Moisture		
LDPE	44	82.96	13.86	0.06	0.00	2.25	0.09	0.78	98.82	0.29	0.11	45.49	42.47
HDPE	10	83.28	14.06	0.05	0.00	0.18	0.59	1.83	96.71	1.18	0.27	45.55	42.48
PP	39	83.25	13.96	0.06	0.01	0.06	1.75	0.92	98.02	0.37	0.69	45.31	42.27
PS	7	89.37	8.06	0.43	0.00	0.05	1.41	0.68	93.4	5.49	0.44	40.54	38.78

Table 3A. The proximate and ultimate composition of LDPE

No	Proximate composition, wt %				Ultimate composition, wt %						Reference
	Ash	Volatile matter	Fixed carbons	Moisture	C	H	N	Cl	S	O	
1	0.00	99.70	0.00	0.30	85.70	14.20	0.05	0.00	0.00	0.05	(Park et al., 2012)
2	0.40	99.60	0.00	0.00	85.50	14.30		0.00	0.20	0.00	(Aboulkas and El Bouadili, 2010)
3	1.57	96.76	1.68	0.00	69.67	10.12	0.09	0.00	0.90	0.00	(Rajendran et al., 2020)

4					85.70	13.00	0.09	0.00	18.55	0.00	(Rajendran et al., 2020)
5	0.12	99.85	0.00	0.03	85.60	13.40	0.26	0.00	0.00	0.74	(Sharuddin et al., 2017)
6	0.00	99.80	0.20	0.10	83.67	16.33	0.00	0.00	0.00	0.00	(Silvarrey and Phan, 2016)
7	0.08	99.95	0.00	0.01	86.32	14.43	0.00	0.00	0.21	0.00	(Saad et al., 2021)
8	0.00	99.70	0.00	0.30							(Mortezaeikia et al., 2021)
9	0.40	99.60	0.00	0.00							(Mortezaeikia et al., 2021)
10	3.55	95.08	1.22	0.15							(Mortezaeikia et al., 2021)
11	1.99	97.85	0.16	0.18							(Mortezaeikia et al., 2021)
12	1.05	98.62	0.28	0.05	75.69	11.25	0.00	0.00	0.00	0.00	(Akgün et al., 2021)
13	0.15	99.65	0.00	0.20	83.00	16.75	0.00	0.00	0.25	0.00	(Dubdub and Al-Yaari, 2020)
Mean	0.78	98.85	0.30	0.11	82.32	13.75	0.06	0.00	2.23	0.09	Calculated

Table 4A. The proximate and ultimate composition of HDPE

No	Proximate composition, wt %				Ultimate composition, wt %						Reference
	Ash	Volatile matter	Fixed carbons	Moisture	C	H	N	Cl	S	O	
1	0.60	99.40	0.00	0.00	85.50	14.20	0.00	0.00	0.30	0.00	(Aboulkas and El Bouadili, 2010)
2	0.20	97.50	1.01	0.00	83.90	14.90	0.05	0.00	0.00	0.74	(Rajendran et al., 2020)
3	0.22	99.77	0.00	0.01	86.99	12.12	0.27	0.00	0.07	0.56	(Sharuddin et al., 2017)
4	0.18	99.81	0.01	0.00	84.74	11.65	0.02	0.00	0.66	0.00	(Ahmad et al., 2013)
5	1.40	98.57	0.03	0.00	83.73	15.52	0.01	0.00	0.00	0.00	(Heikkinen et al., 2004)

6	4.98	94.77	0.00	0.25	78.18	12.84	0.06	0.00	0.08	3.61	(Yao et al., 2018)
7	10.40	77.70	11.90	0.10	73.33	13.28	0.00	0.00	0.00	0.00	(Silvarrey and Phan, 2016)
8	0.38	99.27	0.00	0.72	85.39	14.23	0.02	0.00	0.23	0.37	(Saad et al., 2021)
9	0.18	99.81	0.01	0.80							(Mortezaeikia et al., 2021)
10	1.40	98.57	0.03	0.74							(Mortezaeikia et al., 2021)
11	0.22	99.38	0.00	0.41	82.77	16.92	0.00	0.00	0.29	0.00	(Dubdub and Al-Yaari, 2020)
Mean	1.83	96.78	1.18	0.28	82.73	13.96	0.05	0.00	0.18	0.59	Calculated

Table 5A. The proximate and ultimate composition of PP.

No	Proximate composition, wt %				Ultimate composition, wt %						Reference
	Ash	Volatile matter	Fixed carbons	Moisture	C	H	N	Cl	S	O	
1	0.00	99.70	0.00	0.30	86.10	13.70	0.00	0.00	0.00	0.20	(Park et al., 2012)
2	0.90	99.10	0.00	0.00	85.10	14.40	0.00	0.00	0.00	0.00	(Aboulkas and El Bouadili, 2010)
3	0.67	99.44	0.00	0.00	77.52	14.22	0.10	0.00	0.00	7.46	(Rajendran et al., 2020)
4					86.10	13.70	0.10	0.00	0.00	0.20	(Rajendran et al., 2020)
5	0.36	99.64	0.00	0.00	86.88	12.50	0.28	0.00	0.03	0.32	(Sharuddin et al., 2017)
6	1.99	97.85	0.16	0.18							(Heikkinen et al., 2004)
7	1.06	98.54	0.00	0.40	83.74	13.71	0.02	0.00	0.08	0.98	(Yao et al., 2018)
8	3.55	95.08	1.22	0.15	80.30	13.20	0.00	0.06	0.00	0.00	(Jung et al., 2010)
9	0.00	97.70	2.30	0.10	83.25	16.75	0.00	0.00	0.00	0.00	(Silvarrey and Phan, 2016)

10	0.39	95.00	0.00	5.68	78.85	12.74	0.04	0.00	0.23	8.38	(Saad et al., 2021)
11	0.29	99.63	0.00	0.08	85.00	14.73	0.04	0.00	0.23	0.00	(Dubdub and Al-Yaari, 2020)
Mean	0.92	98.17	0.37	0.69	83.28	13.97	0.06	0.01	0.06	1.75	Calculated

Table 6A. The proximate and ultimate composition of PS.

No	Proximate composition, wt %				Ultimate composition, wt %						Reference
	Ash	Volatile matter	Fixed carbons	Moisture	C	H	N	Cl	S	O	
1	0.00	99.50	0.20	0.30	92.70	7.90	0.00	0.00	0.00	0.00	(Park et al., 2012)
2	0.00	52.01	47.99	0.00	83.10	7.82	0.21	0.00	0.00	0.00	(Rajendran et al., 2020)
3					92.70	7.90	0.21	0.00	0.00	8.88	(Rajendran et al., 2020)
4	0.22	99.78	0.00	0.00	91.57	7.80	0.15	0.00	0.04	0.45	(Sharuddin et al., 2017)
5	0.50	99.30	0.00	0.20	90.40	8.56	0.07	0.00	0.08	0.18	(Yao et al., 2018)
6	0.00	98.80	1.20	1.00	89.81	7.48	2.71	0.00	0.00	0.00	(Silvarrey and Phan, 2016)
7	5.23	98.25	0.00	1.72	89.91	8.14	0.11	0.00	0.23	1.84	(Saad et al., 2021)
8	0.00	99.63	0.12	0.25							(Mortezaeikia et al., 2021)
9	0.00	99.50	0.20	0.30							(Mortezaeikia et al., 2021)
10	0.18	99.59	0.00	0.24	90.47	9.43	0.00	0.00	0.08	0.00	(Dubdub and Al-Yaari, 2020)
Mean	0.68	94.04	5.52	0.45	90.08	8.13	0.43	0.00	0.05	1.42	Calculated

Table 7A. Chemical composition of crude oil in Aspen plus simulation for C1 and D1 scenarios.

Component name	Alias in Aspen	Mass fraction, wt%
Toluene	C7H18	6.9
Dimethyl-heptene	1-TRA-01	1.4
Ethyl-benzene	ETHYL-01	6.3
Xylenes	O-XYL-01	2.1
Nonene	1-NON-01	2
Styrene	STYRE-01	16.4
a-Methyl-styrene	C9H10	2.2
Decene	1-DEC_01	3.7
Undecene	1-UND-01	3.6
Dodecene	1-DOD-01	3.1
Naphthalene	NAPTH-01	2.5
Tridecene	1-TRI-01	3.5
Tridecane	N-TRI-01	1.3
Tetradecene	1-TET-01	3.9
Tetradecane	N-TET-01	1.4
Pentadecene	1-PEN-01	3.6
Pentadecane	N-PEN-01	1.4
Hexadecene	1-HEX-01	3.6
Hexadecane	N-HEX-01	2.8
Heptadecene	1-HEP-01	3.5
Heptadecane	N-HEP-01	1.9
Octadecene	1-OCT_01	5.6
Octadecane	N-OCT-01	1.7
Nonadecene	1-NON-02	5.6
Nonadecane	N-NON-01	2
Eicosene	1-EIC-01	2.6
Eicosane	N-EIC-01	3.6
Heneicosane	N-HEN-01	1.8

Table 8A. Chemical composition of gas in Aspen plus simulation for C1 and D1 scenarios.

Component name	Alias in Aspen	Mass fraction, wt%
Hydrogen	H2	0.9
Carbon monoxide	CARBO-01	6.8
Carbon dioxide	CARBO-02	11.8
Methane	CH4	26.2
Ethane	ETHAN-01	17.9
Ethene	ETHYL-02	9.4
Propene	PROPY-01	14.2
Butene	BUTENE	12.8

Table 9A. Chemical composition of volatiles obtained from the fast pyrolysis in Aspen plus simulation for C2 and D2 scenarios.

Component name	Alias in Aspen	Mass fraction, wt%
Hydrogen	H2	0.01
Methane	CH4	0.29
Ethane	C2H6	0.53
ETHYLENE	ETHYL-01	0.45
PROPANE	C3H8	0.41
PROPYLENE	PROPY-01	1.7
N-BUTANE	N-BUT-01	0.11
ISOBUTANE	ISOBU-01	0.024
1-BUTENE	1-BUT-01	0.23
ISOBUTYLENE	ISOBU-02	0.34
1,2-BUTADIENE	1:2-B-01	0.025
N-PENTANE	N-PEN-01	0.75
2-PENTENE,-(CIS+TRANS)	C5H10	0.75
N-HEXANE	N-HEX-01	0.8
2-HEXENE,-(CIS+TRANS)	C6H12	0.8
N-HEPTANE	C7H16	0.41
2-HEPTENE	C7H14	0.41
N-OCTANE	C8H18	0.335

2-OCTENE	C8H16	0.335
N-NONANE	C9H20	1.8
1-NONENE	1-NON-01	1.8
2,4-DIMETHYLHEPTANE	2:4-D-01	2.4
N-DECANE	N-DEC-01	0.425
1-DECENE	01-Dec-01	0.425
N-UNDECANE	N-UND-01	0.295
1-UNDECENE	1-UND-01	0.295
N-DODECANE	N-DOD-01	0.45
1-DODECENE	1-DOD-01	0.45
N-TRIDECANE	N-TRI-01	0.31
1-TRIDECENE	1-TRI-01	0.31
N-TETRADECANE	N-TET-01	0.4
N-PENTADECANE	N-PEN-02	0.4
1-TETRADECENE	1-TET-01	0.4
1-PENTADECENE	1-PEN-01	0.4
1-HEXADECENE	1-HEX-01	0.4
1-HEPTADECENE	1-HEP-01	0.4
N-HEXADECANE	N-HEX-02	0.35
N-HEPTADECANE	N-HEP-01	0.35
1-OCTADECENE	01-Oct-01	0.35
1-NONADECENE	1-NON-02	0.35
1-EICOSENE	1-EIC-01	0.35
BENZENE	BENZE-01	0.014
TOLUENE	1:2-D-01	0.5
STYRENE	STYRE-01	6.3
ETHYLBENZENE	ETHYL-02	0.15
ALPHA-METHYL-STYRENE	ALPHA-01	0.29
N-OCTADECANE	N-OCT-01	0.44
N-NONADECANE	N-NON-01	0.44
N- HEXADECYLCYCLOPENTANE	N-HEX-03	0.44
1-DOCOSENE	1-DOC-01	0.44
CYCLOTRICOSANE	CYCLO-01	0.44
N-EICOSANE	N-EIC-01	0.4

N-HENEICOSANE	N-HEN-01	0.4
1-TETRACOSENE	1-TET-02	0.4
C25H50	C25H5-01	0.4
1-HEXACOSENE	1-HEX-02	0.4
N-DOCOSANE	N-DOC-01	0.42
N-TRICOSANE	N-TRI-02	0.42
C27H54-N1	C27H5-01	0.42
1-OCTACOSENE	01-Oct-02	0.42
1-NONACOSENE	1-NON-03	0.42
N-TETRACOSANE	N-TET-02	0.42
1-CYCLOHEXYLNONADECANE	1-CYC-01	0.42
1-TRIACONTENE	1-TRI-02	0.42
C31H62-N2	C31H6-01	0.42
C32H64-N4	C32H6-01	0.42
N-HEXACOSANE	N-HEX-04	0.42
N-HEPTACOSANE	N-HEP-02	0.42
C34H68-N2	17-TR-01	0.42
C35H70	C35H7-01	0.42
N-OCTACOSANE	N-OCT-02	0.42
N-NONACOSANE	N-NON-02	0.42
1-HEXATRIACONTENE	1-HEX-03	0.42
13-DODECYL-12-PENTACOSENE	13-DO-01	0.42
N-TRIACONTANE	N-TRI-03	0.42
N-HENTRIACONTANE	N-HEN-02	0.42
C39H78	C39H7-01	0.42
1-TETRACONTENE	1-TET-03	0.42
N-DOTRIACONTANE	N-DOT-01	0.7
N-TRITRIACONTANE	N-TRI-04	0.7
CYCLODOTETRACONTANE	CYCLO-02	0.7
3-METHHLTRITRIACONTANE	3-MET-01	0.7
2-METHYLTETRATRIACONTANE	2-MET-01	0.7
CYCLOPENTATETRACONTANE	CYCLO-03	0.7
N-HEXATRIACONTANE	N-HEX-05	0.7

N-HEPTATRIACONTANE	N-HEP-03	0.7
CYCLOOCTATETRACONTANE	CYCLO-04	0.7
13-DODECYLHEXACOSANE	13-DO-02	16.71
N-NONATRIACONTANE	N-NON-03	16.71
C40H82-N1	C40H8-01	16.726

Table 10A. Virtual components representing gas, oil and wax hydrocarbons of obtained volatiles from the fast pyrolysis for C2 and D2 scenarios.

Component name	Alias in Aspen	Mass fraction, wt%
Hydrogen	H2	0.011
Methane	CH4	0.29
Ethane	C2H6	0.53
ETHYLENE	ETHYL-01	0.45
PROPANE	C3H8	0.41
PROPYLENE	PROPY-01	2.429
N-PENTANE	C5H12	10.59
N-DECANE	N-DEC-01	2.96
N-TETRADECANE	N-TET-01	1.6
N-HEXADECANE	N-HEX-01	1.5
BENZENE	BENZE-01	0.014
TOLUENE	1:2-D-01	0.5
STYRENE	STYRE-01	6.3
ETHYLBENZENE	ETHYL-02	0.15
ALPHA-METHYL-STYRENE	ALPHA-01	0.29
N-OCTADECANE	N-OCT-01	5.46
N-OCTACOSANE	N-OCT-02	14.28
OCTATRIACONTANE	OCTAT-01	50.146

Table 11A. Chemical composition of diesel obtained from NMPW for C1 and D1 scenarios.

Component name	Alias in Aspen	Mass fraction, wt%
Toluene	C7H8	8.14

Dimethyl-heptene	1-TRA-01	1.65
Ethyl-benzene	ETHYL-01	7.43
Xylenes	O-XYL-01	2.48
Nonene	1-NON-01	2.35
Styrene	STYRE-01	19.35
a-Methyl-styrene	C9H10	2.6
Decene	1-DEC_01	4.37
Undecene	1-UND-01	4.25
Dodecene	1-DOD-01	3.66
Naphthalene	NAPTH-01	2.95
Tridecene	1-TRI-01	4.13
Tridecane	N-TRI-01	1.53
Tetradecene	1-TET-01	4.6
Tetradecane	N-TET-01	1.65
Pentadecene	1-PEN-01	4.24
Pentadecane	N-PEN-01	1.65
Hexadecene	1-HEX-01	4.25
Hexadecane	N-HEX-01	3.3
Heptadecene	1-HEP-01	4.13
Heptadecane	N-HEP-01	2.24
Octadecene	1-OCT_01	6.58
Octadecane	N-OCT-01	1.97
Nonadecene	1-NON-02	0.44
Nonadecane	N-NON-01	0.05
C20+		<0.01

Table 12A. Chemical composition of cleaned syngas obtained from NMPW for C2 and D2 scenarios.

Component name	Alias in Aspen	Mass fraction, wt%
Hydrogen	H2	7.89
Methane	CH4	<0.01
Ethane	C2H6	<0.01
ETHYLENE	ETHYL-01	<0.01

PROPANE	C3H8	<0.01
PROPYLENE	PROPY-01	<0.01
N-PENTANE	C5H12	<0.01
Steam	H2O	36.91
Carbon monoxide	CO	54.36

Table 13A. Chemical composition of the gas used as fuel to produce heating energy for the C1 and D1 scenarios.

Component name	Alias in Aspen	Mass fraction, wt%
Hydrogen	H2	0.9
Carbon monoxide	CO	6.8
Carbon dioxide	CO2	11.8
Methane	CH4	26.2
Ethane	ETHAN-01	17.9
Ethene	ETHYL-02	9.4
Propene	PROPY-01	14.2
Butene	BUTENE	12.8

Table 14A. Chemical composition of the residue used as fuel to produce heating energy for the C1 and D1 scenarios.

Component name	Alias in Aspen	Mass fraction, wt%
Nonadecene	1-NON-02	34.4
Nonadecane	N-NON-01	12.9
Eicosene	1-EIC-01	17.1
Eicosane	N-EIC-01	23.7
Heneicosane	N-HEN-01	11.8

Table 15A. Consumer Price Index (CPI) from 2010 to 2023 for UK (Gooding, 2023).

No	Year	CPI
1	2010	89.423
2	2011	93.415
3	2012	96.057
4	2013	98.521
5	2014	99.96
6	2015	100
7	2016	100.660
8	2017	103.361
9	2018	105.922
10	2019	107.819
11	2020	108.736
12	2021	111.551
13	2022	121.664
14	2023	130.545

Table 16A. The Chemical Engineering Plant Cost Index (CEPCI) from 2001 to 2022 (Chemical Engineering, 2023).

No	Year	CEPCI
1	2001	394.3
2	2002	395.6
3	2003	402
4	2004	444.2
5	2005	468.2
6	2006	499.6
7	2007	525.4
8	2008	575.4
9	2009	521.9
10	2010	550.8
11	2011	585.7
12	2012	584.6

13	2013	567.3
14	2014	576.1
15	2015	556.8
16	2016	541.7
17	2017	567.5
18	2018	603.1
19	2019	607.5
20	2020	596.2
21	2021	708.8
22	2022	816

Table 17A. The average prices of electricity and gas based on the consumption scale for non-domestic sector in UK in the reference year (Department for Energy Security and Net Zero, 2023a).

Name	Annual consumption, MWh	Price, pence per kWh
Electricity: very small	0-20	23.21
Electricity: small	20-499	19.36
Electricity: small/medium	500-1,999	23.28
Electricity: medium	2000-19,999	19.5
Electricity: large	20,000-69,999	18.39
Electricity: very large	70,000-150,000	19.34
Electricity: extra large	>150,000	19.13
Gas: very small	0-20	7.024
Gas: small	20-499	4.256
Gas: medium	500-1,999	4.539
Gas: large	2000-19,999	4.641
Gas: very large	20,000-69,999	5.034

Table 18A. The GWP breakdown of the four scenarios based on the stages involved in the production of hydrogen and diesel in percentages.

Stages	Scenarios			
	C1	D1	C2	D2
MPW collection and transportation to sorting facility	0.52%	0.31%	0.06%	0.05%
MPW sorting	1.76%	1.05%	0.20%	0.18%
Extra sorting	0.54%	0.32%	0.06%	0.05%
Bailing	0.29%	0.00%	0.03%	0.00%
MPW transportation to the pyrolysis facility	0.92%	0.00%	0.10%	0.00%
Impurities transportation to the incineration plant	0.10%	0.00%	0.01%	0.00%
Dryer	4.74%	5.82%	0.49%	1.03%
Pyrolysis/Pyrolysis-Catalytic Reforming	36.67%	57.49%	60.70%	64.57%
Oil distillation	10.18%	8.94%	0.37%	0.35%
PSA (pressure swing adsorption)	0.00%	0.00%	0.34%	0.30%
Impurities incineration	37.34%	22.23%	4.21%	3.74%
Acid washing	0.00%	0.00%	14.61%	13.01%
Diesel transportation to the oil refinery plant, and back to Glasgow	0.90%	0.27%	0.03%	0.01%
Fuel station	5.98%	3.56%	0.17%	0.15%
Ash transportation to landfill	0.05%	0.03%	0.00%	0.00%
Hydrogen compression and storage	0.00%	0.00%	0.96%	0.86%
Compressed hydrogen transportation	0.00%	0.00%	0.01%	0.00%
Refuelling hydrogen fuel vehicles	0.00%	0.00%	0.08%	0.08%
Wastewater treatment	0.00%	0.00%	17.56%	15.63%

References

- ABOULKAS, A. & EL BOUADILI, A. 2010. Thermal degradation behaviors of polyethylene and polypropylene. Part I: Pyrolysis kinetics and mechanisms. *Energy Conversion and Management*, 51, 1363-1369.
- ACOMB, J. C., WU, C. & WILLIAMS, P. T. 2016. The use of different metal catalysts for the simultaneous production of carbon nanotubes and hydrogen from pyrolysis of plastic feedstocks. *Applied Catalysis B: Environmental*, 180, 497-510.
- ADVISORS, D., DE WIT, W., HAMILTON, A., SCHEER, R., STAKES, T. & ALLAN, S. 2019. Solving plastic pollution through accountability. *WWF—World Wide Fund For Nature, Gland, Switzerland*.
- AFZAL, S., SINGH, A., NICHOLSON, S. R., UEKERT, T., DESVEAUX, J. S., TAN, E. C., DUTTA, A., CARPENTER, A. C., BALDWIN, R. M. & BECKHAM, G. T. 2023. Techno-economic analysis and life cycle assessment of mixed plastic waste gasification for production of methanol and hydrogen. *Green Chemistry*, 25, 5068-5085.
- AGILYX 2024.
- AGUADO, J., SERRANO, D. & ESCOLA, J. 2008. Fuels from waste plastics by thermal and catalytic processes: a review. *Industrial & Engineering Chemistry Research*, 47, 7982-7992.
- AHAMED, A., VEKSHA, A., YIN, K., WEERACHANCHAI, P., GIANNIS, A. & LISAK, G. 2020. Environmental impact assessment of converting flexible packaging plastic waste to pyrolysis oil and multi-walled carbon nanotubes. *Journal of hazardous materials*, 390, 121449.
- AHMAD, I., KHAN, M. I., ISHAQ, M., KHAN, H., GUL, K. & AHMAD, W. 2013. Catalytic efficiency of some novel nanostructured heterogeneous solid catalysts in pyrolysis of HDPE. *Polymer Degradation and Stability*, 98, 2512-2519.

- AKGÜN, H., YAPICI, E., GÜNKAYA, Z., ÖZKAN, A. & BANAR, M. 2021. Utilization of liquid product through pyrolysis of LDPE and C/LDPE as commercial wax. *Environmental Science and Pollution Research*, 28, 45971-45984.
- AL-QADRI, A. A., AHMED, U., JAMEEL, A. G. A., AHMAD, N., ZAHID, U., ZEIN, S. H. & NAQVI, S. R. 2023. Process design and techno-economic analysis of dual hydrogen and methanol production from plastics using energy integrated system. *International Journal of Hydrogen Energy*, 48, 10797-10811.
- AL-RUMAIHI, A., SHAHBAZ, M., MCKAY, G. & AL-ANSARI, T. 2023. Investigation of co-pyrolysis blends of camel manure, date pits and plastic waste into value added products using Aspen Plus. *Fuel*, 340, 127474.
- AL-SABAGH, A., YEHIA, F., ESHAQ, G., RABIE, A. & ELMETWALLY, A. 2016. Greener routes for recycling of polyethylene terephthalate. *Egyptian Journal of Petroleum*, 25, 53-64.
- ALLY, J. & PRYOR, T. 2016. Life cycle costing of diesel, natural gas, hybrid and hydrogen fuel cell bus systems: An Australian case study. *Energy Policy*, 94, 285-294.
- ÁLVAREZ, J., ORDÓÑEZ, S., ROSAL, R., SASTRE, H. & DíEZ, F. V. 1999. A new method for enhancing the performance of red mud as a hydrogenation catalyst. *Applied Catalysis A: General*, 180, 399-409.
- ANENE, A. F., FREDRIKSEN, S. B., SÆTRE, K. A. & TOKHEIM, L.-A. 2018. Experimental study of thermal and catalytic pyrolysis of plastic waste components. *Sustainability*, 10, 3979.
- ANTONOPOULOS, I., FARACA, G. & TONINI, D. 2021. Recycling of post-consumer plastic packaging waste in the EU: Recovery rates, material flows, and barriers. *Waste Management*, 126, 694-705.

- ARGYLE, M. D. & BARTHOLOMEW, C. H. 2015. Heterogeneous catalyst deactivation and regeneration: a review. *Catalysts*, 5, 145-269.
- ARREGI, A., SEIFALI ABBAS-ABADI, M., LOPEZ, G., SANTAMARIA, L., ARTETXE, M., BILBAO, J. & OLAZAR, M. 2020. CeO₂ and La₂O₃ promoters in the steam reforming of polyolefinic waste plastic pyrolysis volatiles on Ni-based catalysts. *ACS Sustainable Chemistry & Engineering*, 8, 17307-17321.
- ASCHER, S., GORDON, J., BONGIOVANNI, I., WATSON, I., HERMANNSSON, K., GILLESPIE, S., SARANGI, S., BIAKHMETOV, B., BHARGAVA, P. C. & BHASKAR, T. 2024. Trigeneration based on the pyrolysis of rural waste in India: Environmental impact, economic feasibility and business model innovation. *Science of The Total Environment*, 921, 170718.
- ASCHER, S., WATSON, I., WANG, X. & YOU, S. 2019. Township-based bioenergy systems for distributed energy supply and efficient household waste re-utilisation: Techno-economic and environmental feasibility. *Energy*, 181, 455-467.
- ATABANI, A. E., SILITONGA, A. S., BADRUDDIN, I. A., MAHLIA, T., MASJUKI, H. & MEKHILEF, S. 2012. A comprehensive review on biodiesel as an alternative energy resource and its characteristics. *Renewable and sustainable energy reviews*, 16, 2070-2093.
- AUPRETRE, F., DESCORME, C. & DUPREZ, D. 2002. Bio-ethanol catalytic steam reforming over supported metal catalysts. *Catalysis Communications*, 3, 263-267.
- AWAJA, F. & PAVEL, D. 2005. Recycling of PET. *European polymer journal*, 41, 1453-1477.
- BANK, M. S., SWARZENSKI, P. W., DUARTE, C. M., RILLIG, M. C., KOELMANS, A. A., METIAN, M., WRIGHT, S., PROVENCHER, J. F., SANDEN, M. & JORDAAN,

- A. 2021. Global Plastic Pollution Observation System to Aid Policy. *Environmental Science & Technology*.
- BARBARIAS, I., LOPEZ, G., ARTETXE, M., ARREGI, A., BILBAO, J. & OLAZAR, M. 2018. Valorisation of different waste plastics by pyrolysis and in-line catalytic steam reforming for hydrogen production. *Energy Conversion and Management*, 156, 575-584.
- BENAVIDES, P. T., SUN, P., HAN, J., DUNN, J. B. & WANG, M. 2017. Life-cycle analysis of fuels from post-use non-recycled plastics. *Fuel*, 203, 11-22.
- BIAKHMETOV, B., DOSTIYAROV, A., OK, Y. S. & YOU, S. 2023. A review on catalytic pyrolysis of municipal plastic waste. *Wiley Interdisciplinary Reviews: Energy and Environment*, e495.
- BIAKHMETOV, B., LI, Y., ZHAO, Q., DOSTIYAROV, A., FLYNN, D. & YOU, S. 2025. Transportation and process modelling-assisted techno-economic assessment of resource recovery from non-recycled municipal plastic waste. *Energy Conversion and Management*, 324, 119273.
- BIAKHMETOV, B., LI, Y., ZHAO, Q., OK, Y. S., DOSTIYAROV, A., PARK, Y.-K., FLYNN, D. & YOU, S. 2024. Comparing carbon-saving potential of the pyrolysis of non-recycled municipal plastic waste: Influences of system scales and end products. *Journal of Cleaner Production*, 143140.
- BIAKHMETOV, B., YOU, S. & DOSTIYAROV, A. 2022. Sustainable waste management and circular economy. *Low Carbon Stabilization and Solidification of Hazardous Wastes*. Elsevier.
- BIBBY, D. M., HOWE, R. F. & MCLELLAN, G. D. 1992. Coke formation in high-silica zeolites. *Applied Catalysis A: General*, 93, 1-34.

- BODZAY, B. & BÁNHEGYI, G. 2016. Polymer waste: controlled breakdown or recycling? *International Journal of Design Sciences & Technology*, 22.
- BORA, R. R., WANG, R. & YOU, F. 2020. Waste polypropylene plastic recycling toward climate change mitigation and circular economy: energy, environmental, and technoeconomic perspectives. *ACS Sustainable Chemistry & Engineering*, 8, 16350-16363.
- BORRELLE, S. B., RINGMA, J., LAW, K. L., MONNAHAN, C. C., LEBRETON, L., MCGIVERN, A., MURPHY, E., JAMBECK, J., LEONARD, G. H. & HILLEARY, M. A. 2020. Predicted growth in plastic waste exceeds efforts to mitigate plastic pollution. *Science*, 369, 1515-1518.
- BORSODI, N., MISKOLCZI, N., ANGYAL, A., BARTHA, L., KOHÁN, J. & LENGYEL, A. Hydrocarbons obtained by pyrolysis of contaminated waste plastics. 45th International Petroleum Conference, Bratislava, Slovak Republic, 2011.
- BORSODI, N., SZENTES, A., MISKOLCZI, N., WU, C. & LIU, X. 2016. Carbon nanotubes synthesized from gaseous products of waste polymer pyrolysis and their application. *Journal of Analytical and Applied Pyrolysis*, 120, 304-313.
- BRITISH PLASTIC FEDERATION 2024. Plastic Recycling.
- BROWNSORT, P. A., SCOTT, V. & HASZELDINE, R. S. 2016. Reducing costs of carbon capture and storage by shared reuse of existing pipeline—Case study of a CO₂ capture cluster for industry and power in Scotland. *International Journal of Greenhouse Gas Control*, 52, 130-138.
- BUCCI, K., TULIO, M. & ROCHMAN, C. 2020. What is known and unknown about the effects of plastic pollution: A meta-analysis and systematic review. *Ecological Applications*, 30, e02044.

- BUDSAEREECHAI, S., HUNT, A. J. & NGERNYEN, Y. 2019. Catalytic pyrolysis of plastic waste for the production of liquid fuels for engines. *RSC advances*, 9, 5844-5857.
- BURGESS, J. UK must remove barriers to green hydrogen to meet 5-GW 2030 target: RenewableUK.
- BURGESS, M., HOLMES, H., SHARMINA, M. & SHAVER, M. P. 2021. The future of UK plastics recycling: one bin to rule them all. *Resources, Conservation and Recycling*, 164, 105191.
- CAI, N., LI, X., XIA, S., SUN, L., HU, J., BARTOCCI, P., FANTOZZI, F., WILLIAMS, P. T., YANG, H. & CHEN, H. 2021. Pyrolysis-catalysis of different waste plastics over Fe/Al₂O₃ catalyst: High-value hydrogen, liquid fuels, carbon nanotubes and possible reaction mechanisms. *Energy Conversion and Management*, 229, 113794.
- CALERO, M., MARTÍN-LARA, M. Á., GODOY, V., QUESADA, L., MARTÍNEZ, D., PEULA, F. & SOTO, J. M. 2018. Characterization of plastic materials present in municipal solid waste: Preliminary study for their mechanical recycling. *Detritus*, 104.
- CARLSON, E. L., PICKFORD, K. & NYGA-ŁUKASZEWSKA, H. 2023. Green hydrogen and an evolving concept of energy security: Challenges and comparisons. *Renewable Energy*, 219, 119410.
- CASTANO, P., ELORDI, G., OLAZAR, M., AGUAYO, A. T., PAWELEC, B. & BILBAO, J. 2011. Insights into the coke deposited on HZSM-5, H β and HY zeolites during the cracking of polyethylene. *Applied Catalysis B: Environmental*, 104, 91-100.
- ÇEPELIOĞULLAR, Ö. & PÜTÜN, A. E. 2013. Utilization of two different types of plastic wastes from daily and industrial life. *Journal of Selcuk University Natural and Applied Science*, 2, 694-706.

- CHANDRAN, M., TAMILKOLUNDU, S. & MURUGESAN, C. 2020. Characterization studies: waste plastic oil and its blends. *Energy Sources, Part A: Recovery, Utilization, and Environmental Effects*, 42, 281-291.
- CHEMICAL ENGINEERING 2023. The Chemical Engineering Plant Cost Index (CEPCI).
- CHEN, C., JIN, Y. & CHI, Y. 2014a. Effects of moisture content and CaO on municipal solid waste pyrolysis in a fixed bed reactor. *Journal of analytical and applied pyrolysis*, 110, 108-112.
- CHEN, D., YIN, L., WANG, H. & HE, P. 2014b. Pyrolysis technologies for municipal solid waste: a review. *Waste management*, 34, 2466-2486.
- CHEN, Z., ZHANG, X., CHE, L., PENG, H., ZHU, S., YANG, F. & ZHANG, X. 2020. Effect of volatile reactions on oil production and composition in thermal and catalytic pyrolysis of polyethylene. *Fuel*, 271, 117308.
- CHEN, Z., ZHANG, X., YANG, F., PENG, H., ZHANG, X., ZHU, S. & CHE, L. 2021. Deactivation of a Y-zeolite based catalyst with coke evolution during the catalytic pyrolysis of polyethylene for fuel oil. *Applied Catalysis A: General*, 609, 117873.
- CHIN, B. L. F., YUSUP, S., AL SHOAIBI, A., KANNAN, P., SRINIVASAKANNAN, C. & SULAIMAN, S. A. 2014. Kinetic studies of co-pyrolysis of rubber seed shell with high density polyethylene. *Energy conversion and management*, 87, 746-753.
- CIVANCIK-USLU, D., NHU, T. T., VAN GORP, B., KRESOVIC, U., LARRAIN, M., BILLEN, P., RAGAERT, K., DE MEESTER, S., DEWULF, J. & HUYSVELD, S. 2021. Moving from linear to circular household plastic packaging in Belgium: Prospective life cycle assessment of mechanical and thermochemical recycling. *Resources, Conservation and Recycling*, 171, 105633.
- CLARK, H. & WU, H. 2016. The sustainable development goals: 17 goals to transform our world. *Furthering the work of the United Nations*, 36-54.

- COELHO, P. M., CORONA, B., TEN KLOOSTER, R. & WORRELL, E. 2020. Sustainability of reusable packaging-Current situation and trends. *Resources, Conservation & Recycling: X*, 100037.
- CUNANAN, C., TRAN, M.-K., LEE, Y., KWOK, S., LEUNG, V. & FOWLER, M. 2021. A review of heavy-duty vehicle powertrain technologies: Diesel engine vehicles, battery electric vehicles, and hydrogen fuel cell electric vehicles. *Clean Technologies*, 3, 474-489.
- DAGLE, R. A., DAGLE, V., BEARDEN, M. D., HOLLADAY, J. D., KRAUSE, T. R. & AHMED, S. 2017. An overview of natural gas conversion technologies for co-production of hydrogen and value-added solid carbon products.
- DAI, L., KARAKAS, O., CHENG, Y., COBB, K., CHEN, P. & RUAN, R. 2023. A review on carbon materials production from plastic wastes. *Chemical Engineering Journal*, 453, 139725.
- DAI, L., ZHOU, N., LV, Y., CHENG, Y., WANG, Y., LIU, Y., COBB, K., CHEN, P., LEI, H. & RUAN, R. 2022. Pyrolysis technology for plastic waste recycling: A state-of-the-art review. *Progress in Energy and Combustion Science*, 93, 101021.
- DAS, A. K., HANSDAH, D., MOHAPATRA, A. K. & PANDA, A. K. 2020. Energy, exergy and emission analysis on a DI single cylinder diesel engine using pyrolytic waste plastic oil diesel blend. *Journal of the Energy Institute*, 93, 1624-1633.
- DAVIDSON, M. G., FURLONG, R. A. & MCMANUS, M. C. 2021. Developments in the Life Cycle Assessment of Chemical Recycling of Plastic Waste—A Review. *Journal of Cleaner Production*, 126163.
- DE-LA-TORRE, G. E. 2020. Microplastics: an emerging threat to food security and human health. *Journal of food science and technology*, 57, 1601-1608.

DE MARCO, I., CABALLERO, B. M., LÓPEZ, A., LARESGOITI, M., TORRES, A. & CHOMÓN, M. J. 2009. Pyrolysis of the rejects of a waste packaging separation and classification plant. *Journal of Analytical and Applied Pyrolysis*, 85, 384-391.

DE SOUZA MACHADO, A. A., KLOAS, W., ZARFL, C., HEMPEL, S. & RILLIG, M. C. 2018. Microplastics as an emerging threat to terrestrial ecosystems. *Global change biology*, 24, 1405-1416.

DEFRA (DEPARTMENT OF ECONOMIC AND SOCIAL AFFAIRS POPULATION DIVISION) 2018. Digest of Waste and Resource Statistics- 2018 Edition.

DEGNAN, T. F. 2000. Applications of zeolites in petroleum refining. *Topics in Catalysis*, 13, 349-356.

DEPARTMENT FOR BUSINESS, E. I. S. 2021. Sub-national road transport fuel consumption in the United Kingdom, 2005 to 2019.

DEPARTMENT FOR ENERGY SECURITY & NET ZERO 2023a. Hydrogen production delivery roadmap.

DEPARTMENT FOR ENERGY SECURITY & NET ZERO 2023b. Hydrogen Strategy Update to the Market: August 2023.

DEPARTMENT FOR ENERGY SECURITY & NET ZERO 2023c. Hydrogen Transport and Storage Cost Report.

DEPARTMENT FOR ENERGY SECURITY AND NET ZERO 2019. Road fuel consumption and the UK motor vehicle fleet.

DEPARTMENT FOR ENERGY SECURITY AND NET ZERO 2021. Hydrogen Production Costs 2021.

DEPARTMENT FOR ENERGY SECURITY AND NET ZERO 2023a. Gas and electricity prices in the non-domestic sector.

DEPARTMENT FOR ENERGY SECURITY AND NET ZERO 2023b. Traded carbon values used for modelling purposes, 2023.

DEPARTMENT FOR ENERGY SECURITY AND NET ZERO 2024. Energy Trends and Prices statistical release: 25 January 2024.

DEPARTMENT FOR ENERGY SECURITY AND NET ZERO AND DEPARTMENT FOR BUSINESS, E. I. S. 2022. Hydrogen infrastructure requirements up to 2035.

DIRECTIVE, E. 2008. Directive 2008/98/EC of the European Parliament and of the Council of 19 November 2008 on waste and repealing certain Directives. *Official Journal of the European Union L*, 312.

DISSANAYAKE, P. D., KIM, S., SARKAR, B., OLESZCZUK, P., SANG, M. K., HAQUE, M. N., AHN, J. H., BANK, M. S. & OK, Y. S. 2022. Effects of microplastics on the terrestrial environment: A critical review. *Environmental Research*, 112734.

DOUBILET, P., BEGG, C. B., WEINSTEIN, M. C., BRAUN, P. & MCNEIL, B. J. 1985. Probabilistic sensitivity analysis using Monte Carlo simulation: a practical approach. *Medical decision making*, 5, 157-177.

DUBDUB, I. & AL-YAARI, M. 2020. Pyrolysis of mixed plastic waste: I. kinetic study. *Materials*, 13, 4912.

EAMSIRI, A., JACKSON, W. R., PRATT, K. C., CHRISTOV, V. & MARSHALL, M. 1992. Activated red mud as a catalyst for the hydrogenation of coals and of aromatic compounds. *Fuel*, 71, 449-453.

EDINA SOCIETY DIGIMAP SERVICE 2011. Output Area Classification [FileGeoDatabase geospatial data], Scale 1:2500, Tiles: GB, Updated: 27 March 2011, ONS, Using: EDINA Society Digimap Service, <<https://digimap.edina.ac.uk>>, Downloaded: 2022-10-01 17:00:45.519.

- EDINA SOCIETY DIGIMAP SERVICE 2022a. OS Open Roads [SHAPE geospatial data], Scale 1:25000, Tiles: ns, Updated: 29 March 2022, Ordnance Survey (GB), Using: EDINA Digimap Ordnance Survey Service, <<https://digimap.edina.ac.uk>>, Downloaded: 2022-10-09 15:39:35.096.
- EDINA SOCIETY DIGIMAP SERVICE 2022b. OS Open UPRN [GeoPackage geospatial data], Scale 1:1000, Tiles: GB, Updated: 15 March 2022, Ordnance Survey (GB), Using: EDINA Digimap Ordnance Survey Service, <<https://digimap.edina.ac.uk>>, Downloaded: 2022-10-10 12:57:17.288.
- EDINA SOCIETY DIGIMAP SERVICE 2022c. UKBuildings [FileGeoDatabase geospatial data], Scale 1:5000, Tiles: GB, Updated: 1 September 2022, Verisk, Using: EDINA Verisk Digimap Service, <<https://digimap.edina.ac.uk>>, Downloaded: 2023-08-29 18:02:57.303.
- EDJABOU, M. E., TAKOU, V., BOLDRIN, A., PETERSEN, C. & ASTRUP, T. F. 2021. The influence of recycling schemes on the composition and generation of municipal solid waste. *Journal of Cleaner Production*, 295, 126439.
- ELLEN MACARTHUR FOUNDATION 2016. The New Plastics Economy: Rethinking the future of plastics.
- ELLEN MACARTHUR FOUNDATION 2020. The Global Commitment 2020 Progress Report.
- ELLEN MACARTHUR FOUNDATION 2023. The Global Commitment 2023 Progress Report.
- ELLEN MACARTHUR FOUNDATION, M. E. 2019. Completing the Picture: how the circular economy tackles climate change.
- ELORDI, G., OLAZAR, M., LOPEZ, G., AMUTIO, M., ARTETXE, M., AGUADO, R. & BILBAO, J. 2009. Catalytic pyrolysis of HDPE in continuous mode over zeolite

- catalysts in a conical spouted bed reactor. *Journal of Analytical and Applied Pyrolysis*, 85, 345-351.
- EPA 2023. CHP Benefits.
- ERDOĞAN, S., BALKI, M. K. & SAYIN, C. 2019. The effect on the knock intensity of high viscosity biodiesel use in a DI diesel engine. *Fuel*, 253, 1162-1167.
- ERIKSSON, O. & FINNVEDEN, G. 2009. Plastic waste as a fuel-CO₂-neutral or not? *Energy & Environmental Science*, 2, 907-914.
- EUROPEAN COMMISSION 2020. A new Circular Economy Action Plan for a Cleaner and More Competitive Europe.
- EUROPEAN COMMISSION 2024. A EUROPEAN STRATEGY FOR PLASTICS IN A CIRCULAR ECONOMY.
- EUROPEAN COMMISSION 2018. Directive 2008/98/EC on waste (Waste Framework Directive).
- FADILLAH, G., FATIMAH, I., SAHRONI, I., MUSAWWA, M. M., MAHLIA, T. M. I. & MURAZA, O. 2021. Recent progress in low-cost catalysts for pyrolysis of plastic waste to fuels. *Catalysts*, 11, 837.
- FAISAL, F., RASUL, M., CHOWDHURY, A. A., SCHALLER, D. & JAHIRUL, M. 2023a. Uncovering the differences: A comparison of properties of crude plastic pyrolytic oil and distilled and hydrotreated plastic diesel produced from waste and virgin plastics as automobile fuels. *Fuel*, 350, 128743.
- FAISAL, F., RASUL, M., JAHIRUL, M. & CHOWDHURY, A. A. 2023b. Waste plastics pyrolytic oil is a source of diesel fuel: A recent review on diesel engine performance, emissions, and combustion characteristics. *Science of The Total Environment*, 163756.

- FAISAL, F., RASUL, M., JAHIRUL, M. & SCHALLER, D. 2023c. Pyrolytic conversion of waste plastics to energy products: A review on yields, properties, and production costs. *Science of The Total Environment*, 861, 160721.
- FANG, Y., LI, X., ASCHER, S., LI, Y., DAI, L., RUAN, R. & YOU, S. 2023. Life cycle assessment and cost benefit analysis of concentrated solar thermal gasification of biomass for continuous electricity generation. *Energy*, 284, 128709.
- FANG, Y., LI, X., WANG, X., DAI, L., RUAN, R. & YOU, S. 2024. Machine learning-based multi-objective optimization of concentrated solar thermal gasification of biomass incorporating life cycle assessment and techno-economic analysis. *Energy Conversion and Management*, 302, 118137.
- FERNÁNDEZ, Y., ARENILLAS, A. & MENÉNDEZ, J. 2011. Microwave Heating Applied to Pyrolysis, *Advances in Induction and Microwave Heating of Mineral and Organic Materials*, Stanisław Grundas (Ed.), ISBN: 978-953-307-522-8. *InTech, InTech*.
- FOSTER, S. 2008. Domestic mixed plastics packaging waste management options. *Waste and Resources Action Programme (WRAP): Oxford, UK*, 1-77.
- FRIEDLINGSTEIN, P., JONES, M. W., O'SULLIVAN, M., ANDREW, R. M., HAUCK, J., PETERS, G. P., PETERS, W., PONGRATZ, J., SITCH, S. & LE QUÉRÉ, C. 2019. Global carbon budget 2019. *Earth System Science Data*, 11, 1783-1838.
- FUKUSHIMA, M., SHIOYA, M., WAKAI, K. & IBE, H. 2009. Toward maximizing the recycling rate in a Sapporo waste plastics liquefaction plant. *Journal of material cycles and waste management*, 11, 11-18.
- GARCIA-GUTIERREZ, P., AMADEI, A. M., KLENERT, D., NESSI, S., TONINI, D., TOSCHES, D., ARDENTE, F. & SAVEYN, H. 2023. Environmental and economic assessment of plastic waste recycling. *A Comparison of Mechanical, Physical, Chemical Recycling and Energy Recovery of Plastic Waste*.

- GARFORTH, A., FIDDY, S., LIN, Y.-H., GHANBARI-SIAKHALI, A., SHARRATT, P. & DWYER, J. 1997. Catalytic degradation of high density polyethylene: an evaluation of mesoporous and microporous catalysts using thermal analysis. *Thermochimica Acta*, 294, 65-69.
- GEAR, M., SADHUKHAN, J., THORPE, R., CLIFT, R., SEVILLE, J. & KEAST, M. 2018. A life cycle assessment data analysis toolkit for the design of novel processes—A case study for a thermal cracking process for mixed plastic waste. *Journal of cleaner production*, 180, 735-747.
- GEISLER, C. H. & MARAVELIAS, C. T. 2021. Economic, energetic, and environmental analysis of lignocellulosic biorefineries with carbon capture. *Applied Energy*, 302, 117539.
- GERVET, B. 2007. The use of crude oil in plastic making contributes to global warming. *Lulea: Lulea University of Technology*.
- GEYER, R. 2020. Production, use, and fate of synthetic polymers. *Plastic Waste and Recycling*. Elsevier.
- GIACOVELLI, C. 2018. Single-Use Plastics: A Roadmap for Sustainability (rev. 2).
- GLASGOW CITY COUNCIL 2015. Tackling Glasgow's waste cleansing and waste strategy and action plan 2015 to 2020.
- GLASGOW CITY COUNCIL 2019. Glasgow City Council On Road To Zero Emissions Vehicle Fleet.
- GLASGOW CITY COUNCIL 2021. Fully electric bin lorry sees Glasgow driving ahead on zero emissions.
- GLASGOW CITY COUNCIL 2023a. Bin Replacement Programme: Frequently Asked Questions.

- GLASGOW CITY COUNCIL 2023b. Glasgow City Council Neighbourhoods, Regeneration and Sustainability Charges 2023/24.
- GLASGOW CITY COUNCIL 2023c. Waste and Recycling FAQs.
- GLASGOW CITY COUNCIL 2025. Household Waste Recycling Centres.
- GOODING, P. 2023. Consumer price inflation.
- GRADUS, R. 2020. Postcollection separation of plastic recycling and design-for-recycling as solutions to low cost-effectiveness and plastic debris. *Sustainability*, 12, 8415.
- GRANT, M. L., LAVERS, J. L., HUTTON, I. & BOND, A. L. 2021. Seabird breeding islands as sinks for marine plastic debris. *Environmental Pollution*, 116734.
- GREENMANTRA TECHNOLOGIES 2024.
- GRIFFITHS, O. G., O'BYRNE, J. P., TORRENTE-MURCIANO, L., JONES, M. D., MATTIA, D. & MCMANUS, M. C. 2013. Identifying the largest environmental life cycle impacts during carbon nanotube synthesis via chemical vapour deposition. *Journal of cleaner production*, 42, 180-189.
- GROOTEN, M. & ALMOND, R. E. 2018. Living planet report-2018: aiming higher. *Living planet report-2018: aiming higher*.
- GUO, P., CHEN, X., GAO, X., SONG, H. & SHEN, H. 2007. Fabrication and mechanical properties of well-dispersed multiwalled carbon nanotubes/epoxy composites. *Composites science and Technology*, 67, 3331-3337.
- GUPTA, R., MCROBERTS, R., YU, Z., SMITH, C., SLOAN, W. & YOU, S. 2022. Life cycle assessment of biodiesel production from rapeseed oil: Influence of process parameters and scale. *Bioresource Technology*, 360, 127532.
- HAFEEZ, S., PALLARI, E., MANOS, G. & CONSTANTINOU, A. 2019. Catalytic conversion and chemical recovery. *Plastics to energy*. Elsevier.

- HAIG, S., MORRISH, L., MORTON, R., ONWUAMAEGBU, U., SPELLER, P. & WILKINSON, S. 2018. Plastics to oil products: Final report. *Zero Waste Scotland*.
- HAUGEN, M. J., FLYNN, D., GREENING, P., TICHLER, J., BLYTHE, P. & BOIES, A. M. 2022. Electrification versus hydrogen for UK road freight: Conclusions from a systems analysis of transport energy transitions. *Energy for Sustainable Development*, 68, 203-210.
- HEIKKINEN, J., HORDIJK, J. D., DE JONG, W. & SPLIETHOFF, H. 2004. Thermogravimetry as a tool to classify waste components to be used for energy generation. *Journal of Analytical and Applied Pyrolysis*, 71, 883-900.
- HERNADI, K., FONSECA, A., NAGY, J. B., SISKA, A. & KIRICSI, I. 2000. Production of nanotubes by the catalytic decomposition of different carbon-containing compounds. *Applied Catalysis A: General*, 199, 245-255.
- HOLGER, R., UDO, J., CLINT, F., ALEXANDER, M. Z. F., SANTOSH, A. & MIRIAM, B. D. 2019. A Circular Solution to Plastic Waste.
- HONUS, S., KUMAGAI, S., FEDORKO, G., MOLNÁR, V. & YOSHIOKA, T. 2018a. Pyrolysis gases produced from individual and mixed PE, PP, PS, PVC, and PET—Part I: Production and physical properties. *Fuel*, 221, 346-360.
- HONUS, S., KUMAGAI, S., MOLNÁR, V., FEDORKO, G. & YOSHIOKA, T. 2018b. Pyrolysis gases produced from individual and mixed PE, PP, PS, PVC, and PET—Part II: Fuel characteristics. *Fuel*, 221, 361-373.
- HORODYTSKA, O., CABANES, A. & FULLANA, A. 2019. Plastic waste management: current status and weaknesses. *Plastics in the Aquatic Environment-Part I: Current Status and Challenges*. Springer.

- HUANG, J., JIANG, Y., MARTHALA, V. R., BRESSEL, A., FREY, J. & HUNGER, M. 2009. Effect of pore size and acidity on the coke formation during ethylbenzene conversion on zeolite catalysts. *Journal of Catalysis*, 263, 277-283.
- HUANG, J., VEKSHA, A., JUN, T. F. J. & LISAK, G. 2022. Upgrading waste plastic derived pyrolysis gas via chemical looping cracking–gasification using Ni–Fe–Al redox catalysts. *Chemical Engineering Journal*, 438, 135580.
- HYDROGEN UK 2023. Economic Impact Assessment for the Hydrogen Sector to 2030.
- HYDROGEN VALLEY PLATFORM 2024. Hydrogen cost and sales prices.
- IAN, T. 2023. United Kingdom Emission Trading System (UK-ETS) carbon pricing from January 2022 to July 2023.
- IEA 2021. Fuel economy in the United Kingdom.
- IKÄHEIMO, J., PURSIHEIMO, E., KIVILUOMA, J. & HOLTTINEN, H. 2019. Role of power to liquids and biomass to liquids in a nearly renewable energy system. *IET Renewable Power Generation*, 13, 1179-1189.
- IMPERATIVES, S. 1987. Report of the World Commission on Environment and Development: Our common future. *Accessed Feb, 10*, 1-300.
- INAYAT, A., KLEMENCOVA, K., GRYSKOVA, B., SOKOLOVA, B. & LESTINSKY, P. 2021. Thermo-catalytic pyrolysis of polystyrene in batch and semi-batch reactors: A comparative study. *Waste Management & Research*, 39, 260-269.
- INDUSTRIES, K. 2024.
- INSHAKOVA, E., INSHAKOVA, A. & GONCHAROV, A. Engineered nanomaterials for energy sector: Market trends, modern applications and future prospects. IOP Conference Series: Materials Science and Engineering, 2020. IOP Publishing, 032031.

- ISAACS, J. A., TANWANI, A., HEALY, M. & DAHLBEN, L. 2010. Economic assessment of single-walled carbon nanotube processes. *Journal of Nanoparticle Research*, 12, 551-562.
- ISMAIL, H. Y., ABBAS, A., AZIZI, F. & ZEAITER, J. 2017. Pyrolysis of waste tires: A modeling and parameter estimation study using Aspen Plus®. *Waste management*, 60, 482-493.
- ISO 2006a. ISO 14040:2006 Environmental management — Life cycle assessment — Principles and framework.
- ISO 2006b. ISO 14044:2006 Environmental management — Life cycle assessment — Requirements and guidelines.
- JAMBECK, J. R., GEYER, R., WILCOX, C., SIEGLER, T. R., PERRYMAN, M., ANDRADY, A., NARAYAN, R. & LAW, K. L. 2015. Plastic waste inputs from land into the ocean. *Science*, 347, 768-771.
- JANUSZEWICZ, K., HUNICZ, J., KAZIMIERSKI, P., RYBAK, A., SUCHOCKI, T., DUDA, K. & MIKULSKI, M. 2023. An experimental assessment on a diesel engine powered by blends of waste-plastic-derived pyrolysis oil with diesel. *Energy*, 281, 128330.
- JAUNICH, M. K., LEVIS, J. W., DECAROLIS, J. F., GASTON, E. V., BARLAZ, M. A., BARTELT-HUNT, S. L., JONES, E. G., HAUSER, L. & JAIKUMAR, R. 2016. Characterization of municipal solid waste collection operations. *Resources, Conservation and Recycling*, 114, 92-102.
- JEPSEN, E. M. & DE BRUYN, P. N. 2019. Pinniped entanglement in oceanic plastic pollution: A global review. *Marine pollution bulletin*, 145, 295-305.
- JESWANI, H., KRÜGER, C., RUSS, M., HORLACHER, M., ANTONY, F., HANN, S. & AZAPAGIC, A. 2021. Life cycle environmental impacts of chemical recycling via

- pyrolysis of mixed plastic waste in comparison with mechanical recycling and energy recovery. *Science of The Total Environment*, 769, 144483.
- JIANG, Y., LI, X., LI, C., ZHANG, L., ZHANG, S., LI, B., WANG, S. & HU, X. 2022. Pyrolysis of typical plastics and coupled with steam reforming of their derived volatiles for simultaneous production of hydrogen-rich gases and heavy organics. *Renewable Energy*, 200, 476-491.
- JUNG, S.-H., CHO, M.-H., KANG, B.-S. & KIM, J.-S. 2010. Pyrolysis of a fraction of waste polypropylene and polyethylene for the recovery of BTX aromatics using a fluidized bed reactor. *Fuel processing technology*, 91, 277-284.
- KAEWLUAN, S. & PIPATMANOMAI, S. 2011. Gasification of high moisture rubber woodchip with rubber waste in a bubbling fluidized bed. *Fuel Processing Technology*, 92, 671-677.
- KAMINSKY, W., PREDEL, M. & SADIKI, A. 2004. Feedstock recycling of polymers by pyrolysis in a fluidised bed. *Polymer degradation and stability*, 85, 1045-1050.
- KANATTUKARA, B. V., SINGH, G., SARKAR, P., CHOPRA, A., SINGH, D., MONDAL, S., KAPUR, G. S. & RAMAKUMAR, S. S. V. 2023. Catalyst-mediated pyrolysis of waste plastics: tuning yield, composition, and nature of pyrolysis oil. *Environmental Science and Pollution Research*, 1-17.
- KARAMARKOVIC, R. & KARAMARKOVIC, V. 2010. Energy and exergy analysis of biomass gasification at different temperatures. *Energy*, 35, 537-549.
- KARIMI, S., BIBAK, F., MESHKANI, F., RASTEGARPANAH, A., DENG, J., LIU, Y. & DAI, H. 2021. Promotional roles of second metals in catalyzing methane decomposition over the Ni-based catalysts for hydrogen production: a critical review. *International Journal of Hydrogen Energy*, 46, 20435-20480.

- KAZA, S., YAO, L., BHADA-TATA, P. & VAN WOERDEN, F. 2018. *What a waste 2.0: a global snapshot of solid waste management to 2050*, World Bank Publications.
- KERSHAW, P. J. 2016. Marine plastic debris and microplastics—Global lessons and research to inspire action and guide policy change.
- KHOO, H. H. 2009. Life cycle impact assessment of various waste conversion technologies. *Waste management*, 29, 1892-1900.
- KHOO, H. H. 2019. LCA of plastic waste recovery into recycled materials, energy and fuels in Singapore. *Resources, Conservation and Recycling*, 145, 67-77.
- KIM, I., KIM, J. & LEE, J. 2020. Dynamic analysis of well-to-wheel electric and hydrogen vehicles greenhouse gas emissions: Focusing on consumer preferences and power mix changes in South Korea. *Applied Energy*, 260, 114281.
- KRÜGER, C., RUSS, M., GONZALEZ, M. & HORLACHER, M. 2020. Evaluation of pyrolysis with LCA—3 case studies. *BASF*, no. July.
- KÜHN, S. & VAN FRANEKER, J. A. 2020. Quantitative overview of marine debris ingested by marine megafauna. *Marine pollution bulletin*, 151, 110858.
- KUMAGAI, S. & YOSHIOKA, T. 2016. Feedstock recycling via waste plastic pyrolysis. *Journal of the Japan Petroleum Institute*, 59, 243-253.
- KUMAR, M., XIONG, X., HE, M., TSANG, D. C., GUPTA, J., KHAN, E., HARRAD, S., HOU, D., OK, Y. S. & BOLAN, N. S. 2020. Microplastics as pollutants in agricultural soils. *Environmental Pollution*, 265, 114980.
- KUMAR, S. & SINGH, R. 2011. Recovery of hydrocarbon liquid from waste high density polyethylene by thermal pyrolysis. *Brazilian journal of chemical engineering*, 28, 659-667.
- KUNWAR, B., CHENG, H., CHANDRASHEKARAN, S. R. & SHARMA, B. K. 2016. Plastics to fuel: a review. *Renewable and Sustainable Energy Reviews*, 54, 421-428.

- LAPUERTA, M., ARMAS, O. & RODRIGUEZ-FERNANDEZ, J. 2008. Effect of biodiesel fuels on diesel engine emissions. *Progress in energy and combustion science*, 34, 198-223.
- LASE, I. S., TONINI, D., CARO, D., ALBIZZATI, P. F., CRISTÓBAL, J., ROOSEN, M., KUSENBERG, M., RAGAERT, K., VAN GEEM, K. M. & DEWULF, J. 2023. How much can chemical recycling contribute to plastic waste recycling in Europe? An assessment using material flow analysis modeling. *Resources, Conservation and Recycling*, 192, 106916.
- LEBRETON, L. & ANDRADY, A. 2019. Future scenarios of global plastic waste generation and disposal. *Palgrave Communications*, 5, 1-11.
- LI, A., LI, X., LI, S., REN, Y., SHANG, N., CHI, Y., YAN, J. & CEN, K. 1999. Experimental studies on municipal solid waste pyrolysis in a laboratory-scale rotary kiln. *Energy*, 24, 209-218.
- LI, Q.-L., SHAN, R., WANG, S.-X., YUAN, H.-R. & CHEN, Y. 2023. Production of carbon nanotubes via catalytic pyrolysis of waste plastics over Ni/Al₂O₃ catalyst: The influence of plastic types. *Journal of Analytical and Applied Pyrolysis*, 106318.
- LI, Y., DING, Z., SHAKERIN, M. & ZHANG, N. 2020. A multi-objective optimal design method for thermal energy storage systems with PCM: A case study for outdoor swimming pool heating application. *Journal of Energy Storage*, 29, 101371.
- LILJENSTRÖM, C. & FINNVEDEN, G. 2015. Data for separate collection and recycling of dry recyclable materials. KTH Royal Institute of Technology.
- LIU, W.-W., AZIZ, A., CHAI, S.-P., MOHAMED, A. R. & HASHIM, U. 2013. Synthesis of single-walled carbon nanotubes: Effects of active metals, catalyst supports, and metal loading percentage. *Journal of Nanomaterials*, 2013, 63-63.

- LLANO, J. J., ROSAL, R., SASTRE, H. & DÍEZ, F. V. 1994. Catalytic hydrogenation of anthracene oil with red mud. *Fuel*, 73, 688-694.
- LOPEZ-URIONABARRENECHEA, A., DE MARCO, I., CABALLERO, B., LARESGOITI, M. & ADRADOS, A. 2015. Upgrading of chlorinated oils coming from pyrolysis of plastic waste. *Fuel Processing Technology*, 137, 229-239.
- LÓPEZ, A., DE MARCO, I., CABALLERO, B., ADRADOS, A. & LARESGOITI, M. 2011a. Deactivation and regeneration of ZSM-5 zeolite in catalytic pyrolysis of plastic wastes. *Waste management*, 31, 1852-1858.
- LOPEZ, A., DE MARCO, I., CABALLERO, B., LARESGOITI, M. & ADRADOS, A. 2011. Influence of time and temperature on pyrolysis of plastic wastes in a semi-batch reactor. *Chemical Engineering Journal*, 173, 62-71.
- LÓPEZ, A., DE MARCO, I., CABALLERO, B., LARESGOITI, M., ADRADOS, A. & ARANZABAL, A. 2011b. Catalytic pyrolysis of plastic wastes with two different types of catalysts: ZSM-5 zeolite and Red Mud. *Applied Catalysis B: Environmental*, 104, 211-219.
- LÓPEZ, A., DE MARCO, I., CABALLERO, B., LARESGOITI, M., ADRADOS, A. & TORRES, A. 2011c. Pyrolysis of municipal plastic wastes II: Influence of raw material composition under catalytic conditions. *Waste Management*, 31, 1973-1983.
- LÓPEZ, A., DE MARCO, I., CABALLERO, B. M., LARESGOITI, M. & ADRADOS, A. 2010. Pyrolysis of municipal plastic wastes: Influence of raw material composition. *Waste Management*, 30, 620-627.
- LOPEZ, G., ARTETXE, M., AMUTIO, M., BILBAO, J. & OLAZAR, M. 2017. Thermochemical routes for the valorization of waste polyolefinic plastics to produce fuels and chemicals. A review. *Renewable and Sustainable Energy Reviews*, 73, 346-368.

- LOZANOVSKI, A., SCHULLER, O., FALTENBACHER, M., BODE, M., FINKBEINER, M. & CHOMKHAMRSRI, K. 2011. Guidance document for performing LCAs on fuel cells and H₂ technologies. *Retrieved February, 10, 2015.*
- LUBERTI, M. & AHN, H. 2022. Review of Polybed pressure swing adsorption for hydrogen purification. *International Journal of Hydrogen Energy.*
- LUCAS, A., SILVA, C. A. & NETO, R. C. 2012. Life cycle analysis of energy supply infrastructure for conventional and electric vehicles. *Energy Policy*, 41, 537-547.
- LUDLOW-PALAFIX, C. & CHASE, H. A. 2001. Microwave-induced pyrolysis of plastic wastes. *Industrial & engineering chemistry research*, 40, 4749-4756.
- LUI, J., PAUL, M. C., SLOAN, W. & YOU, S. 2022a. Techno-economic feasibility of distributed waste-to-hydrogen systems to support green transport in Glasgow. *International Journal of Hydrogen Energy*, 47, 13532-13551.
- LUI, J., SLOAN, W., PAUL, M. C., FLYNN, D. & YOU, S. 2022b. Life cycle assessment of waste-to-hydrogen systems for fuel cell electric buses in Glasgow, Scotland. *Bioresource Technology*, 359, 127464.
- MA, C., YU, J., WANG, B., SONG, Z., XIANG, J., HU, S., SU, S. & SUN, L. 2017. Catalytic pyrolysis of flame retarded high impact polystyrene over various solid acid catalysts. *Fuel Processing Technology*, 155, 32-41.
- MAGNOUX, P., ROGER, P., CANAFF, C., FOUICHE, V., GNEP, N. & GUISET, M. 1987. New technique for the characterization of carbonaceous compounds responsible for zeolite deactivation. *Studies in surface science and catalysis*. Elsevier.
- MANGESH, V., PADMANABHAN, S., TAMIZHDURAI, P., NARAYANAN, S. & RAMESH, A. 2020a. Combustion and emission analysis of hydrogenated waste polypropylene pyrolysis oil blended with diesel. *Journal of hazardous materials*, 386, 121453.

- MANGESH, V., PADMANABHAN, S., TAMIZHDURAI, P. & RAMESH, A. 2020b. Experimental investigation to identify the type of waste plastic pyrolysis oil suitable for conversion to diesel engine fuel. *Journal of Cleaner Production*, 246, 119066.
- MANI, M., NAGARAJAN, G. & SAMPATH, S. 2011. Characterisation and effect of using waste plastic oil and diesel fuel blends in compression ignition engine. *Energy*, 36, 212-219.
- MANIGANDAN, S., RYU, J. I., KUMAR, T. P. & ELGENDI, M. 2023. Hydrogen and ammonia as a primary fuel—A critical review of production technologies, diesel engine applications, and challenges. *Fuel*, 352, 129100.
- MANISCALCO, M., LA PAGLIA, F., IANNOTTA, P., CAPUTO, G., SCARGIALI, F., GRISAFI, F. & BRUCATO, A. 2021. Slow pyrolysis of an LDPE/PP mixture: kinetics and process performance. *Journal of the Energy Institute*.
- MANOS, G., YUSOF, I. Y., PAPAYANNAKOS, N. & GANGAS, N. H. 2001. Catalytic cracking of polyethylene over clay catalysts. Comparison with an ultrastable Y zeolite. *Industrial & engineering chemistry research*, 40, 2220-2225.
- MANZOLINI, G., MACCHI, E. & GAZZANI, M. 2013. CO₂ capture in natural gas combined cycle with SEWGS. Part B: Economic assessment. *International Journal of Greenhouse Gas Control*, 12, 502-509.
- MARCILLA, A., BELTRÁN, M. & NAVARRO, R. 2009. Evolution of products during the degradation of polyethylene in a batch reactor. *Journal of Analytical and Applied Pyrolysis*, 86, 14-21.
- MARTINS, A. H., ROUBOA, A. & MONTEIRO, E. 2023. On the green hydrogen production through gasification processes: A techno-economic approach. *Journal of Cleaner Production*, 383, 135476.

- MASTRAL, F., ESPERANZA, E., GARCÍA, P. & JUSTE, M. 2002. Pyrolysis of high-density polyethylene in a fluidised bed reactor. Influence of the temperature and residence time. *Journal of Analytical and Applied Pyrolysis*, 63, 1-15.
- MCKINSEY CENTER FOR BUSINESS AND ENVIRONMENT 2015. Stemming the Tide: Land-based strategies for a plastic- free ocean.
- MELLO, M., RUTTO, H. & SEODIGENG, T. 2023. Waste tire pyrolysis and desulfurization of tire pyrolytic oil (TPO)—A review. *Journal of the Air & Waste Management Association*, 73, 159-177.
- MEYERS, R. A. 2016. *Handbook of petroleum refining processes*, McGraw-Hill Education.
- MILLARD, R. 2022. Ukraine crisis exposes UK reliance on Russian diesel. *Telegraph*.
- MISKOLCZI, N., ANGYAL, A., BARTHA, L. & VALKAI, I. 2009. Fuels by pyrolysis of waste plastics from agricultural and packaging sectors in a pilot scale reactor. *Fuel Processing Technology*, 90, 1032-1040.
- MISKOLCZI, N., BARTHA, L. & DEÁK, G. 2006. Thermal degradation of polyethylene and polystyrene from the packaging industry over different catalysts into fuel-like feed stocks. *Polymer degradation and stability*, 91, 517-526.
- MORTEZAEIKIA, V., TAVAKOLI, O. & KHODAPARASTI, M. S. 2021. A review on kinetic study approach for pyrolysis of plastic wastes using thermogravimetric analysis. *Journal of Analytical and Applied Pyrolysis*, 160, 105340.
- MUKHERJEE, A., OKOLIE, J. A., NIU, C. & DALAI, A. K. 2022. Techno–Economic analysis of activated carbon production from spent coffee grounds: Comparative evaluation of different production routes. *Energy Conversion and Management: X*, 14, 100218.
- MURATA, K., SATO, K. & SAKATA, Y. 2004. Effect of pressure on thermal degradation of polyethylene. *Journal of Analytical and Applied Pyrolysis*, 71, 569-589.

- MUSHARAVATI, F., KHOSHNEVISAN, A., ALIRAHMI, S. M., AHMADI, P. & KHANMOHAMMADI, S. 2022. Multi-objective optimization of a biomass gasification to generate electricity and desalinated water using Grey Wolf Optimizer and artificial neural network. *Chemosphere*, 287, 131980.
- NAKASAKA, Y., NISHIMURA, J.-I., TAGO, T. & MASUDA, T. 2015. Deactivation mechanism of MFI-type zeolites by coke formation during n-hexane cracking. *Chemical Engineering Journal*, 278, 159-165.
- NISANTH, H. & KUMAR, B. 2019. Observations on the entanglement of plastic debris in seabirds of the family Laridae along Kerala Coast, India. *Journal of Aquatic Biology & Fisheries/ Vol, 7*, 115-119.
- NISAR, J., ALI, G., SHAH, A., IQBAL, M., KHAN, R. A., ANWAR, F., ULLAH, R. & AKHTER, M. S. 2019. Fuel production from waste polystyrene via pyrolysis: Kinetics and products distribution. *Waste management*, 88, 236-247.
- NIUTECH ENVIRONMENT TECHNOLOGY CORPORATION 2024.
- OK, Y. S. 2020. Particulate Plastics in Terrestrial and Aquatic Environments.
- ONWUDILI, J. A., MUHAMMAD, C. & WILLIAMS, P. T. 2019. Influence of catalyst bed temperature and properties of zeolite catalysts on pyrolysis-catalysis of a simulated mixed plastics sample for the production of upgraded fuels and chemicals. *Journal of the Energy Institute*, 92, 1337-1347.
- OUDERJI, Z. H., GUPTA, R., MCKEOWN, A., YU, Z., SMITH, C., SLOAN, W. & YOU, S. 2023. Integration of anaerobic digestion with heat Pump: Machine learning-based technical and environmental assessment. *Bioresource Technology*, 369, 128485.
- PAN, D., SU, F., LIU, H., LIU, C., UMAR, A., CASTAÑEDA, L., ALGADI, H., WANG, C. & GUO, Z. 2021. Research progress on catalytic pyrolysis and reuse of waste plastics and petroleum sludge. *ES Materials & Manufacturing*, 11, 3-15.

- PANERU, B., PANERU, B., SAPKOTA, S. C., MANDAL, D. K. & GIRI, P. 2024. Techno-economic analysis of hydrogen production from waste plastics and storage plant in the context of Japan. *International Journal of Hydrogen Energy*, 95, 53-70.
- PARK, S. S., SEO, D. K., LEE, S. H., YU, T.-U. & HWANG, J. 2012. Study on pyrolysis characteristics of refuse plastic fuel using lab-scale tube furnace and thermogravimetric analysis reactor. *Journal of analytical and applied pyrolysis*, 97, 29-38.
- PATIL, V., ADHIKARI, S. & CROSS, P. 2018. Co-pyrolysis of lignin and plastics using red clay as catalyst in a micro-pyrolyzer. *Bioresource technology*, 270, 311-319.
- PE INTERNATIONAL 2015. LCA of Management Options for Polymer Waste from Bank Notes. Final Study Report.
- PEETERS, A., FAAIJ, A. & TURKENBURG, W. 2007. Techno-economic analysis of natural gas combined cycles with post-combustion CO₂ absorption, including a detailed evaluation of the development potential. *International Journal of Greenhouse gas control*, 1, 396-417.
- PI, A. E., DAI, Q., HAN, J. & WANG, M. 2016. Life Cycle Analysis of Emerging Hydrogen Production Technologies. *Argonne National Laboratory: Lemont, IL, USA*, 1-5.
- PIRES COSTA, L., VAZ DE MIRANDA, D. B. M. & PINTO, J. C. 2022. Critical Evaluation of Life Cycle Assessment Analyses of Plastic Waste Pyrolysis. *ACS Sustainable Chemistry & Engineering*.
- PLASTIC2OIL 2024.
- PLASTIC ADVANCED RECYCLING CORP 2024.
- PLASTICS EUROPE 2020. Plastics – the Facts 2020.
- POPULATION UK 2023. Glasgow Population 2022.

- POTTING, J., HEKKERT, M. P., WORRELL, E. & HANEMAAIJER, A. 2017. Circular economy: measuring innovation in the product chain. *Planbureau voor de Leefomgeving*.
- PRABU, S. & CHIANG, K.-Y. 2022. Highly active Ni-Mg-Al Ni–Mg–Al catalyst effect on carbon nanotube production from waste biodegradable plastic catalytic pyrolysis. *Environmental Technology & Innovation*, 28, 102845.
- PRAVEENKUMAR, T., SEKAR, M., PASUPULETI, R. R., GAVUROVÁ, B., KUMAR, G. A. & KUMAR, M. V. 2024. Current technologies for plastic waste treatment for energy recovery, it's effects on poly aromatic hydrocarbons emission and recycling strategies. *Fuel*, 357, 129379.
- PREDEL, M. & KAMINSKY, W. 2000. Pyrolysis of mixed polyolefins in a fluidised-bed reactor and on a pyro-GC/MS to yield aliphatic waxes. *Polymer Degradation and Stability*, 70, 373-385.
- PROMEKO 2024.
- QUANTUM LIFECYCLE 2024.
- QUINTEIRO, P., GRECO, F., DA CRUZ TARELHO, L. A., RIGHI, S., ARROJA, L. & DIAS, A. C. 2020. A comparative life cycle assessment of centralised and decentralised wood pellets production for residential heating. *Science of The Total Environment*, 730, 139162.
- QURESHI, M. S., OASMAA, A., PIHKOLA, H., DEVIATKIN, I., TENHUNEN, A., MANNILA, J., MINKKINEN, H., POHJAKALLIO, M. & LAINE-YLIJOKI, J. 2020. Pyrolysis of plastic waste: opportunities and challenges. *Journal of Analytical and Applied Pyrolysis*, 104804.
- RAC FOUNDATION 2024. UK petrol and diesel consumption.

- RAGAERT, K., DELVA, L. & VAN GEEM, K. 2017. Mechanical and chemical recycling of solid plastic waste. *Waste Management*, 69, 24-58.
- RAJAK, U., PANCHAL, M., VEZA, I., AĞBULUT, Ü., VERMA, T. N., SARİDEMİR, S. & SHENDE, V. 2022. Experimental investigation of performance, combustion and emission characteristics of a variable compression ratio engine using low-density plastic pyrolyzed oil and diesel fuel blends. *Fuel*, 319, 123720.
- RAJENDRAN, K. M., CHINTALA, V., SHARMA, A., PAL, S., PANDEY, J. K. & GHODKE, P. 2020. Review of catalyst materials in achieving the liquid hydrocarbon fuels from municipal mixed plastic waste (MMPW). *Materials Today Communications*, 24, 100982.
- RAM, L. & MASTO, R. 2014. Fly ash for soil amelioration: a review on the influence of ash blending with inorganic and organic amendments. *Earth-Science Reviews*, 128, 52-74.
- RAMALINGAM, S., RAJENDRAN, S., GANESAN, P. & GOVINDASAMY, M. 2018. Effect of operating parameters and antioxidant additives with biodiesels to improve the performance and reducing the emissions in a compression ignition engine—A review. *Renewable and Sustainable Energy Reviews*, 81, 775-788.
- RATH, L. K., CHOU, V. H. & KUEHN, N. J. 2011. Assessment of hydrogen production with CO₂ capture volume 1: baseline state-of-the-art plants. National Energy Technology Laboratory (NETL), Pittsburgh, PA, Morgantown, WV
- RODRIGUEZ, I., VALDIVIEZO, L., HARDEN, T. & HUNAG, X. 2018. Transforming non-recyclable plastics to fuel oil using thermal pyrolysis. *Chemical Engineering Department, Grove School of Engineering, The City College of New York*.
- ROMAN, L., SCHUYLER, Q., WILCOX, C. & HARDESTY, B. D. 2020. Plastic pollution is killing marine megafauna, but how do we prioritize policies to reduce mortality? *Conservation Letters*, e12781.

- RONALD LONG, K. P. A. A. Z. 2011. Optimising hydrogen production and use.
- RUBIN, E. S., CHEN, C. & RAO, A. B. 2007. Cost and performance of fossil fuel power plants with CO₂ capture and storage. *Energy policy*, 35, 4444-4454.
- RUTHVEN, D. M. & PRESSURE, F. 1994. Swing adsorption. *New York: VCH Publishers*, 1, 235.
- SAAD, J. M., WILLIAMS, P. T., ZHANG, Y. S., YAO, D., YANG, H. & ZHOU, H. 2021. Comparison of waste plastics pyrolysis under nitrogen and carbon dioxide atmospheres: A thermogravimetric and kinetic study. *Journal of Analytical and Applied Pyrolysis*, 156, 105135.
- SAHU, J., MAHALIK, K., NAM, H. K., LING, T. Y., WOON, T. S., BIN ABDUL RAHMAN, M. S., MOHANTY, Y., JAYAKUMAR, N. & JAMUAR, S. 2014. Feasibility study for catalytic cracking of waste plastic to produce fuel oil with reference to M alaysia and simulation using ASPEN Plus. *Environmental Progress & Sustainable Energy*, 33, 298-307.
- SAMADDER, S., PRABHAKAR, R., KHAN, D., KISHAN, D. & CHAUHAN, M. 2017. Analysis of the contaminants released from municipal solid waste landfill site: a case study. *Science of the Total Environment*, 580, 593-601.
- SANTAMARIA, L., LOPEZ, G., FERNANDEZ, E., CORTAZAR, M., ARREGI, A., OLAZAR, M. & BILBAO, J. 2021. Progress on catalyst development for the steam reforming of biomass and waste plastics pyrolysis volatiles: a review. *Energy & Fuels*, 35, 17051-17084.
- SANTAWEESUK, C. & JANYALERTADUN, A. 2017. The production of fuel oil by conventional slow pyrolysis using plastic waste from a municipal landfill. *International Journal of Environmental Science and Development*, 8, 168.

- SARKAR, B., DISSANAYAKE, P. D., BOLAN, N. S., DAR, J. Y., KUMAR, M., HAQUE, M. N., MUKHOPADHYAY, R., RAMANAYAKA, S., BISWAS, J. K. & TSANG, D. C. 2021. Challenges and opportunities in sustainable management of microplastics and nanoplastics in the environment. *Environmental Research*, 112179.
- SAUVÉ, S., BERNARD, S. & SLOAN, P. 2016. Environmental sciences, sustainable development and circular economy: Alternative concepts for trans-disciplinary research. *Environmental Development*, 17, 48-56.
- SAVINELLI, B., FERNÁNDEZ, T. V., GALASSO, N. M., D'ANNA, G., PIPITONE, C., PRADA, F., ZENONE, A., BADALAMENTI, F. & MUSCO, L. 2020. Microplastics impair the feeding performance of a Mediterranean habitat-forming coral. *Marine environmental research*, 155, 104887.
- SAVOCA, M. S., MCINTURF, A. G. & HAZEN, E. L. 2021. Plastic ingestion by marine fish is widespread and increasing. *Global Change Biology*.
- SCHADE, A., MELZER, M., ZIMMERMANN, S., SCHWARZ, T., STOEWE, K. & KUHN, H. 2024. Plastic Waste Recycling— A Chemical Recycling Perspective. *ACS Sustainable Chemistry & Engineering*, 12, 12270-12288.
- SCHIRMER, J., KIM, J. & KLEMM, E. 2001. Catalytic degradation of polyethylene using thermal gravimetric analysis and a cycled-spheres-reactor. *Journal of analytical and applied pyrolysis*, 60, 205-217.
- SCOTTISH ENTERPRISE 2023. Hydrogen demand in Scotland: a mapping of industrial and transport applications.
- SCOTTISH ENVIRONMENT PROTECTION AGENCY 2015. Waste Classification.
- SCOTTISH ENVIRONMENT PROTECTION AGENCY 2019. Climate Change Plan: third report on proposals and policies 2018-2032 (RPP3).

SCOTTISH ENVIRONMENT PROTECTION AGENCY 2023. Scottish household waste generation and management (tonnes).

SCOTTISH GOVERNMENT 2022. Scottish Greenhouse Gas Statistics 2020.

SCOTTISH POWER 2024. Get paid for generating green electricity.

SEKAR, M., PONNUSAMY, V. K., PUGAZHENDHI, A., NIŽETIĆ, S. & PRAVEENKUMAR, T. 2022. Production and utilization of pyrolysis oil from solidplastic wastes: A review on pyrolysis process and influence of reactors design. *Journal of environmental management*, 302, 114046.

SEPA 2024. Waste from all sources: summary document and commentary text.

SEREFENTSE, R., RUWONA, W., DANHA, G. & MUZENDA, E. 2019. A review of the desulphurization methods used for pyrolysis oil. *Procedia manufacturing*, 35, 762-768.

SERRA, A. C., MILATO, J. V., FAILLACE, J. G. & CALDERARI, M. R. 2022. Reviewing the use of zeolites and clay based catalysts for pyrolysis of plastics and oil fractions. *Brazilian Journal of Chemical Engineering*, 1-33.

SERRANO, D., AGUADO, J. & ESCOLA, J. 2012. Developing advanced catalysts for the conversion of polyolefinic waste plastics into fuels and chemicals. *ACS Catalysis*, 2, 1924-1941.

SGN AND WOOD 2021. North East Network & Industrial Cluster Development – Summary Report.

SHAHABUDDIN, M., KRISHNA, B. B., BHASKAR, T. & PERKINS, G. 2020. Advances in the thermo-chemical production of hydrogen from biomass and residual wastes: Summary of recent techno-economic analyses. *Bioresource Technology*, 299, 122557.

SHARUDDIN, S. D. A., ABNISA, F., DAUD, W. M. A. W. & AROUA, M. K. 2016. A review on pyrolysis of plastic wastes. *Energy conversion and management*, 115, 308-326.

- SHARUDDIN, S. D. A., ABNISA, F., DAUD, W. M. A. W. & AROUA, M. K. 2017. Energy recovery from pyrolysis of plastic waste: Study on non-recycled plastics (NRP) data as the real measure of plastic waste. *Energy Conversion and Management*, 148, 925-934.
- SHEN, M., YE, S., ZENG, G., ZHANG, Y., XING, L., TANG, W., WEN, X. & LIU, S. 2020. Can microplastics pose a threat to ocean carbon sequestration? *Marine pollution bulletin*, 150, 110712.
- SILVARREY, L. D. & PHAN, A. 2016. Kinetic study of municipal plastic waste. *International journal of hydrogen energy*, 41, 16352-16364.
- SINGH, B., STRØMMAN, A. H. & HERTWICH, E. 2011. Life cycle assessment of natural gas combined cycle power plant with post-combustion carbon capture, transport and storage. *International Journal of Greenhouse Gas Control*, 5, 457-466.
- SINGH, E., KUMAR, A., KHAPRE, A., SAIKIA, P., SHUKLA, S. K. & KUMAR, S. 2020. Efficient removal of arsenic using plastic waste char: Prevailing mechanism and sorption performance. *Journal of Water Process Engineering*, 33, 101095.
- SINGH, N., HUI, D., SINGH, R., AHUJA, I., FEO, L. & FRATERNALI, F. 2017. Recycling of plastic solid waste: A state of art review and future applications. *Composites Part B: Engineering*, 115, 409-422.
- SINGH, R. K., RUJ, B., SADHUKHAN, A. & GUPTA, P. 2019. Impact of fast and slow pyrolysis on the degradation of mixed plastic waste: Product yield analysis and their characterization. *Journal of the Energy Institute*, 92, 1647-1657.
- SOBKO, A. Generalized van der Waals-Berthelot equation of state. *Doklady Physics*, 2008. Springer, 416-419.
- SOMOZA-TORNOS, A., GONZALEZ-GARAY, A., POZO, C., GRAELLS, M. S., ESPUÑA, A. & GUILLÉN-GOSÁLBEZ, G. 2020. Realizing the potential high benefits of circular

- economy in the chemical industry: ethylene monomer recovery via polyethylene pyrolysis. *ACS Sustainable Chemistry & Engineering*, 8, 3561-3572.
- SPALLINA, V., PANDOLFO, D., BATTISTELLA, A., ROMANO, M. C., ANNALAND, M. V. S. & GALLUCCI, F. 2016. Techno-economic assessment of membrane assisted fluidized bed reactors for pure H₂ production with CO₂ capture. *Energy conversion and management*, 120, 257-273.
- STATISTA 2022. Forecast cost of domestically produced and imported green hydrogen in Europe in 2024 and 2030.
- STATISTA 2025. Forecasted consumer price index (CPI) inflation in the United Kingdom (UK) from 2020 to 2024, by institution.
- STEIGER, J. H. 2010. Monte Carlo Investigations.
- STEVEN, O. & ASHLEY, R. 2022. Comparing the Costs of Alternative Waste Treatment Options. *WRAP: Banbury, UK*.
- SUN, J., LUO, J., MA, R., LIN, J. & FANG, L. 2023. Effects of microwave and plastic content on the sulfur migration during co-pyrolysis of biomass and plastic. *Chemosphere*, 314, 137680.
- THE RENEWABLE ENERGY HUB 2023. The Smart Export Guarantee in 2022.
- THE SCOTTISH PARLAMENT 2023. Earnings in Scotland 2022.
- U.S. DEPARTMENT OF ENERGY 2024a. All-Electric Vehicles.
- U.S. DEPARTMENT OF ENERGY 2024b. FUEL CELL TECHNOLOGIES PROGRAM.
- UK, G. 2020. Government takes historic step towards net-zero with end of sale of new petrol and diesel cars by 2030.
- UK GOVERNMENT 2023. Developing the UK Emissions Trading Scheme: Main Response.
- UMENWEKE, G. C., PACE, R. B., SANTILLAN-JIMENEZ, E. & OKOLIE, J. A. 2023. Techno-economic and life-cycle analyses of sustainable aviation fuel production via

- integrated catalytic deoxygenation and hydrothermal gasification. *Chemical Engineering Journal*, 452, 139215.
- VALENTE, A., IRIBARREN, D. & DUFOUR, J. 2019. Life cycle sustainability assessment of hydrogen from biomass gasification: A comparison with conventional hydrogen. *International Journal of Hydrogen Energy*, 44, 21193-21203.
- VAN CANEGHEM, J., VAN ACKER, K., DE GREEF, J., WAUTERS, G. & VANDECASTEELE, C. 2019. Waste-to-energy is compatible and complementary with recycling in the circular economy. *Clean Technologies and Environmental Policy*, 21, 925-939.
- VAN DER SPEK, M., BANET, C., BAUER, C., GABRIELLI, P., GOLDTHORPE, W., MAZZOTTI, M., MUNKEJORD, S. T., RØKKE, N. A., SHAH, N. & SUNNY, N. 2022. Perspective on the hydrogen economy as a pathway to reach net-zero CO₂ emissions in Europe. *Energy & Environmental Science*, 15, 1034-1077.
- VAN EMMERIK, T. & SCHWARZ, A. 2020. Plastic debris in rivers. *Wiley Interdisciplinary Reviews: Water*, 7, e1398.
- VOSS, C. 2005. Applications of pressure swing adsorption technology. *Adsorption*, 11, 527-529.
- WANG, C., XIAN, Z., JIN, X., LIANG, S., CHEN, Z., PAN, B., WU, B., OK, Y. S. & GU, C. 2020. Photo-aging of polyvinyl chloride microplastic in the presence of natural organic acids. *Water Research*, 183, 116082.
- WANG, F., QUAN, C., LIU, H., LANG, L., YUAN, H., YIN, X., WANG, J. & GAO, N. 2023a. Energy and exergy analysis based on an energy saving process of waste tires pressurized catalytic reforming. *Energy Conversion and Management*, 289, 117191.
- WANG, J., JIANG, J., SUN, Y., WANG, X., LI, M., PANG, S., RUAN, R., RAGAUSKAS, A. J., OK, Y. S. & TSANG, D. C. 2021. Catalytic degradation of waste rubbers and

- plastics over zeolites to produce aromatic hydrocarbons. *Journal of Cleaner Production*, 309, 127469.
- WANG, S., SUN, Y., SHAN, R., GU, J., HUHE, T., LING, X., YUAN, H. & CHEN, Y. 2023b. Polypropylene Pyrolysis and Steam Reforming over Fe-based Catalyst Supported on Activated Carbon for the Production of Hydrogen-Rich Syngas. *Carbon Resources Conversion*.
- WANG, Y., CAI, N., YANG, H. & WU, C. 2022a. Application of carbon nanotubes from waste plastics as filler to epoxy resin composite. *ACS Sustainable Chemistry & Engineering*, 10, 2204-2213.
- WANG, Z., LI, J., RANGAIAH, G. P. & WU, Z. 2022b. Machine learning aided multi-objective optimization and multi-criteria decision making: Framework and two applications in chemical engineering. *Computers & Chemical Engineering*, 165, 107945.
- WEXLER, P., ANDERSON, B. D., GAD, S. C. & DE PEYSTER, A. 2005. *Encyclopedia of toxicology*, Academic Press.
- WILLIAMS, K., KHODIER, A. & BENTLEY, P. 2023. PAHs, PCBs and Environmental Contamination in Char Products. *Biochar-Productive Technologies, Properties and Applications*. IntechOpen.
- WILLIAMS, P. T. 2020. Hydrogen and carbon nanotubes from pyrolysis-catalysis of waste plastics: A review. *Waste and Biomass Valorization*, 1-28.
- WU, C., NAHIL, M. A., MISKOLCZI, N., HUANG, J. & WILLIAMS, P. T. 2014. Processing real-world waste plastics by pyrolysis-reforming for hydrogen and high-value carbon nanotubes. *Environmental science & technology*, 48, 819-826.

- WU, C. & WILLIAMS, P. T. 2013. Advanced thermal treatment of wastes for fuels, chemicals and materials recovery. *Waste as a Resource*. Royal Society of Chemistry Publishers London.
- WU, W., XU, H., SHI, B. & KUO, P.-C. 2023. Techno-economic analysis of plastic wastes-based polygeneration processes. *Chemical Engineering and Processing-Process Intensification*, 184, 109297.
- YADAV, G., SINGH, A., NICHOLSON, S. R. & BECKHAM, G. T. 2022. Techno-Economic Analysis and Life Cycle Assessment for Pyrolysis of Mixed Waste Plastics. National Renewable Energy Lab.(NREL), Golden, CO (United States).
- YANG, R. T. 1997. *Gas separation by adsorption processes*, World Scientific.
- YAO, D. & WANG, C.-H. 2020. Pyrolysis and in-line catalytic decomposition of polypropylene to carbon nanomaterials and hydrogen over Fe-and Ni-based catalysts. *Applied Energy*, 265, 114819.
- YAO, D., YANG, H., CHEN, H. & WILLIAMS, P. T. 2018. Co-precipitation, impregnation and so-gel preparation of Ni catalysts for pyrolysis-catalytic steam reforming of waste plastics. *Applied Catalysis B: Environmental*, 239, 565-577.
- YI, C. Q., BOJENG, M. N. I. B. H. B. H., KAMIS, S. K. B. H., MUBARAK, N. M., KARRI, R. R. & AZRI, H. 2024. Production of hydrogen using plastic waste via Aspen Hysys simulation. *Scientific Reports*, 14, 4934.
- YOU, S., WANG, W., DAI, Y., TONG, Y. W. & WANG, C.-H. 2016. Comparison of the co-gasification of sewage sludge and food wastes and cost-benefit analysis of gasification and incineration-based waste treatment schemes. *Bioresource Technology*, 218, 595-605.
- YUAN, X., KUMAR, N. M., BRIGLJEVIĆ, B., LI, S., DENG, S., BYUN, M., LEE, B., LIN, C. S. K., TSANG, D. C. & LEE, K. B. 2022. Sustainability-inspired upcycling of waste

polyethylene terephthalate plastic into porous carbon for CO₂ capture. *Green Chemistry*.

YUAN, X., WANG, X., SARKAR, B. & OK, Y. S. 2021. The COVID-19 pandemic necessitates a shift to a plastic circular economy. *Nature Reviews Earth & Environment*, 2, 659-660.

ZERO WASTE SCOTLAND 2010. The composition of municipal solid waste in Scotland. *Zero Waste Scotland, Stirling*.

ZHENG, J. & SUH, S. 2019. Strategies to reduce the global carbon footprint of plastics. *Nature Climate Change*, 9, 374-378.